BEILSTEIN JOURNAL OF ORGANIC CHEMISTRY

Organometallic chemistry

Edited by Bernd F. Straub and Lutz Gade

Generated on 06 November 2026, 09:36

Imprint

Beilstein Journal of Organic Chemistry
www.bjoc.org
ISSN 1860-5397
Email: journals-support@beilstein-institut.de

The *Beilstein Journal of Organic Chemistry* is published by the Beilstein-Institut zur Förderung der Chemischen Wissenschaften.

Beilstein-Institut zur Förderung der Chemischen Wissenschaften
Trakehner Straße 7–9
60487 Frankfurt am Main
Germany
www.beilstein-institut.de

The copyright to this document as a whole, which is published in the *Beilstein Journal of Organic Chemistry*, is held by the Beilstein-Institut zur Förderung der Chemischen Wissenschaften. The copyright to the individual articles in this document is held by the respective authors, subject to a Creative Commons Attribution license.

BEILSTEIN JOURNAL OF ORGANIC CHEMISTRY

Organometallic chemistry

Bernd F. Straub*[1], Rolf Gleiter[1], Claudia Meier[2] and Lutz H. Gade*[3]

Editorial

Open Access

Address:
[1]Organisch-Chemisches Institut, Universität Heidelberg, Im Neuenheimer Feld 270, D-69120 Heidelberg, Germany, [2]Department Chemie, Ludwig-Maximilians-Universität München, Butenandtstrasse 5–13 (Haus F), D-81377 München, Germany and [3]Anorganisch-Chemisches Institut, Universität Heidelberg, Im Neuenheimer Feld 270, D-69120 Heidelberg, Germany

Email:
Bernd F. Straub* - straub@oci.uni-heidelberg.de; Lutz H. Gade* - lutz.gade@uni-heidelberg.de

* Corresponding author

Beilstein J. Org. Chem. **2016,** *12,* 2216–2221.
doi:10.3762/bjoc.12.213

Received: 19 September 2016
Accepted: 29 September 2016
Published: 19 October 2016

This article is part of the Thematic Series "Organometallic chemistry".

Guest Editors: B. F. Straub and L. H. Gade

© 2016 Straub et al.; licensee Beilstein-Institut.
License and terms: see end of document.

This Thematic Series is dedicated to the memory of Professor Peter Hofmann (Figure 1) whose research work included many seminal contributions to the field of organometallic chemistry [1-3]. Organometallic chemistry has therefore been chosen as the topic of this Thematic Series of the *Beilstein Journal of Organic Chemistry*. Over a period of many decades, the chemistry of metal–carbon bonds has given rise to an ever-growing field of fundamental research and applied science, merging the reactivity of inorganic complexes with the structural diversity of organic compounds. The contributions in this Thematic Series reflect the broad impact of organometallic compounds in various fields of modern chemical research. These include the tailoring of new ancillary ligands, the investigation of more active and more selective homogeneous catalysts, catalytic transformations in the total synthesis of natural products, the theoretical and kinetic unravelling of reaction mechanisms, and the verification of rare coordination modes. These various facets underline the importance of organometallic chemistry in its own right, but also demonstrate the vital role that research in organometallic chemistry plays as a provider of invaluable tools for other chemistry sub-disciplines.

We thank the authors for their excellent contributions and are grateful for the commitment and the support of the Beilstein-Institut and its staff who made this Thematic Series possible.



Figure 1: Peter Hofmann.

Peter Hofmann, a multifaceted organometallic chemist

Peter Hofmann died unexpectedly in Heidelberg on August 15, 2015, having retired from his chair position of organic chemistry at Heidelberg University just a few months before [4-155].

Peter Hofmann was born on January 12, 1947 in the Franconian city of Nuremberg, Germany, where he spent most of his youth. After the Abitur, his final secondary school examinations in 1966, he studied chemistry at the University of Erlangen-Nuremberg. In 1973, he received a doctorate with honors for his research on photochemical reactions of oxepin and thiepin derivatives in the group of Hans Hofmann [4-8,10,12,18]. Despite their identical family names, he and his doctoral supervisor were not related; Hof(f)mann is an unusually prevalent surname among distinguished German chemists.

In the time between his Ph.D. and postdoctoral research, he began his studies on vicinal triketones and their electronic structure [13,33,41].

Peter Hofmann joined the research group of Roald Hoffmann, the chemistry Nobel laureate of 1981, where he studied the electronic structure of organo-transition metal complexes by extended Hückel model calculations [14,17,20,28,39,49,50,54,57]. In 1978, he completed his habilitation in Erlangen, mentored by Paul von Ragué Schleyer, and was promoted to professor in 1980. Following a three-month visiting professorship in Berkeley in 1980, he was appointed to a visiting professorship in Munich in 1981 that was converted into a permanent academic position. Working with Ernst Otto Fischer, the chemistry Nobel laureate of 1973, he benefited from an ideal research environment that enabled him to compare his theoretical analyses and predictions with experimental data [34-38,40,42,43,45-60,62,63,65,74]. As an accomplished communicator of his research results, Peter Hofmann was a much sought-after visiting professor in the following years, which led to stints at the Universities of Bern, Ulm, TU and FU Berlin, Heidelberg, Rennes, Strasbourg, and Madison Wisconsin. In 1995, he declined the offer of a professorship from the Free University of Amsterdam and accepted a call to a chair position at Heidelberg University. He thus became one of the very few chemists with a history of research and teaching in theoretical, organic and inorganic chemistry. His research interests combined all three fields, with a focus on homogeneous catalysis with transition metal complexes. Bidentate donor ligands with a small bite angle such as bis(di-*tert*-butylphosphino)methane (dtbpm) were a unique feature of his work [61,67,70-72,80,81,84,86,93,94,97,100,101,103,107,124,128,148,149] that ultimately enabled C–Si activation of organosilanes and the C–C activation of oxiranes by coordinatively unsaturated platinum species [66,149]. In the mechanism of the Dötz reaction, he found that chromacyclobutene structures were unrealistic intermediates and instead proposed vinylcarbene complexes as much more stable isomers [64,68,88]. Other research projects of his group included the synthesis of ruthenium–carbene complexes with *cis*-dichloro ligands for olefin metathesis catalysis [86,87,90,91,98-100,108,132,138,147], the characterization of copper–carbene complexes as intermediates in the cyclopropanation of alkenes [102,106,113,119,120], as well as detailed studies into the mechanism of the hydroformylation of alkenes. An improved understanding of this industrially important process was achieved by a combination of ligand design for the rhodium catalysts, kinetic studies, and high-level quantum-chemical calculations [126,135,142,145,146,152,155].

In 2006, he initiated the foundation of the “Catalysis Research Laboratory” (CaRLa), a cooperation of Ludwighafen’s BASF and Heidelberg University, for which he acted as scientific head until October 2014. Postdocs from all over the world studied industrially important processes focusing on their fundamental principles [110,112,115,121,123,126,127]. The biennial “Heidelberg Forum of Molecular Catalysis” (HFMC), organized by Peter Hofmann until 2013, has been one of the most visible scientific events of Heidelberg’s chemical institutes.

Peter Hofmann was initiator, and until July 2009 chairman, of the SFB 623 “Molecular Catalysts: Structure and Functional Design”. As dean and vice-dean, he was actively involved in the affairs of the Heidelberg Faculty of Chemistry and Geosciences for six years. He received numerous awards and distinctions, including 2008 the Emil-Fischer medal of the GDCh and memberships in the Heidelberg Academy of Science and Humanities as well as the Academy of Science of North Rhine-Westphalia.

Peter Hofmann was an archetypical scientist and teacher, and in many respects a role model for colleagues and students. His scientific work revealed a high degree of intellectual creativity and deep chemical understanding, leading to modern and original research. He was reliable, honest and forthright in the interaction with his colleagues and students and enthusiastic when discussing any scientific problem. He preferred science over science politics and found it difficult to hide an aversion towards pomposity and concealed mediocrity, while being supportive towards less established junior colleagues.

We will remember Peter Hofmann as a tolerant, cooperative and amiable colleague.

Bernd F. Straub, Rolf Gleiter, Claudia Meier and Lutz H. Gade

Heidelberg, September 2016

References

1. ORCID entry for Peter Hofmann. http://orcid.org/0000-0003-2568-4608
2. ResearcherID entry for Peter Hofmann. http://www.researcherid.com/rid/A-4852-2016
3. Gleiter, R.; Straub, B. F. *Nachr. Chem.* **2016,** *64,* 370.
4. Hofmann, H.; Hofmann, P. *Tetrahedron Lett.* **1971,** *12,* 4055–4056. doi:10.1016/S0040-4039(01)97360-5
5. Hofmann, H.; Meyer, B.; Hofmann, P. *Angew. Chem., Int. Ed. Engl.* **1972,** *11,* 423–424. doi:10.1002/anie.197204231
6. Hofmann, H.; Hofmann, P. *Chem. Ber.* **1973,** *106,* 3571–3577. doi:10.1002/cber.19731061114
7. Hofmann, H.; Hofmann, P. *Justus Liebigs Ann. Chem.* **1974,** 1301–1314. doi:10.1002/jlac.197419740817
8. Hofmann, H.; Hofmann, P. *Chem. Ber.* **1974,** *107,* 2259–2264. doi:10.1002/cber.19741070710
9. Bischof, P.; Gleiter, R.; Hofmann, P. *J. Chem. Soc., Chem. Commun.* **1974,** 767–768. doi:10.1039/c39740000767
10. Hofmann, H.; Hofmann, P. *Justus Liebigs Ann. Chem.* **1975,** 1797–1807. doi:10.1002/jlac.197519751008
11. Hofmann, P.; Gleiter, R. *Tetrahedron Lett.* **1975,** *16,* 159–162. doi:10.1016/S0040-4039(00)72496-8
12. Hofmann, H.; Hofmann, P. *Justus Liebigs Ann. Chem.* **1975,** 1571–1575. doi:10.1002/jlac.197519750904
13. Bischof, P.; Gleiter, R.; Hofmann, P. *Helv. Chim. Acta* **1975,** *58,* 2130–2135. doi:10.1002/hlca.19750580725
14. Hoffmann, R.; Hofmann, P. *J. Am. Chem. Soc.* **1976,** *98,* 598–604. doi:10.1021/ja00418a046
15. Gleiter, R.; Bartetzko, R.; Hofmann, P.; Scharf, H.-D. *Angew. Chem., Int. Ed. Engl.* **1977,** *16,* 400–401. doi:10.1002/anie.197704001
16. Hofmann, P. *Angew. Chem., Int. Ed. Engl.* **1977,** *16,* 536–537. doi:10.1002/anie.197705361
17. Albright, T. A.; Hofmann, P.; Hoffmann, R. *J. Am. Chem. Soc.* **1977,** *99,* 7546–7557. doi:10.1021/ja00465a025
18. Hofmann, H.; Hofmann, P. *Justus Liebigs Ann. Chem.* **1977,** 1597–1609. doi:10.1002/jlac.197719771003
19. Hofmann, P. *Z. Naturforsch., B* **1978,** *33,* 251–260.
20. Albright, T. A.; Hoffmann, R.; Hofmann, P. *Chem. Ber.* **1978,** *111,* 1591–1602. doi:10.1002/cber.19781110440
21. Hofmann, P. *Angew. Chem., Int. Ed. Engl.* **1979,** *18,* 554–556. doi:10.1002/anie.197905541
22. Gleiter, R.; Bartetzko, R.; Hofmann, P. *Z. Naturforsch., B* **1980,** *35,* 1166–1170.
23. Hofmann, P.; Albright, T. A. *Angew. Chem., Int. Ed. Engl.* **1980,** *19,* 728–729. doi:10.1002/anie.198007281
24. Jutzi, P.; Karl, A.; Hofmann, P. *Angew. Chem., Int. Ed. Engl.* **1980,** *19,* 484–485. doi:10.1002/anie.198004841
25. Jutzi, P.; Kohl, F.; Hofmann, P.; Krüger, C.; Tsay, Y. H. *Chem. Ber.* **1980,** *113,* 757–769. doi:10.1002/cber.19801130233
26. Gleiter, R.; Hofmann, P.; Schang, P.; Sieber, A. *Tetrahedron* **1980,** *36,* 655–659. doi:10.1016/0040-4020(80)88009-4
27. Albright, T. A.; Hofmann, P.; Rossi, A. R. *Z. Naturforsch., B* **1980,** *35,* 343–351.
28. Pinhas, A. R.; Albright, T. A.; Hofmann, P.; Hoffmann, R. *Helv. Chim. Acta* **1980,** *63,* 29–49. doi:10.1002/hlca.19800630105
29. Böhm, M. C.; Daub, J.; Gleiter, R.; Hofmann, P.; Lappert, M. F.; Öfele, K. *Chem. Ber.* **1980,** *113,* 3629–3646. doi:10.1002/cber.19801131121
30. Hofmann, P. *Fresenius' Z. Anal. Chem.* **1980,** *304,* 262–263. doi:10.1007/BF00488803
31. Koehler, F. H.; Hofmann, P.; Prössdorf, W. *J. Am. Chem. Soc.* **1981,** *103,* 6359–6367. doi:10.1021/ja00411a016
32. Schubert, U.; Neugebauer, D.; Hofmann, P.; Schilling, B. E. R.; Fischer, H.; Motsch, A. *Chem. Ber.* **1981,** *114,* 3349–3365. doi:10.1002/cber.19811141015
33. Beck, E.; Hofmann, P.; Sieber, A. *Tetrahedron Lett.* **1981,** *22,* 4683–4686. doi:10.1016/S0040-4039(01)83012-4
34. Jutzi, P.; Kohl, F.; Krüger, C.; Wolmershäuser, G.; Hofmann, P.; Stauffert, P. *Angew. Chem., Int. Ed. Engl.* **1982,** *21,* 70. doi:10.1002/anie.198200701
35. Hofmann, P.; Stauffert, P.; Schore, N. E. *Chem. Ber.* **1982,** *115,* 2153–2174. doi:10.1002/cber.19821150612
36. Ackermann, K.; Hofmann, P.; Koehler, F. H.; Kratzer, H.; Krist, H.; Ofele, K.; Schmidt, H. R. *Z. Naturforsch., B* **1983,** *38,* 1313–1324.
37. Werner, H.; Kraus, H.-J.; Schubert, U.; Ackermann, K.; Hofmann, P. *J. Organomet. Chem.* **1983,** *250,* 517–536. doi:10.1016/0022-328X(83)85075-X
38. Hofmann, P.; Padmanabhan, M. *Organometallics* **1983,** *2,* 1273–1284. doi:10.1021/om50004a002
39. Albright, T. A.; Hofmann, P.; Hoffmann, R.; Lillya, C. P.; Dobosh, P. A. *J. Am. Chem. Soc.* **1983,** *105,* 3396–3411. doi:10.1021/ja00349a004
40. Schore, N. E.; Young, S. J.; Olmstead, M. M.; Hofmann, P. *Organometallics* **1983,** *2,* 1769–1780. doi:10.1021/om50006a012
41. Hofmann, P.; Sieber, A.; Beck, E.; Schubert, U. *Z. Naturforsch., B* **1983,** *38,* 1192–1198.
42. Kohl, F. X.; Schlüter, E.; Jutzi, P.; Krüger, C.; Wolmershäuser, G.; Hofmann, P.; Stauffert, P. *Chem. Ber.* **1984,** *117,* 1178–1193. doi:10.1002/cber.19841170331
43. Köhler, F. H.; Geike, W. A.; Hofmann, P.; Schubert, U.; Stauffert, P. *Chem. Ber.* **1984,** *117,* 904–914. doi:10.1002/cber.19841170305
44. Nørskov-Lauritsen, L.; Bürgi, H.-B.; Hofmann, P.; Schmidt, H. R. *Helv. Chim. Acta* **1985,** *68,* 76–82. doi:10.1002/hlca.19850680110
45. Benn, R.; Cibura, K.; Hofmann, P.; Jonas, K.; Rufinska, A. *Organometallics* **1985,** *4,* 2214–2221. doi:10.1021/om00131a027
46. Kreissl, F. R.; Sieber, W. J.; Hofmann, P.; Riede, J.; Wolfgruber, M. *Organometallics* **1985,** *4,* 788–792. doi:10.1021/om00123a029
47. Kläui, W.; Schmidt, K.; Bockmann, A.; Hofmann, P.; Schmidt, H. R.; Stauffert, P. *J. Organomet. Chem.* **1985,** *286,* 407–418. doi:10.1016/0022-328X(85)80054-1
48. Hofmann, P.; Frede, M.; Stauffert, P.; Lasser, W.; Thewalt, U. *Angew. Chem., Int. Ed. Engl.* **1985,** *24,* 712–713. doi:10.1002/anie.198507121
49. Hofmann, P.; Stauffert, P.; Tatsumi, K.; Nakamura, A.; Hoffmann, R. *Organometallics* **1985,** *4,* 404–406. doi:10.1021/om00121a040
50. Tatsumi, K.; Nakamura, A.; Hofmann, P.; Stauffert, P.; Hoffmann, R. *J. Am. Chem. Soc.* **1985,** *107,* 4440–4451. doi:10.1021/ja00301a012
51. Gleiter, R.; Koppel, H.; Hofmann, P.; Schmidt, H. R.; Ellermann, J. *Inorg. Chem.* **1985,** *24,* 4020–4023. doi:10.1021/ic00218a012
52. Werner, H.; Ulrich, B.; Schubert, U.; Hofmann, P.; Zimmer-Gasser, B. *J. Organomet. Chem.* **1985,** *297,* 27–42. doi:10.1016/0022-328X(85)80394-6
53. Jutzi, P.; Hampel, B.; Stroppel, K.; Krüger, C.; Angermund, K.; Hofmann, P. *Chem. Ber.* **1985,** *118,* 2789–2797. doi:10.1002/cber.19851180720
54. Tatsumi, K.; Nakamura, A.; Hofmann, P.; Hoffmann, R.; Moloy, K. G.; Marks, T. J. *J. Am. Chem. Soc.* **1986,** *108,* 4467–4476. doi:10.1021/ja00275a037

55. Hofmann, P.; Rösch, N. *J. Chem. Soc., Chem. Commun.* **1986,** 843–844. doi:10.1039/C39860000843
56. Hofmann, P.; Perez Moya, L. A.; Kain, I. *Synthesis* **1986,** 43–44. doi:10.1055/s-1986-31470
57. Hofmann, P.; Beck, E.; Hoffmann, M. D.; Sieber, A. *Liebigs Ann. Chem.* **1986,** 1779–1786. doi:10.1002/jlac.198619861011
58. Hofmann, P.; Schmidt, H. R. *Angew. Chem., Int. Ed. Engl.* **1986,** *25,* 837–839. doi:10.1002/anie.198608371
59. Karsch, H. H.; Milewski-Mahrla, B.; Besenhard, J. O.; Hofmann, P.; Stauffert, P.; Albright, T. A. *Inorg. Chem.* **1986,** *25,* 3811–3821. doi:10.1021/ic00241a022
60. Hofmann, P.; Roesch, N.; Schmidt, H. R. *Inorg. Chem.* **1986,** *25,* 4470–4478. doi:10.1021/ic00245a006
61. Hofmann, P.; Heiss, H.; Mueller, G. *Z. Naturforsch., B* **1987,** *42,* 395–409.
62. Sieber, W. J.; Wolfgruber, M.; Tran-Huy, N. H.; Schmidt, H. R.; Heiss, H.; Hofmann, P.; Kreissl, F. R. *J. Organomet. Chem.* **1988,** *340,* 341–351. doi:10.1016/0022-328X(88)80027-5
63. Klein, H. F.; Helwig, M.; Koch, U.; Lull, G.; Tadic, M.; Krueger, C.; Hofmann, P. *Z. Naturforsch., B* **1988,** *43,* 1427–1438.
64. Hofmann, P.; Hämmerle, M. *Angew. Chem., Int. Ed. Engl.* **1989,** *28,* 908–910. doi:10.1002/anie.198909081
65. Hofmann, P.; Stauffert, P.; Frede, M.; Tatsumi, K. *Chem. Ber.* **1989,** *122,* 1559–1577. doi:10.1002/cber.19891220828
66. Hofmann, P.; Heiss, H.; Neiteler, P.; Müller, G.; Lachmann, J. *Angew. Chem., Int. Ed. Engl.* **1990,** *29,* 880–882. doi:10.1002/anie.199008801
67. Hofmann, P.; Perez Moya, L. A.; Krause, M. E.; Kumberger, O.; Mueller, G. *Z. Naturforsch., B* **1990,** *45,* 897–908.
68. Hofmann, P.; Haemmerle, M.; Unfried, G. *New J. Chem.* **1991,** *15,* 769–789.
69. Herberich, G. E.; Englert, U.; Wesemann, L.; Hofmann, P. *Angew. Chem., Int. Ed. Engl.* **1991,** *30,* 313–315. doi:10.1002/anie.199103131
70. Hofmann, P.; Perez-Moya, L. A.; Steigelmann, O.; Riede, J. *Organometallics* **1992,** *11,* 1167–1176. doi:10.1021/om00039a024
71. Hofmann, P.; Meier, C.; Englert, U.; Schmidt, M. U. *Chem. Ber.* **1992,** *125,* 353–365. doi:10.1002/cber.19921250212
72. Hofmann, P.; Unfried, G. *Chem. Ber.* **1992,** *125,* 659–661. doi:10.1002/cber.19921250319
73. Helm, S. W.; Linti, G.; Nöth, H.; Channareddy, S.; Hofmann, P. *Chem. Ber.* **1992,** *125,* 73–86. doi:10.1002/cber.19921250113
74. Beckhaus, R.; Flatau, S.; Trojanov, S.; Hofmann, P. *Chem. Ber.* **1992,** *125,* 291–299. doi:10.1002/cber.19921250204
75. Albinati, A.; Eckert, J.; Hofmann, P.; Rüegger, H.; Venanzi, L. M. *Inorg. Chem.* **1993,** *32,* 2377–2390. doi:10.1021/ic00063a029
76. Filippou, A. C.; Hofmann, P.; Kiprof, P.; Schmidt, H. R.; Wagner, C. *J. Organomet. Chem.* **1993,** *459,* 233–247. doi:10.1016/0022-328X(93)86076-T
77. Blümel, J.; Hofmann, P.; Köhler, F. H. *Magn. Reson. Chem.* **1993,** *31,* 2–6. doi:10.1002/mrc.1260310103
78. Herberich, G. E.; Englert, U.; Marken, F.; Hofmann, P. *Organometallics* **1993,** *12,* 4039–4045. doi:10.1021/om00034a041
79. Seyferth, D.; Hoke, J. B.; Dewan, J. C.; Hofmann, P.; Schnellbach, M. *Organometallics* **1994,** *13,* 3452–3464. doi:10.1021/om00021a020
80. Hofmann, P.; Meier, C.; Hiller, W.; Heckel, M.; Riede, J.; Schmidt, M. U. *J. Organomet. Chem.* **1995,** *498,* C29. doi:10.1016/0022-328X(95)05682-F
81. Hofmann, P.; Meier, C.; Hiller, W.; Heckel, M.; Riede, J.; Schmidt, M. U. *J. Organomet. Chem.* **1995,** *490,* 51–70. doi:10.1016/0022-328X(94)05173-9
82. Leoni, P.; Pasquali, M.; Fadini, L.; Albinati, A.; Hofmann, P.; Metz, M. *J. Am. Chem. Soc.* **1997,** *119,* 8625–8629. doi:10.1021/ja970262+
83. Ward, T. R.; Schafer, O.; Daul, C.; Hofmann, P. *Organometallics* **1997,** *16,* 3207–3215. doi:10.1021/om9700369
84. Straub, B. F.; Hofmann, P. *Inorg. Chem. Commun.* **1998,** *1,* 350–353. doi:10.1016/S1387-7003(98)00099-9
85. Lippmann, E.; Kerscher, T.; Aechter, B.; Robl, C.; Beck, W.; Price, D. W.; Metz, M.; Hofmann, P. *J. Organomet. Chem.* **1998,** *556,* 207–217. doi:10.1016/S0022-328X(97)00718-3
86. Hansen, S. M.; Rominger, F.; Metz, M.; Hofmann, P. *Chem. – Eur. J.* **1999,** *5,* 557–566. doi:10.1002/(SICI)1521-3765(19990201)5:2<557::AID-CHEM557>3.0.CO;2-A
87. Hansen, S. M.; Volland, M. A. O.; Rominger, F.; Eisenträger, F.; Hofmann, P. *Angew. Chem., Int. Ed.* **1999,** *38,* 1273–1276. doi:10.1002/(SICI)1521-3773(19990503)38:9<1273::AID-ANIE1273>3.0.CO;2-0
88. Fischer, H.; Hofmann, P. *Organometallics* **1999,** *18,* 2590–2592. doi:10.1021/om980958r
89. Straub, B. F.; Eisenträger, F.; Hofmann, P. *Chem. Commun.* **1999,** 2507–2508. doi:10.1039/a907928i
90. Hofmann, P.; Volland, M. A. O.; Hansen, S. M.; Eisenträger, F.; Gross, J. H.; Stengel, K. *J. Organomet. Chem.* **2000,** *606,* 88–92. doi:10.1016/S0022-328X(00)00288-6
91. Adlhart, C.; Volland, M. A. O.; Hofmann, P.; Chen, P. *Helv. Chim. Acta* **2000,** *83,* 3306–3311. doi:10.1002/1522-2675(20001220)83:12<3306::AID-HLCA3306>3.0.CO;2-7
92. Straub, B. F.; Rominger, F.; Hofmann, P. *Organometallics* **2000,** *19,* 4305–4309. doi:10.1021/om000430y
93. Straub, B. F.; Rominger, F.; Hofmann, P. *Inorg. Chem. Commun.* **2000,** *3,* 214–217. doi:10.1016/S1387-7003(00)00043-5
94. Straub, B. F.; Rominger, F.; Hofmann, P. *Inorg. Chem.* **2000,** *39,* 2113–2119. doi:10.1021/ic991173w
95. Straub, B. F.; Rominger, F.; Hofmann, P. *Chem. Commun.* **2000,** 1611–1612. doi:10.1039/b004173o
96. Hofmann, P.; Meier, C.; Maier, A.; Steck, O.; Sporys, V.; Rominger, F. *Z. Kristallogr. - New Cryst. Struct.* **2000,** *215,* 609–614. doi:10.1515/ncrs-2000-0466
97. Straub, B. F.; Rominger, F.; Hofmann, P. *Inorg. Chem. Commun.* **2000,** *3,* 358–360. doi:10.1016/S1387-7003(00)00098-8
98. Volland, M. A. O.; Adlhart, C.; Kiener, C. A.; Chen, P.; Hofmann, P. *Chem. – Eur. J.* **2001,** *7,* 4621–4632. doi:10.1002/1521-3765(20011105)7:21<4621::AID-CHEM4621>3.0.CO;2-C
99. Volland, M. A. O.; Straub, B. F.; Gruber, I.; Rominger, F.; Hofmann, P. *J. Organomet. Chem.* **2001,** *617,* 288–291. doi:10.1016/S0022-328X(00)00598-2
100. Volland, M. A. O.; Hofmann, P. *Helv. Chim. Acta* **2001,** *84,* 3456–3469. doi:10.1002/1522-2675(20011114)84:11<3456::AID-HLCA3456>3.0.CO;2-P
101. Urtel, H.; Bikzhanova, G. A.; Grotjahn, D. B.; Hofmann, P. *Organometallics* **2001,** *20,* 3938–3949. doi:10.1021/om010503t

102. Straub, B. F.; Hofmann, P. *Angew. Chem., Int. Ed.* **2001,** *40,* 1288–1290. doi:10.1002/1521-3773(20010401)40:7<1288::AID-ANIE1288>3.0.CO;2-6
103. Urtel, H.; Meier, C.; Eisenträger, F.; Rominger, F.; Joschek, J. P.; Hofmann, P. *Angew. Chem., Int. Ed.* **2001,** *40,* 781–784. doi:10.1002/1521-3773(20010216)40:4<781::AID-ANIE7810>3.0.CO;2-T
104. Volland, M. A. O.; Rominger, F.; Eisenträger, F.; Hofmann, P. *J. Organomet. Chem.* **2002,** *641,* 220–226. doi:10.1016/S0022-328X(01)01361-4
105. Schultz, M.; Straub, B. F.; Hofmann, P. *Acta Crystallogr., Sect. C: Cryst. Struct. Commun.* **2002,** *58,* M256–M257. doi:10.1107/S0108270102002706
106. Straub, B. F.; Gruber, I.; Rominger, F.; Hofmann, P. *J. Organomet. Chem.* **2003,** *684,* 124–143. doi:10.1016/S0022-328X(03)00520-5
107. Eisenträger, F.; Göthlich, A.; Gruber, I.; Heiss, H.; Kiener, C. A.; Krüger, C.; Notheis, J. U.; Rominger, F.; Scherhag, G.; Schultz, M.; Straub, B. F.; Volland, M. A. O.; Hofmann, P. *New J. Chem.* **2003,** *27,* 540–550. doi:10.1039/b210114a
108. Volland, M. A. O.; Hansen, S. M.; Rominger, F.; Hofmann, P. *Organometallics* **2004,** *23,* 800–816. doi:10.1021/om030655j
109. Gross, J. H.; Nieth, N.; Linden, H. B.; Blumbach, U.; Richter, F. J.; Tauchert, M. E.; Tompers, R.; Hofmann, P. *Anal. Bioanal. Chem.* **2006,** *386,* 52–58. doi:10.1007/s00216-006-0524-0
110. Deglmann, P.; Ember, E.; Hofmann, P.; Pitter, S.; Walter, O. *Chem. – Eur. J.* **2007,** *13,* 2864–2879. doi:10.1002/chem.200600396
111. Messaoudi, A.; Deglmann, P.; Braunstein, P.; Hofmann, P. *Inorg. Chem.* **2007,** *46,* 7899–7909. doi:10.1021/ic700761e
112. Fernández, P.; Pritzkow, H.; Carbó, J. J.; Hofmann, P.; Enders, M. *Organometallics* **2007,** *26,* 4402–4412. doi:10.1021/om070173y
113. Hofmann, P.; Shishkov, I. V.; Rominger, F. *Inorg. Chem.* **2008,** *47,* 11755–11762. doi:10.1021/ic801443y
114. Göthlich, A. P. V.; Tensfeldt, M.; Rothfuss, H.; Tauchert, M. E.; Haap, D.; Rominger, F.; Hofmann, P. *Organometallics* **2008,** *27,* 2189–2200. doi:10.1021/om701140c
115. Crewdson, P.; Bryce, D. L.; Rominger, F.; Hofmann, P. *Angew. Chem., Int. Ed.* **2008,** *47,* 3454–3457. doi:10.1002/anie.200705204
116. Schnetz, T.; Röder, M.; Rominger, F.; Hofmann, P. *Dalton Trans.* **2008,** 2238–2240. doi:10.1039/b802684j
117. Richmond, J. P.; Banwell, M.; Bellus, D.; Muniz, K.; Narasaka, K.; Okamoto, Y.; Okuda, J.; Schlosser, M.; Shinkai, I.; Tatsuta, K.; van Koten, G.; You, X.-Z.; Aggarwal, V. K.; Aida, T.; Alper, H.; Bai, C.; Bhattacharyya, K.; Blaser, H.-U.; Pugin, B.; Spindler, F.; Brown, J. M.; Buchwald, S. L.; Chan, A. S. C.; Chatani, N.; Denmark, S. E.; Diederich, F.; Doyle, M. P.; Fu, G.; Fujishima, A.; Hanessian, S.; Hashimoto, S.; Hayashi, M.; Hiyama, T.; Hofmann, P.; Hou, Z.; Imamoto, T.; Izawa, K.; Jacobsen, E.; Katsuki, T.; Kim, S.; Kobayashi, S.; Komatsu, K.; Kumobayashi, H.; Kuendig, E. P.; Lee, E.; Leitner, W.; Ley, S. V.; Lipshutz, B.; Yixin, L.; Maruoka, K.; Murahashi, S.-I.; Murai, S.; Nicolaou, K. C.; Nishiyama, H.; Ohkuma, T.; Ohta, T.; Oshima, K.; Otera, J.; Pfaltz, A.; Reetz, M. T.; Ricci, A.; Sawamoto, M.; Scalone, M.; Sharpless, K. B.; Sheldon, R.; Snieckus, V.; Sodeoka, M.; Tokunaga, M.; Tomioka, K.; Umezawa, Y.; Uozumi, Y.; Wong, C.-H.; Wong, H. N. C.; Yamamoto, Y.; Zhu, D. *Adv. Synth. Catal.* **2008,** *350,* 1925–1941.
118. Shishkov, I. V.; Rominger, F.; Hofmann, P. *Organometallics* **2009,** *28,* 3532–3536. doi:10.1021/om801097f
119. Shishkov, I. V.; Rominger, F.; Hofmann, P. *Organometallics* **2009,** *28,* 1049–1059. doi:10.1021/om8007376
120. Shishkov, I. V.; Rominger, F.; Hofmann, P. *Dalton Trans.* **2009,** 1428–1435. doi:10.1039/b813790k
121. Schneider, N.; Finger, M.; Haferkemper, C.; Bellemin-Laponnaz, S.; Hofmann, P.; Gade, L. H. *Chem. – Eur. J.* **2009,** *15,* 11515–11529. doi:10.1002/chem.200901594
122. Schneider, N.; Finger, M.; Haferkemper, C.; Bellemin-Laponnaz, S.; Hofmann, P.; Gade, L. H. *Angew. Chem., Int. Ed.* **2009,** *48,* 1609–1613. doi:10.1002/anie.200804993
123. Tauchert, M. E.; Kaiser, T. R.; Göthlich, A. P. V.; Rominger, F.; Warth, D. C. M.; Hofmann, P. *ChemCatChem* **2010,** *2,* 674–682. doi:10.1002/cctc.201000022
124. Urtel, H.; Meier, C.; Rominger, F.; Hofmann, P. *Organometallics* **2010,** *29,* 5496–5503. doi:10.1021/om100413m
125. Schnetz, T.; Rominger, F.; Hofmann, P. *Acta Crystallogr., Sect. E: Struct. Rep. Online* **2010,** *66,* m453–n454. doi:10.1107/S1600536810010263
126. Smith, S. E.; Rosendahl, T.; Hofmann, P. *Organometallics* **2011,** *30,* 3643–3651. doi:10.1021/om200334g
127. Tauchert, M. E.; Warth, D. C. M.; Braun, S. M.; Gruber, I.; Ziesak, A.; Rominger, F.; Hofmann, P. *Organometallics* **2011,** *30,* 2790–2809. doi:10.1021/om200164f
128. Schultz, M.; Eisenträger, F.; Regius, C.; Rominger, F.; Hanno-Igels, P.; Jakob, P.; Gruber, I.; Hofmann, P. *Organometallics* **2012,** *31,* 207–224. doi:10.1021/om200715w
129. Kühnel, E.; Shishkov, I. V.; Rominger, F.; Oeser, T.; Hofmann, P. *Organometallics* **2012,** *31,* 8000–8011. doi:10.1021/om300701u
130. Lejkowski, M. L.; Lindner, R.; Kageyama, T.; Bódizs, G. É.; Plessow, P. N.; Müller, I. B.; Schäfer, A.; Rominger, F.; Hofmann, P.; Futter, C.; Schunk, S. A.; Limbach, M. *Chem. – Eur. J.* **2012,** *18,* 14017–14025. doi:10.1002/chem.201201757
131. Nägele, P.; Herrlich (neé Blumbach), U.; Rominger, F.; Hofmann, P. *Organometallics* **2013,** *32,* 181–191. doi:10.1021/om300963t
132. Salem, H.; Schmitt, M.; Herrlich (née Blumbach), U.; Kühnel, E.; Brill, M.; Nägele, P.; Bogado, A. L.; Rominger, F.; Hofmann, P. *Organometallics* **2013,** *32,* 29–46. doi:10.1021/om300487r
133. Brill, M.; Kühnel, E.; Scriban, C.; Rominger, F.; Hofmann, P. *Dalton Trans.* **2013,** *42,* 12861–12864. doi:10.1039/c3dt51777b
134. Wetzel, A.; Wöckel, S.; Schelwies, M.; Brinks, M. K.; Rominger, F.; Hofmann, P.; Limbach, M. *Org. Lett.* **2013,** *15,* 266–269. doi:10.1021/ol303075h
135. Schmidt, S.; Abkai, G.; Rosendahl, T.; Rominger, F.; Hofmann, P. *Organometallics* **2013,** *32,* 1044–1052. doi:10.1021/om301027x
136. Plessow, P. N.; Weigel, L.; Lindner, R.; Schäfer, A.; Rominger, F.; Limbach, M.; Hofmann, P. *Organometallics* **2013,** *32,* 3327–3338. doi:10.1021/om400262b
137. Chalkley, M. J.; Guard, L. M.; Hazari, N.; Hofmann, P.; Hruszkewycz, D. P.; Schmeier, T. J.; Takase, M. K. *Organometallics* **2013,** *32,* 4223–4238. doi:10.1021/om400415c
138. Brown, C. C.; Plessow, P. N.; Rominger, F.; Limbach, M.; Hofmann, P. *Organometallics* **2014,** *33,* 6754–6759. doi:10.1021/om5005429
139. Ye, X.; Plessow, P. N.; Brinks, M. K.; Schelwies, M.; Schaub, T.; Rominger, F.; Paciello, R.; Limbach, M.; Hofmann, P. *J. Am. Chem. Soc.* **2014,** *136,* 5923–5929. doi:10.1021/ja409368a
140. Brendel, M.; Braun, C.; Rominger, F.; Hofmann, P. *Angew. Chem., Int. Ed.* **2014,** *53,* 8741–8745. doi:10.1002/anie.201401024

141. Wöckel, S.; Plessow, P.; Schelwies, M.; Brinks, M. K.; Rominger, F.; Hofmann, P.; Limbach, M. *ACS Catal.* **2014,** *4,* 152–161. doi:10.1021/cs4009418
142. Abkai, G.; Schmidt, S.; Rosendahl, T.; Rominger, F.; Hofmann, P. *Organometallics* **2014,** *33,* 3212–3214. doi:10.1021/om401139u
143. Plessow, P. N.; Schäfer, A.; Limbach, M.; Hofmann, P. *Organometallics* **2014,** *33,* 3657–3668. doi:10.1021/om500151h
144. Huguet, N.; Jevtovikj, I.; Gordillo, A.; Lejkowski, M. L.; Lindner, R.; Bru, M.; Khalimon, A. Y.; Rominger, F.; Schunk, S. A.; Hofmann, P.; Limbach, M. *Chem. – Eur. J.* **2014,** *20,* 16858–16862. doi:10.1002/chem.201405528
145. Schmidt, S.; Baráth, E.; Prommnitz, T.; Rosendahl, T.; Rominger, F.; Hofmann, P. *Organometallics* **2014,** *33,* 6018–6022. doi:10.1021/om500643t
146. Schmidt, S.; Deglmann, P.; Hofmann, P. *ACS Catal.* **2014,** *4,* 3593–3604. doi:10.1021/cs500718v
147. Brown, C. C.; Rominger, F.; Limbach, M.; Hofmann, P. *Inorg. Chem.* **2015,** *54,* 10126–10140. doi:10.1021/acs.inorgchem.5b00513
148. Brill, M.; Marrwitz (née Eisenhauer), D.; Rominger, F.; Hofmann, P. *J. Organomet. Chem.* **2015,** *775,* 137–151. doi:10.1016/j.jorganchem.2014.04.008
149. Plessow, P. N.; Carbo, J. J.; Schaefer, A.; Hofmann, P. *Organometallics* **2015,** *34,* 3764–3773. doi:10.1021/acs.organomet.5b00435
150. Brendel, M.; Engelke, R.; Desai, V. G.; Rominger, F.; Hofmann, P. *Organometallics* **2015,** *34,* 2870–2878. doi:10.1021/acs.organomet.5b00204
151. Brendel, M.; Wenz, J.; Shishkov, I. V.; Rominger, F.; Hofmann, P. *Organometallics* **2015,** *34,* 669–672. doi:10.1021/om501229b
152. Schmidt, S.; Baráth, E.; Larcher, C.; Rosendahl, T.; Hofmann, P. *Organometallics* **2015,** *34,* 841–847. doi:10.1021/om501015z
153. Stieber, S. C. E.; Huguet, N.; Kageyama, T.; Jevtovikj, I.; Ariyananda, P.; Gordillo, A.; Schunk, S. A.; Rominger, F.; Hofmann, P.; Limbach, M. *Chem. Commun.* **2015,** *51,* 10907–10909. doi:10.1039/C5CC01932J
154. Brill, M.; Rominger, F.; Hofmann, P. *Organometallics* **2015,** *34,* 506–521. doi:10.1021/om501145b
155. Mormul, J.; Mulzer, M.; Rosendahl, T.; Rominger, F.; Limbach, M.; Hofmann, P. *Organometallics* **2015,** *34,* 4102–4108. doi:10.1021/acs.organomet.5b00538

License and Terms

This is an Open Access article under the terms of the Creative Commons Attribution License (http://creativecommons.org/licenses/by/4.0), which permits unrestricted use, distribution, and reproduction in any medium, provided the original work is properly cited.

The license is subject to the *Beilstein Journal of Organic Chemistry* terms and conditions: (http://www.beilstein-journals.org/bjoc)

The definitive version of this article is the electronic one which can be found at: doi:10.3762/bjoc.12.213

BEILSTEIN JOURNAL OF ORGANIC CHEMISTRY

A modular approach to neutral P,N-ligands: synthesis and coordination chemistry

Vladislav Vasilenko‡, Torsten Roth‡, Clemens K. Blasius, Sebastian N. Intorp, Hubert Wadepohl and Lutz H. Gade*

Full Research Paper

Open Access

Address:
Anorganisch-Chemisches Institut, Universität Heidelberg, Im Neuenheimer Feld 270, 69120 Heidelberg, Germany

Email:
Lutz H. Gade* - lutz.gade@uni-heidelberg.de

* Corresponding author ‡ Equal contributors

Keywords:
P,N-ligands; phosphanylformamidines; phosphine imines; transition metal complexes

Beilstein J. Org. Chem. **2016,** *12,* 846–853.
doi:10.3762/bjoc.12.83

Received: 11 February 2016
Accepted: 12 April 2016
Published: 29 April 2016

This article is part of the Thematic Series "Organometallic chemistry". Dedicated to the memory of Peter Hofmann.

Guest Editor: B. F. Straub

© 2016 Vasilenko et al; licensee Beilstein-Institut.
License and terms: see end of document.

Abstract

We report the modular synthesis of three different types of neutral κ^2-P,N-ligands comprising an imine and a phosphine binding site. These ligands were reacted with rhodium, iridium and palladium metal precursors and the structures of the resulting complexes were elucidated by means of X-ray crystallography. We observed that subtle changes of the ligand backbone have a significant influence on the binding geometry und coordination properties of these bidentate P,N-donors.

Introduction

P,N-ligands have been applied in a wide variety of chemical reactions ranging from hydrogenations [1,2] and allylic substitutions [3,4] to Heck reactions [5] and conjugate additions to enones [6]. Their popularity arises from the inherent electronic disparity of the phosphorus and the nitrogen donor groups, rendering one binding site a soft π-acceptor featuring a pronounced *trans* effect and the other site a hard σ-donor [7]. In addition, the steric and electronic properties of both donor groups can in principle be varied separately, rendering modular construction approaches particularly appealing [8].

Driven by our recent efforts to provide easily accessible, modular ligand families [9,10], we have explored three different possibilities to expand the portfolio of P,N-ligands (**L1**–**L3**, Figure 1). We reasoned that suitable candidates should be accessible on a multigram scale in excellent yields starting from commercially available reagents and ideally involving a maximum of two steps. In addition, the resulting ligand families

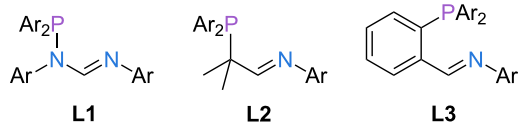


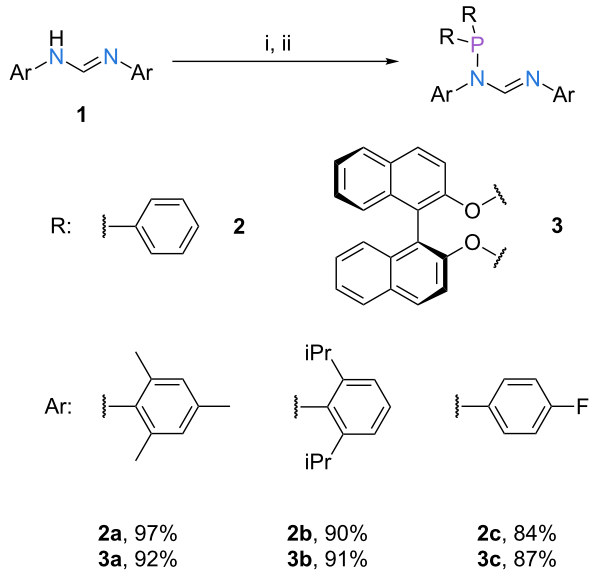
Figure 1: P,N-ligand frameworks studied in this work.

should provide nitrogen and phosphorus donors with varying donor strength (amidine vs imine, phosphine vs heteroatom-bound phosphorus) and different bite angles (five- vs six-membered chelate rings).

Results and Discussion

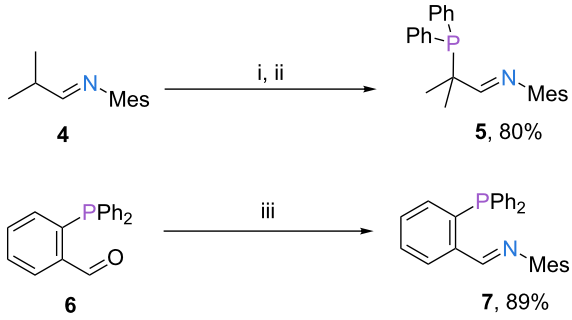
Ligand synthesis

We based the preparation of the ligand systems **L1**–**L3** on a simple construction principle, i.e., only reactions of carbon- or nitrogen-nucleophiles with chlorophosphines, and condensations of amines with aldehydes were employed. For the synthesis of the *N*-phosphanylformamidine derivatives **2** and **3** we prepared a set of three aromatic formamidines (**1a**–**c**) starting from triethyl orthoformate and aromatic amines. Low-temperature lithiation of **1** and addition to achiral (R = Ph) and axially chiral (R_2 = BINOL) chlorophosphines R_2PCl gave ligands **2** and **3** in excellent yields (Scheme 1) [11]. If the correct stoichiometry is maintained throughout the reaction, the resulting mixtures do not require a purification step beyond a filtration from toluene or hexane to remove residual lithium chloride. As has been pointed out by Dyer et al. for the structurally related *N*-phosphanylamidines, there are several distinct conformers of ligands **2a**–**c** and **3a**–**c** that can exist in solution, depending on the orientation of the phosphorus lone pair, the geometry of the C=N double bond and the orientation of the substituents of the C–N single bond [12]. Notably, all synthesized derivatives feature a single signal in the ^{31}P NMR spectrum at room temperature, indicating that a relatively fast interconversion of the different conformers occurs at ambient conditions. However, with increasing steric bulk of the aromatic nitrogen substituents, a substantial line broadening is observed, indicating the rise of the isomerization barrier through steric repulsion of the neighboring groups [11].



Scheme 1: Synthesis of *N*-phosphanylformamidines **2** and **3**. Reaction conditions: (i) *t*-BuLi, THF, −78 °C to rt, 1 h; (ii) R_2PCl, THF, −78 °C to rt, overnight.

The methodology for the synthesis of compounds **2** and **3** was also applied to the preparation of phosphine imine ligand **5**. Instead of a formamidine precursor, imine **4** was employed as the nucleophile. Deprotonation of **4** at low temperature and addition of the resulting C-nucleophile to chlorodiphenylphosphine gave the desired product in good yield (Scheme 2) [13]. This modification renders the phosphorus donor site more electron rich and also results in a more robust P–C bond compared to ligands **2** and **3**.



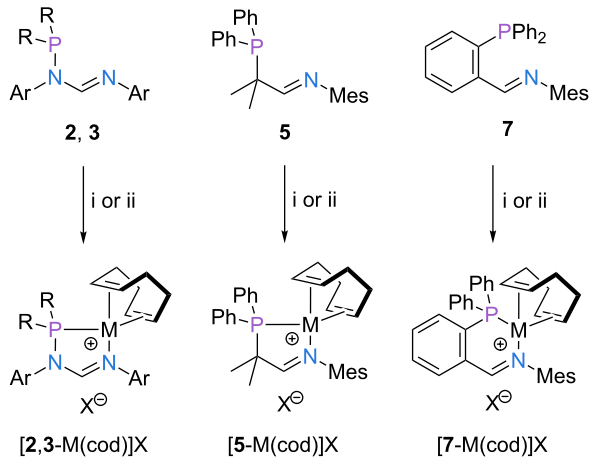
Scheme 2: Synthesis of phosphanylformamidines **5** and **7**. Reaction conditions: (i) *t*-BuLi, THF, −78 °C to rt, 1 h; (ii) Ph_2PCl, THF, −78 °C to rt, overnight; (iii) NH_2Mes, toluene, 135 °C, 20 h.

For the preparation of ligand **7** the order of bond formations of the previous protocols was reversed, that means, the carbon–nitrogen bond was formed in the second step of the synthesis. Condensation of aldehyde **6** with mesitylamine gave ligand **7** in good yield [14-16].

The connectivity of the ligands **2**, **3**, **5** and **7** imposes a varying level of rigidity on these bidentate donors, with distinct consequences for their coordination chemistry (vide infra).

Complex synthesis

In the next step of our study we set out to explore the coordination chemistry and structural properties of the synthesized ligands with rhodium(I/III), iridium(I/III) and palladium(II) precursors. Reaction of ligands **2** and **3** with (i) preformed $[Rh(cod)_2]BF_4$ and (ii) stoichiometric amounts of $[Ir(cod)Cl]_2$ in the presence of $AgBF_4$ gave the corresponding rhodium(I) and iridium(I) complexes [**2**,**3**-M(cod)]BF_4 in good to excellent yields (Scheme 3). In a similar fashion, analogous complexes of ligands **5** and **7** were prepared.



Scheme 3: Synthesis of complexes [**2**-M(cod)]X, [**3**-M(cod)]X, [**5**-M(cod)]X and [**7**-M(cod)]X. M = Rh, Ir; X = BF_4^- or OTf^-. Reaction conditions: (i) $[Rh(cod)_2]BF_4$, DCM, rt, 30 min; (ii) $[Ir(cod)Cl]_2$, $AgBF_4$ or AgOTf, DCM, rt, 30 min. Ar = mesityl, 2,6-diisopropylphenyl, 4-fluorophenyl; R = phenyl or BINOL. Yields: [**2a**-Rh(cod)]BF_4 = 85%, [**2b**-Rh(cod)]BF_4 = 75%, [**2c**-Rh(cod)]BF_4 = 88%, [**3a**-Rh(cod)]BF_4 = 74%, [**3b**-Rh(cod)]BF_4 = 90%, [**3c**-Rh(cod)]BF_4 = 81%, [**2a**-Ir(cod)]BF_4 = 77%, [**2b**-Ir(cod)]BF_4 = 80%, [**2c**-Ir(cod)]BF_4 = 88%, [**3a**-Ir(cod)]BF_4 = 65%, [**3b**-Ir(cod)]BF_4 = 81%, [**3c**-Ir(cod)]BF_4 = 82%, [**5**-Rh(cod)]BF_4 = 52%, [**5**-Ir(cod)]OTf = 67%, [**7**-Rh(cod)]BF_4 = 92%, [**7**-Ir(cod)]BF_4 = 85%.

It should be noted that ligands **2**, **5**, and **7** feature a distinct shift of the ^{31}P NMR resonance to lower fields upon complexation of a rhodium(I) or iridium(I) center, whereas a shift to higher fields is observed for ligand **3** [11]. We were able to obtain single crystals of compounds [**2a**-Rh(cod)]BF_4, [**2b**-Rh(cod)]BF_4, of the corresponding iridium complexes and of complexes [**5**-Rh(cod)]BF_4, [**5**-Ir(cod)]OTf and [**7**-Rh(cod)]BF_4 suitable for X-ray analysis by layering solutions of the complexes in dichloromethane with toluene and pentane. Instructive examples of the structural properties of selected complexes are illustrated in Figure 2. An overview of characteristic bonding properties of all crystallized compounds can be found in Table 1.

The five-membered metallacyclic derivatives of ligands **2** and **5** feature an almost planar κ^2-P,N chelate ring with bite angles of approx. 81–82°. Notably, increasing the number of atoms that are part of the chelate ring leads to a slightly folded structure with only minor changes in the bite angle (87°). The nitrogen-attached aryl substituent typically displays an orientation which is perpendicular to the plane of the metallacycle [17]. The P–M bond lengths in all complexes are within the expected range of 2.23–2.27 Å, as are the metal−imine bonds (2.08–2.15 Å) [18,19]. The close structural resemblance between the rhodium

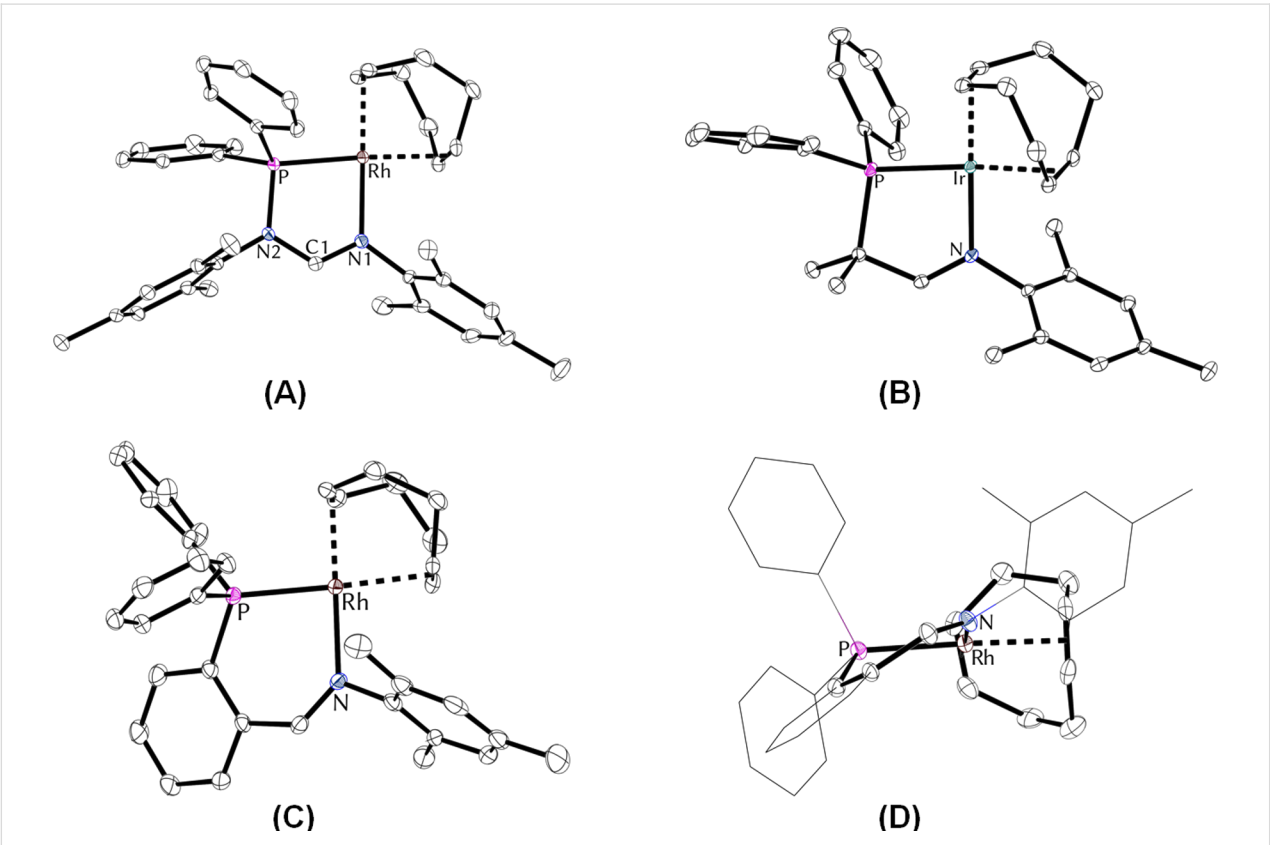


Figure 2: Molecular structures of [**2a**-Rh(cod)]$^+$ (A), [**5**-Ir(cod)]$^+$ (B), and [**7**-Rh(cod)]$^+$ (C,D). Anisotropic displacement ellipsoids are set at the 50% probability level. Hydrogen atoms have been omitted for clarity. For selected bond lengths and angles see Table 1.

Table 1: Selected structural parameters of the crystallized complexes[a].

	P–M [Å]	N–M [Å]	α[b] [°]	β[c] [°]
[**2a**-Rh(cod)]BF_4	2.2338(10) [2.2351(10)]	2.0890(19) [2.0885(19)]	122.25(19) [122.35(19)]	81.69(5) [81.60(5)]
[**2b**-Rh(cod)]BF_4	2.2487(10) [2.2452(10)]	2.0981(18) [2.0907(18)]	122.57(17) [122.55(17)]	81.42(5) [81.75(5)]
[**2a**-Ir(cod)]BF_4	2.2447(18) [2.2389(17)]	2.083(6) [2.082(6)]	122.4(7) [122.3(6)]	81.49(16) [81.94(16)]
[**2b**-Ir(cod)]BF_4	2.2522(7) [2.2473(7)]	2.088(2) [2.080(2)]	123.1(3) [122.9(3)]	81.83(7) [81.89(7)]
[**5**-Rh(cod)]BF_4	2.2580(10)	2.1128(12)	122.24(11)	81.49(3)
[**5**-Ir(cod)]OTf	2.2698(9)	2.1087(15)	122.33(13)	81.59(4)
[**7**-Rh(cod)]BF_4	2.2653(12) [2.2587(12), 2.2654(12)]	2.131(4) [2.129(4), 2.155(4)]	129.1(4) [128.9(4), 130.0(4)]	86.65(10) [87.32(10), 87.66(10)]

[a]Where applicable, values for crystallographically independent molecules are provided in square brackets. [b]α Denotes the N–C–N angle (complexes derived from ligands **2**) or the N–C–C angle (complexes derived from ligands **5** and **7**), respectively. [c]β Denotes the N–M–P angle.

and iridium complexes is notable and can be attributed to the similar atomic radii of these metals [20].

Moreover, the N–C–N angles of the formamidine unit closely resemble those found in related amidinium salts, thus indicating that no significant ring strain is present. The M−C_{cod} bonds located *trans* to the P atoms are slightly longer (av 2.11 Å) than the M−C_{cod} bonds *trans* to the imino group (av 2.04 Å), suggesting a dominant *trans* influence of the phosphorus donor function compared to the imino group. The differing bond lengths within the N−C−N unit (mean 1.30 vs 1.35 Å) may indicate little or no delocalization of the positive charge via the metallacycle. Remarkably, introduction of the sterically more demanding 2,6-di(isopropyl)phenyl group as the *N*-aryl substituent induced only slight structural changes (complexes of ligand **2a** vs **2b**), mostly in the orientation of the phenyl rings of the phosphorus donor and the position of the cyclooctadiene co-ligand.

To further explore the binding properties of the P,N-ligand scaffold, ligands **2a** and **5** were reacted with the Lewis-acidic precursors $[Cp^*RhCl_2]_2$ and $[Cp^*IrI_2]_2$ (Figure 3). As has been pointed out for the analogous Rh(I) and Ir(I) compounds, complexation is accompanied by a ^{31}P NMR shift to lower fields (from 49.7 ppm to 108.9 ppm and 80.6 ppm for the Rh(III) and Ir(III) complexes of **2a**, respectively). The structures of [**2a**-Cp*IrI]BF_4, and [**5**-Cp*IrI]BF_4 were confirmed unambiguously by single-crystal X-ray diffraction. The solid-state structure of [**2a**-Cp*IrI]BF_4 confirms the tetrahedral environment of the iridium center, rendering the two faces of the complex inequivalent (Figure 4, left). Similar findings were made for complex [**5**-Cp*IrI]BF_4 (Figure 4, right). This is also reflected in the NMR spectra of both complexes, featuring a distinct set of resonances for each methyl group of the mesityl substituent.

Despite the changes in the oxidation state of the metal center, only subtle deviations in the bond lengths of the chelate ligands were observed upon going from the Ir(I) to the Ir(III) complexes (in complexes of ligand **2a**: avg. 2.418 Å to 2.270 Å for the P–Ir bond and 2.083 Å to 2.132 Å for the N–Ir bond; in complexes of ligand **5**: 2.270 Å to 2.305 Å for the P–Ir bond and 2.109 Å to 2.136 Å for the N–Ir bond). Similarly, no major structural changes of the ligand backbone were detected for the different oxidation states.

Furthermore, due to the importance of palladium in common transition-metal-catalyzed transformations [21], we decided to explore the reactivity of the three P,N-ligand families with the widely used precursors $[Pd(cod)Cl_2]$ and $[Pd(allyl)Cl]_2$ (Figure 5). Addition of ligand **2a** to a solution of $[Pd(cod)Cl_2]$ in DCM gave complex [**2a**-$PdCl_2$] in good yield. In the presence of $AgBF_4$ complex [**2a**-$PdCl_2$] was converted to the

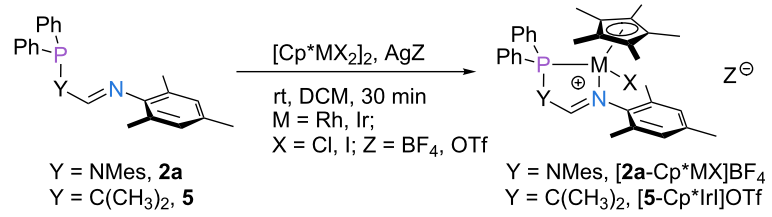


Figure 3: Coordination of ligands **2a** and **5** to Rh(III) and Ir(III) precursors. Yields: [**2a**-Cp*RhCl]BF_4 = 87%, [**2a**-Cp*IrI]BF_4 = 76%, [5-Cp*IrI]OTf = 80%.

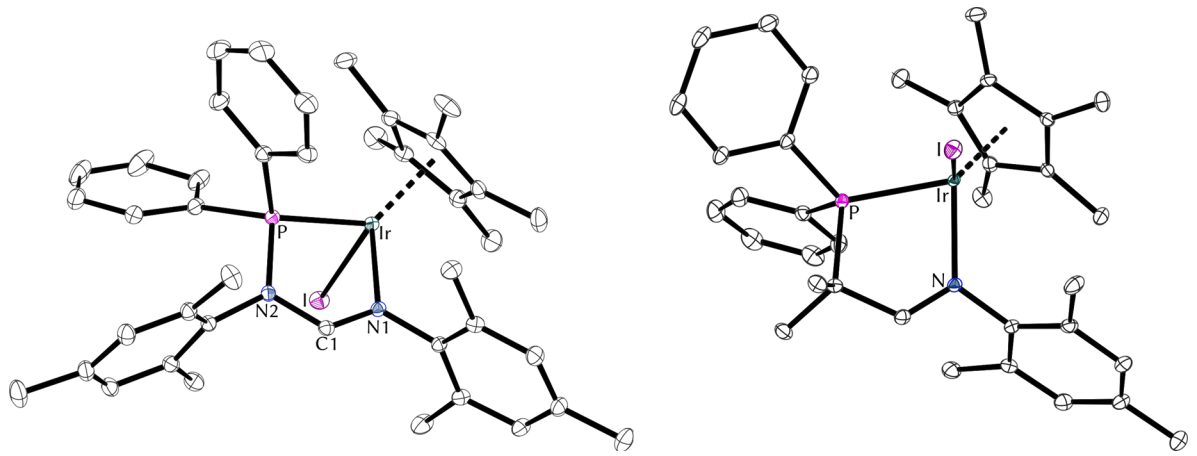


Figure 4: Molecular structures of [**2a**-Cp*IrI]$^+$ (left) and [**5**-Cp*IrI]$^+$ (right). Anisotropic displacement ellipsoids set at the 50% probability level. Hydrogen atoms have been omitted for clarity. For selected bond lengths and angles see Table 2.

Table 2: Selected structural parameters of the crystallized complexes [**2a**-Cp*IrI]BF_4 and [**5**-Cp*IrI]OTf.

	P–Ir [Å]	N–Ir [Å]	α[a] [°]	β[b] [°]
[**2a**-Cp*IrI]BF_4	2.2695(7)	2.1322(15)	122.05(14)	80.42(4)
[**5**-Cp*IrI]OTf	2.3052(8)	2.136(2)	124.4(2)	79.75(6)

[a]α Denotes the N–C–N angle ([**2a**-Cp*IrI]BF_4) or the N–C–C angle ([**5**-Cp*IrI]OTf), respectively. [b]β Denotes the N–Ir–P angle.

cationic palladium species [**2a**-PdCl]BF_4, which is dimeric in the solid state [11]. Similarly, Pd(allyl) complexes of ligands **2a**, **5** and **7** were obtained from mixtures of the respective ligand, $[Pd(allyl)Cl]_2$ and $AgBF_4$ or AgOTf as the chloride scavenger in DCM (Figure 5B).

We were able to obtain single crystals of [**2a**-$PdCl_2$] and [**5**-Pd(2-Me-allyl)]OTf suitable for X-ray diffraction analysis (Figure 6). For an overview of metric parameters of all palladium complexes see Table 3.

The solid-state structures of [**2a**-$PdCl_2$] (Figure 6, left) and its cationic congener $[\mathbf{2a}\text{-PdCl}]_2(BF_4)_2$ (Figure 5) show distinct similarities. Bond lengths and bond angles of the chelate ring agree well, underlining that halide abstraction is effectively compensated by the bridging chlorides (Table 3). Significant structural deviations are only observed for the Pd–Cl bonds, where significantly longer bonds were found for the cationic species (*trans*-nitrogen 2.31 Å vs 2.33 Å and *trans*-phosphorus 2.33 Å vs 2.42 Å). As has been observed for the corresponding rhodium and iridium complexes (vide supra), the structure of complex [**5**-Pd(allyl)]OTf is slightly folded, which is also accompanied by longer P–Pd and N–Pd bonds (cf. Table 2 and Table 3).

Conclusion

The work described in this paper shows that three related neutral κ^2-P,N-ligand families **L1**–**L3** are accessible via straightforward condensation protocols. All ligand classes can be synthesized starting from cheap, commercially available reagents on a multigram scale. Notably, relatively small changes in the ligand backbone, i.e., C/N-exchange or increasing the chelate ring size, have a significant impact on the ligand geometry and its coordination properties. Thus, complexes of **L1** with rhodium, iridium and palladium form planar chelate rings, structures based on **L2** are slightly folded, whereas complexes of **L3** exhibit a strong deviation from planarity. In summary, these results may be utilized for the design, preparation and structural elucidation of novel late transition metal complexes. Investigations into their potential as precatalysts for organic transformations are currently underway in our laboratory and will be reported in due course.

Experimental

General procedure for the preparation of ligands **2**, **3** and **5**

To a solution of the formamidine or imine (15.0 mmol, 1.0 equiv) in 150 mL of THF at −78 °C was added dropwise a solution of *tert*-butyllithium in pentane (15.0 mmol, 1.0 equiv,

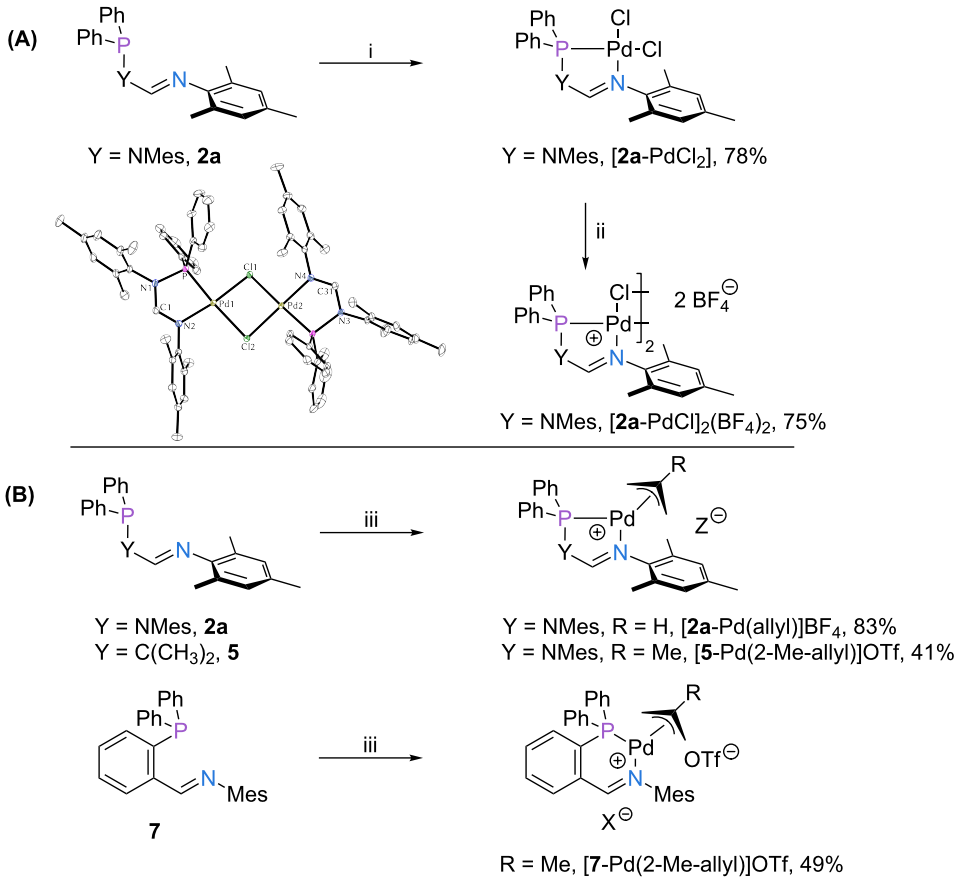


Figure 5: Formation of palladium complexes of ligands **2a**, **5** and **7**. (A) Formation of [**2a**-$PdCl_2$] and [**2a**-$PdCl]_2(BF_4)_2$, and molecular structure of the dimer [**2a**-$PdCl]_2^{2+}$. Anisotropic displacement ellipsoids set at the 50% probability level. Hydrogen atoms have been omitted for clarity. (B) Formation of Pd(allyl) complexes of ligands **2a**, **5**, and **7**. Reaction conditions: (i) DCM, [Pd(cod)Cl_2], rt, 30 min; (ii) DCM, $AgBF_4$, rt, 30 min; (iii) DCM, [Pd(allyl)Cl]$_2$ or [Pd(2-Me-allyl)Cl]$_2$, $AgBF_4$ or AgOTf, rt, 30 min.

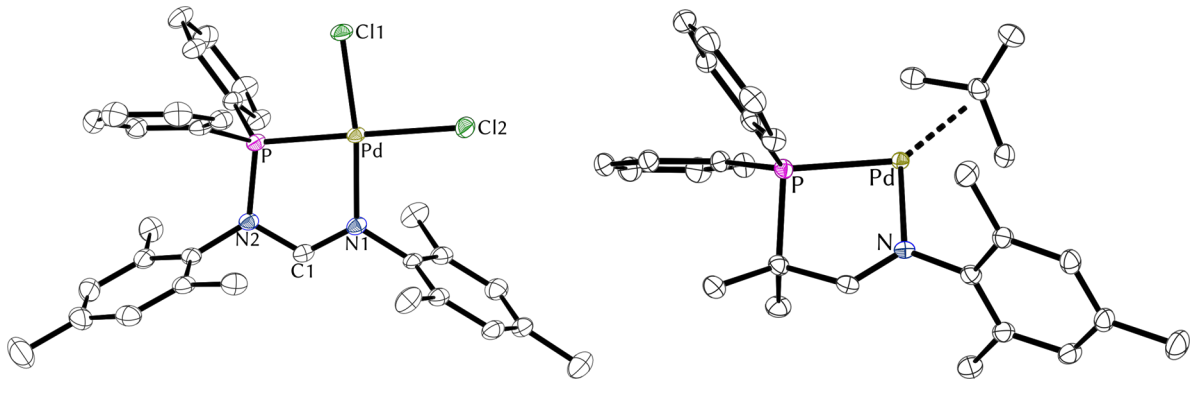


Figure 6: Molecular structures of [**2a**-$PdCl_2$] (left) and [**5**-Pd(2-Me-allyl)]$^+$ (right). Anisotropic displacement ellipsoids set at the 50% probability level. Hydrogen atoms have been omitted for clarity.

1.9 M). The reaction was left at this temperature for 30 min, warmed to rt and stirred for 1 h. This mixture was added to a solution of the chlorophosphine (15.0 mmol, 1.0 equiv) in 150 mL of THF at −78 °C, stirred for 30 min at this temperature and warmed to rt overnight. The solvent was removed under reduced pressure and the residue was taken up in 300 mL

Table 3: Selected structural parameters of the crystallized complexes [**2a**-$PdCl_2$], [**2a**-$PdCl]_2(BF_4)_2$ and [**5**-Pd(allyl)]OTf.

	P–Pd [Å]	N–Pd [Å]	α[a] [°]	β[b] [°]
[**2a**-$PdCl_2$]	2.1823(7)	2.043(2)	121.5(2)	83.59(7)
[**2a**-$PdCl]_2BF_4$[c]	2.1861(11) [2.1848(10)]	2.007(2) [2.019(2)]	121.4(2) [121.4(3)]	83.62(7) [83.69(7)]
[**5**-Pd(2-Me-allyl)]OTf	2.2806(14)	2.107(3)	122.2(3)	82.24(8)

[a]α Denotes the N–C–N angle ([**2a**-$PdCl_2$], [**2a**-$PdCl]_2BF_4$) or the N–C–C angle ([**5**-Pd(allyl)]OTf), respectively. [b]β Denotes the N–Pd–P angle. [c]Values for the second palladium center of the dimer are provided in square brackets.

of toluene. The mixture was then filtered through a plug of Celite© and the solvent was evaporated in vacuo yielding the desired product which was used without further purification in the subsequent metalation steps. For compound numbering and the preparation of ligand **7**, see Supporting Information File 1.

General procedure for the preparation of metal complexes: A solution of the ligand (100 µmol, 1.0 equiv) in 5 mL of DCM was added to the metal precursor [M]–X (100 µmol, 1.0 equiv) and the mixture was stirred for 30 minutes. At this point, the product was either isolated by layering with toluene and pentane yielding the desired neutral product or $AgBF_4$ (alternatively AgOTf) (100 µmol, 1.0 equiv) was added to produce the cationic complex. The suspension was then stirred in the dark for another 30 minutes, the solid residue was filtered off and the filtrate was layered with toluene and pentane, and stored at −40 °C. This procedure yielded a powder or in several cases single crystals suitable for X-ray diffraction. The solid was then washed with pentane and dried under high vacuum for several days to remove residual solvent. Alternatively, the complexes can be synthesized starting from a preformed cationic precursor [M]–BF_4 (or [M]–OTf). In this case, a solution of the ligand (100 µmol, 1.0 equiv) in 5 mL DCM was added to the metal precursor [M]–BF_4 (100 µmol, 1.0 equiv). The mixture was stirred for 30 minutes, filtered, layered with toluene and pentane and stored at −40 °C. Additional purification steps were carried out as described above. For details see Supporting Information File 1.

Supporting Information

Supporting Information File 1

Experimental procedures and analytical data.
[http://www.beilstein-journals.org/bjoc/content/supplementary/1860-5397-12-83-S1.pdf]

Supporting Information File 2

Crystal structure data.
[http://www.beilstein-journals.org/bjoc/content/supplementary/1860-5397-12-83-S2.cif]

Acknowledgements

We gratefully acknowledge the award of a Ph.D. grant to T. R. from the Landesgraduiertenförderung (LGF Funding Program of the state of Baden-Württemberg), the award of a national scholarship (Deutschlandstipendium) to V. V., C. K. B and S. N. I., and the University of Heidelberg for generous funding.

References

1. Roseblade, S. J.; Pfaltz, A. *Acc. Chem. Res.* **2007,** *40,* 1402. doi:10.1021/ar700113g
2. Lightfoot, A.; Schnider, P.; Pfaltz, A. *Angew. Chem., Int. Ed.* **1998,** *37,* 2897. doi:10.1002/(SICI)1521-3773(19981102)37:20<2897::AID-ANIE2897>3.0.CO;2-8
3. Helmchen, G. *J. Organomet. Chem.* **1999,** *576,* 203. doi:10.1016/S0022-328X(98)01059-6
4. Kazmaier, U., Ed. *Transition Metal Catalyzed Enantioselective Allylic Substitution in Organic Synthesis;* Springer: Berlin, Heidelberg, 2012; Vol. 38. doi:10.1007/978-3-642-22749-3
5. Loiseleur, O.; Hayashi, M.; Keenan, M.; Schmees, N.; Pfaltz, A. *J. Organomet. Chem.* **1999,** *576,* 16. doi:10.1016/S0022-328X(98)01049-3
6. Hu, X.; Chen, H.; Zhang, X. *Angew. Chem., Int. Ed.* **1999,** *38,* 3518. doi:10.1002/(SICI)1521-3773(19991203)38:23<3518::AID-ANIE3518>3.0.CO;2-P
7. Pfaltz, A.; Drury III, W. J. *Proc. Natl. Acad. Sci. U. S. A.* **2004,** *101,* 5723. doi:10.1073/pnas.0307152101
8. Guiry, P. J.; Saunders, C. P. *Adv. Synth. Catal.* **2004,** *346,* 497. doi:10.1002/adsc.200303138
9. Roth, T.; Wadepohl, H.; Wright, D. S.; Gade, L. H. *Chem. – Eur. J.* **2013,** *19,* 13823. doi:10.1002/chem.201302327
10. Roth, T.; Vasilenko, V.; Benson, C. G. M.; Wadepohl, H.; Wright, D. S.; Gade, L. H. *Chem. Sci.* **2015,** *6,* 2506. doi:10.1039/C4SC03966A
11. Carney, M. J.; Small, B. L.; Sydora, O. L. Phosphinyl Formamidine Compounds, Metal Complexes, Catalyst Systems, and their use to Oligomerize or Polymerize Olefins. WO 2015/094207 A1, June 25, 2015.
12. Baiget, L.; Batsanov, A. S.; Dyer, P. W.; Fox, M. A.; Hanton, M. J.; Howard, J. A. K.; Lane, P. K.; Solomon, S. A. *Dalton Trans.* **2008,** 1043. doi:10.1039/B715736C
13. Daugulis, O.; Brookhart, M. *Organometallics* **2002,** *21,* 5926. doi:10.1021/om0206305
14. Xue, Z.; Linh, N. T. B.; Noh, S. K.; Lyoo, W. S. *Angew. Chem.* **2008,** *120,* 6526. doi:10.1002/ange.200801647
15. Yoshida, H.; Shirakawa, E.; Kurahashi, T.; Nakao, Y.; Hiyama, T. *Organometallics* **2000,** *19,* 5671. doi:10.1021/om000828u

16. Shirakawa, E.; Nakao, Y.; Murota, Y.; Hiyama, T. *J. Organomet. Chem.* **2003,** *670,* 132. doi:10.1016/S0022-328X(02)02153-8
17. Nolan, S. P. *N-Heterocyclic Carbenes: Effective Tools for Organometallic Synthesis;* Wiley-VCH, 2014. doi:10.1002/9783527671229
18. Roth, T.; Vasilenko, V.; Wadepohl, H.; Wright, D. S.; Gade, L. H. *Inorg. Chem.* **2015,** *54,* 7636. doi:10.1021/acs.inorgchem.5b01292
19. Hilgraf, R.; Pfaltz, A. *Adv. Synth. Catal.* **2005,** *347,* 61. doi:10.1002/adsc.200404168
20. Slater, J. C. *J. Chem. Phys.* **1964,** *41,* 3199. doi:10.1063/1.1725697
21. Tsuji, J. *Palladium Reagents and Catalysts;* Wiley, 2004. doi:10.1002/0470021209

License and Terms

This is an Open Access article under the terms of the Creative Commons Attribution License (http://creativecommons.org/licenses/by/2.0), which permits unrestricted use, distribution, and reproduction in any medium, provided the original work is properly cited.

The license is subject to the *Beilstein Journal of Organic Chemistry* terms and conditions: (http://www.beilstein-journals.org/bjoc)

The definitive version of this article is the electronic one which can be found at: doi:10.3762/bjoc.12.83

BEILSTEIN JOURNAL OF ORGANIC CHEMISTRY

Modular synthesis of the pyrimidine core of the manzacidins by divergent Tsuji–Trost coupling

Sebastian Bretzke[1], Stephan Scheeff[2], Felicitas Vollmeyer[2], Friederike Eberhagen[2], Frank Rominger[1] and Dirk Menche[*2]

Full Research Paper

Open Access

Address:
[1]Institut für Organische Chemie, Ruprecht-Karls Universität Heidelberg, Im Neuenheimer Feld 270, 69120 Heidelberg, Germany and [2]Kekulé-Institut für Organische Chemie und Biochemie, Universität Bonn, Gerhard-Domagk-Strasse 1, 53121 Bonn, Germany

Email:
Dirk Menche[*] - dirk.menche@uni-bonn.de

* Corresponding author

Keywords:
cross-metathesis; natural products; pyrimidines; Tsuji–Trost reaction; synthetic methods

Beilstein J. Org. Chem. **2016,** *12,* 1111–1121.
doi:10.3762/bjoc.12.107

Received: 18 March 2016
Accepted: 13 May 2016
Published: 02 June 2016

This article is part of the Thematic Series "Organometallic chemistry" and is dedicated to the memory of Peter Hofmann. With deep gratitude I remember the joint time at the University of Heidelberg. He has been a role model in many ways.

Guest Editor: B. F. Straub

© 2016 Bretzke et al; licensee Beilstein-Institut.
License and terms: see end of document.

Abstract

The design, development and application of an efficient procedure for the concise synthesis of the 1,3-*syn*- and *anti*-tetrahydropyrimidine cores of manzacidins are reported. The intramolecular allylic substitution reaction of a readily available joint urea-type substrate enables the facile preparation of both diastereomers in high yields. The practical application of this approach is demonstrated in the efficient and modular preparation of the authentic heterocyclic cores of manzacidins, structurally unique bromopyrrole alkaloids of marine origin. Additional features of this route include the stereoselective generation of the central amine core with an appending quaternary center by an asymmetric addition of a Grignard reagent to a chiral *tert*-butanesulfinyl ketimine following an optimized Ellman protocol and a cross-metathesis of a challenging homoallylic urea substrate, which proceeds in good yields in the presence of an organic phosphoric acid.

Introduction

Chiral pyrimidine motifs constitute prevalent structural features in a variety of potent natural products and bioactive agents [1-5]. As exemplified by the marine natural products manzazidins A and C [2-5], they may be characterized by diverse configurations, including synthetically challenging quaternary centers. Owing to their pronounced biological activities, several synthetic routes have been reported to access these important substructures [6-22]. The manzacidins have first been isolated by the group of Kobayashi from the marine sponge *Hymeniacidon* sp. in the early nineties of the last century [2]. The compounds have demonstrated potent antifungal activity [3], and acted as α-adrenoceptor blockers, antagonists of the

serotonergic receptor and/or actomyosin ATPase activators [23-25]. As shown in Figure 1 for the most prominent representatives, manzacidins A (**1**) and C (**2**), their unique architecture is characterized by an ester-linked bromopyrrole carboxylic acid and a tetrahydropyrimidine ring in which one of the amino groups is attached to a quaternary carbon center. Due to their intriguing structures in combination with the promising biological properties this class of bromopyrrole alkaloids has attracted great interest from synthetic chemists and a variety of elegant total syntheses has been reported [6-22]. Inspired by an innovative concept for heterocycles synthesis recently developed in our group [26-31], we became interested to devise a novel and a more versatile route to the central heterocyclic core of these marine metabolites. The method is based on a late-stage diversification strategy involving a Tsuji–Trost reaction of the urea-type joint precursor **5**. In contrast to existing routes, this approach enables a more versatile elaboration of different configurations as present in the manzacidins and/or originally postulated for this class of marine natural products. Notably, the absolute configuration of manzacidin C was initially proposed as shown in Figure 1 [2] and subsequently revised by a total synthesis [6] which adds to the importance of a flexible route to such substructures. Herein we report in full detail the design, development and application of an innovative strategy for the high-yielding synthesis of 1,3-*syn*- and *anti*-configured tetrahydropyrimidinones, based on an allylic substitution reaction of a joint precursor **5**. Subsequently this strategy is successfully applied to the synthesis of the authentic pyrimidine cores **3** and **4** of manzacidin A (**1**) and *ent*-manzacidin C (**2**).

Results and Discussion

General synthetic concept

As part of our ongoing efforts to the design of novel tandem reactions for the synthesis of complex natural products [29,32-37], we have developed an innovative concept for heterocycles synthesis [26-31]. As shown in Scheme 1, this approach that further advances and generalizes several individual reports by other groups [38-43], is based on a sequential nucleophilic addi-

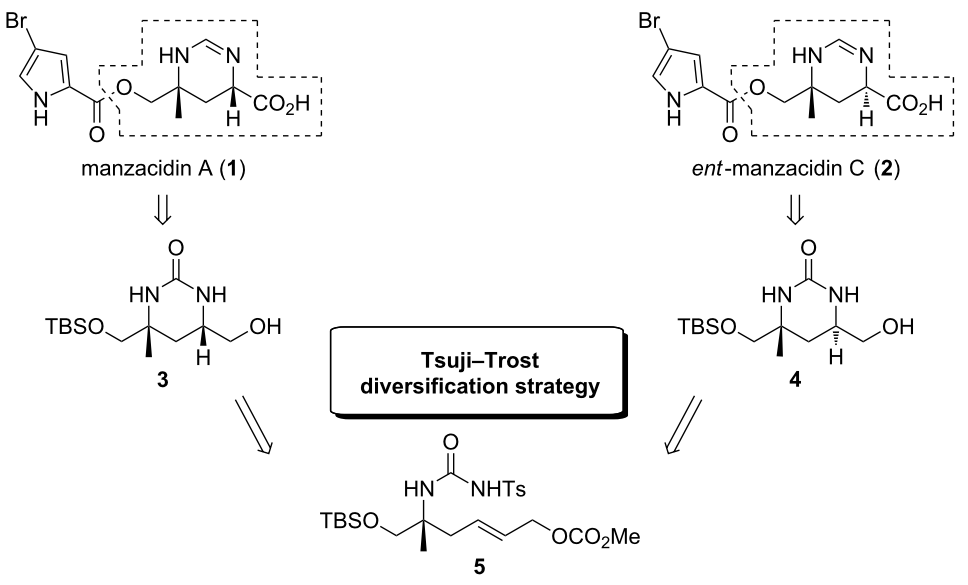
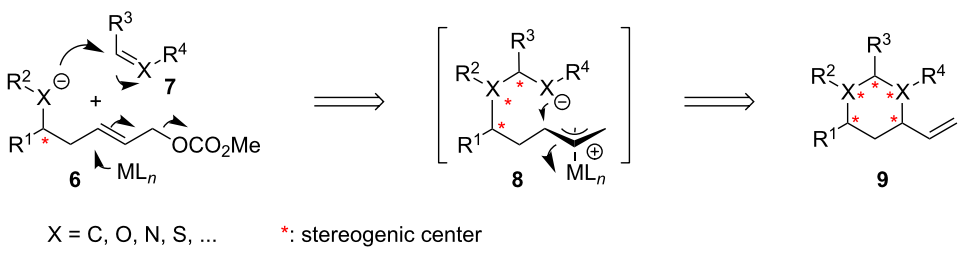


Figure 1: Modular concept for manzacidin synthesis based on a Tsuji–Trost coupling of joint intermediate **5**.



Scheme 1: General concept for heterocycles synthesis based on a nucleophilic addition and Tsuji–Trost coupling.

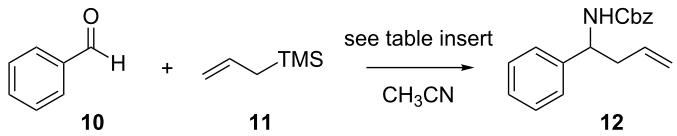
tion and an intramolecular allylic substitution reaction. It relies on the coupling of different homoallylic nucleophiles of general type **6** to diverse electrophiles **7** such as Michael acceptors, or heteroolefins as for example imines, carbonyls or allene homologs. The resulting homologated nucleophile **8** may then be trapped in an intramolecular fashion by a π-allyl complex, which may concomitantly form from **6** through activation of the homoallylic functionality with a suitable transition metal catalyst. According to this concept, variously substituted 6-membered heterocycles of type **9** may be obtained in a general and concise fashion. Notably, this anionic relay process may directly generate up to four new stereogenic centers and thus demonstrates a high increase in structural complexity from readily available starting materials.

Evaluation of the concept by a model study

As a prelude to the targeted substitution pattern of the manzacidins, we first evaluated the applicability of this process for a modular synthesis of 1,3-*syn*- and *anti*-tetrahydropyrimidinones using the simplified amine substrate **12**. Parts of this model study have already been reported in preliminary form [31]. Homoallylic amines of type **12** may be efficiently obtained through multicomponent reactions. These involve the nucleophilic allylation of imines which may be generated in situ by the condensation of an amine and a carbonyl compound. As shown in Scheme 2, two such procedures were evaluated within the preliminary study. The first protocol that we analyzed was reported by the group of Tian. It involves a four-component coupling of aldehyde **10** with CbzCl for activation of the nitrogen source, HMDS and allyltrimethylsilane (**11**) in the presence of catalytic amounts of $FeSO_4$ [44]. In our hands, this process enabled an efficient access to the desired homoallylic amine **12** in essentially quantitative yields. The other protocol was reported by Phukan and involves an iodine-catalyzed condensation of aldehyde **10** with benzylcarbamate and allyltrimethylsilane (**11**) [45]. Unfortunately, this route was found to be less effective in terms of isolated yields and scalability. Thus, the iron-catalyzed procedure was applied and multigram quantities of **12** were readily obtained.

As shown in Scheme 3, we next focused on the further derivatization of amine **12** towards suitably functionalized urea substrates **15** or **19**. Inspired by a work of Garcia [39], we initially intended to use isocyanate for both, the introduction of the urea motif and for the functionalization of the terminal homoallylic alcohol. Consequently, we evaluated the conversion of **14** to **15**. The required substrate **14** was prepared from amine **12** by cross-metathesis with 2-butene-1,4-diol (**13**) in the presence of Grubbs-II catalyst **21**. However, in the subsequent coupling reactions of **14** with TsNCO it became apparent that this homoallylic amine was too unreactive to enable a double addition to access **15** directly. Therefore, a stepwise approach towards **19** was pursued instead. This involved either a coupling of **12** first with isocyanate to give **16** followed by a cross-metathesis or starting with the cross-metathesis to **18** and subsequent installment of the urea motif. As shown in the table inserted in Scheme 3 for selected cross-metatheses of Cbz-protected amide **12** and its urea-derivative **16** with butene **17**, a different reactivity of **12** and **16** was observed. While **16** proved too unreactive for the coupling reaction under various conditions (e.g., entries 1 and 2), the homologation of the Cbz-protected amine **12** to **18** could be realized. Preparative useful yields (69%) were obtained with Grubbs-II catalyst (**21**) in toluene at elevated temperatures (entry 3), while lower conversions were observed with other catalysts (**20**, **22**) or in dichloromethane (entries 4 and 5). Finally, for the installment of the required urea motif into **18**, tosylisocyanate in combination with strong bases was required to achieve useful degrees of conversion towards the desired precursor **19**. The best results were obtained with BuLi, as previously communicated [31], while weaker bases (NEt_3, LHMDS, DBU, proton sponge) and less electron-deficient isocyanates resulted in lower yields.

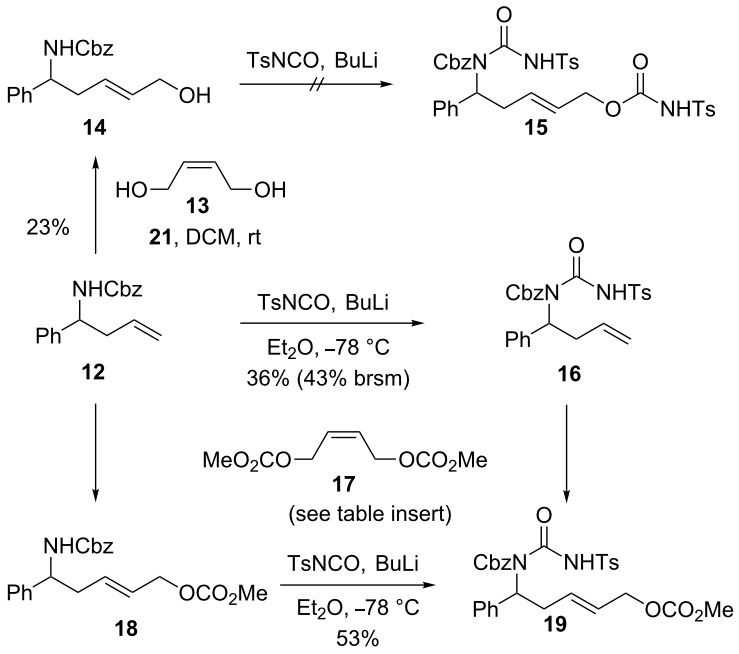
We then turned our attention to the pivotal intramolecular allylic substitution reaction of **19** to access *syn*- and *anti*-pyrimidinones **23** and **24**. As previously reported [31], this diastereodivergent coupling could indeed be realized as shown in Scheme 4. Based on a report of Garcia for a related system we first evaluated $Pd_2(dba)_3$ with different phosphite ligands [39].



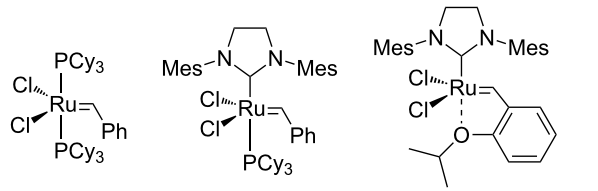
10 **11** **12**

entry	reagent	catalyst	yield (%)	
1	CbzCl/HMDS	$FeSO_4$	95	[44]
2	$CbzNH_2$	I_2	66	[45]

Scheme 2: Synthesis of homoallylic alcohol **12** by multi-component reactions.

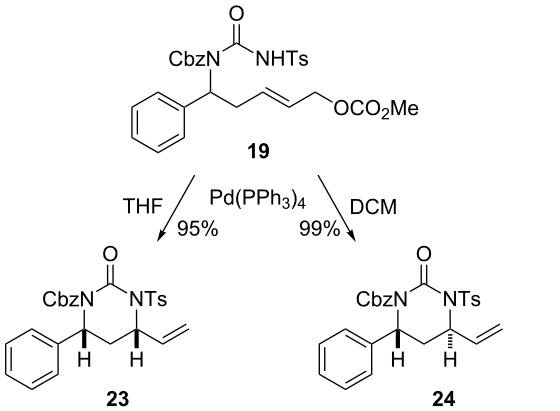


entry	substrate	catalyst	conditions	yield (%)
1	**16**	**20** (5 mol %)	toluene, 80 °C	– (**19**)
2	**16**	**22** (5 mol %)	toluene, 80 °C	– (**19**)
3	**12**	**21** (5 mol %)	toluene, 80 °C	69 (**18**)
4	**12**	**22** (5 mol %)	DCM, 50 °C	60 (**18**)
5	**12**	**22** (5 mol %)	toluene, 80 °C	43 (**18**)



Grubbs-I (**20**) Grubbs-II (**21**) Hoveyda–Grubbs-II (**22**)

Scheme 3: Preparation of urea-type cyclization precursor **19**.

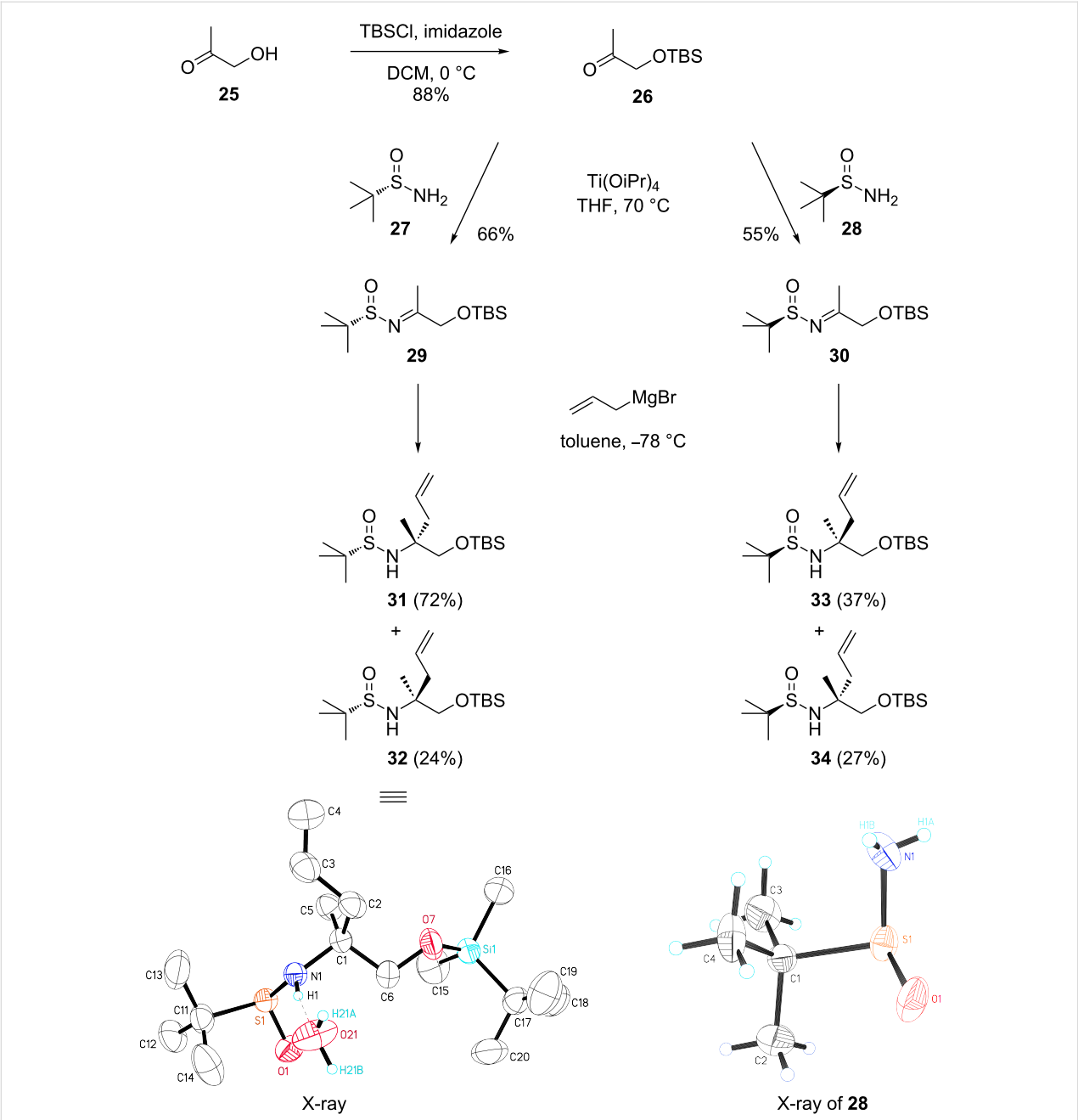


Scheme 4: Stereodivergent synthesis of 1,3-*syn*- and *anti*-tetrahydropyrimidinones [31].

However, the best results were obtained with the stable catalyst $Pd(PPh_3)_4$ and depending on the solvent used, either the *syn*-isomer **23** or the *anti*-isomer **24** could be selectively obtained.

Application of the concept for manzacidin core synthesis

After proofing the general adaptability of our synthetic concept, we next evaluated the applicability of this procedure for the synthesis of the authentic manzacidin substrate. As shown in Scheme 5, we first focused on the stereoselective synthesis of the chiral amine core of these alkaloids. For the synthesis of the nitrogen appending the quaternary center we tested a method developed by the Ellman group [46,47], which relies on an asymmetric addition of organometallic reagents to enantiopure *tert*-butanesulfinyl ketimines of type **29** and **30**. Although the group of Lee had already communicated the synthesis of **33**

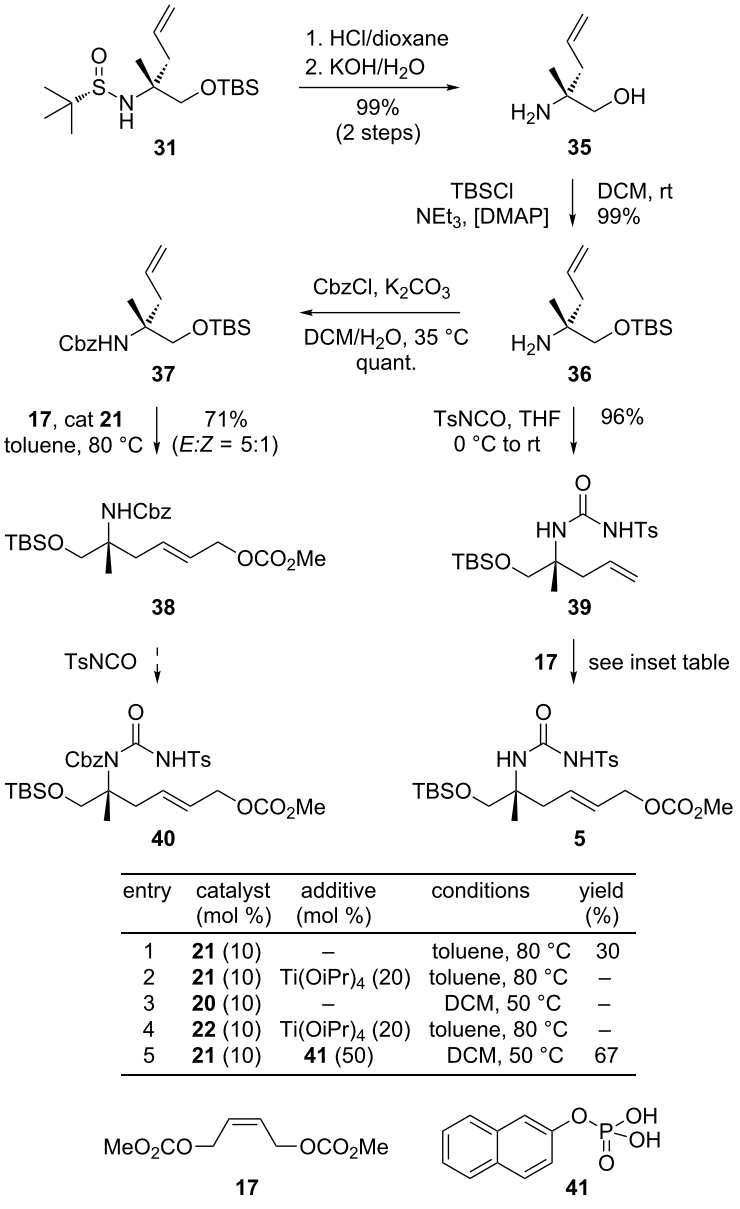


Scheme 5: Stereoselective synthesis of all possible stereoisomers of the manzacidin core amine by asymmetric addition to chiral *tert*-butanesulfinyl ketimines.

using this approach [48], no full details have been given. In addition, the reported yields were only moderate and the stereochemistry appeared not to have been rigorously assigned. Therefore, we evaluated this type of asymmetric addition in more general terms and analyzed the addition reactions of allylmagnesium bromide both to **29** and **30**. Notably, this route would allow to access all possible stereoisomers of the manzacidins, in agreement with the stereochemical diversity of this class of natural products. In detail, the synthesis of **29** and **30** involved a condensation of hydroxyacetone (**25**)-derived ketone **26** [49] with S_S- and R_S-*tert*-butanesulfinamides **27** and **28**, respectively. As an improvement to the original procedure [46-48], we applied $Ti(OiPr)_4$ as Lewis acid instead of the reported $Ti(OEt)_4$, which resulted in higher yields and a more reliable process in our hands. In agreement with the results of Lee the addition of allylmagnesium bromide to **30** lead to **33** in only moderate yields and low selectivity towards **34**. We then studied the coupling of **29** in more detail to target amine **31** that

bears the correct configuration required for manzacidin A. Possibly, the higher selectivity observed for the conversion of **29** as compared to **30** may be due to initial problems during the work-up. Finally, the addition could be effected giving the desired diastereomer **31** in high yields (72%) and the minor isomer **32** that was likewise obtained (24%) could be readily removed by column chromatography. The configuration of **31** was initially assigned by Mosher ester analysis of the free amine **36** (Scheme 6) and finally proven in an indirect manner by an X-ray crystallography of the minor diastereomer **32**. Within the course of this study also an X-ray structure of *tert*-butylsulfinylamine **28** was obtained. Remarkably, these types of substances have not been broadly evaluated by X-ray structural analysis which adds to the importance of this general evaluation.

Next, we focused on further homologation towards a suitably functionalized urea precursor **5** for the envisioned Tsuji–Trost cyclization. As shown in Scheme 6, this involved an acidic cleavage of the sulfinamide followed by basic treatment to give free amine **35**. After protection of the primary hydroxy group as TBS ether, we first evaluated the synthesis of derivative **40**, in analogy to our model study. Accordingly, the free amine **36** was Cbz-protected following the Schotten–Baumann method [50]. The obtained amide **37** was then homologated by cross-metathesis with butenedicarboxylate **17** in the presence of Grubbs-II



entry	catalyst (mol %)	additive (mol %)	conditions	yield (%)
1	**21** (10)	–	toluene, 80 °C	30
2	**21** (10)	$Ti(OiPr)_4$ (20)	toluene, 80 °C	–
3	**20** (10)	–	DCM, 50 °C	–
4	**22** (10)	$Ti(OiPr)_4$ (20)	toluene, 80 °C	–
5	**21** (10)	**41** (50)	DCM, 50 °C	67

Scheme 6: Synthesis of the authentic cyclization precursor **5**.

catalyst (**21**) applying our conditions developed above (Scheme 3). However, with the resulting homologated amide **38** in hand we were not able to install the required urea moiety with tosylisocyanate, despite considerable efforts with various bases, solvents or variation of temperature and equivalents. These results again demonstrated the difficulties to install the urea function in a sterically hindered and electronically unreactive Cbz-protected amine substrate, which is in agreement with our observations above. Therefore, we decided to continue our route with the free amine **36** instead, which was directly coupled with TSNCO to give **39** in high yield. The reaction took place even without an additional base, which shows the strong influence of the amine protective group on this type of condensation. Importantly, at this stage, the structure of **39** was fully confirmed by X-ray crystallography. As shown in Figure 2, this urea derivative is present as an unsymmetrical dimer in the crystal lattice, which is stabilized by two hydrogen bonds between the urea oxygen atoms and the tosyl-protected nitrogens. This also unambiguously confirms the absolute configuration of **39** and corroborates our prediction of the asymmetric adduct **31**.

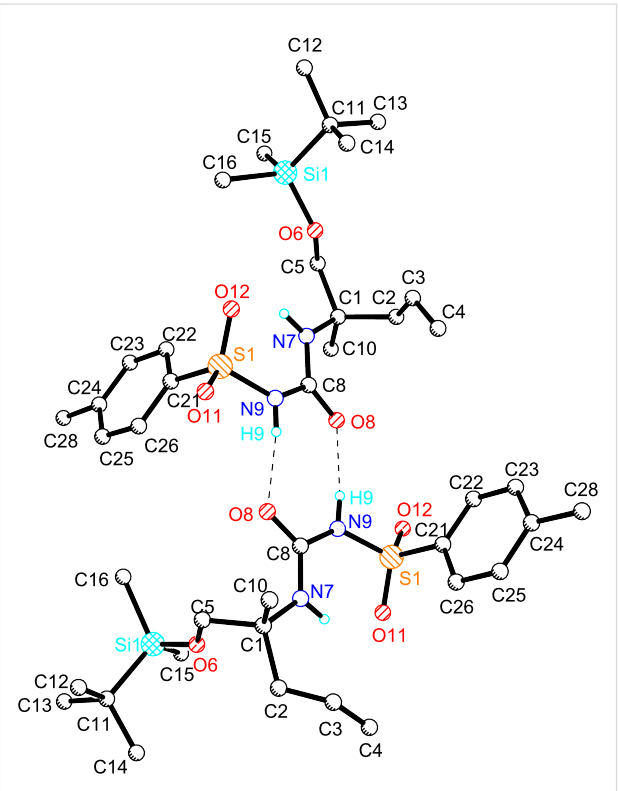


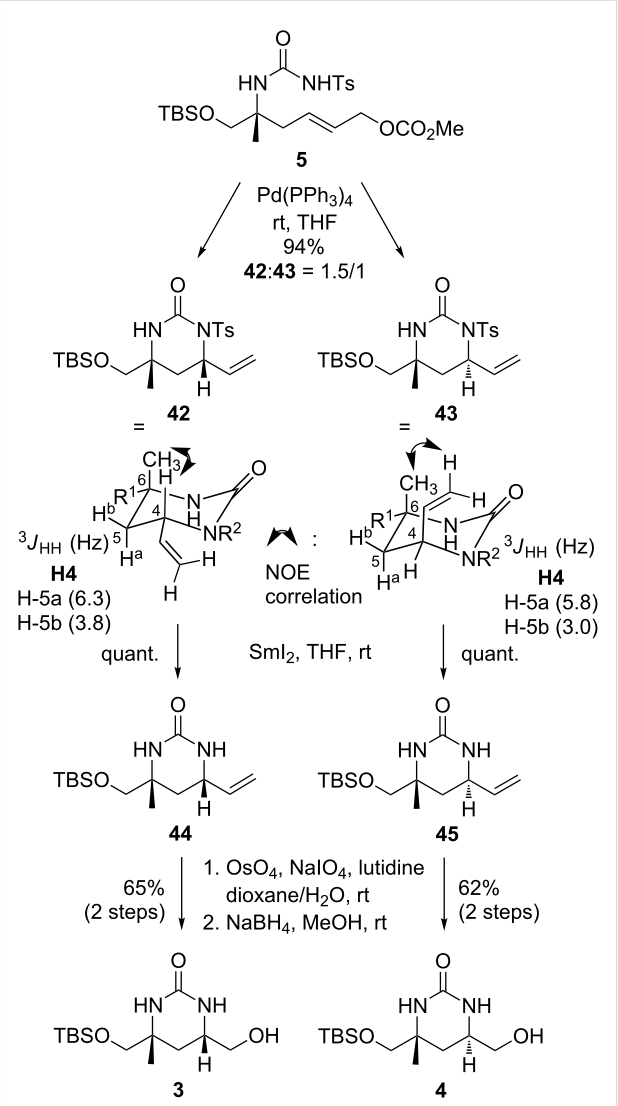
Figure 2: X-ray structure of **39**.

We then attempted the installation of the required allylic carbonate on **39** by cross-metathesis with **17**. However, initial attempts following our protocol developed above with Grubbs-II catalyst (**21**) resulted in only moderate conversion (inserted table in Scheme 6, entry 1). Also, the application of other catalysts with or without additional additives to impede a possibly unfavorable amine coordination of the reactive ruthenium intermediates [51] did not improve the reaction outcome (entries 2–4). Following reports from Nolan and Prunet [52], as well as from Steinke and Vilar [53] we finally evaluated tricyclohexylphosphane oxides and organic phosphoric acid, which had been reported to have beneficial effects in the cross-metathesis of related substrates. In the presence of catalytic amounts of phosphoric acid **41** [53], the coupling of **39** with **17** could indeed be realized in useful yields in a reliable fashion. Optimal results included treatment of **39** with 2.5 equiv of dicarbonate **17**, 50 mol % naphthylphosphoric acid and 10 mol % Grubbs-II catalyst, giving the desired urea derivative **5** in good yield (67%), considering the general difficulties observed for such substrates in cross-metathesis reactions.

With precursor **5** in hand the desired cyclization towards **42** and **43** could then be efficiently realized in a straightforward manner giving the desired *syn*- and *anti*- tetrahydropyrimidinones in a joint fashion with a ratio of 1.5:1. Following the protocol developed above, excellent yields (94%) were obtained in this coupling. As compared to the model substrate **19** (see Scheme 4) no selectivity was observed in this coupling, which could also not be modified by other solvents. Possibly this may be due to the missing Cbz group of **5** as compared to **19**. The configuration of both products was assigned by NMR methods based on characteristic NOE correlations and vicinal coupling constants as shown in Scheme 7. For further conversion to key intermediates **3** and **4**, the tosyl groups of **42** and **43** were removed with SmI_2 [54,55] giving the free amides **44** and **45**. The terminal double bonds were then oxidized by dihydroxylation with OsO_4 and periodate cleavage [56,57], and the resulting aldehydes (not shown) were reduced to the terminal alcohols with $NaBH_4$, giving the desired pyrimidinones **3** and **4**. These compounds represent key intermediates which may be transformed into the targeted natural products **1** and **2** following previously established protocols [6,31].

Conclusion

In summary, we have reported in full details the design, development and application of an efficient method for the synthesis of the tetrahydropyrimidinone core of the manzacidins by a divergent intramolecular allylic substitution reaction. The application of this approach enabled a highly concise access to the authentic heterocyclic cores of the manzacidins, structurally unique natural products of marine origin. Additional notable features of our modular route also include the generation of an amine appending quaternary center by an optimized Ellman protocol for the asymmetric allyl-Grignard addition to enan-



Scheme 7: Divergent Tsuji–Trost coupling and completion of the synthesis of authentic pyrimidinones **3** and **4**.

tiopure *tert*-butanesulfinyl ketimines and an efficient cross-metathesis of an unreactive urea substrate in the presence of an organic phosphoric acid. It is expected that these strategies and tactics will find applications in functional target synthesis and stimulate further studies for modular heterocycle synthesis.

Experimental

Preparation of **31** by asymmetric addition of allylmagnesium bromide to **29**

In a flame-dried flask (S_S)-*N*-(1-((*tert*-butyldimethylsilyl)oxy)propan-2-ylidene)-2-methylpropane-2-sulfinamide (**29**, 1.37 g, 4.70 mmol, 1.0 equiv) was dissolved in 12 mL toluene and the solution was cooled to −78 °C. To this mixture allylmagnesium bromide (1.0 M in Et_2O, 7.05 mL, 7.05 mmol, 1.5 equiv) was slowly added and the reaction was stirred for 1 h at −78 °C. The reaction was quenched with a solution of saturated Na_2SO_4, warmed to rt, filtered, washed with ethyl acetate and finally purified by column chromatography on silica gel (120 g) with ethyl acetate/hexane 1:9 as eluent, which yielded the desired diasteromers **31** (major diastereomer) and **32** (minor diastereomer) as light yellow oils (96 %, dr = 1:3). Major diastereomer S_SR (1.13 g, 3.39 mmol, 72%): R_f 0.1 (ethyl acetate/hexane 1:9); $[\alpha]^{20}_D$ +58.2 (*c* 1.00, $CHCl_3$); ^{1}H NMR (300.13 MHz, $CDCl_3$) δ 0.06 (s, 6H), 0.91 (s, 9H), 1.19 (s, 12H), 2.48 (dd, *J* = 4.1 Hz, 7.4 Hz, 2H), 3.32 (d, *J* = 9.3 Hz, 1H), 3.49 (d, *J* = 9.3 Hz, 1H), 3.72 (bs, 1H), 5.11 (d, *J* = 10.4 Hz, 1H), 5.12 (d, *J* = 16.7 Hz, 1H), 5.80 (ddt, *J* = 7.4 Hz, 10.4 Hz, 17.8 Hz, 1H); ^{13}C NMR (75.47 MHz, $CDCl_3$) δ −5.5, 18.2, 22.1, 22.6, 25.8, 43.0, 55.5, 58.1, 69.2, 118.7, 133.8; HRMS–FAB (*m*/*z*): $[M + H]^+$ calcd for $C_{16}H_{36}NO_2SSi$, 334.2231; found, 334.2227. Minor diastereomer S_SS (371 mg, 1.11 mmol, 24%): R_f 0.13 (ethyl acetate/hexane 1:9); $[\alpha]^{20}_D$ +39.2 (*c* 1.00, $CHCl_3$); ^{1}H NMR (300.13 MHz, $CDCl_3$) δ 0.07 (s, 3H), 0.08 (s, 3H), 0.91 (s, 9H), 1.20 (s, 9H), 1.28 (s, 3H), 2.22 (dd, *J* = 8.0 Hz, 13.7 Hz, 1H), 2.37 (dd, *J* = 6.7 Hz, 14.0 Hz, 1H), 3.48 (d, *J* = 9.3 Hz, 1H), 3.53 (d, *J* = 9.6 Hz, 1H), 3.77 (bs, 1H), 5.09 (d, *J* = 17.8 Hz, 1H), 5.10 (d, *J* = 10.7 Hz, 1H), 5.78 (ddt, *J* = 8.0 Hz, 10.7 Hz, 17.3 Hz, 1H); ^{13}C NMR (75.47 MHz, $CDCl_3$) δ −5.6, 18.2, 22.3, 22.7, 25.8, 43.1, 55.6, 58.1, 69.9, 118.5, 133.6; HRMS–ESI (*m*/*z*): $[M + H]^+$ calcd for $C_{16}H_{36}NO_2SSi$, 334.2231; found, 334.2231.

Preparation of **39** by addition of TsNCO to amine **36**

p-TsNCO (0.6 mL, 4.13 mmol, 1.1 equiv) was slowly added to a stirred solution of (*R*)-1-((*tert*-butyldimethylsilyl)oxy)-2-methylpent-4-en-2-amine (**36**, 902 mg, 3.93 mmol) in dry THF (3.9 mL) at 0 °C and stirring was continued at rt for 5 h. The solvent was removed under reduced pressure and purification of the residue by column chromatography on silica gel (cyclohexane/ethyl acetate 4:1) yielded the desired product (1.61 g, 3.77 mmol, 96%) as a colorless solid. R_f 0.29 (cyclohexane/ethyl acetate 4:1); mp 84 °C; $[\alpha]^{20}_D$ −2.3 (*c* 0.5, $CHCl_3$); ^{1}H NMR (300.13 MHz, $CDCl_3$) δ 0.09 (s, 6H), 0.93 (s, 9H), 1.24 (s, 3H), 2.43 (d, *J* = 8.0 Hz, 2H), 2.44 (s, 3H), 3.44 (d, *J* = 9.8 Hz, 1H), 3.58 (d, *J* = 9.8 Hz, 1H), 4.99 (dd, *J* = 10.1, 2.1 Hz, 1H), 5.04 (dd, *J* = 17.2, 2.1 Hz, 1H), 5.58 (ddt, *J* = 17.2, 10.1, 8.0 Hz, 1H), 6.84 (brs, 1H), 7.30 (d, *J* = 8.1 Hz, 2H), 7.77 (d, *J* = 8.1 Hz, 2H); ^{13}C NMR (75.47 MHz, $CDCl_3$) δ −5.4, 18.5, 21.4, 21.8, 26.0, 40.1, 57.3, 67.8, 118.8, 127.2, 129.9, 133.3, 137.0, 144.7, 150.3; HRMS–ESI (*m*/*z*): $[M + Na]^+$ calcd for $C_{20}H_{34}N_2NaO_4SSi$, 449.1901; found, 449.1892. CCDC 1461909 (**39**) contains the supplementary crystallographic data for this paper. These data can be obtained free of charge from The Cambridge Crystallographic Data Centre via http://www.ccdc.cam.ac.uk/data_request/cif.

Preparation of **5** by cross-metathesis of **39** with **17**

To a solution of (*R*)-*N*-((1-((*tert*-butyldimethylsilyl)oxy)-2-methylpent-4-en-2-yl)carbamoyl)-4-methylbenzenesulfonamide (**39**, 50.0 mg, 0.12 mmol, 1.0 equiv), (*Z*)-(but-2-ene-1,4-diyl)dimethyl dicarbonate (**17**, 60.0 mg, 0.29 mmol, 2.5 equiv) and naphthylphosphoric acid (**41**, 15.0 mg, 67.0 µmol, 0.5 equiv) in dry and degassed dichloromethane (1 mL) was added Grubbs-II catalyst (**21**, 10.0 mg, 11.8 µmol, 10 mol %) and the resulting mixture was stirred overnight at 50 °C under an argon atmosphere. Concentration in vacuo and purification by column chromatography on silica gel (10 g) with ethyl acetate/hexane 1:9 as eluent yielded the desired allylic carbonate as brown oil (41.3 mg, 80.4 µmol, 67%): R_f 0.30 (ethyl acetate/hexane 1:3); $[\alpha]^{20}_D$ −2.9 (*c* 1.00, $CHCl_3$); ^{1}H NMR (300.13 MHz, $CDCl_3$) δ 0.09 (s, 6H), 0.93 (s, 9H), 1.24 (s, 3H), 2.44 (m, 5H), 3.44 (d, *J* = 9.8 Hz, 1H), 3.56 (d, *J* = 9.8 Hz, 1H), 3.79 (s, 3H), 4.49 (d, *J* = 4.7 Hz, 2H), 5.60 (m, 2H), 6.87 (s, 1H), 7.31 (d, *J* = 8.1 Hz, 2H), 7.77 (d, *J* = 8.3 Hz, 2H), 8.42 (bs, 1H); ^{13}C NMR (75.47 MHz, $CDCl_3$) δ −5.6, 18.3, 21.3, 21.6, 25.8, 38.5, 54.8, 57.1, 67.7, 68.2, 127.0, 127.5, 129.9, 131.0, 136.7, 144.8, 149.8, 155.6; HRMS–ESI (*m*/*z*): $[M + H]^+$ calcd for $C_{23}H_{39}N_2O_7SSi$, 515.2242; found, 515.2247; HRMS–ESI (*m*/*z*): $[M + Na]^+$ calcd for $C_{23}H_{38}N_2O_7SSiNa$, 537.2061; found, 537.2065.

Tsuji–Trost coupling of **5** to **42** and **43**

A solution of $Pd(PPh_3)_4$ (432 mg, 3.73 µmol, 20 mol %) in dry THF (300 mL) was added to a stirred solution of (*R*,*E*)-6-((*tert*-butyldimethylsilyl)oxy)-5-methyl-5-(3-tosylureido)hex-2-en-1-ylmethyl carbonate (**5**, 959 mg, 1.86 mmol) in dry THF (300 mL) at rt and stirring was continued for 18 h until the color of the solution changed from yellow to red. The solvent was removed under reduced pressure and purification of the residue by column chromatography on silica gel (cyclohexane/ethyl acetate 4:1) yielded the desired products **42** and **43** (766 mg, 1.75 mmol, 94%, dr 1:1.5 *anti*/*syn*) as off-white solids. **42**: mp 129 °C; $[\alpha]^{20}_D$ −20.3 (*c* 0.5, $CHCl_3$); ^{1}H NMR (400.13 MHz, $CDCl_3$) δ 0.00 (s, 6H), 0.86 (s, 9H), 1.18 (s, 3H), 1.92 (dd, *J* = 14.2, 6.3 Hz, 1H), 2.10 (dd, *J* = 14.2, 3.6 Hz, 1H), 2.39 (s, 3H), 3.35–3.43 (m, 2H), 5.12–5.16 (m, 1H), 5.18 (dd, *J* = 10.5, 1.5 Hz, 1H), 5.25 (dd, *J* = 17.2, 1.5 Hz, 1H), 5.45 (brs, 1H), 5.79 (ddd, *J* = 17.2, 10.5, 5.4 Hz, 1H), 7.25 (d, *J* = 8.3 Hz, 2H), 7.89 (d, *J* = 8.3 Hz, 2H); ^{13}C NMR (100.62 MHz, $CDCl_3$) δ −5.4, −5.4, 18.2, 21.7, 25.9, 27.1, 35.8, 55.1, 56.3, 69.1, 116.8, 129.0, 129.1, 137.1, 137.2, 144.2, 151.4; HRMS–EI (*m*/*z*): $[M - C_4H_9]^+$ calcd for $C_{17}H_{25}N_2NaO_7SSi$, 381.1304; found, 381.1307. **43**: mp 127 °C; $[\alpha]^{20}_D$ −12.8 (*c* 0.5, $CHCl_3$); ^{1}H NMR (400.13 MHz, $CDCl_3$) δ 0.02 (s, 3H), 0.03 (s, 3H), 0.85 (s, 9H), 1.20 (s, 3H), 1.89 (dd, *J* = 13.9, 3.2 Hz, 1H), 2.05 (dd, *J* = 13.9, 5.8 Hz, 1H), 2.05 (dd, *J* = 13.9, 5.8 Hz, 1H), 2.39 (s, 3H), 3.25 (d, *J* = 9.4 Hz, 1H), 3.34 (d, *J* = 9.4 Hz, 1H), 5.30–5.17 (m, 4H), 5.88 (ddd, *J* = 16.9, 10.5, 6.0 Hz, 1H), 7.25 (d, *J* = 8.3 Hz, 2 H), 7.90 (d, *J* = 8.3 Hz, 2H); ^{13}C NMR (100.62 MHz, $CDCl_3$) δ −5.4, −5.5, 18.3, 21.7, 25.6, 25.9, 36.3, 55.0, 56.3, 71.6, 117.0, 129.0, 129.2, 137.1, 144.2, 151.3; HRMS–EI (*m*/*z*): $[M - C_4H_9]^+$ calcd for $C_{17}H_{25}N_2NaO_7SSi$, 381.1307; found, 381.1309.

Supporting Information

Supporting Information File 1

Full experimental details, characterization data of all products, copies of ^{1}H and ^{13}C NMR spectra and X-ray crystallographic data for **28**, **32** and **39**.
[http://www.beilstein-journals.org/bjoc/content/supplementary/1860-5397-12-107-S1.pdf]

Acknowledgements

Generous financial support by the DFG is most gratefully acknowledged. We thank Andreas J. Schneider for HPLC-support and Michael Morgen for exploratory studies.

References

1. Patil, A. D.; Kumar, N. V.; Kokke, W. C.; Bean, M. F.; Freyer, A. J.; De Brosse, C.; Mai, S.; Truneh, A.; Faulkner, D. J.; Carte, B.; Breen, A. L.; Hertzberg, R. P.; Johnson, P. K.; Westley, J. W.; Potts, B. C. M. *J. Org. Chem.* **1995,** *60,* 1182–1188. doi:10.1021/jo00110a021
2. Kobayashi, J.; Kanda, F.; Ishibashi, M.; Shigemori, H. *J. Org. Chem.* **1991,** *56,* 4574–4576. doi:10.1021/jo00014a052
3. Tsukamoto, S.; Tane, K.; Ohta, T.; Matsunaga, S.; Fusetani, N.; van Soest, R. W. M. *J. Nat. Prod.* **2001,** *64,* 1576–1578. doi:10.1021/np010280b
4. Jahn, T.; König, G. M.; Wright, A. D.; Wörheide, G.; Reitner, J. *Tetrahedron Lett.* **1997,** *38,* 3883–3884. doi:10.1016/S0040-4039(97)00846-0
5. Aiello, A.; D'Esposito, M.; Fattourusso, E.; Menna, M.; Müller, W. E. G.; Perović-Ottstadt, S.; Schröder, H. C. *Bioorg. Med. Chem.* **2006,** *14,* 17–24. doi:10.1016/j.bmc.2005.07.057
6. Namba, K.; Shinada, T.; Teramoto, T.; Ohfune, Y. *J. Am. Chem. Soc.* **2000,** *122,* 10708–10709. doi:10.1021/ja002556s
7. Wehn, P. M.; Du Bois, J. *J. Am. Chem. Soc.* **2002,** *124,* 12950–12951. doi:10.1021/ja028139s
8. Woo, J. C. S.; MacKay, D. B. *Tetrahedron Lett.* **2003,** *44,* 2881–2883. doi:10.1016/S0040-4039(03)00431-3
9. Drouin, C.; Woo, J. C. S.; MacKay, D. B.; Lavigne, R. M. A. *Tetrahedron Lett.* **2004,** *45,* 7197–7199. doi:10.1016/j.tetlet.2004.08.038
10. Kano, T.; Hashimoto, T.; Maruoka, K. *J. Am. Chem. Soc.* **2006,** *128,* 2174–2175. doi:10.1021/ja056851u
11. Wang, Y.; Liu, X.; Deng, L. *J. Am. Chem. Soc.* **2006,** *128,* 3928–3930. doi:10.1021/ja060312n
12. Sibi, M. P.; Stanley, L. M.; Soeta, T. *Org. Lett.* **2007,** *9,* 1553–1556. doi:10.1021/ol070364x

13. Shinada, T.; Ikebe, E.; Oe, K.; Namba, K.; Kawasaki, M.; Ohfune, Y. *Org. Lett.* **2007,** *9,* 1765–1767. doi:10.1021/ol0704789
14. Tran, K.; Lombardi, P. J.; Leighton, J. L. *Org. Lett.* **2008,** *10,* 3165–3167. doi:10.1021/ol8011869
15. Shinada, T.; Ikebe, E.; Oe, K.; Namba, K.; Kawasaki, M.; Ohfune, Y. *Org. Lett.* **2010,** *12,* 2170. doi:10.1021/ol1006339
16. Ichikawa, Y.; Okumura, K.; Matsuda, Y.; Hasegawa, T.; Nakamura, M.; Fujimoto, A.; Masuda, T.; Nakano, K.; Kotsuki, H. *Org. Biomol. Chem.* **2012,** *10,* 614–622. doi:10.1039/C1OB06559A
17. Sankar, K.; Rahman, H.; Das, P. P.; Bhimireddy, E.; Sridhar, B.; Mohapatra, D. K. *Org. Lett.* **2012,** *14,* 1082–1085. doi:10.1021/ol203466m
18. Shinada, T.; Oe, K.; Ohfune, Y. *Tetrahedron Lett.* **2012,** *53,* 3250–3253. doi:10.1016/j.tetlet.2012.04.042
19. Yoshimura, T.; Kinoshita, T.; Yoshioka, H.; Kawabata, T. *Org. Lett.* **2013,** *15,* 864–867. doi:10.1021/ol303568f
20. Nagatomo, M.; Nishiyama, H.; Fujino, H.; Inoue, M. *Angew. Chem., Int. Ed.* **2015,** *127,* 1557–1561. doi:10.1002/ange.201410186
21. Hashimoto, T.; Maruoka, K. *Org. Biomol. Chem.* **2008,** *6,* 829–835. doi:10.1039/B716062C
22. Ohfune, Y.; Oe, K.; Namba, K.; Shinada, T. *Heterocycles* **2012,** *85,* 2617–2649. doi:10.3987/REV-12-746
23. Urban, S.; de Almeida Leone, P.; Carroll, A. R.; Fechner, G. A.; Smith, J.; Hooper, J. N. A.; Quinn, R. J. *J. Org. Chem.* **1999,** *64,* 731–735. doi:10.1021/jo981034g
24. Kobayashi, J.; Inaba, K.; Tsuda, M. *Tetrahedron* **1997,** *53,* 16679–16682. doi:10.1016/S0040-4020(97)10097-7
25. Kato, T.; Shizuri, Y.; Izumida, H.; Yokoyama, A.; Endo, M. *Tetrahedron Lett.* **1995,** *36,* 2133–2136. doi:10.1016/0040-4039(95)00194-H
26. Herkommer, D.; Schmalzbauer, B.; Menche, D. *Nat. Prod. Rep.* **2014,** *31,* 456–467. doi:10.1039/C3NP70093C
27. Tang, B.; Wang, L.; Menche, D. *Synlett* **2013,** *24,* 625–629. doi:10.1055/s-0032-1318300
28. Wang, L.; Menche, D. *J. Org. Chem.* **2012,** *77,* 10811–10823. doi:10.1021/jo302102x
29. Wang, L.; Menche, D. *Angew. Chem.* **2012,** *124,* 9559–9562. doi:10.1002/ange.201203911
Angew. Chem., Int. Ed. **2012,** *51,* 9425–9427. doi:10.1002/anie.201203911
30. Wang, L.; Li, P.; Menche, D. *Angew. Chem.* **2010,** *122,* 9456–9460. doi:10.1002/ange.201003304
Angew. Chem., Int. Ed. **2010,** *49,* 9270–9273. doi:10.1002/anie.201003304
31. Morgen, M.; Bretzke, S.; Li, P.; Menche, D. *Org. Lett.* **2010,** *12,* 4494–4497. doi:10.1021/ol101755m
32. Debnar, T.; Dreisigacker, S.; Menche, D. *Chem. Commun.* **2013,** *49,* 725–727. doi:10.1039/C2CC37678D
33. Dieckmann, M.; Menche, D. *Org. Lett.* **2013,** *15,* 228–231. doi:10.1021/ol3033303
34. Schrempp, M.; Thiede, S.; Herkommer, D.; Gansäuer, A.; Menche, D. *Chem. – Eur. J.* **2015,** *21,* 16266–16271. doi:10.1002/chem.201502263
35. Thiede, S.; Winterscheid, P. M.; Hartmann, J.; Schnakenburg, G.; Essig, S.; Menche, D. *Synthesis* **2016,** *48,* 697–709. doi:10.1055/s-0035-1561278
36. Herkommer, D.; Thiede, S.; Wosniok, P. R.; Dreisigacker, S.; Tian, M.; Debnar, T.; Irschik, H.; Menche, D. *J. Am. Chem. Soc.* **2015,** *137,* 4086–4089. doi:10.1021/jacs.5b01894
37. Menche, D.; Arikan, F.; Li, J.; Rudolph, S. *Org. Lett.* **2007,** *9,* 267–270. doi:10.1021/ol062715y
38. Alouane, N.; Boutier, A.; Baron, C.; Vrancken, E.; Mangeney, P. *Synthesis* **2006,** 885–889. doi:10.1055/s-2006-926340
39. Broustal, G.; Ariza, X.; Campagne, J.-M.; Garcia, J.; Georges, Y.; Marinetti, A.; Robiette, R. *Eur. J. Org. Chem.* **2007,** 4293–4297. doi:10.1002/ejoc.200700503
40. Fraunhoffer, K. J.; White, M. C. *J. Am. Chem. Soc.* **2007,** *129,* 7274–7276. doi:10.1021/ja071905g
41. Amador, M.; Ariza, X.; Garcia, J.; Sevilla, S. *Org. Lett.* **2002,** *4,* 4511–4514. doi:10.1021/ol0270428
42. Butler, D. C. D.; Inman, G. A.; Alper, H. *J. Org. Chem.* **2000,** *65,* 5887–5890. doi:10.1021/jo000608q
43. Xie, Y.; Yu, K.; Gu, Z. *J. Org. Chem.* **2014,** *79,* 1289–1302. doi:10.1021/jo402681z
44. Song, Q.-Y.; Yang, B.-L.; Tian, S.-K. *J. Org. Chem.* **2007,** *72,* 5407–5410. doi:10.1021/jo0704558
45. Phukan, P. *J. Org. Chem.* **2004,** *69,* 4005–4006. doi:10.1021/jo0498462
46. Cogan, D. A.; Liu, G.; Ellman, J. *Tetrahedron* **1999,** *55,* 8883–8904. doi:10.1016/S0040-4020(99)00451-2
47. Tang, T. P.; Volkman, S. K.; Ellman, J. A. *J. Org. Chem.* **2001,** *66,* 8772–8778. doi:10.1021/jo0156868
48. Yendapally, R.; Lee, R. E. *Bioorg. Med. Chem. Lett.* **2008,** *18,* 1607–1611. doi:10.1016/j.bmcl.2008.01.065
49. Li, H.; Hong, J.-H. *Bull. Korean Chem. Soc.* **2008,** *29,* 847–850. doi:10.5012/bkcs.2008.29.4.847
50. Herrington, P. M.; Owen, C. E.; Gage, J. R. *Org. Process Res. Dev.* **2001,** *5,* 80–83. doi:10.1021/op0002949
51. Formentín, P.; Gimeno, N.; Steinke, J. H. G.; Vilar, R. *J. Org. Chem.* **2005,** *70,* 8235–8238. doi:10.1021/jo051120y
52. Bourgeois, D.; Pancrazi, A.; Nolan, S. P.; Prunet, J. *J. Organomet. Chem.* **2002,** *643–644,* 247–252. doi:10.1016/S0022-328X(01)01269-4
53. Gimeno, N.; Formentín, P.; Steinke, J. H. G.; Vilar, R. *Eur. J. Org. Chem.* **2007,** 918–924. doi:10.1002/ejoc.200600908
54. Goulaouic-Dubois, C.; Guggisberg, A.; Hesse, M. *Tetrahedron* **1995,** *51,* 12573–12582. doi:10.1016/0040-4020(95)00811-L
55. Knowles, H. S.; Parsons, A. F.; Pettifer, R. M.; Rickling, S. *Tetrahedron* **2000,** *56,* 979–988. doi:10.1016/S0040-4020(00)00025-9
56. Pappo, R.; Allen, D. S., Jr.; Lemieux, R. U.; Johnson, W. S. *J. Org. Chem.* **1956,** *21,* 478–479. doi:10.1021/jo01110a606
57. Yu, W.; Mei, Y.; Kang, Y.; Hua, Z.; Jin, Z. *Org. Lett.* **2004,** *6,* 3217–3219. doi:10.1021/ol0400342

License and Terms

This is an Open Access article under the terms of the Creative Commons Attribution License (http://creativecommons.org/licenses/by/2.0), which permits unrestricted use, distribution, and reproduction in any medium, provided the original work is properly cited.

The license is subject to the *Beilstein Journal of Organic Chemistry* terms and conditions: (http://www.beilstein-journals.org/bjoc)

The definitive version of this article is the electronic one which can be found at: doi:10.3762/bjoc.12.107

BEILSTEIN JOURNAL OF ORGANIC CHEMISTRY

Chiral cyclopentadienylruthenium sulfoxide catalysts for asymmetric redox bicycloisomerization

Barry M. Trost*, Michael C. Ryan and Meera Rao

Full Research Paper

Open Access

Address:
Department of Chemistry, Stanford University, Stanford, California 94305-5580, USA

Email:
Barry M. Trost* - bmtrost@stanford.edu

* Corresponding author

Keywords:
asymmetric catalysis; [3.1.0] bicycles; [4.1.0] bicycles; cycloisomerization; 1,6-enyne; 1,7-enyne; ruthenium catalysis; sulfoxide

Beilstein J. Org. Chem. **2016,** *12,* 1136–1152.
doi:10.3762/bjoc.12.110

Received: 16 March 2016
Accepted: 03 May 2016
Published: 07 June 2016

This article is part of the Thematic Series "Organometallic chemistry" and is dedicated to the memory of Prof. Peter Hofmann.

Guest Editor: L. Gade

© 2016 Trost et al; licensee Beilstein-Institut.
License and terms: see end of document.

Abstract

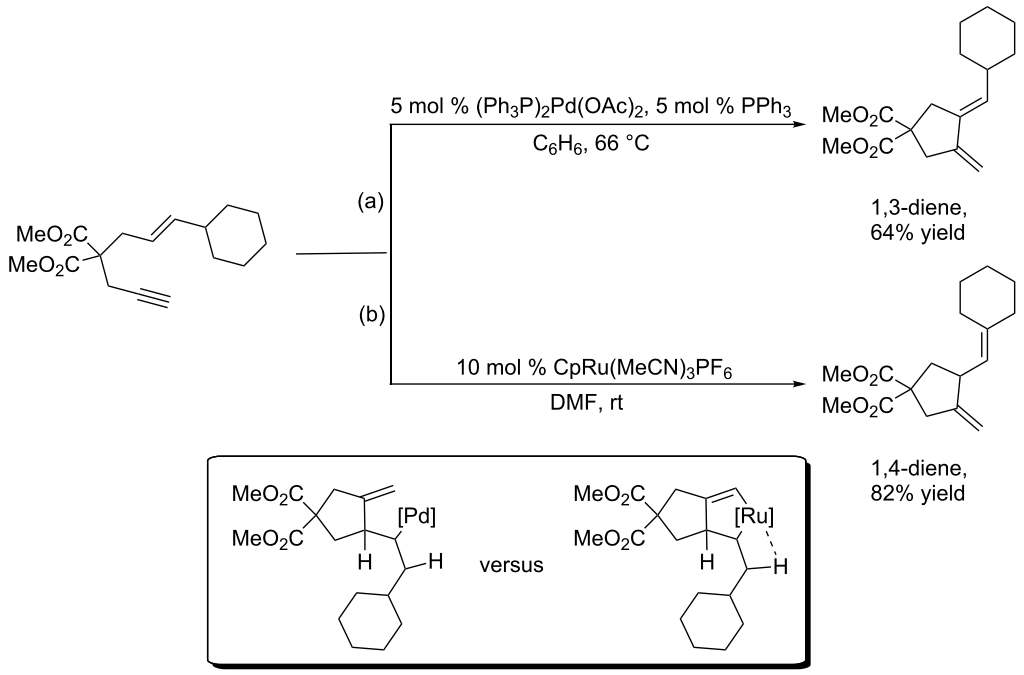
A full account of our efforts toward an asymmetric redox bicycloisomerization reaction is presented in this article. Cyclopentadienylruthenium (CpRu) complexes containing tethered chiral sulfoxides were synthesized via an oxidative [3 + 2] cycloaddition reaction between an alkyne and an allylruthenium complex. Sulfoxide complex **1** containing a *p*-anisole moiety on its sulfoxide proved to be the most efficient and selective catalyst for the asymmetric redox bicycloisomerization of 1,6- and 1,7-enynes. This complex was used to synthesize a broad array of [3.1.0] and [4.1.0] bicycles. Sulfonamide- and phosphoramidate-containing products could be deprotected under reducing conditions. Catalysis performed with enantiomerically enriched propargyl alcohols revealed a matched/mismatched effect that was strongly dependent on the nature of the solvent.

Introduction

Due to their prevalence in natural products [1], medicinal targets [2], and materials [3], organic chemists have made the construction of cyclic, organic molecules one of the most important areas of research in their discipline. Of the available methods to affect cyclization, transition metal-catalyzed enyne cycloisomerizations [4] have been recognized as an atom- [5], step- [6], and redox-economical [7] class of reactions that are able to stitch together cyclic molecules quickly and efficiently.

The very first enyne cycloisomerization reactions were reported by the Trost group while they were synthesizing substrates intended for thermal Alder–ene reactions [8]. They serendipitously discovered that palladium(II) salts catalyzed the cyclization of 1,6-enynes at much lower temperatures compared to the thermal process [9], which normally requires temperatures in excess of 200 °C (Scheme 1, path a).

More recently, the same research group disclosed a $CpRu(MeCN)_3PF_6$-catalyzed variant of the same reaction that proceeds even at room temperature [10]. The ruthenium process differs from the initially-discovered palladium reaction in that it produces cyclic 1,4-dienes exclusively; no olefin isomerization



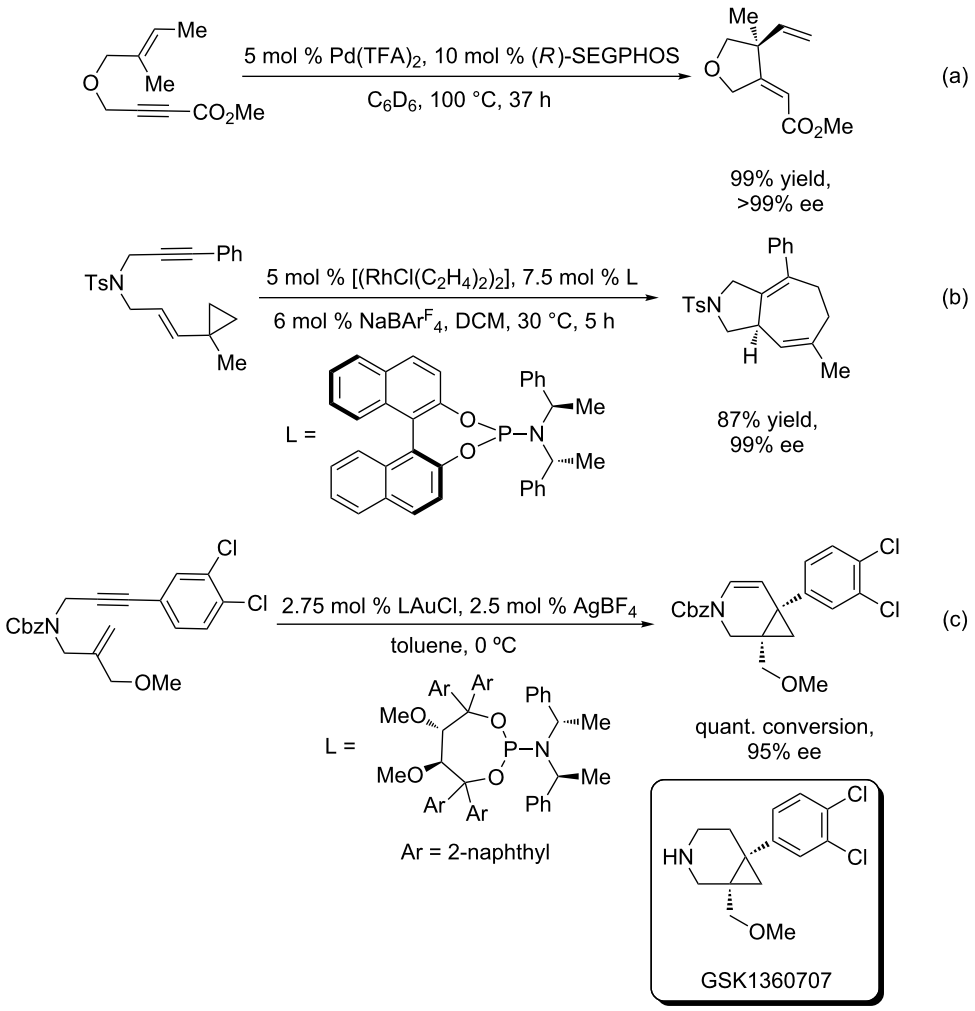
Scheme 1: Divergent behavior of the palladium and ruthenium-catalyzed Alder–ene reaction.

is detected (Scheme 1, path b). Moreover, ruthenium can tolerate many sensitive functional groups, such as free alcohols, silyl enol ethers, and ketones, which makes it an attractive metal for late stage functionalization and elaboration of complex molecules. It is thought that the origin of ruthenium's divergent behavior stems from a difference in reaction mechanism. Whereas the palladium-catalyzed Alder–ene reaction proceeds through an initial hydrometallation of a palladium hydride intermediate, ruthenium is speculated to first form a ruthenacyclopentene prior to β-hydride elimination. Since the hydrogen leading to the 1,3-diene is inaccessible to the ruthenacyclopentene, it must exclusively abstract the exocyclic hydrogen, which results in 1,4-diene formation. Palladium, which is not restricted to a metallacycle, is free to choose either hydrogen, and therefore performs β-hydride elimination on the allylic hydrogen.

Recognizing that enantioenriched, cyclic molecular architectures hold a particular interest to the chemical community, especially in the fields of natural product synthesis and drug design, researchers have made a significant effort to discover asymmetric variations of enyne cycloisomerization reactions [11,12]. Researchers have used a variety of transition metals to affect asymmetric enyne cycloisomerization [13-23]. In particular, Mikami has disclosed a palladium-catalyzed asymmetric enyne cycloisomerization where a tetrahydrofuran containing a quaternary, all-carbon stereocenter is created in excellent yield and selectivity [24] (Scheme 2a). Unfortunately, the scope of this reaction is rather limited, as this is the only example presented in the paper. Mechanistic studies performed by the same group on this system support a hydropalladation/cyclization/β-hydride elimination mechanism. Rhodium catalysis of simple 1,6-enynes displayed a broader scope than Mikami's palladium system, although none of the examples contained a quaternary stereocenter [25].

Asymmetric enyne cycloisomerization reactions can be extended beyond the construction of 1,4-dienes, depending on the transition metal used and the adjacent functionality on the substrate in question. For example, Hayashi has shown that a rhodium/phosphoramidite catalysis is particularly effective for asymmetric [5 + 2] cycloaddition reactions (Scheme 2b). The (*S*,*R*,*R*)-diastereomer of the Feringa-style phosphoramidite ligand proved to be crucial to both the yield and enantioselectivity of this reaction, as there was a severe matched/mismatched effect observed with another diastereomer. In contrast to the ruthenium-catalyzed [5 + 2] cycloaddition of enynes, which is thought to proceed through a ruthenacyclopentene intermediate [26], it has been proposed that rhodium first undergoes oxidative cyclization with the vinylcyclopropane prior to alkyne insertion.

The asymmetric enyne cycloisomerization reaction has been shown to be instrumental in the construction of medicinal chemistry targets. For example, the Fürstner group realized that



Scheme 2: Some asymmetric enyne cycloisomerization reactions.

gold catalysis would be particularly suited for the construction of the [4.1.0] bicyclic piperidine core of GSK1360707 [27], a triple-uptake inhibitor developed by GlaxoSmithKline [28,29] (Scheme 2c). The construction of this interesting molecular scaffold was a motivator of much of our early work on the ruthenium-catalyzed redox bicycloisomerization reaction (vide infra). Unlike ruthenium and palladium enyne cycloisomerization, which operate via metallacycle formation or hydrometallation, gold acts as a π-acid, increasing the electrophilicity of the alkyne by η^2 coordination. The pendant alkene cyclizes on the alkyne, and the resulting tertiary carbocation is trapped by a gold carbenoid intermediate to form the fused cyclopropane.

While there had been reports of utilizing chiral ruthenium complexes for asymmetric catalysis prior to our studies [30-40], there had previously been no reported examples of asymmetric ruthenium-catalyzed cycloisomerization reactions in the literature. In 2011, our research group disclosed the ruthenium-catalyzed redox bicycloisomerization of 1,6- and 1,7-enynes to construct structurally complex [3.1.0] and [4.1.0] bicycles containing vicinal, quaternary all-carbon stereocenters [41] (Figure 1a). The proposed mechanism of this fascinating reaction involves chloride abstraction of the ruthenium catalyst by indium(III) triflate and phosphine ligand dissociation. The propargyl alcohol then coordinates to the now coordinatively unsaturated cyclopentadienylruthenium (CpRu) fragment in a bidentate fashion and undergoes a redox isomerization reaction wherein the carbinol proton performs a 1,2-hydride shift. The resulting vinylruthenium intermediate can be seen as a resonance structure of a ruthenium carbene, which coordinates to a pendant alkene, performs a [2 + 2] cycloaddition to form a ruthenacyclobutane, and reductively eliminates to generate the bicyclic product.

Intrigued by the possibility of rendering this reaction asymmetric, we wondered if an appropriate choice of catalyst,

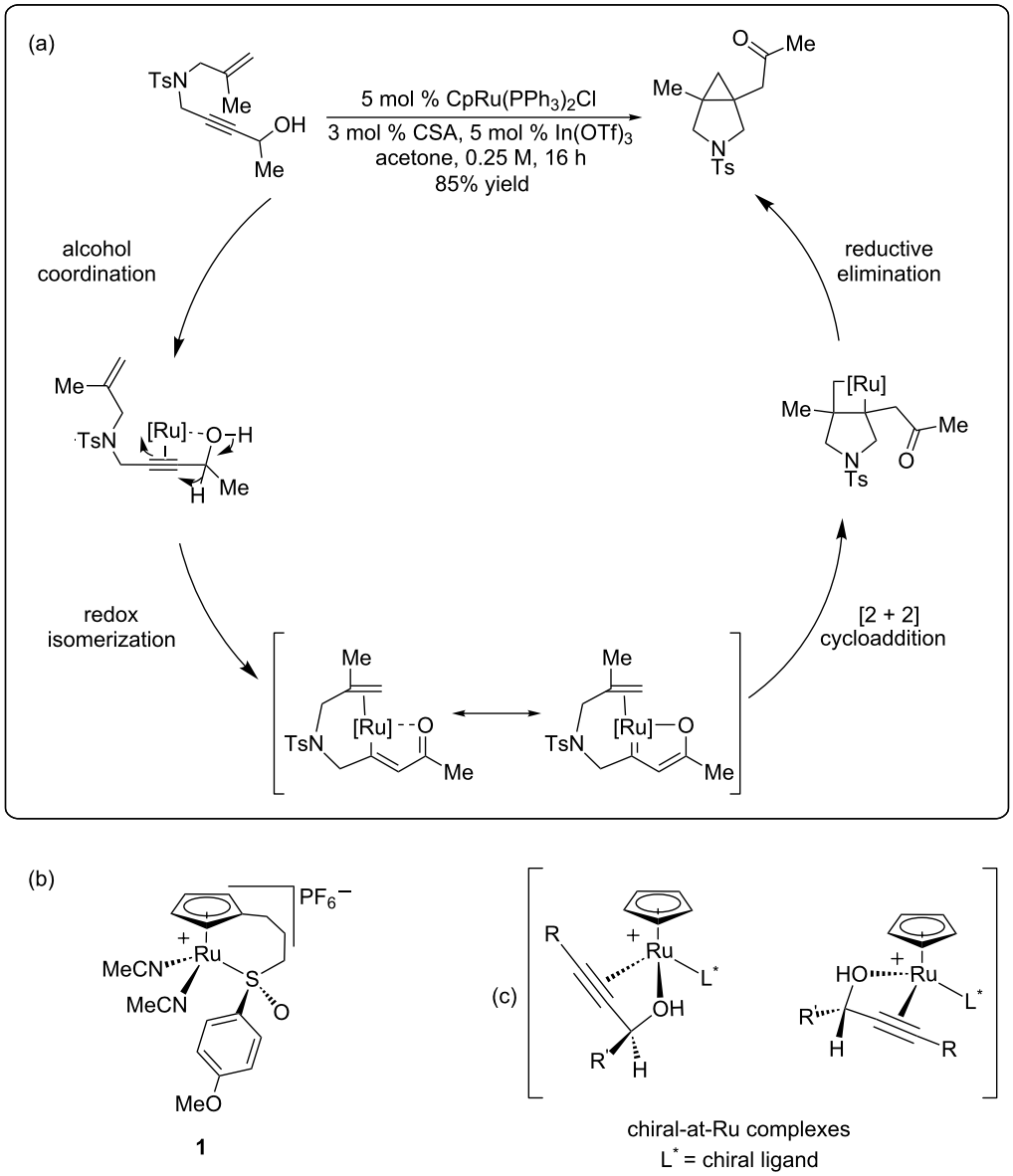


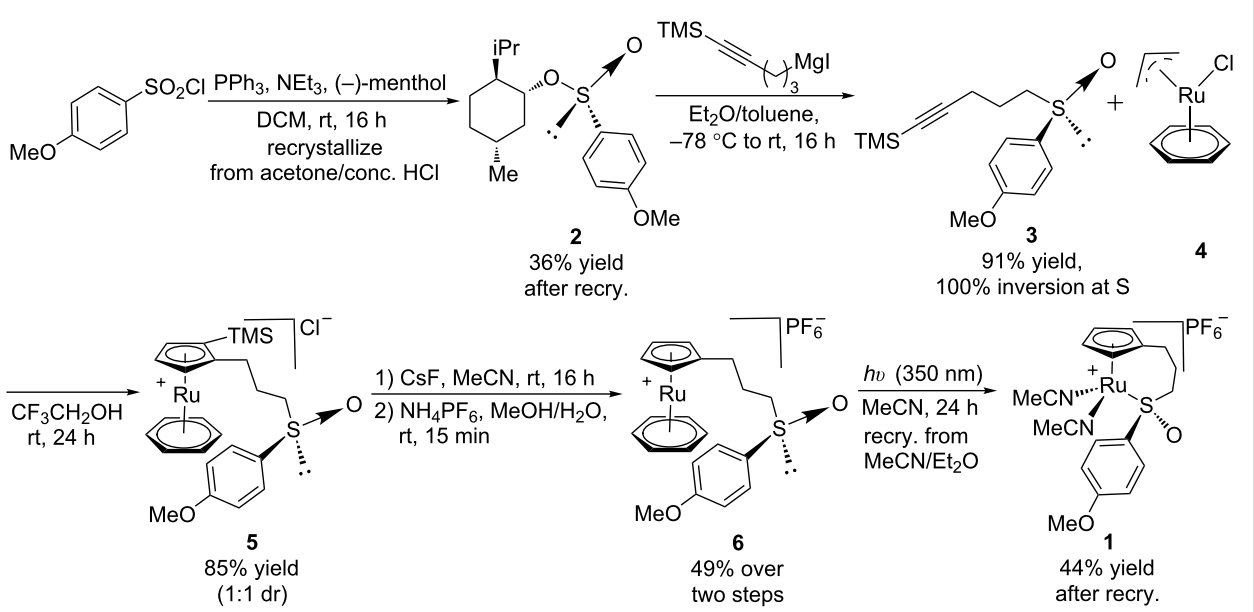
Figure 1: (a) Mechanism for the redox biscycloisomerization reaction. (b) Ruthenium catalyst containing a tethered chiral sulfoxide. (c) Possible diastereomeric complexes formed from alcohol coordination.

namely the chiral CpRu-sulfoxide catalysts **1** our group developed for asymmetric allylic substitution reactions [42] (Figure 1b), would be able to impart sufficiently useful enantioselectivities on these complex, drug-like molecules. While the idea certainly was appealing at first glance, this reaction is complicated by the fact that the 1,6- and 1,7-enyne substrates contain a stereogenic center that, upon coordination to ruthenium, create diastereomeric, chiral-at-ruthenium complexes (Figure 1c). It was unclear a priori whether this transfer of stereochemical information would have an adventitious, negligible, or detrimental impact on the enantioselectivity of the reaction. With this important consideration in mind, we began our search for an asymmetric ruthenium-catalyzed redox bicycloisomerization reaction [43].

Results and Discussion

Catalyst synthesis

Synthesis of CpRu-sulfoxide complexes requires a six-step sequence that was developed in our group [44]. Scheme 3 outlines the synthetic sequence of *p*-anisyl catalyst **1**. In situ reduction of 4-methoxysulfonyl chloride by triphenylphosphine and trapping with (−)-menthol affords diastereomerically pure sulfinate ester **2** after enrichment by recrystallization [45]. Grignard addition attaches a TMS-protected alkyne of appropriate tether



Scheme 3: Synthesis of *p*-anisyl catalyst **1**.

length via stereospecific nucleophilic displacement of the chiral auxiliary with complete inversion of configuration at the sulfur center [46,47]. Sulfoxide **3** is incorporated into the catalyst via a [3 + 2] oxidative cycloaddition with allylruthenium complex **4**. Desilylation of cationic complex **5**, ion exchange, and photolysis of **6** completes the synthesis of catalyst **1**. Using this strategy, a variety of catalysts including *p*-tolyl, 2-naphthyl, 1-naphthyl, and *tert*-butyl sulfoxide complexes were all synthesized in an analogous fashion. This method has a distinct advantage over a traditional CpRu catalyst synthesis in that the complexes can be made quickly and efficiently without relying on toxic thallium salts to transfer substitutionally complex cyclopentadienyl ligands to ruthenium.

While certainly attractive, the main limitation to this synthetic route is that the diastereomeric mixture of sulfinate esters made in the first step is required to either be a solid that can be recrystallized to diastereomeric purity or be separable by column chromatography. Figure 2 contains the attempted sulfinate ester syntheses that failed using the method described in Scheme 3. An alternate method to synthesize these chiral sulfoxides needed to be explored, preferably one that did not rely on crystallization.

In 2005, the Senanayake group described a process in which (+)-norephedrine-derived oxathiazolidine 2-oxides are used as sulfinyl transfer agents in the synthesis of optically pure sulfox-

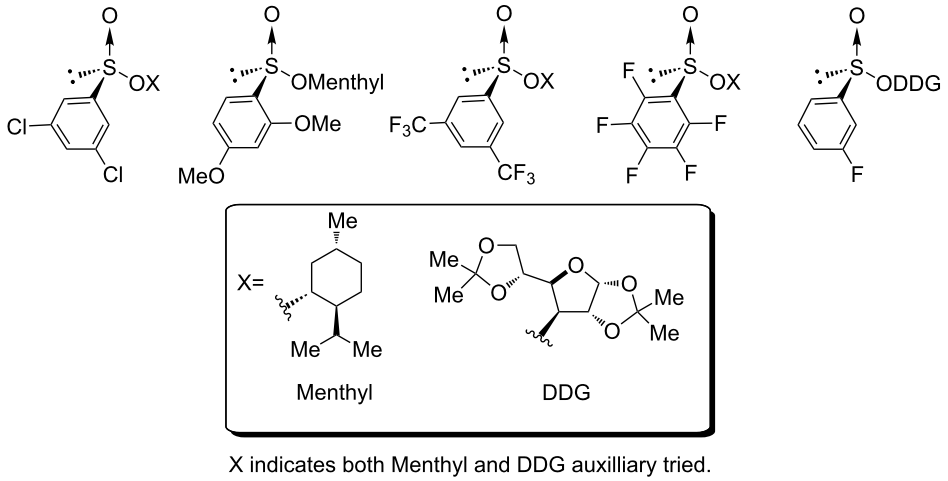


Figure 2: Failed sulfinate ester syntheses.

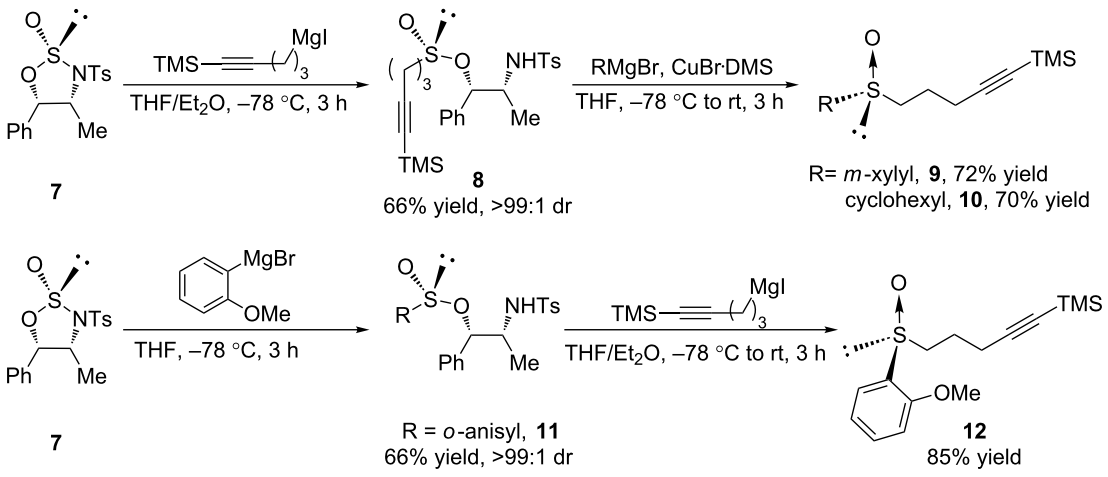
ides and sulfinamides [48]. The application of this method to the synthesis of our chiral sulfoxide tethers is presented in Scheme 4. Tosyl protection of the primary amine of (+)-norephedrine and treatment with thionyl chloride furnishes chiral oxathiazolidine 2-oxide **7** as a single diastereomer in 87% yield over two steps. Heterocycle **7** is a bench stable white powder that can be stored indefinitely in a dessicator without any noticeable decomposition. The sulfonamide moiety activates sulfur towards nucleophilic addition, making the first addition of an organometallic reagent faster than the second. By performing two successive organometallic additions to **7**, one could in principle obtain any desired chiral sulfoxide. Addition of a slight excess of (5-trimethylsilyl)-4-pentynylmagnesium iodide to the auxiliary at −78 °C affords sulfinate ester **8** in a 66% yield and as a single diastereomer. Organocuprate addition to **8** completes the synthesis of tether precursors **9** and **10**. The use of an organocuprate is essential in order to obtain good yields of the desired sulfoxides; the enantiospecificity of this organocuprate addition was checked by comparison of the optical rotation of **3** synthesized by this method with **3** synthesized by the menthyl sulfinate ester method used in Scheme 3. The o-anisyl sulfoxide **12** had to be synthesized in a slightly different manner because the organocuprate addition to **8** failed, most likely due to deactivation of the organometallic by the proximal methoxy group. Instead, sulfinate ester **11** was synthesized and subjected to alkylation with (5-trimethylsilyl)-4-pentynylmagnesium iodide. Because the order of addition was reversed, it is important to note that **12** has the opposite absolute configuration. In this way, sulfoxides containing *m*-xylyl, *o*-methoxyphenyl, and cyclohexyl groups have been made and carried through the remainder of the standard catalyst synthesis as outlined in Scheme 3. None of the catalysts made through this method could be synthesized through separation of sulfinate ester diastereomers.

Substrate synthesis

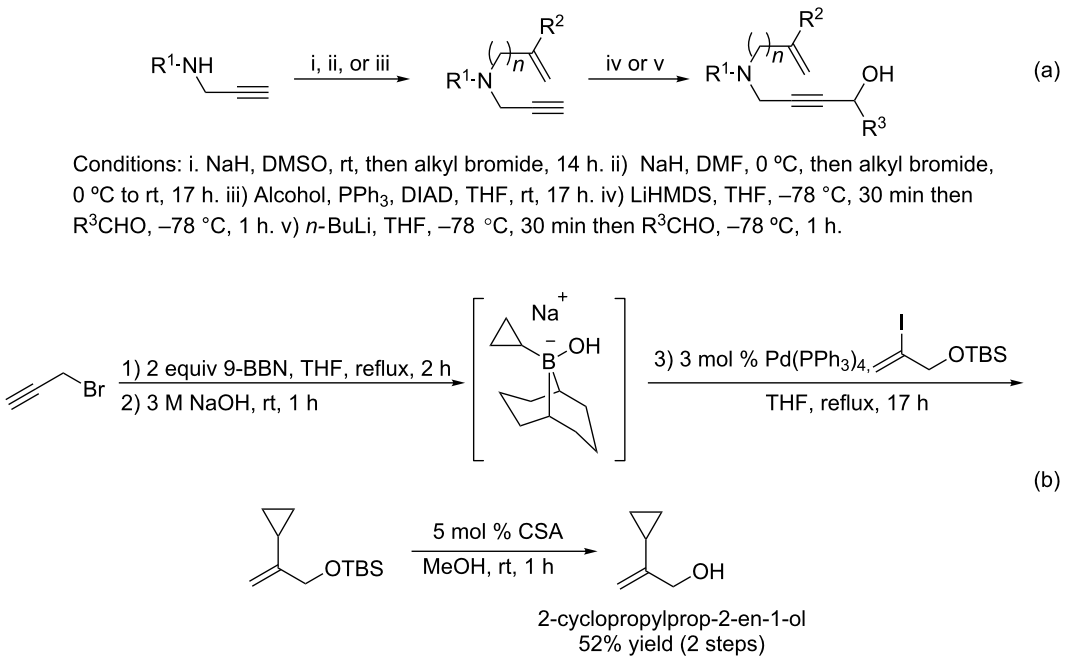
The substrates for the enyne bicycloisomerization reaction can be readily accessed in two steps. Alkylation of a secondary propargylamide can be achieved by sodium hydride deprotonation of its acidic proton and S_N2 substitution of a substituted propargyl bromide (Scheme 5a). Alternatively, the same propargylamide can be alkylated under Mitsunobu conditions with a desired primary alcohol. One such alcohol, 2-cyclopropylprop-2-en-1-ol, can be synthesized using a modified Suzuki coupling procedure developed by Soderquist [49] (Scheme 5b). A cyclopropyl boronate can be generated from propargyl bromide, 9-BBN, and aqueous sodium hydroxide. This reactive intermediate can be used in situ for the subsequent coupling reaction, which constructs the desired allyl alcohol after deprotection in a 52% yield over two steps. After alkylation, the newly-formed enynes can then be deprotonated with either *n*-BuLi or LiHMDS and trapped with an aldehyde to form a substituted propargyl alcohol. With a convenient route towards these enyne substrates in hand, we set our sights on optimizing the asymmetric enyne bicycloisomerization reaction.

Initial experiments and reaction optimization

Due to the similarity of **14** to the triple-uptake inhibitor GSK1360707 (see Scheme 2), we decided to initiate our efforts on 1,7-enyne sulfonamide **13** for reaction optimization. Table 1 showcases our initial experiments. With 3 mol % of CpRu-sulfoxide catalyst **1** in THF at 40 °C, **14** could be obtained in a 69% yield and a promising 26.5:73.5 er (Table 1, entry 1). This important first experiment establishes that **1** not only efficiently catalyzes redox bicycloisomerization, but also that the ligated chiral sulfoxide can induce asymmetry in the [4.1.0] bicyclic product. Indeed, we have shown through control experiments that $CpRu(MeCN)_3PF_6$ does not catalyze this reaction without added ligands, implying that the sulfoxide must be bound to the

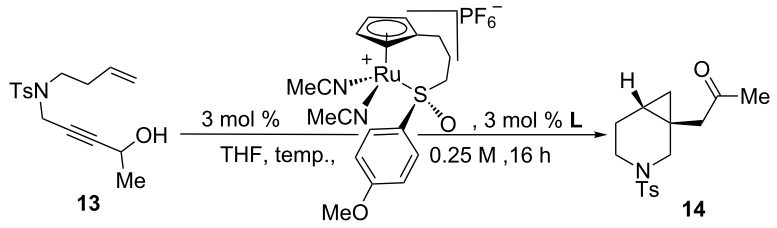


Scheme 4: Using norephedrine-based oxathiazolidine-2-oxide **7** for chiral sulfoxide synthesis.



Scheme 5: (a) General synthetic sequence to access enyne bicycloisomerization substrates (b) Synthesis of 2-cyclopropylprop-2-en-1-ol using a modified Suzuki coupling reaction developed by Soderquist.

Table 1: Initial result for the asymmetric redox bicycloisomerization of 1,7-enyne **13** with chiral CpRu-sulfoxide complex **1** and the effect of added ligands.



entry	ligand	temp. (°C)	conversion (%)[a]	yield (%)	er[b]
1	none	40	100	69	26.5:73.5
2	none	60	100	89	26.0:74.0
3	PPh_3	60	0	n.r.	–
4	$P(OPh)_3$	60	0	n.r.	–
5	(+)-(*R*)-methyl *p*-tolyl sulfoxide	60	100	74	28.0:72.0
6	(+)-(*R*)-methyl *p*-tolyl sulfoxide	40	50	22	41.5:58.5
7	(−)-(*S*)-methyl *p*-tolyl sulfoxide	40	0	N.R.	–
8	(±)-*N*-(*p*-tosyl) methyl *p*-tolyl sulfimide	40	50	22	50.0:50.0

[a]Determined by NMR integration. [b]Determined by chiral HPLC.

metal in order for the reaction to proceed. Raising the temperature to 60 °C had a negligible impact on enantioselectivity (Table 1, entry 2).

Our proposed mechanism of the racemic redox bicycloisomerization reaction necessitates the decomplexation of one phosphine ligand before catalysis can occur (vide supra). In other words, ruthenium must have two open coordination sites in order to bind the substrate. To test if there is a similar requirement for **1**, we decided to add one catalyst equivalent of an auxiliary ligand to test its impact on reaction rate, conversion, and enantioselectivity. Added phosphorous-based ligands only

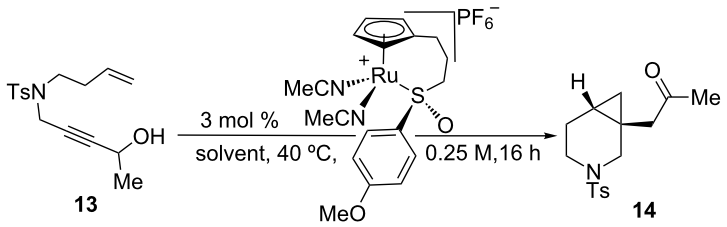
served to completely shut down all reactivity (Table 1, entries 3 and 4). At 60 °C, 3 mol % of chiral (+)-(*R*)-methyl *p*-tolyl sulfoxide had no impact on the reaction, indicating negligible binding of the ligand to the metal (Table 1, entry 5). In general, untethered, exogenous sulfoxides are poorer ligands to ruthenium than phosphines or phosphites. As the reaction temperature is lowered to 40 °C, however, one begins to see a significant decrease in reaction rate and conversion (Table 1, entry 6). The enantioselectivity of the reaction also drops to 41.5:58.5 er Interestingly, (−)-(*S*)-methyl *p*-tolyl sulfoxide completely inhibited any reaction at 40 °C (Table 1, entry 7). Finally, the more electron-withdrawing (±)-*N*-*p*-tosyl methyl *p*-tolyl sulfimide (*p*-CH_3Ph(S=NTs)CH_3) also reduced both conversion and er.

As seen in Table 2, the redox bicycloisomerization reaction is compatible with a number of solvents that have vastly different steric profiles and dielectric constants. The nature of the solvent also had a significant impact on the enantiomeric ratios. Switching from THF to acetone, we observed a dramatic reversal in enantioselectivity, going from 26.5:73.5 to 67.0:33.0, respectively (Table 2, entry 2). Changing the reaction temperature had no impact on the er, similar to the temperature studies done in THF (Table 2, entries 3 and 4).

Initially, we thought that this difference in selectivity between acetone and THF was due to their drastically different steric profiles, so we tested bulkier analogues of these solvents, 2,5-dimethyl THF (mixture of *cis* and *trans*, entry 5) and 3-methyl-2-butanone (Table 2, entry 6). Complex **1** catalyzed the redox bicycloisomerization reaction less efficiently in both solvents. Chlorinated (Table 2, entry 7), aromatic (entry 8), ester (entry 9), and alcohol (entry 10) solvents were all tried, with inferior results to acetone and THF and without any obvious trends in selectivity apparent. Finally, alternative ethereal solvents like 1,4-dioxane (Table 2, entry 11) and DME (entry 12) were checked, as well as the effect of adding a small volume percentage of *N*,*N*-dimethylformamide (Table 2, entries 13 and 14). No improvement in enantioselectivity was observed.

The effect of catalyst structure on the selectivity of the redox bicycloisomerization reaction was explored in both acetone and THF, due to the differential nature of both of these solvents (Table 3). *p*-Tolyl and 2-naphthyl sulfoxide complexes **15** and **16** were both able to catalyze the reaction to complete conversion, although the enantiomeric ratios of **14** were lower than in the *p*-anisyl case. Curiously, the bulkier 1-naphthyl sulfoxide complex **17** was completely ineffective, most likely due to deli-

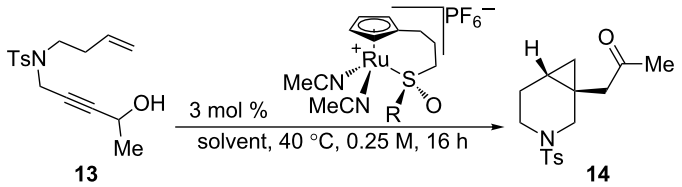
Table 2: Solvent effects on asymmetric redox bicycloisomerization reaction as described in [43].

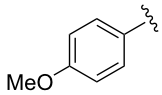
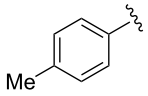
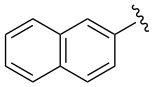
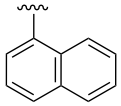
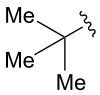
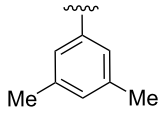
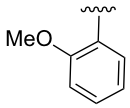
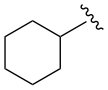


entry	solvent	conversion (%)[a]	yield (%)	er[b]
1	THF	100	69	26.5:**73.5**
2	acetone	100	72	**67.0**:33.0
3[c]	acetone	100	69	**67.0**:33.0
4[d]	acetone	91	n.d.[e]	**66.0**:34.0
5[c]	2,5-Me_2THF[f]	50	17	26.5:**73.5**
6[c]	iPr Me ketone	70	47	**57.5**:42.5
7	DCE	100	66	**60.5**:39.5
8	toluene	59	n.d.[e]	31.5:**68.5**
9	EtOAc	100	65	37.0:**63.0**
10	MeOH	100	80	45.0:**55.0**
11	1,4-dioxane	100	59	32.0:**68.0**
12	DME	100	56	27.0:**73.0**
13	THF[g]	62	13	41.0:**59.0**
14	acetone[g]	88	56	**61.0**:39.0

[a]Determined by NMR integration. [b]Determined by chiral HPLC. [c]Reaction performed at 60 degrees. [d]Reaction performed at room temperature. [e]Not determined due to inseparability from starting substrate. [f]Mixture of *cis* and *trans*. [g]2 vol % DMF added.

Table 3: Effect of the catalyst structure on the redox bicycloisomerization as described in [43].



entry	R	solvent	conversion (%)[a]	yield (%)	er[b]
1	 **1**	acetone THF	100 100	72 69	**67.0**:33.0 26.5:**73.5**
2	 **15**	acetone THF	100 100	72 53	**64.5**:35.5 41.0:**59.0**
3	 **16**	acetone THF	100 100	72 58	**60.5**:39.5 31.5:**68.5**
4	 **17**	acetone THF	0 0	n.r. n.r.	– –
5	 **18**	acetone THF	100 93	69 44	40.5:**59.5** 43.5:**56.5**
6	 **19**	acetone THF	50 82	11 36	**52.0**:48.0 **54.0**:46.0
7[c]	 **20**	acetone THF	100 63	50 30	27.5:**72.5** 22.0:**78.0**
8	 **21**	acetone THF	100 100	70 57	**73.5**:26.5 47.5:**52.5**

[a]Determined by NMR integration. [b]Determined by chiral HPLC. [c]Catalyst enantiomer opposite to the one shown.

gation of the sulfoxide prior to coordination of the substrate (Table 3, entry 4). The more electron-rich, bulky *t*-butyl sulfoxide catalyst **18**, was able to maintain coordination to ruthenium, though the enantiomeric ratios obtained were unsatisfactory (Table 3, entry 5). *m*-Xylyl **19** was similarly disappointing (Table 3, entry 6). However, *o*-anisyl **20** was interesting in that it was able to maintain high enantiomeric ratios of **14** in both THF and acetone and with the same absolute configuration (Table 3, entry 7). This could possibly be due to a chelation effect wherein the *o*-methoxy group acts as a hemilabile ligand, changing the steric and electronic environment around the metal center. Since **20** displayed inferior conversions and yields, however, it was eschewed in favor of complex **1**. Cyclohexyl **21** was also an excellent catalyst in terms of reactivity, but again

this system did not prove to be differential towards the enantiomeric ratio of **14**.

Before moving forward with complex **1**, we wondered how these complexes compare to other catalyst/ligand systems in terms of reactivity (Table 4). After all, complexing an achiral, commercially available catalyst $CpRu(MeCN)_3PF_6$ with a chiral ligand would constitute a much simpler solution to the development of an asymmetric redox bicycloisomerization reaction. To compare the efficiency of each catalyst system, we decided to run the reaction for a shorter period of time, stop the reaction, and check the conversion by proton NMR.

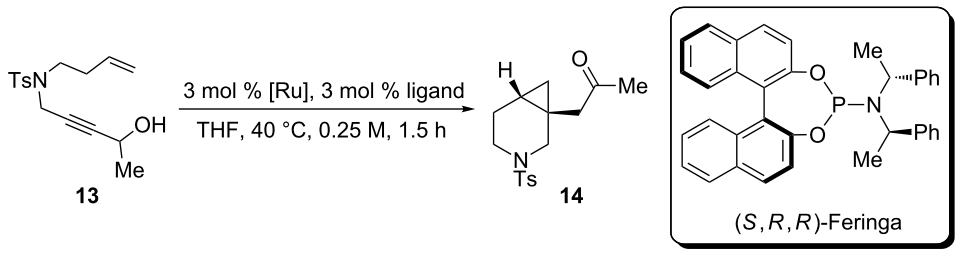
As seen in Table 4, when this experiment is performed with 3 mol % complex **1**, a 54% conversion is observed after 1.5 hours (entry 1). When the same experiment is conducted with 3 mol % of $CpRu(MeCN)_3PF_6$ and 3 mol % triphenylphosphine, the reaction only proceeds to 15% conversion, indicating that the tethered sulfoxide complex is much more efficient at catalyzing redox bicycloisomerization (Table 4, entry 2). As one would expect from the lessons learned in the previous studies, chiral bidentate (*R*)-BINAP completely inhibits any reactivity (Table 4, entry 3). Surprisingly, monodentate (*S,S,R*)-Feringa was also an ineffective ligand for this process, which underscores the stringent electronic requirements a ligand must have in order to promote redox bicycloisomerization (Table 4, entry 4). To date, the only effective ligands for redox bicycloisomerization have been triaryl phosphines, biaryl sulfoxides, or monoaryl monoalkyl sulfoxides. After 1.5 hours, (*S*)-methyl *p*-tolyl sulfoxide also showed no conversion (Table 4, entry 5).

Since subtle changes in the structure of the enyne substrate could have a significant impact on enantioselectivity, variations of the substituent on nitrogen were examined (Table 5). These reactions were conducted in THF, as this solvent provided the highest enantioselectivities in the [4.1.0] system. Incorporating electron rich or electron poor aromatics on the sulfonamide resulted in diminished reactivities and selectivities, as seen in the cases of entries 2 and 3 (Table 5). Surprisingly, 2-biphenyl sulfonamide **26** gave an unimproved 26.0:74.0 er, despite the increased steric bulk on the substrate (Table 5, entry 4). Further increasing the Lewis basicity of the nitrogen completely shuts down catalyst activity, as can be seen in the case of the benzhydryl tertiary amine **28** (Table 5, entry 5). Phosphoramidate **31** could be obtained in good yield and with an increased enantioselectivity when compared to the parent sulfonamide (Table 5, entry 6). Amide **32** also reacted, but with a lower conversion and yield, possibly due to increased coordination of the amide to the Lewis acidic ruthenium center (Table 5, entry 7). Gratifyingly, utilizing the bulkier 2,4,6-triisopropylbenzenesulfonyl group (Tris) significantly improved the er of protected piperidine **35** to 15.0:85.0. Because of its differential impact on selectivity, this protecting group was pursued more broadly in the substrate scope.

Substrate scope

Unfortunately, the conditions developed for the Tris-protected [4.1.0] bicycle **35** did not extend to other similarly protected 1,7-enynes [43]. We decided to shift our focus from 1,7- to 1,6-enynes to determine if bicyclic [3.1.0] pyrrolidines are more broadly accessible to our synthetic method (Table 6). While the 1,6-enyne substrates **36** and **38** exhibited the desired reactivity

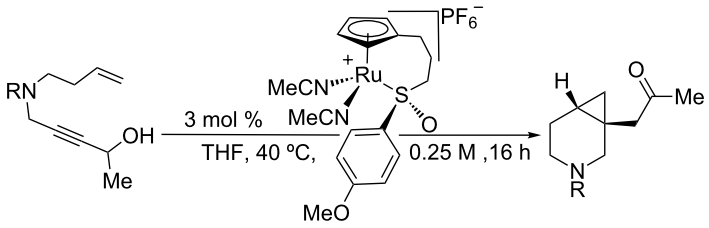
Table 4: Comparison of complex **1** to other catalyst systems as described in [43].

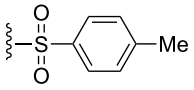
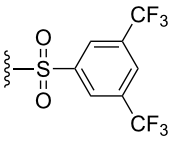
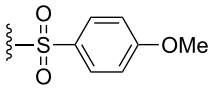
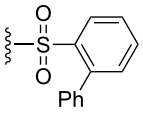
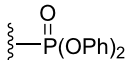
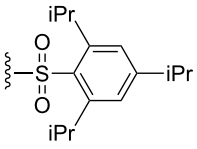


entry	[Ru]	ligand	conversion (%)[a]
1	**1**	none	54
2	$CpRu(MeCN)_3PF_6$	PPh_3	15
3	$CpRu(MeCN)_3PF_6$	(*R*)-BINAP	0
4	$CpRu(MeCN)_3PF_6$	(*S,S,R*)-Feringa	0
5	$CpRu(MeCN)_3PF_6$	(*S*)-methyl *p*-tolyl sulfoxide	0

[a]Determined by ^1H NMR.

Table 5: Effect of the nitrogen protecting group on reactivity and enantioselectivity as described in [43].



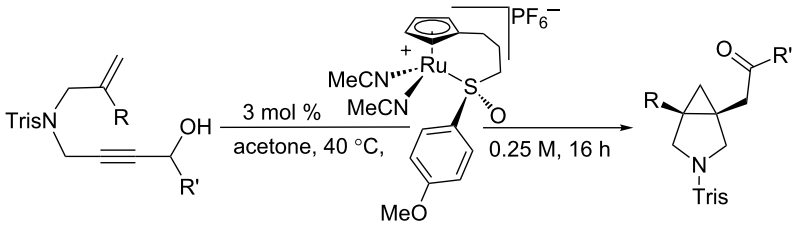
entry	R	substrate	product	yield (%)	er[a,b]
1		**13**	**14**	69	26.5:**73.5**
2		**22**	**23**	21	31.5:**68.5**
3		**24**	**25**	n.d.[c]	43.5:**56.5**
4		**26**	**27**	59	26.0:**74.0**
5		**28**	**29**	n.r.[d]	–
6		**30**	**31**	52	21.0:**79.0**
7		**32**	**33**	45[e]	26.5:**73.5**
8		**34**	**35**	56	15.0:**85.0**

[a]Determined by chiral HPLC. [b](Enantiomer A:Enantiomer B). Absolute configuration not determined. Bold indicates major enantiomer. [c]n.d.= not determined. Conversion ~30%. [d]n.r. = no reaction. [e]Conversion ~50%.

in THF, the enantioselectivities for the process were poor. Considering how impactful a judicious choice of solvent had on the enantioselectivity of the [4.1.0] bicycles, we decided to try the same reactions in acetone. Pleasingly, exceptional yields and enantioselectivities of **37** and **39** were obtained in this solvent, surpassing those obtained for **35**. Catalyst **1** exhibits excellent functional group compatibility. Substrates containing remote electron-neutral aromatic rings **40**, alkenes **42**, and alkynes **44** are all tolerated and remain intact under the reaction conditions. The reaction can also tolerate branching at the internal position of the pendant olefin, as polycyclic **46** and **48** displayed excellent enantiomeric ratios. It is also important to point out that no ring opening of either **49** or its vinylcyclopropane precursor **48** was observed. Finally, styrenyl substrates like **50** can be used for redox bicycloisomerization, but their pyrrolidine products are isolated in somewhat diminished enantioselectivities.

After examining the scope of the redox bicycloisomerization reaction for the synthesis of Tris-protected [3.1.0] pyrrolidines,

Table 6: Tris-protected [3.1.0] bicyclic pyrrolidines made by redox bicycloisomerization[a].

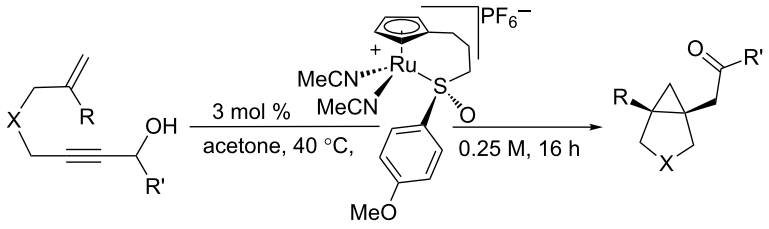


entry	R	R'	enyne	product	Yield (%)	er
1	Me	Me	**36**	**37**	78 85	56.0:44.0[b] 90.5:9.5
2	Me	iPr	**38**	**39**	47 75	64.0:36.0[b] 98.5:1.5
3[c]	Me	Bn	**40**	**41**	88	92.0:8.0
4	Me	-$(CH_2)_8CH{=}CH_2$	**42**	**43**	57	93.0:7.0
5[d]	Me	-$(CH_2)_4C{\equiv}CH_3$	**44**	**45**	48	90.0:10.0
6	cyclopentyl	iPr	**46**	**47**	42	94.0:6.0
7	cyclopropyl	cyclohexyl	**48**	**49**	75	90.0:10.0
8	*p*-tolyl	Me	**50**	**51**	50	82.5:17.5

[a]Tris = 2,4,6-triisopropylbenzenesulfonyl. [b]Reaction conducted in THF. [c]5 mol % of catalyst used. [d]8.5 mol % of catalyst used.

it occurred to us that protecting groups other than Tris may be equally effective for the [3.1.0] system. The Tris group was chosen during our optimization of the six-membered ring system (Table 5), which may have significantly different requirements necessary to achieve high enantioselectivity. Indeed, when tosyl- or phosphoramidate-protected 1,6-enynes were tested, excellent yields and enantioselectivities were observed (Table 7). Like the Tris substrates, branching at the propargylic and alkenyl positions were well tolerated. Carbocyclic **69** could also be isolated with similar results, although

Table 7: Other substrate tethers for redox bicycloisomerization.



entry	X	R	R'	enyne	product	yield (%)	er
1	-NTs	Me	Me	**52**	**53**	81	94.0:6.0
2	-NTs	Me	Bn	**54**	**55**	84	95.0:5.0
3	-NTs	cyclopentyl	iPr	**56**	**57**	56	91.0:9.0
4	-$NP(O)(OPh)_2$	Me	Me	**58**	**59**	84	98.0:2.0
5[a]	-$NP(O)(OPh)_2$	Me	Bn	**60**	**61**	61	97.0:3.0
6	-$NP(O)(OPh)_2$	cyclopentyl	iPr	**62**	**63**	64	96.0:4.0
7	-$NP(O)(OPh)_2$	Me	cyclohexyl	**64**	**65**	51	96.0:4.0
8	-$NP(O)(OPh)_2$	Ph	Me	**66**	**67**	69	88.0:12.0
9[b]	-$C(CO_2Bn)_2$	Me	iPr	**68**	**69**	49	92.0:8.0

[a]5 mol % of catalyst used. [b]7.5 mol % of catalyst used.

the catalyst loading for this substrate had to be increased to 7.5 mol %. This is most likely due to the tendency of ruthenium to coordinate to certain aromatic rings in a η^6 fashion.

There were a few substrate classes that were not amenable to redox bicycloisomerization (Figure 3). For example, we thought that by increasing the steric bulk on styrenyl-substituted compound **50**, either on the aromatic ring or at the propargylic position, the enantioselectivity would also increase. On the contrary, neither substrate **70** or **71** reacted at all, which indicated to us that this substrate class is very sensitive to steric substitution and where it is placed on the enyne. In other words, while both phenyl substitution and branching at the propargylic position are tolerated on separate enyne substrates (see for example **48** and **50**), putting both moieties on the same substrate results in no reaction. Increasing steric congestion near the sulfonamide (substrate **72**) also inhibits enyne bicycloisomerization, as does placing an additional alkyne in conjugation with the pendant alkene (substrate **73**). Both *cis*- and *trans*-1,2-disubstituted alkenes **74** and **75** were observed to decompose under the standard reaction conditions.

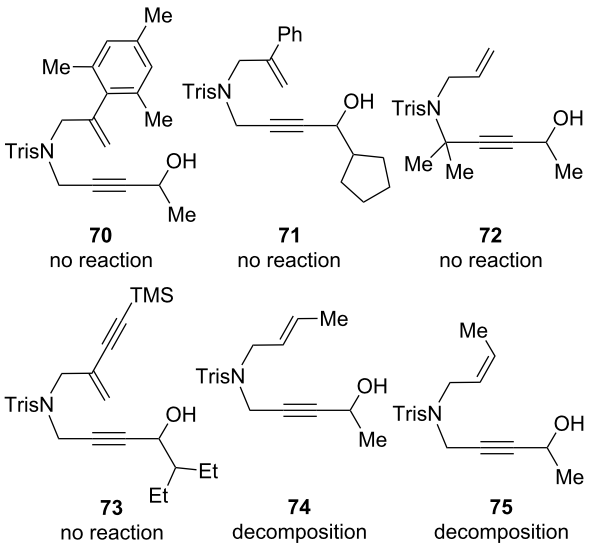
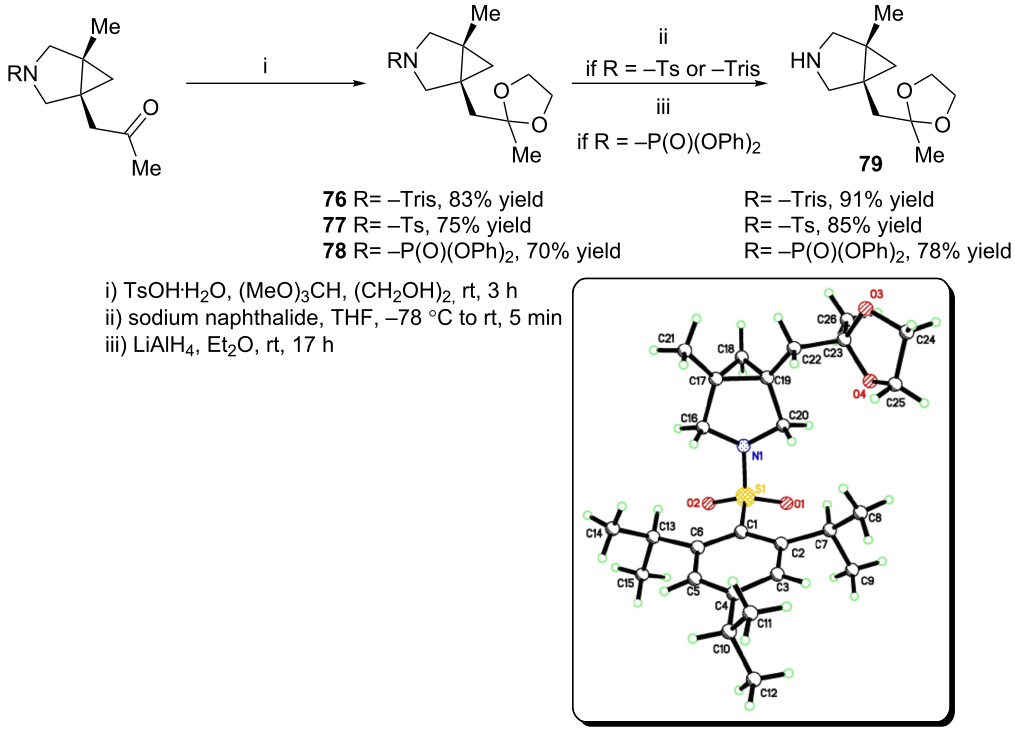


Figure 3: Failed bicycloisomerization substrates. Reactions performed at 40 °C for 16 hours with 3 mol % of catalyst **1** in acetone at a 0.25 M concentration relative to substrate.

The tosyl and 2,4,6-triisopropylbenzenesulfonyl groups on nitrogen can be removed after protection of the ketone as the cyclic acetal by using sodium naphthalide in THF (Scheme 6). After protection, the diphenylphosphoramidate group can also be removed with lithium aluminum hydride in excellent yield. The absolute configuration of the [3.1.0] pyrrolidines was assigned by analogy to **76**, which was determined to be (*R*,*R*) by single crystal X-ray crystallography.



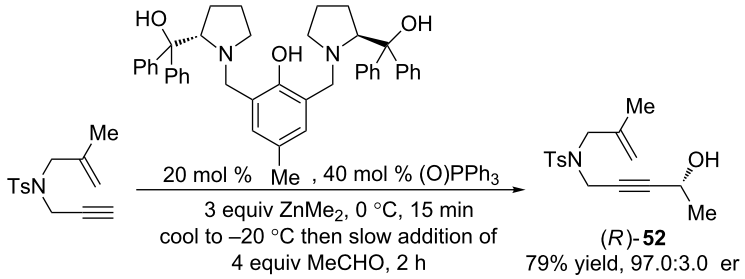
Scheme 6: Deprotection of [3.1.0] bicycles and X-ray crystal structure of **76**.

Mechanistic studies

After having successfully developed this synthetic methodology, a few questions still remained pertaining to the mechanism of the reaction. First, does the propargylic stereocenter on the enyne substrate have a significant impact on the enantioselectivity of the reaction, despite it being destroyed during redox isomerization? Second, what role does the nature of the solvent play in determining enantioselectivity? To answer these questions, we synthesized a 1,6-enyne containing an enantioenriched propargyl alcohol using our group's zinc ProPhenol chemistry (Scheme 7). By employing the opposite enantiomers of the ProPhenol catalyst, either enantiomer of propargyl alcohol can be accessed with this methodology. Additionally, no other attempted synthetic strategy was able to provide (*R*)-**52**, including Noyori and CBS reduction, which highlights the utility of this asymmetric transformation.

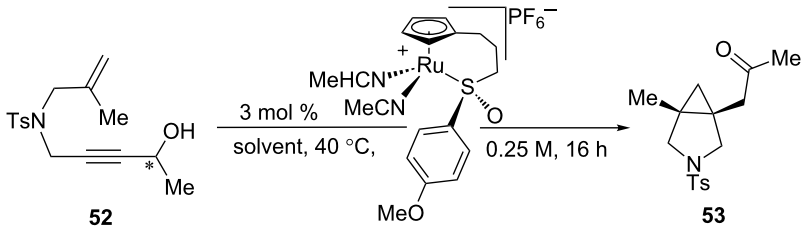
In acetone, the nature of this stereocenter had very little impact on the enantiomeric ratio of the final product, as both (*R*)- and (*S*)-**52** gave results that were almost identical to the racemic substrate (Table 8). Interestingly, however, switching to THF provided drastically different results. While redox bicycloisomerization of (*R*)-**52** was very enantioselective, affording **53** in a 92.0 to 8.0 enantiomeric ratio, (*S*)-**52** performed much worse. Product **53** was isolated in a 68.0 to 32.0 enantiomeric ratio in this case. The same matched/mismatched effect was observed for chiral 1,7-enynes in THF [44]. Based on these results, it is clear that the high enantioselectivity of the redox bicycloisomerization reaction of 1,6-enynes is due to acetone's ability to override any impact the propargylic stereocenter has on the course of the reaction.

Considering the data presented in Table 8, we now propose a working mechanism for the origin of enantioselectivity in the redox bicycloisomerization reaction. There are two important factors to consider when putting together such a mechanism: coordination of the propargyl alcohol on the metal center and facial selectivity for the [2 + 2] cycloaddition. We will look at each in turn. First, coordination by the propargyl alcohol creates four possible diastereomeric, chiral-at-ruthenium intermediates (Figure 4). As long as the metal does not epimerize over the course of the reaction, this transfer of stereochemical informa-



Scheme 7: ProPhenol-catalyzed addition of zinc acetylide to acetaldehyde for the synthesis of a chiral 1,6-enyne substrate.

Table 8: Effect of propargylic stereocenter on enantioselectivity.



entry	solvent	alcohol configuration	yield (%)	er
1	acetone	*rac*	81	94.0:6.0
2	acetone	(*R*)[a]	84	93.5:6.5
3	acetone	(*S*)[a]	81	96.5:3.5
4	THF	*rac*	52	80.0:20.0
5	THF	(*R*)[a]	61	92.0:8.0
6	THF	(*S*)[a]	52	68.0:32.0

[a]Starting alcohol has a 97.0:3.0 er.

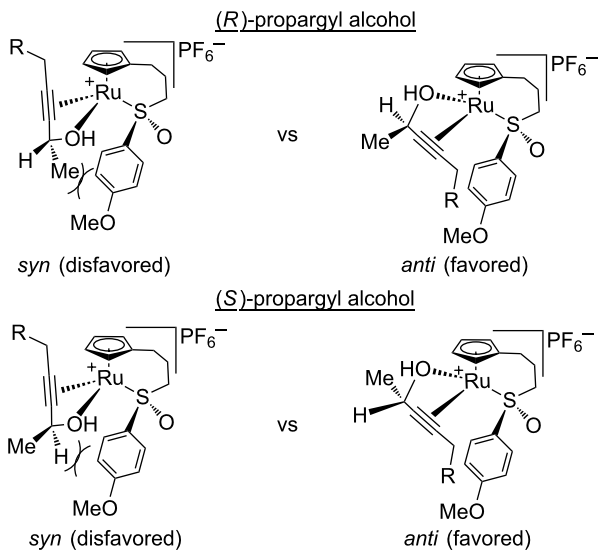
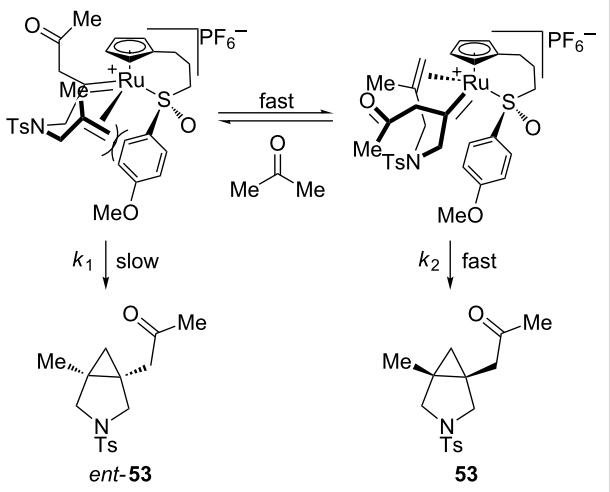


Figure 4: Diastereomeric metal complexes formed after alcohol coordination.

tion can then be transferred back to the substrate following redox isomerization, influencing the overall enantioselectivity of the process. For both the (*R*)- and the (*S*)-propargyl alcohols, the CpRu-sulfoxide catalyst prefers to place the stereocenter away from the steric bulk of the sulfoxide (*anti* configuration). Both *syn* configurations are disfavored, but the *syn*-(*R*)-configuration is energetically more taxing than the *syn*-(*S*)-configuration, creating a larger energy difference between *syn*-(*R*) and *anti*-(*R*). This larger energy difference is reflected in the higher enantioselectivities obtained for the (*R*) enantiomer in THF (Table 8, entry 5). The smaller energetic difference between *syn*-(*S*) and *anti*-(*S*) means that there is less of a preference for either coordination mode, which leads to poorer enantioselectivities in THF (Table 8, entry 6).

We propose that acetone, being more Lewis basic than THF, has the effect of epimerizing the chiral-at-ruthenium intermediates formed prior to [2 + 2] cycloaddition. The rate of epimerization is much faster than the [2 + 2] cycloaddition, creating a classic Curtin–Hammitt scenario wherein all of the substrate is funneled into the observed enantiomer of product (Scheme 8). Rate k_1 is much slower than k_2 due to the severe steric hindrance imposed by the ligated chiral sulfoxide, which block alkene coordination. The pendant olefin prefers to approach the carbene *anti* to the aforementioned sulfoxide, resulting in the observed enantiomer of **53**. In THF, the rate of epimerization is significantly slower than the [2 + 2] cycloaddition, which means that the enantiomeric ratios observed in the products are affected more by the initial coordination of the propargyl alcohol.



Scheme 8: Curtin–Hammitt scenario of redox bicycloisomerization in acetone.

Conclusion

In conclusion, we have developed a ruthenium-catalyzed asymmetric redox bicycloisomerization utilizing a chiral CpRu–sulfoxide complex **1**. This constitutes the first example of an asymmetric ruthenium-catalyzed redox isomerization known to date. We were able to demonstrate that the nitrogen protecting group on the 1,7-enynes had a significant impact on the enantioselectivity of the redox bicycloisomerization as did the choice of solvent. Extending the chemistry to the 1,6-enynes, we showed that these substrates were much more amenable to a wider range of groups on nitrogen, though a significant solvent effect was still observed in these cases. The mechanism of the reaction was then probed by performing the redox isomerization reaction on enantioenriched propargyl alcohols. While a significant matched/mismatched effect was observed in THF, no such effect was seen in acetone. We postulate that there are two different enantiodetermining steps that center around a chosen solvent's ability to epimerize a metal center following redox isomerization.

Supporting Information

Supporting Information File 1

Experimental details and NMR data of new catalysts.
[http://www.beilstein-journals.org/bjoc/content/supplementary/1860-5397-12-110-S1.pdf]

Supporting Information File 2

X-ray crystallography data for **76**.
[http://www.beilstein-journals.org/bjoc/content/supplementary/1860-5397-12-110-S2.cif]

Acknowledgements

We would like to thank the NSF for their generous support (NSF-CHE-1360634).

References

1. Nicolaou, K. C.; Vourloumis, D.; Winssinger, N.; Baran, P. S. *Angew. Chem., Int. Ed.* **2000,** *39,* 44. doi:10.1002/(SICI)1521-3773(20000103)39:1<44::AID-ANIE44>3.0.CO;2-L
2. Babine, R. E.; Bender, S. L. *Chem. Rev.* **1997,** *97,* 1359. doi:10.1021/cr960370z
3. Laurent, B. A.; Grayson, S. M. *Chem. Soc. Rev.* **2009,** *38,* 2202. doi:10.1039/b809916m
4. Michelet, V.; Toullec, P. Y.; Genêt, J.-P. *Angew. Chem., Int. Ed.* **2008,** *47,* 4268. doi:10.1002/anie.200701589
   See for a review on enyne cycloisomerizations.
5. Trost, B. M. *Science* **1991,** *254,* 1471. doi:10.1126/science.1962206
6. Wender, P. A.; Verma, V. A.; Paxton, T. J.; Pillow, T. H. *Acc. Chem. Res.* **2008,** *41,* 40. doi:10.1021/ar700155p
7. Burns, N. Z.; Baran, P. S.; Hoffmann, R. W. *Angew. Chem., Int. Ed.* **2009,** *48,* 2854. doi:10.1002/anie.200806086
8. Trost, B. M.; Lautens, M. *J. Am. Chem. Soc.* **1985,** *107,* 1781. doi:10.1021/ja00292a065
9. Oppolzer, W.; Snieckus, V. *Angew. Chem., Int. Ed. Engl.* **1978,** *17,* 476. doi:10.1002/anie.197804761
   See for a review on thermal ene reactions.
10. Trost, B. M.; Toste, F. D. *J. Am. Chem. Soc.* **2000,** *122,* 714. doi:10.1021/ja993401r
11. Fairlamb, I. J. S. *Angew. Chem., Int. Ed.* **2004,** *43,* 1048. doi:10.1002/anie.200301699
12. Watson, I. D. G.; Toste, F. D. *Chem. Sci.* **2012,** *3,* 2899. doi:10.1039/c2sc20542d
13. Chao, C.-M.; Vitale, M. R.; Toullec, P. Y.; Genêt, J.-P.; Michelet, V. *Chem. – Eur. J.* **2009,** *15,* 1319. doi:10.1002/chem.200802341
14. Watson, I. D. G.; Ritter, S.; Toste, F. D. *J. Am. Chem. Soc.* **2009,** *131,* 2056. doi:10.1021/ja8085005
15. Martínez, A.; García-García, P.; Fernández-Rodríguez, M. A.; Rodríguez, F.; Sanz, R. *Angew. Chem., Int. Ed.* **2010,** *49,* 4633. doi:10.1002/anie.201001089
16. Brissy, D.; Skander, M.; Jullien, H.; Retailleau, P.; Marinetti, A. *Org. Lett.* **2009,** *11,* 2137. doi:10.1021/ol900724z
17. Jullien, H.; Brissy, D.; Sylvain, R.; Retailleau, P.; Naubron, J.-V.; Gladiali, S.; Marinetti, A. *Adv. Synth. Catal.* **2011,** *353,* 1109. doi:10.1002/adsc.201000904
18. Goeke, A.; Kuwano, R.; Ito, Y.; Sawamura, M. *Angew. Chem., Int. Ed. Engl.* **1996,** *35,* 662. doi:10.1002/anie.199606621
19. Zhang, Q.; Lu, X.; Han, X. *J. Org. Chem.* **2001,** *66,* 7676. doi:10.1021/jo0105181
20. Hatano, M.; Mikami, K. *J. Am. Chem. Soc.* **2003,** *125,* 4704. doi:10.1021/ja0292748
21. Shintani, R.; Nakatsu, H.; Takatsu, K.; Hayashi, T. *Chem. – Eur. J.* **2009,** *15,* 8692. doi:10.1002/chem.200901463
22. Nicolaou, K. C.; Li, A.; Ellery, S. P.; Edmonds, D. J. *Angew. Chem., Int. Ed.* **2009,** *48,* 6293. doi:10.1002/anie.200901992
23. Nishimura, T.; Maeda, Y.; Hayashi, T. *Org. Lett.* **2011,** *13,* 3674. doi:10.1021/ol2013236
24. Hatano, M.; Terada, M.; Mikami, K. *Angew. Chem., Int. Ed.* **2001,** *40,* 249. doi:10.1002/1521-3773(20010105)40:1<249::AID-ANIE249>3.0.CO;2-X
25. Cao, P.; Zhang, X. *Angew. Chem., Int. Ed.* **2000,** *39,* 4104. doi:10.1002/1521-3773(20001117)39:22<4104::AID-ANIE4104>3.0.CO;2-X
26. Trost, B. M.; Toste, F. D.; Shen, H. *J. Am. Chem. Soc.* **2000,** *122,* 2379. doi:10.1021/ja993400z
27. Teller, H.; Fürstner, A. *Chem. – Eur. J.* **2011,** *17,* 7764. doi:10.1002/chem.201101346
28. Bertani, B.; Di Fabio, R.; Micheli, F.; Tedesco, G.; Terreni, S. WO 2008031772A1, 2008.
29. Micheli, F.; Cavanni, P.; Andreotti, D.; Arban, R.; Benedetti, R.; Bertani, B.; Bettati, M.; Bettelini, L.; Bonanomi, G.; Braggio, S.; Carletti, R.; Checchia, A.; Corsi, M.; Fazzolari, E.; Fontana, S.; Marchioro, C.; Merlo-Pich, E.; Negri, M.; Oliosi, B.; Ratti, E.; Read, K. D.; Roscic, M.; Sartori, I.; Spada, S.; Tedesco, G.; Tarsi, L.; Terreni, S.; Visentini, F.; Zocchi, A.; Zonzini, L.; Di Fabio, R. *J. Med. Chem.* **2010,** *53,* 4989–5001. doi:10.1021/jm100481d
30. Kündig, E. P.; Saudan, C. M.; Bernardinelli, G. *Angew. Chem., Int. Ed.* **1999,** *38,* 1219–1223. doi:10.1002/(SICI)1521-3773(19990503)38:9<1219::AID-ANIE1219>3.0.CO;2-D
31. Brinkmann, Y.; Madhushaw, R. J.; Jazzar, R.; Bernardinelli, G.; Kündig, E. P. *Tetrahedron* **2007,** *63,* 8413–8419. doi:10.1016/j.tet.2007.06.033
32. Bădoiu, A.; Bernardinelli, G.; Mareda, J.; Kündig, E. P.; Viton, F. *Chem. – Asian J.* **2008,** *3,* 1298–1311. doi:10.1002/asia.200800063
33. Maas, G. *Chem. Soc. Rev.* **2004,** *33,* 183–190. doi:10.1039/b309046a
34. Nishiyama, H. Cyclopropanation with Ruthenium Catalysts. In *Ruthenium Catalysts and Fine Chemistry;* Bruneau, C.; Dixneuf, P. H., Eds.; Topics in Organometallic Chemistry, Vol. 11; Springer: Berlin, Germany, 2004; pp 81–92.
   And references therein.
35. Matsushima, Y.; Onitsuka, K.; Kondo, T.; Mitsudo, T.-a.; Takahashi, S. *J. Am. Chem. Soc.* **2001,** *123,* 10405–10406. doi:10.1021/ja016334l
36. Onitsuka, K.; Matsushima, Y.; Takahashi, S. *Organometallics* **2005,** *24,* 6472–6474. doi:10.1021/om050739n
37. Onitsuka, K.; Okuda, H.; Sasai, H. *Angew. Chem., Int. Ed.* **2008,** *47,* 1454–1457. doi:10.1002/anie.200704457
38. Kanbayashi, N.; Onitsuka, K. *J. Am. Chem. Soc.* **2010,** *132,* 1206–1207. doi:10.1021/ja908456b
39. Kanbayashi, N.; Onitsuka, K. *Angew. Chem., Int. Ed.* **2011,** *50,* 5197–5199. doi:10.1002/anie.201101078
40. Kanbayashi, N.; Takenaka, K.; Okamura, T.-a.; Onitsuka, K. *Angew. Chem., Int. Ed.* **2013,** *52,* 4897–4901. doi:10.1002/anie.201300485
41. Trost, B. M.; Breder, A.; O'Keefe, B. M.; Rao, M.; Franz, A. W. *J. Am. Chem. Soc.* **2011,** *133,* 4766. doi:10.1021/ja200971v
42. Trost, B. M.; Rao, M.; Dieskau, A. P. *J. Am. Chem. Soc.* **2013,** *135,* 18697. doi:10.1021/ja411310w
43. Trost, B. M.; Ryan, M. C.; Rao, M.; Markovic, T. Z. *J. Am. Chem. Soc.* **2014,** *136,* 17422. doi:10.1021/ja510968h
   See for a leading communication on the study presented herein.
44. Rao, M. Development Of Optically Active Cyclopentadienyl Ruthenium Complexes and Their Application in Asymmetric Catalysis. Ph.D. Thesis, Stanford University, Stanford, CA, U.S.A., 2013.

45. Watanabe, Y.; Mase, N.; Tateyama, M.-a.; Toru, T. *Tetrahedron: Asymmetry* **1999,** *10,* 737. doi:10.1016/S0957-4166(99)00066-X
46. Andersen, K. K. *Tetrahedron Lett.* **1962,** *3,* 93. doi:10.1016/S0040-4039(00)71106-3
47. Andersen, K. K.; Gaffield, W.; Papanikolaou, N. E.; Foley, J. W.; Perkins, R. I. *J. Am. Chem. Soc.* **1964,** *86,* 5637. doi:10.1021/ja01078a047
48. Han, Z.; Krishnamurthy, D.; Grover, P.; Fang, Q. K.; Su, X.; Wilkinson, H. S.; Lu, Z.-H.; Magiera, D.; Senanayake, C. H. *Tetrahedron* **2005,** *61,* 6386. doi:10.1016/j.tet.2005.03.122
49. Soderquist, J. A.; Huertas, R.; Leon-Colon, G. *Tetrahedron Lett.* **2000,** *41,* 4251–4255. doi:10.1016/S0040-4039(00)00605-5

License and Terms

This is an Open Access article under the terms of the Creative Commons Attribution License (http://creativecommons.org/licenses/by/2.0), which permits unrestricted use, distribution, and reproduction in any medium, provided the original work is properly cited.

The license is subject to the *Beilstein Journal of Organic Chemistry* terms and conditions: (http://www.beilstein-journals.org/bjoc)

The definitive version of this article is the electronic one which can be found at: doi:10.3762/bjoc.12.110

BEILSTEIN JOURNAL OF ORGANIC CHEMISTRY

Stereoselective synthesis of tricyclic compounds by intramolecular palladium-catalyzed addition of aryl iodides to carbonyl groups

Jakub Saadi, Christoph Bentz, Kai Redies, Dieter Lentz, Reinhold Zimmer and Hans-Ulrich Reissig*

Full Research Paper

Open Access

Address:
Freie Universität Berlin, Institut für Chemie und Biochemie, Takustrasse 3, D-14195 Berlin, Germany

Email:
Hans-Ulrich Reissig* - hreissig@chemie.fu-berlin.de

* Corresponding author

Keywords:
1,2-addition; aryl iodides; ketones; nucleophilic addition; palladium catalysis

Beilstein J. Org. Chem. **2016,** *12,* 1236–1242.
doi:10.3762/bjoc.12.118

Received: 29 March 2016
Accepted: 01 June 2016
Published: 16 June 2016

This article is part of the Thematic Series "Organometallic chemistry" and is dedicated to the memory of Professor Peter Hofmann.

Guest Editor: B. F. Straub

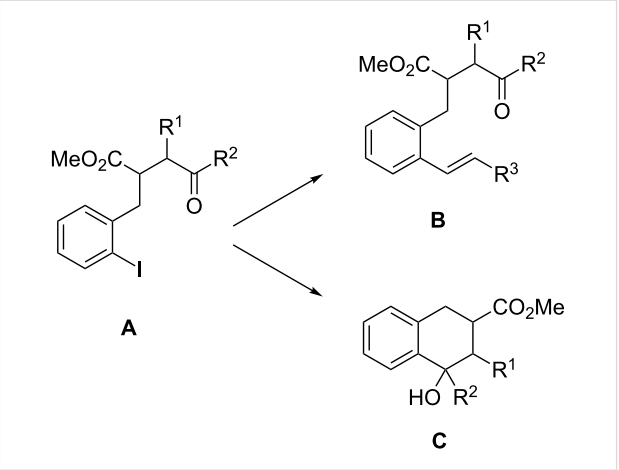
© 2016 Saadi et al.; licensee Beilstein-Institut.
License and terms: see end of document.

Abstract

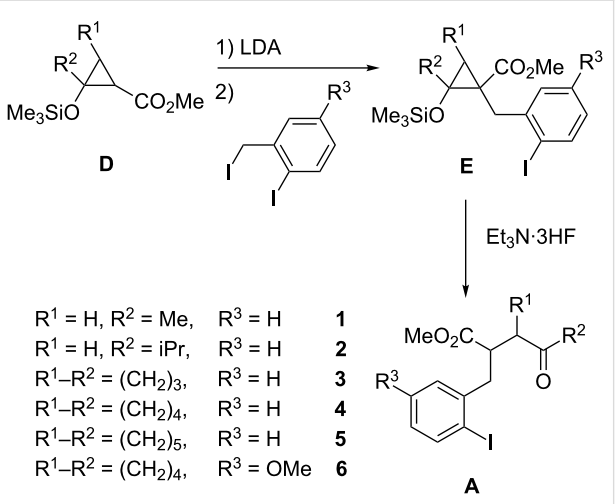
Starting from γ-ketoesters with an *o*-iodobenzyl group we studied a palladium-catalyzed cyclization process that stereoselectively led to bi- and tricyclic compounds in moderate to excellent yields. Four X-ray crystal structure analyses unequivocally defined the structure of crucial cyclization products. The relative configuration of the precursor compounds is essentially transferred to that of the products and the formed hydroxy group in the newly generated cyclohexane ring is consistently in *trans*-arrangement with respect to the methoxycarbonyl group. A transition-state model is proposed to explain the observed stereochemical outcome. This palladium-catalyzed Barbier-type reaction requires a reduction of palladium(II) back to palladium(0) which is apparently achieved by the present triethylamine.

Introduction

For our systematic studies on samarium diiodide promoted cyclizations leading to benzannulated medium-sized rings [1-4] we required starting materials such as alkenyl-substituted compounds **B** (Scheme 1). Obvious precursors for **B** are aryl iodides **A** that smoothly undergo palladium-catalyzed coupling reactions to provide the desired products. However, in one case [**A**: R^1–R^2 = $(CH_2)_4$] typical Heck reaction conditions employing styrene as olefin component not only led to the desired styrene derivative **B** but mainly to the cyclized product **C**. If the reaction was performed without the olefin it provided only the tertiary alcohol **C** in reasonable yield [5]. Similar C–C bond forming reactions of aryl halides that involve an insertion of the



Scheme 1: Planned Heck reaction of **A** to compound **B** and serendipitous discovery of the palladium-catalyzed cyclization to products **C**.



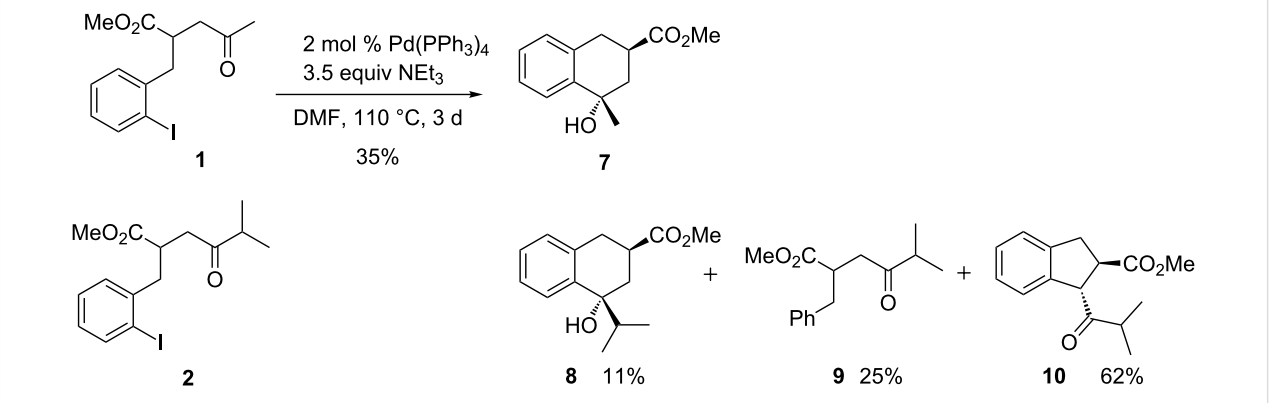
Scheme 2: Synthesis of compounds **A** (**1**–**6**) via methyl 2-siloxycyclopropanecarboxylates **D**, their alkylation to **E** and fluoride-induced ring opening.

intermediate aryl palladium species into a carbonyl group are relatively rare (see discussion below). Therefore this serendipitous discovery led us to investigate the reaction in more detail.

Results

The required γ-ketoesters **A** bearing the aryl iodide substituent were prepared following our well-established route via 2-siloxycyclopropane carboxylates **D** [6,7] that allows a regioselective introduction of the benzylic substituents at the α-carbon [8,9] to give intermediates **E** (Scheme 2). After fluoride-promoted ring opening [10] the desired precursor compounds **A** (**1**–**6**) were obtained in reasonable overall efficacies (for details see Supporting Information File 1).

We start our report with the palladium-catalyzed reactions of simple alkyl ketones **1** and **2** leading to bicyclic products and then continue with the transformations of cyclic ketones **3**–**6** that led to tricyclic compounds. Methyl ketone **1** provided under the reaction conditions (2 mol % $Pd(PPh_3)_4$, 3.5 equivalents NEt_3, DMF, 110 °C, 3 d) that had been optimized with compound **4** a moderate yield of the tetralin derivative **7** formed as a single diastereomer (Scheme 3). Although the configurational assignment is ambiguous in this case, the NMR data and the fact that no γ-lactone is formed strongly support the *trans*-arrangement of the two functional groups as depicted. Under similar conditions (5 mol % $Pd(PPh_3)_4$, 90 °C, 3 d) the isopropyl-substituted ketone **2** furnished a mixture of the related *trans*-compound **8** (11%) together with the de-iodinated product **9** (25%) and the indane derivative **10** as major component (62%). The C–C coupling reaction to **8** seems to be hindered in this case, probably due to the steric bulk of the isopropyl group. The formation of indane derivative **10** occurs by an intramolecular enolate arylation, a reaction that has been discovered by our group some years ago [11,12]. Apparently, under the reaction conditions a ketone enolate of **2** reacts with the iodoarene moiety to form the five-membered ring of **10**. The configura-



Scheme 3: Palladium-catalyzed reactions of methyl ketone **1** to tetralin derivative **7** and of isopropyl-substituted ketone **2** to compounds **8**, **9** and **10**.

tional assignments of compounds **7** and **8** are in agreement with those discussed below, where X-ray crystal structure analyses unequivocally confirmed the relative configurations of cyclization products.

With the cyclic ketones in part considerably higher yields of tricyclic products could be obtained (Schemes 4–6). The cyclopentanone derivative **3** (Scheme 4) had to be used as a mixture of two diastereomers (ca. 2:1) since these were not separable in our hands. Under the standard reaction conditions this ketone furnished a mixture of two diastereomeric tricyclic products **11a** and **11b** in 35% combined yield. The configuration of **11a** was unequivocally determined by an X-ray crystal structure analysis of the corresponding *p*-nitrobenzoate **12a** obtained by esterification of the tertiary alcohol under standard conditions (Scheme 4, Figure 1) [13]. The configuration of the second product **11b** is only tentatively assigned as depicted since the available data do not allow an unambiguous determination. Considering the result obtained with the cycloheptanone derivative where two diastereomers could be assigned by X-ray crystal structure analyses make the proposed *trans*-annulation of the five- and six-membered rings fairly likely.

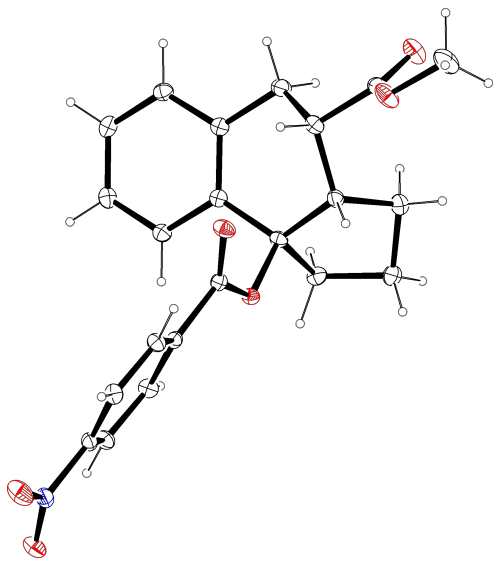
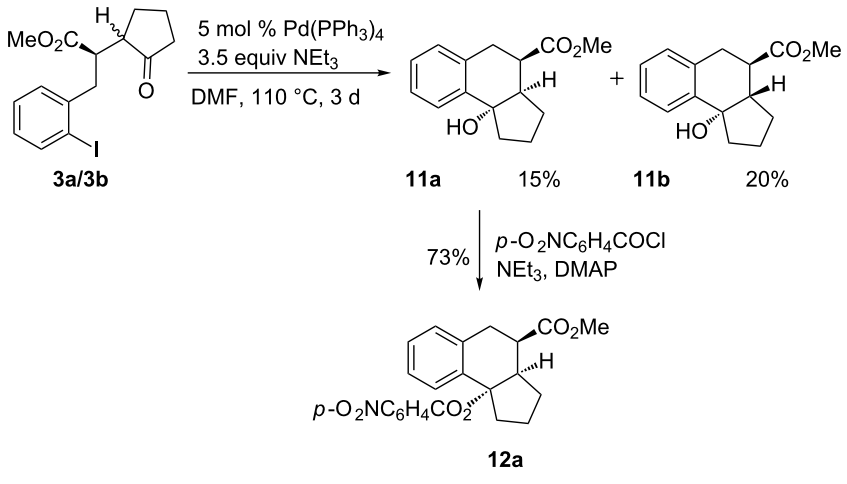
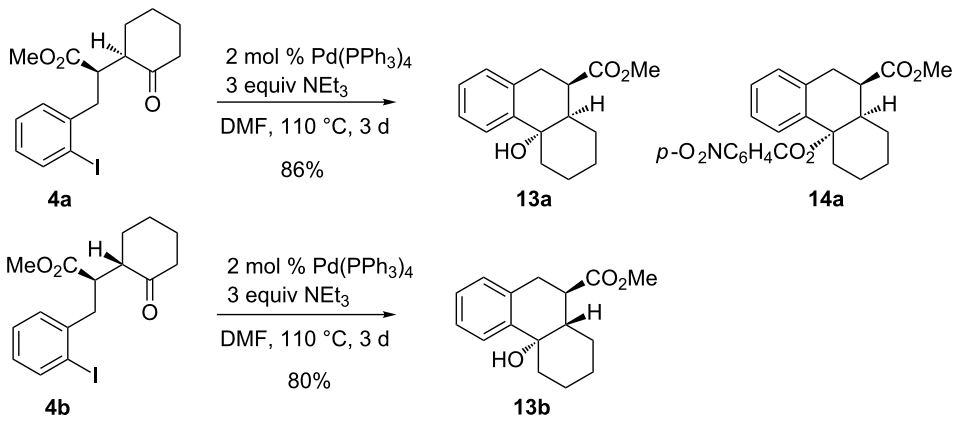


Figure 1: Molecular structure (ORTEP, [14]) of compound **12a** (thermal ellipsoids at 50% probability).

The palladium-catalyzed cyclization discussed in this report was discovered with cyclohexanone derivative **4** and we therefore tried to optimize the reaction conditions with this substrate. After extensive studies investigating different palladium catalysts, bases, additives, temperatures (with and without microwave) and reaction times we found the recorded conditions to be most reliable. A mixture of the two diastereomers **4a**/**4b** (ca. 1:1) furnished the two isomeric cyclization products **13a** and **13b** in varying yields and in several experiments only compound **13a** was isolated. Fortunately, diastereomers **4a** and **4b** could be separated by conventional column chromatography and hence a detailed analysis of the stereochemical features of this transformation was possible. Configurationally homogeneous compound **4a** furnished diastereomerically pure cyclization product **13a** in excellent yield, whereas epimer **4b** was converted into product **13b** in 80% yield, again formed as a single isomer (Scheme 5). An unequivocal configurational assignment of **13a** was possible by the X-ray crystal structure analysis of its corresponding *p*-nitrobenzoate **14a** (Figure 2) [15]. The config-



Scheme 4: Palladium-catalyzed cyclization of diastereomeric cyclopentanone derivatives **3a/3b** to products **11a** and **11b** and synthesis of *p*-nitrobenzoate **12a**.



Scheme 5: Palladium-catalyzed cyclizations of diastereomeric cyclohexanone derivatives **4a** and **4b** leading stereoselectively to products **13a** and **13b** and structure of *p*-nitrobenzoate **14a**.

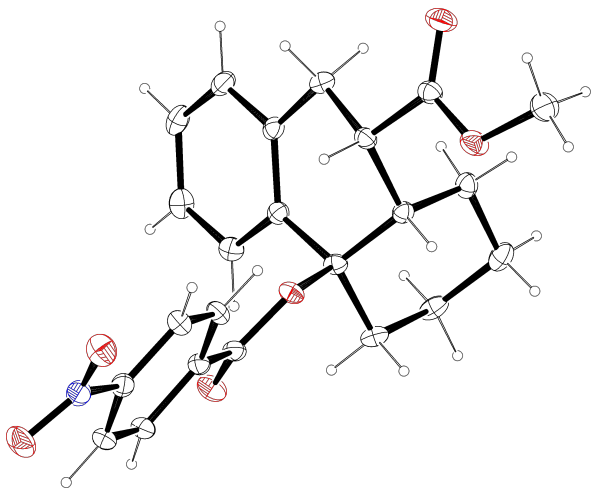
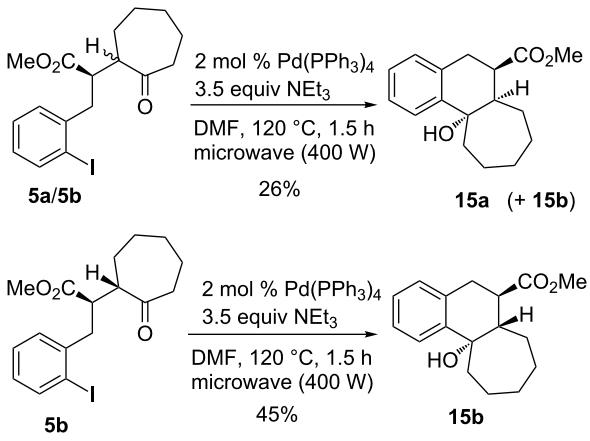


Figure 2: Molecular structure (ORTEP, [14]) of compound **14a** (thermal ellipsoids at 50% probability).



Scheme 6: Palladium-catalyzed cyclizations of cycloheptanone derivatives **5a** and **5b** leading to products **15a** and **15b**.

uration of compound **13b** was tentatively assigned in analogy to its lower and higher homologs.

With cycloheptanone derivatives **5a**/**b** less efficient cyclizations were observed. The mixture of diastereomers **5a**/**5b** (ca. 1:1) provided a mixture of compounds containing the two isomers **15a** and **15b**, from which pure **15a** could be isolated (Scheme 6). A diastereomerically enriched sample of **5b** afforded compound **15b** in 45% yield as a single isomer. These results were obtained employing microwave irradiation (400 W) that allowed considerably shorter reaction times, however, the yields were not strongly influenced by this modification. From both product diastereomers crystals suitable for X-ray crystal structure analyses could be obtained (Figure 3 and Figure 4) [16,17]. Again, the configurations of the precursors are re-

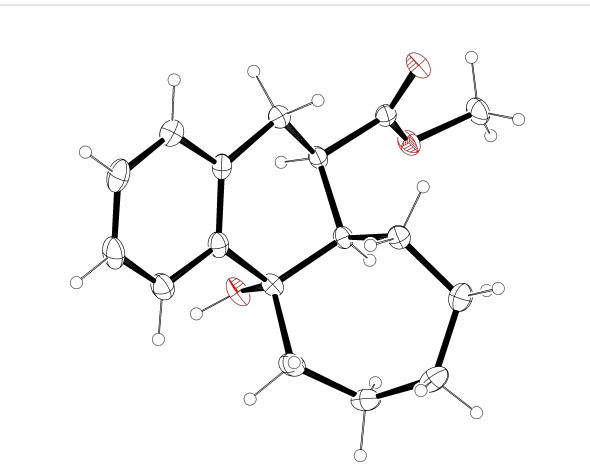


Figure 3: Molecular structure (ORTEP, [14]) of compound **15a** (thermal ellipsoids at 50% probability).

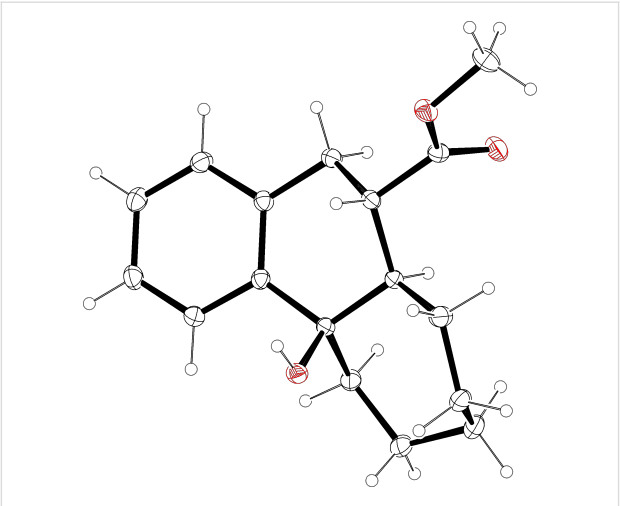


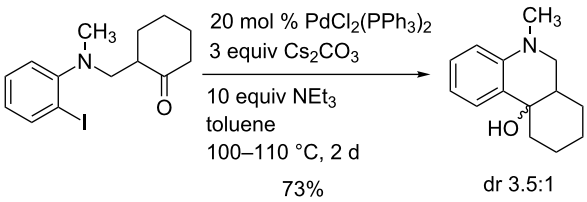
Figure 4: Molecular structure (ORTEP [14]) of compound **15b** (thermal ellipsoids at 50% probability).

flected in the product structure. Compound **5b** provided product **15b** with *trans*-annulation of the two rings and we assume that compound **15a** with *cis*-annulated rings was formed selectively from precursor **5a**.

We also briefly studied the palladium-catalyzed cyclization of *p*-methoxy-substituted aryl iodide **6a**/**b** that led under the standard conditions to a mixture containing compound **16** (Scheme 7). We cannot exclude that other regioisomers or even primarily formed tetralin derivatives are in the crude product mixture, but we isolated only compound **16** in pure form in 24% yield. Not surprisingly, the *p*-methoxy substituent favored the elimination of water from the primary addition product to generate the central double bond of **16**.

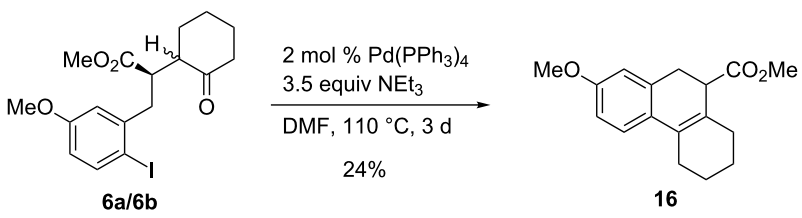
Discussion

The nucleophilic addition of organometallics such as lithium, magnesium or zinc organic compounds to carbonyl groups leading to alcohols is an important standard operation in organic synthesis providing high stereoselectivities in many cases. The in situ generation of the nucleophilic species from the corresponding organic halides in the presence of the carbonyl compound is also known, e.g., the Barbier reaction employing magnesium. The related transformation described in this report very likely involves an arylpalladium species as nucleophile that is in situ generated from the aryl iodide moiety. Similar palladium-catalyzed processes (palladium Barbier reactions) are relatively rare (for a review, see [18]). Early studies were reported by Y. Yamamoto et al. [19] and this group also published examples involving an alkyne palladation step to vinyl palladium intermediates that are able to undergo additions to carbonyl groups [20,21]. Very extensive investigations with a variety of *o*-haloaniline derivatives as precursors have been reported by the group of Solé, Bonjoch and Fernández [22,23]. They also analyzed this reaction and the competing enolate arylation by computational studies [24,25] (for a review, see [26]). Singular contributions employing different systems were contributed by other groups [27-29]. Scheme 8 shows a typical example of Solé et al. [23], related to our systems, furnishing a tricyclic compound in good yield with moderate diastereoselectivity.



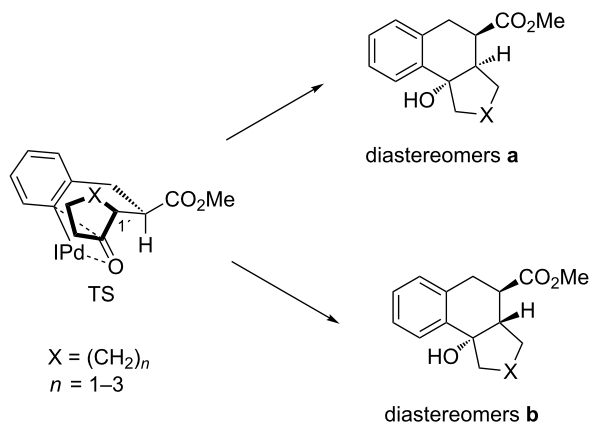
Scheme 8: Typical palladium-catalyzed cyclization of an *o*-iodoaniline derivative to a tricyclic tertiary alcohol as reported by Solé et al. [23].

The transformations described in the present report are highly stereoselective (we hesitate to use the term stereospecific here since the mass balances are often too low to rigorously exclude the formation of other diastereomers) since the configuration of the cyclic precursor ketones **3**–**5** is transferred to that of the cyclization products as shown in Schemes 4–6. Surprisingly, the presence of excess of the base triethylamine and the fairly long reaction times do not lead to noticeable epimerization of the precursor γ-ketoesters that would lead to an erosion of the observed stereoselectivity. In all examples the methoxycarbonyl group and the hydroxy group are arranged *trans* to each other irrespective of the configuration of the third stereogenic center



Scheme 7: Palladium-catalyzed cyclization of *p*-methoxy-substituted aryl iodide **6a**/**6b** to compound **16**.

at the bridgehead. A transition-state model that rationalizes this observation is depicted in Scheme 9. We propose a four-center interaction of the carbonyl moiety with the carbon–palladium bond in the transition state (TS) and due to this highly ordered arrangement only a boat-like transition state with a pseudo-equatorial position of the methoxycarbonyl group seems to be possible. The rigid benzene backbone further restricts the flexibility of the system. This model explains the observed *trans*-arrangement of the methoxycarbonyl group and the hydroxy group leading to diastereomers **a**, if the hydrogen at C-1' is in a pseudo-equatorial position and diastereomers **b** if this atom occupies a pseudo-axial position. This transition state is in accordance with the model that has been proposed on the basis of DFT calculations by Solé and Fernández [24-26].

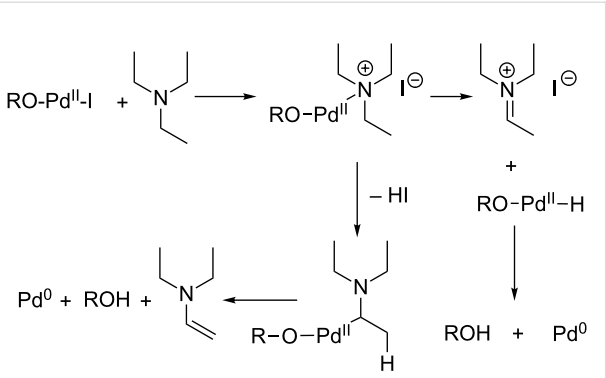


Scheme 9: Proposed transition state (TS) explaining the stereoselective formation of cyclization products.

The intermediate arylpalladium species is certainly generated by the standard oxidative insertion of palladium(0) into the C–I bond of the aryl iodide moiety. After the C–C bond formation leading to the bi- or tricyclic products, palladium(II) has to be reduced back to a palladium(0) species in order to allow a catalytic use of the metal. It is well known that several reagents (alkenes or alcohols [19]) are able to achieve this reduction. We therefore assume that triethylamine is the reducing reagent under the conditions employed in this study [30]. Possible mechanisms for this process leading to the formation of an iminium intermediate or a dehydrogenation of the amine are depicted in Scheme 10.

Conclusion

We have found new examples of intramolecular palladium-catalyzed nucleophilic additions of aryl iodides to alkyl ketones. These additions proceed in the presence of only 2–5 mol % $Pd(PPh_3)_4$ and afford bi- and tricyclic compounds with excellent stereoselectivity and in moderate to very good efficacy. The low mass balance observed in several cases may be due to subsequent reactions such as simple de-iodination of the precursor compounds or elimination of water in the products. However, in general none of these byproducts has been isolated. For compound **2** the bulky isopropyl group slows down the addition to the carbonyl group and an enolate arylation was observed instead as major reaction pathway. Although the scope of the discovered aryl iodide addition to carbonyl groups may be limited it is attractive since only low catalyst loadings are required and interesting products are formed with high stereoselectivity.



Scheme 10: Possible mechanism of the reduction of palladium(II) to palladium(0) by triethylamine (additional ligands at palladium are not depicted for clarity of the presentation).

Supporting Information

Supporting Information File 1

Characterization data and copies of ^{1}H and ^{13}C NMR spectra.
[http://www.beilstein-journals.org/bjoc/content/supplementary/1860-5397-12-118-S1.pdf]

Acknowledgements

Generous support of this work by the Deutsche Forschungsgemeinschaft and by Bayer HealthCare AG is most gratefully acknowledged.

References

1. Berndt, M.; Gross, S.; Hölemann, A.; Reissig, H.-U. *Synlett* **2004,** 422–438. doi:10.1055/s-2004-815429
2. Saadi, J.; Reissig, H.-U. *Synlett* **2009,** 2089–2092. doi:10.1055/s-0029-1217520
3. Saadi, J.; Lentz, D.; Reissig, H.-U. *Org. Lett.* **2009,** *11,* 3334–3337. doi:10.1021/ol901183h
4. Saadi, J.; Brüdgam, I.; Reissig, H.-U. *Beilstein J. Org. Chem.* **2010,** *6,* 1229–1245. doi:10.3762/bjoc.6.141

5. Saadi, J. SmI_2-Induced Cyclizations of Alkenyl- and Alkynyl-Substituted γ-, δ- and ε-Ketoesters – An Approach to Medium-Sized Carbocycles. Ph.D. Thesis, Freie Universität Berlin, Germany, 2009.
6. Reissig, H.-U. *Top. Curr. Chem.* **1988,** *144,* 73–135.
7. Reissig, H.-U.; Zimmer, R. *Chem. Rev.* **2003,** *103,* 1151–1196. doi:10.1021/cr010016n
8. Kunkel, E.; Reichelt, I.; Reissig, H.-U. *Liebigs Ann. Chem.* **1984,** 512–530. doi:10.1002/jlac.198419840311
9. Reichelt, I.; Reissig, H.-U. *Liebigs Ann. Chem.* **1984,** 531–551. doi:10.1002/jlac.198419840312
10. Kunkel, E.; Reichelt, I.; Reissig, H.-U. *Liebigs Ann. Chem.* **1984,** 802–819. doi:10.1002/jlac.198419840416
11. Khan, F. A.; Czerwonka, R.; Reissig, H.-U. *Synlett* **1996,** 533–535. doi:10.1055/s-1996-5483
12. Khan, F. A.; Czerwonka, R.; Reissig, H.-U. *Eur. J. Org. Chem.* **2000,** 3607–3617. doi:10.1002/1099-0690(200011)2000:21<3607::AID-EJOC3607>3.0.CO;2-N
13. CCDC-1469195 (for **12a**) contains the supplementary crystallographic data. These data can be obtained free of charge form The Cambridge Crystallographic Data Centre via http://www.ccdc.cam.ac.uk/data_request/cif.
14. Farrugia, L. J. *J. Appl. Crystallogr.* **1997,** *30,* 565. doi:10.1107/S0021889897003117
15. CCDC-1469196 (for **14a**) contains the supplementary crystallographic data. These data can be obtained free of charge form The Cambridge Crystallographic Data Centre via http://www.ccdc.cam.ac.uk/data_request/cif.
16. CCDC-1469197 (for **15a**) contains the supplementary crystallographic data. These data can be obtained free of charge form The Cambridge Crystallographic Data Centre via http://www.ccdc.cam.ac.uk/data_request/cif.
17. CCDC-1469198 (for **15b**) contains the supplementary crystallographic data. These data can be obtained free of charge form The Cambridge Crystallographic Data Centre via http://www.ccdc.cam.ac.uk/data_request/cif.
18. Yamamoto, Y.; Nakamura, I. *Top. Organomet. Chem.* **2005,** *14,* 211–239. doi:10.1007/b104136
19. Quan, L. G.; Lamrani, M.; Yamamoto, Y. *J. Am. Chem. Soc.* **2000,** *122,* 4827–4828. doi:10.1021/ja000415k
20. Gevorgyan, V.; Quan, L. G.; Yamamoto, Y. *Tetrahedron Lett.* **1999,** *40,* 4089–4092. doi:10.1016/S0040-4039(99)00656-5
21. Quan, L. G.; Gevorgyan, V.; Yamamoto, Y. *J. Am. Chem. Soc.* **1999,** *121,* 3545–3546. doi:10.1021/ja983645w
22. Solé, D.; Vallverdú, L.; Peidró, E.; Bonjoch, J. *Chem. Commun.* **2001,** 1888–1889. doi:10.1039/b105686g
23. Solé, D.; Vallverdú, L.; Solans, X.; Font-Bardía, M.; Bonjoch, J. *J. Am. Chem. Soc.* **2003,** *125,* 1587–1594. doi:10.1021/ja029114w
24. Solé, D.; Mariani, F.; Fernández, I.; Sierra, M. A. *J. Org. Chem.* **2012,** *77,* 10272–10284. doi:10.1021/jo301924e
25. Solé, D.; Fernández, I.; Sierra, M. A. *Chem. – Eur. J.* **2012,** *18,* 6950–6958. doi:10.1002/chem.201102811
26. Solé, D.; Fernández, I. *Acc. Chem. Res.* **2014,** *47,* 168–179. doi:10.1021/ar400104j
27. Zhao, Y.-B.; Mariampillai, B.; Candito, D. A.; Laleu, B.; Li, M.; Lautens, M. *Angew. Chem.* **2009,** *121,* 1881–1884. doi:10.1002/ange.200805780
Angew. Chem., Int. Ed. **2009,** *48,* 1849–1852. doi:10.1002/anie.200805780
28. Jia, Y.-X.; Katayev, D.; Kündig, E. P. *Chem. Commun.* **2010,** *46,* 130–132. doi:10.1039/B917958E
29. Giorgi, G.; Maiti, S.; López-Alvarado, P.; Menéndez, J. C. *Org. Biomol. Chem.* **2011,** *9,* 2722–2730. doi:10.1039/c0ob00526f
30. Coquerel, Y.; Brémond, P.; Rodriguez, J. *J. Organomet. Chem.* **2007,** *692,* 4805–4808. doi:10.1016/j.jorganchem.2007.05.053

License and Terms

This is an Open Access article under the terms of the Creative Commons Attribution License (http://creativecommons.org/licenses/by/2.0), which permits unrestricted use, distribution, and reproduction in any medium, provided the original work is properly cited.

The license is subject to the *Beilstein Journal of Organic Chemistry* terms and conditions: (http://www.beilstein-journals.org/bjoc)

The definitive version of this article is the electronic one which can be found at: doi:10.3762/bjoc.12.118

BEILSTEIN JOURNAL OF ORGANIC CHEMISTRY

Artificial Diels–Alderase based on the transmembrane protein FhuA

Hassan Osseili[‡1], Daniel F. Sauer[‡1], Klaus Beckerle[1], Marcus Arlt[2], Tomoki Himiyama[3], Tino Polen[4], Akira Onoda[3], Ulrich Schwaneberg[2], Takashi Hayashi[3] and Jun Okuda[*1]

Full Research Paper

Open Access

Address:
[1]Institute of Inorganic Chemistry, RWTH Aachen University, Landoltweg 1, 52056 Aachen, Germany, [2]Institute of Biotechnology, RWTH Aachen University, Worringer Weg 1, 52056 Aachen, Germany, [3]Department of Applied Chemistry, Graduate School of Engineering, Osaka University, 2-1 Yamadaoka, Suita 565-0871, Japan and [4]Institute of Bio- and Geosciences IBG-1: Biotechnology, Forschungszentrum Jülich GmbH, 52425 Jülich, Germany

Email:
Jun Okuda[*] - jun.okuda@ac.rwth-aachen.de

* Corresponding author ‡ Equal contributors

Keywords:
artificial Diels-Alderase; biohybrid catalysis; copper enyzme; membrane protein

Beilstein J. Org. Chem. **2016,** *12,* 1314–1321.
doi:10.3762/bjoc.12.124

Received: 02 April 2016
Accepted: 10 June 2016
Published: 24 June 2016

This article is part of the Thematic Series "Organometallic chemistry".

Guest Editor: L. Gade

© 2016 Osseili et al.; licensee Beilstein-Institut.
License and terms: see end of document.

Abstract

Copper(I) and copper(II) complexes were covalently linked to an engineered variant of the transmembrane protein *Ferric hydroxamate uptake protein component A* (FhuA ΔCVF^{tev}). Copper(I) was incorporated using an *N*-heterocyclic carbene (NHC) ligand equipped with a maleimide group on the side arm at the imidazole nitrogen. Copper(II) was attached by coordination to a terpyridyl ligand. The spacer length was varied in the back of the ligand framework. These biohybrid catalysts were shown to be active in the Diels–Alder reaction of a chalcone derivative with cyclopentadiene to preferentially give the *endo* product.

Introduction

So-called artificial metalloenzymes have attracted attention over the last decade [1-9]. Incorporation of an organometallic cofactor into proteins offers new possibilities to expand the reaction repertoire catalyzed by natural enzymes to non-natural reactions. With this approach man-made metalloproteins as asymmetric transfer hydrogenases [10,11], Suzukiases [12], metatheases [13-20], epoxidases [21], Diels–Alderases [22-27] and others have been reported. The Diels–Alder reaction is a powerful C–C bond formation reaction, widely used in organic chemistry, e.g., for the synthesis of natural products [28]. This reaction is known to be catalyzed by Lewis acids such as a Cu(II) complex [29]. Additionally, structurally defined catalysts are found to influence the *endo*/*exo* ratio as well as the enantioselectivity [30]. Artificial Diels–Alderases have also been reported to show good *endo*/*exo* selectivities as well as high enantioselectivities in a benchmark reaction of azachalcone with cyclopentadiene [22-27].

The artificial Diels–Alderases reported so far used soluble proteins, where the binding site of Cu(II) was formed either by site-

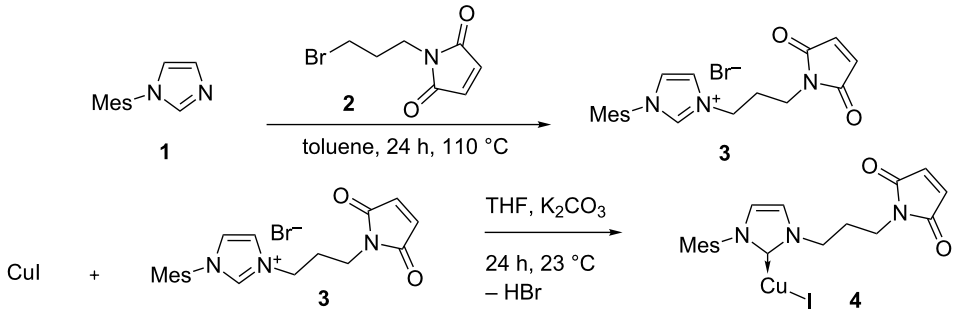
directed mutagenesis [22,23], by incorporation of a suitable ligand, or copper complex in an apo-protein [24-27]. Here we report on the use of the robust transmembrane protein *Ferric hydroxamate uptake protein component A* (FhuA) as host for defined Cu(I) NHC or Cu(II) terpyridyl complexes with a maleimide moiety. By covalently bonding these copper complexes to the protein artificial Diels–Alderases based on a membrane protein have been obtained.

Results and Discussion

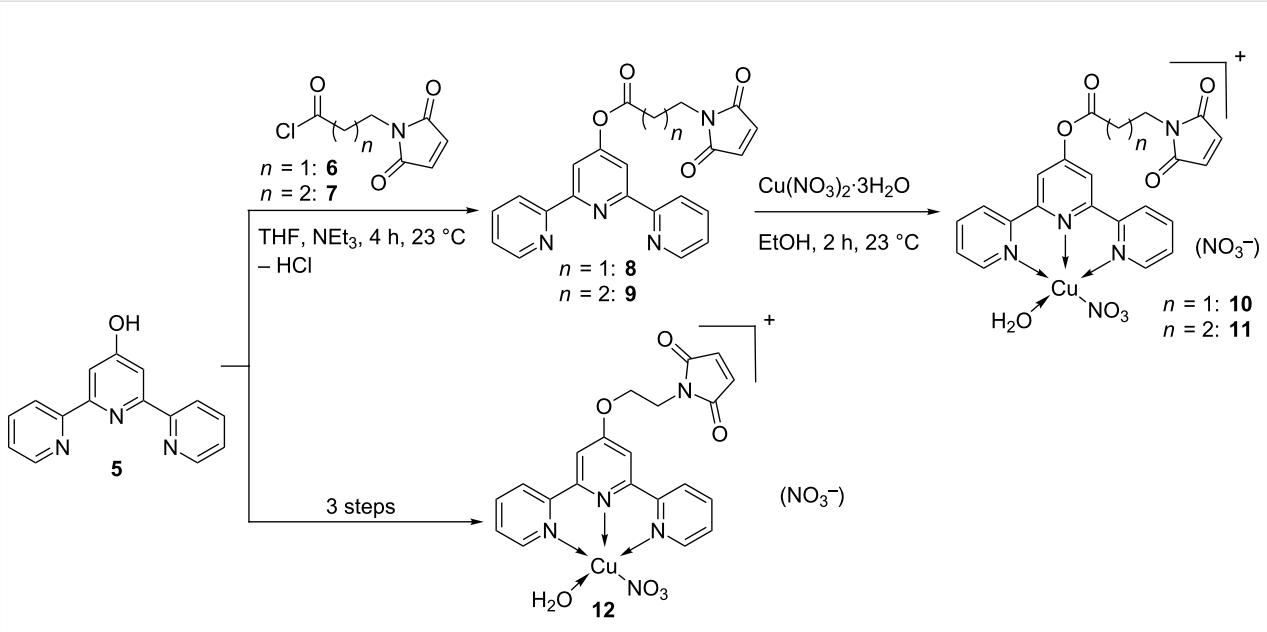
Synthesis of the metal complexes

As the protein host, the FhuA ΔCVF^{tev} variant of the *Ferric hydroxamate uptake protein component A* (FhuA) was chosen [31]. This protein was shown to be suitable to harbor Grubbs–Hoveyda type catalysts for olefin metathesis [17,18]. To anchor Cu(I) in the protein FhuA ΔCVF^{tev} that contains a cysteine residue at position 545 for conjugation [31], an NHC ligand containing a maleimide function was prepared (Scheme 1).

The imidazolium salt **3** was synthesized by nucleophilic substitution of mesityl imidazol **1** with maleimide derivative **2**. These salts were used to generate the Cu(I) NHC complexes **4** upon deprotonation with K_2CO_3. Complex **4** contains only one NHC ligand at the copper, as shown by elemental analysis and ESIMS. Attempts to coordinate Cu(II) to the NHC ligand failed. However, the terpyridyl (terpy) ligand is a promising candidate to support Cu(II) ions. Therefore, the terpy framework containing an alcohol function on the 4 position of the central pyridine was chosen (Scheme 2).



Scheme 1: Syntheses to Cu(I) complex bearing a NHC ligand.



Scheme 2: Synthesis of Cu(II) terpyridyl complexes.

By either esterification or nucleophilic attack, the spacer with the maleimide group was attached. The ligand was treated with one equivalent of $Cu(NO_3)_2 \cdot 3H_2O$ leading to the Cu(II) complexes **10–12**.

By using the established anchoring strategy, the Cu(I) and Cu(II) complexes (**4** and **10–12**) were anchored covalently inside the β-barrel structure. After anchoring, the protein was refolded by dialysis (Scheme 3).

Anchoring of all complexes was successful. Titration of the free cysteine with the fluorescence dye ThioGlo® indicated that more than 95% of the cysteine residues were conjugated for each catalyst.

Renaturing of the protein was successful in the case of the terpy ligand framework (for clarity of the location of the catalyst, see Figure S1 in Supporting Information File 1). After 3 days of dialysis against SDS-solution, excess catalyst **10–12** was removed. Additional 3 days of dialysis against PE-PEG solution renatured the protein structure to give the expected β-barrel structure, as indicated by CD spectra (Figure 1).

The CD spectra show a minimum at around 215 nm and a maximum at 195 nm, as expected for β-barrel proteins such as FhuA [17,18,31]. This finding suggests correct refolding of the protein. Additionally, the temperature stability of the new conjugate **17** was evaluated.

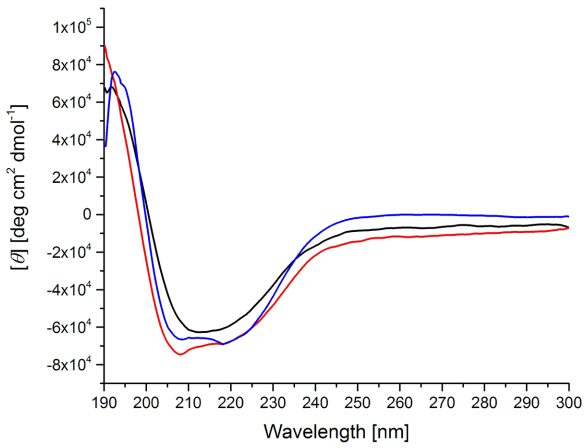
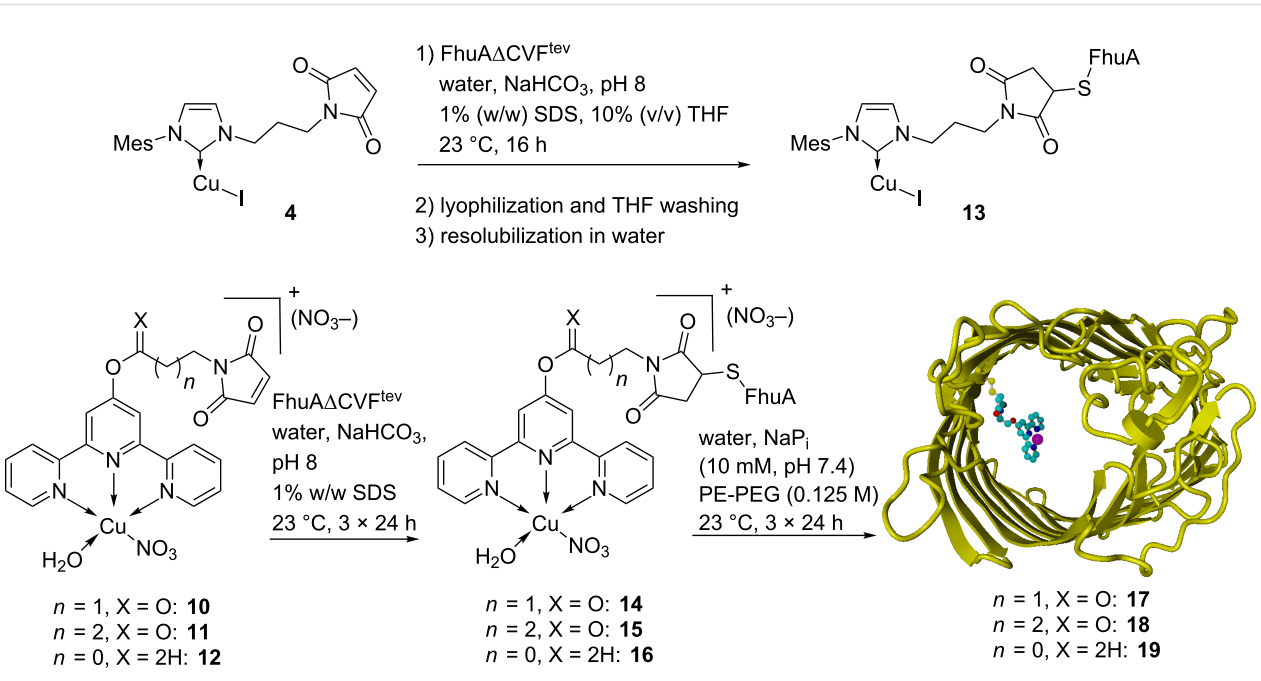


Figure 1: CD spectra of refolded catalysts **17–19** (red: **17**, black: **18**, blue: **19**).

The temperature-dependent CD spectra indicate correct folding of the catalyst in the temperature range from 4 °C to 64 °C (Figure 2). This is in agreement with previously reported stability analysis of the wild-type FhuA and the FhuA mutant with its "cork" domain removed (FhuA Δ1-159) [31].

The Cu(I) NHC-containing protein could not be renatured. We speculate that during the refolding procedure Cu(I) was oxidized to Cu(II) by contamination with air. Cu(II) led to protein aggregation and precipitation. This was shown in an independent experiment. When one equiv of $Cu(NO_3)_2 \cdot 3H_2O$ was



Scheme 3: Anchoring and refolding of the biohybrid copper complexes.

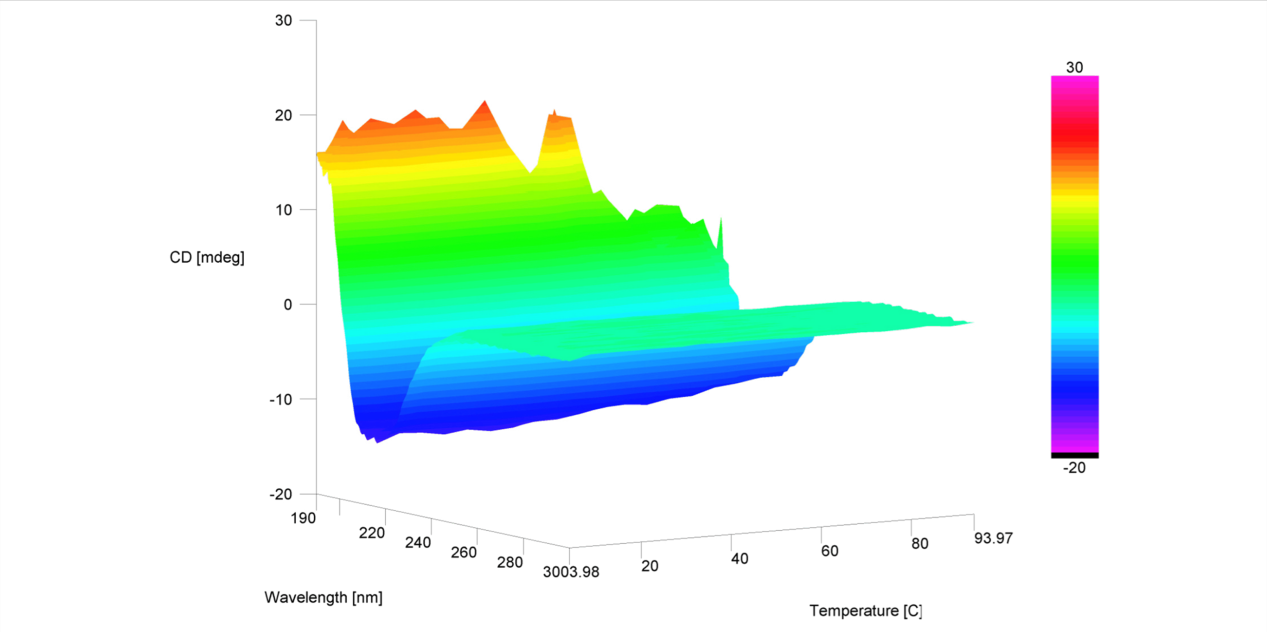


Figure 2: Temperature-dependent CD spectra of catalyst **17**.

added to a solution of FhuA ΔCVF^{tev}, the protein precipitated rapidly and quantitatively.

MALDI–TOF–MS analysis for the whole biohybrid catalyst was difficult due to the high mass of approximately 64 kDa. However, digestion into smaller fragments is possible with the deliberately introduced TEV cleavage site [17,18]. The fragment containing the Cu complex was cut out and analyzed separately (Figure 3).

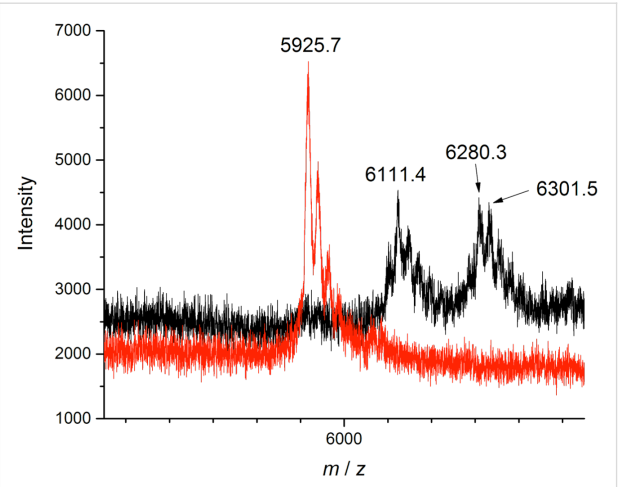
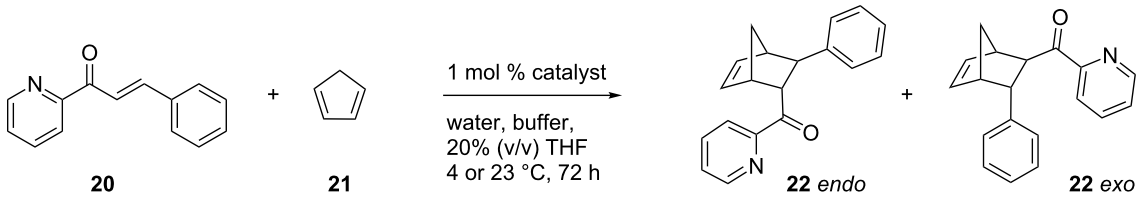


Figure 3: MALDI–TOF mass spectra (black: **17**, red: FhuAΔCVF^{tev}).

Digestion of biohybrid catalyst **17** was successful. Comparison of the MALDI–TOF– MS spectrum with FhuA ΔCVF^{tev} (calcd (M + Na$^+$): m/z = 5925 Da; found: m/z = 5925 Da) indicates successful coupling. The signal of m/z = 6301 Da indicates the FhuA fragment with the attached ligand framework (calcd (M): m/z = 6302 Da; found: m/z = 6301 Da). The signal of m/z = 6111 Da results from saponification of the ester and the maleimide moiety (calcd (M + H_2O + Na$^+$): m/z = 6111 Da, found: m/z = 6111 Da). We were unable to detect the copper ion in the MALDI–TOF–MS.

The isolated biohybrid catalysts were tested in the Diels–Alder reaction of azachalcone **20** and cyclopentadiene (**21**, Table 1). We evaluated first the background reaction of this Diels–Alder reaction in the detergents and buffer solutions we used for the biohybrid catalysts. Since SDS precipitates at 4 °C and the solution becomes heterogeneous, we decided to perform the reactions in SDS at 23 °C. After 3 days, the reaction showed 62% conversion with an *endo* to *exo* ratio of 70:30 (Table 1, entry 2). Since detergents such as SDS influences the reaction significantly, this value is in good agreement with previously reported results [32]. In PE-PEG at 4 °C the conversion was lower; the *endo*/*exo* ratio was ca. 55:45 (Table 1, entry 1). Using CuI in SDS, the conversion increased slightly, showing the same selectivity (Table 1, entry 5). When using Cu(II) as a catalyst, the conversion was complete in both detergent solutions, but no change in selectivity was observed (Table 1, entries 3 and 4). CuI NHC complex **4** showed the same activity and selectivity as CuI (Table 1, entry 6). By using the bioconjugate **13**, the conversion with 62% is comparable with the protein-free catalysts or CuI itself, but the selectivity significantly changed the *endo* product preferred (Table 1, entry 7). By using the Cu(II) complexes **10–12** in the refolding buffer: the conver-

Table 1: Diels–Alder reaction catalyzed by the biohybrid catalysts.



20 + **21** → **22** *endo* + **22** *exo*

Entry	Catalyst	Buffer	Temp. [°C]	Conv.[a] [%]	*endo*/*exo*[b]
1	–	PE-PEG[c]	4	20	55/45
2	–	SDS[d]	23	62	70/30
3	$Cu(NO_3)_2{\cdot}3H_2O$	PE-PEG[c]	4	95	54/46
4	$Cu(NO_3)_2{\cdot}3H_2O$	SDS[d]	23	94	65/35
5	CuI	SDS[d]	23	78	70/30
6	**4**	SDS[d]	23	75	67/33
7	**13**	SDS[d]	23	62	90/10
8	**10**	PE-PEG[c]	4	21	65/35
9	**11**	PE-PEG[c]	4	33	56/44
10	**12**	PE-PEG[c]	4	12	66/34
11	**14**	SDS[d]	23	92	90/10
12	**15**	SDS[d]	23	87	89/11
13	**16**	SDS[d]	23	91	89/11
14	**17**	PE-PEG[c]	4	69	96/4
15	**18**	PE-PEG[c]	4	15	66/34
16	**19**	PE-PEG[c]	4	64	98/2

[a]Determined by ^{1}H NMR in $CDCl_3$ and HPLC. [b]Determined by HPLC. [c]PE-PEG (0.125 M), sodium phosphate buffer (100 mM, pH 7.4).
[d]SDS (1% w/w), pH 7.5 (adjusted with $NaHCO_3$).

sion decreased with an *endo*/*exo* ratio of approximately 60/40 (Table 1, entry 8–10). Upon attaching the catalyst to the protein in the partially folded state, the selectivity increased to 90% *endo* with high conversions independent of the spacer length (Table 1, entry 11–13). The refolded biohybrid catalysts **17** and **19** showed good conversion with almost quantitative *endo* product formation (Table 1, entries 14 and 16). Catalyst **18** with the longest spacer unit, however, showed moderate activity and loss of *endo* selectivity. This is explained by the high flexibility of this catalyst within the β-barrel structure of the refolded protein (Table 1, entry 15). Based on these catalysis results, we hypothesize that the protein environment is sterically rather demanding, which is even more pronounced in the refolded state. The absence of any enantioselectivity suggests that no preferential orientation of the substrate at the active site within the barrel structure is possible. Notably, no protein precipitated during catalysis, showing the advantageous feature of membrane proteins in terms of robustness as compared to soluble proteins [15].

Conclusion

Herein, we report the synthesis of Cu(I) NHC and Cu(II) terpyridyl complexes equipped with a maleimide moiety which underwent covalent conjugation at the cysteine residue 545 of the transmembrane protein FhuAΔCVF^{tev}. These biohybrid conjugates were analyzed by CD spectroscopy, MALDI–TOF–MS, ThioGlo fluorescence titration, and BCA assay. All employed methods indicate the folded structure of FhuA ΔCVF^{tev} and a high occupancy of the only accessible cysteine residue within this β-barrel protein.

The biohybrid catalysts showed high activity and high *endo* selectivity in the Diels–Alder reaction of substrate **20** with cyclopentadiene (**21**). A comparison with other reported artificial Diels–Alderases is not meaningful because of the utilization of detergents in the present case, which increases the stability towards the Diels–Alder reaction conditions. However, similar trends with respect to both activity and *endo* selectivity were observed. The cavity of FhuA appears to enhance the reaction as reported by Hayashi et al. for nitrobindin [26], Reetz et al. for serum albumin [22,23], and Roelfes et al. for Lactococcal multidrug resistance Regulator (LmrR) [25]. Furthermore, the increased *endo* selectivity is in agreement with other protein-modified catalysts reported so far [22-27].

Experimental

General considerations

All manipulations were performed under argon atmosphere using standard Schlenk or glove box techniques. Prior to use, glassware was dried overnight at 130 °C and solvents were dried, distilled and degassed using standard methods. Catalysis with Cu(II) complexes were performed under ambient conditions. NMR measurements were performed on a Bruker Avance II 400 or a Bruker Avance III HD 400 spectrometer at ambient temperature unless otherwise mentioned. The chemical shifts (δ ppm) in the ^{1}H and ^{13}C NMR spectra were referenced to the residual proton signals of the deuterated solvents and reported relative to tetramethylsilane [33]. Abbreviations for NMR spectra: s (singlet), d (doublet), t (triplet), quint (quintet), m (multiplet). Elemental analyses were performed on an elementar vario EL machine. CD spectra were recorded on a JASCO J-1100 equipped with a single position Peltier cell holder. MALDI–TOF spectra were recorded on an Ultraflex III TOF/TOF mass spectrometer (Bruker Daltonics). High resolution ESI–TOF–MS were performed on a Thermo Finnigan LCQ Deca XP Plus spectrometer. CuI and $Cu(NO_3)_2{\cdot}3H_2O$ were purchased from Sigma-Aldrich and used as recieved. Cyclopentadiene was freshly distilled before used. Compounds **1** [34], **2** [35], **5** [36], **6** [37], **7** [37], **12** [26], **20** [32] and FhuAΔCVF^{tev} [17] were synthesized according to literature procedures.

Syntheses

Synthesis and characterization of IMesBr **3**

A solution of 1-(3-bromopropyl)-1*H*-pyrrol-2,5-dione (1.69 g, 7.75 mmol, 1.00 equiv) and 1-(mesityl)-1*H*-imidazole (1.66 g, 8.91 mmol, 1.10 equiv) in toluene (35 mL) was stirred in a closed Schlenk tube for 24 h at 110 °C. The colorless precipitate was filtered, washed with toluene (3 × 15 mL) and dried under vacuum to afford analytically pure imidazolium salt **1** (2.58 g, 6.40 mmol, 83%) as colorless powder. ^{1}H NMR (400 MHz, CD_2Cl_2) δ 10.32 (s, 1H, NC*H*N), 8.07 (s, 1H, C*H*=CH), 7.28 (s, 1H, CH=C*H*), 7.05 (s, 2H, aryl C*H*), 6.73 (s, 2H, C*H*=C*H*), 4.68 (t, $^{3}J_{HH}$ = 6.85 Hz, 2H, CH_2), 3.58 (t, $^{3}J_{HH}$ = 6.42 Hz, 2H, CH_2), 2.35 (s, 3H, *p*-CH_3), 2.34 (quint, $^{3}J_{HH}$ = 6.72 Hz, 2H, CH_2), 2.10 (s, 6H, *o*-*Me*); ^{13}C NMR (100 MHz, CD_2Cl_2) δ 171.5 (*C*=O), 141.9, 139.0 (N*C*HN), 135.0 (*C*H=*C*H), 134.9, 131.3, 130.2, 123.8 (*C*H=*C*H), 123.7, 48.0 (*C*H$_2$), 34.5 (*C*H$_2$), 30.2 (*C*H$_2$), 21.4 (*p*-*Me*), 18.0 (*o*-*Me*); ESIMS (+) *m*/*z* (%): calcd for $(C_{19}H_{22}N_3O_2)^+$, 324.171; found, 324.170 (100).

Synthesis and characterization of NHC-Cu(I)I complex **4**

The Imidazolium salt **3** (200 mg, 0.495 mmol, 1.00 equiv), K_2CO_3 (280 mg, 2.02 mmol, 4.00 equiv) and CuI (95 mg, 0.495 mmol, 1.00 equiv) was stirred in THF (5 mL) for 24 h at 23 °C. The solvent was evaporated under vacuum and the residue was dissolved in dichloromethane (4 mL). After filtering over Celite® the solvent was evaporated under vacuum and the residue dried under vacuum to afford CuI NHC complex **6** (150 mg, 0.292 mmol, 59%) as orange powder. ^{1}H NMR (400 MHz, $CDCl_3$) δ 7.19 (s, 1H, C*H*=CH), 7.28 (s, 1H, CH=C*H*), 6.93 (s, 2H, aryl C*H*), 6.83 (s, 2H, C*H*=C*H*), 4.21 (t, $^{3}J_{HH}$ = 6.72 Hz, 2H, CH_2), 3.58 (t, $^{3}J_{HH}$ = 6.72 Hz, 2H, CH_2), 2.31 (s, 3H, *p*-*Me*), 2.16 (quint, $^{3}J_{HH}$ = 6.72 Hz, 2H, CH_2), 2.00 (s, 6H, *o*-*Me*); ^{13}C NMR (100 MHz, $CDCl_3$,) δ 181.7 (N*C*N), 170.6 (*C*=O), 139.0, 135.4, 134.9, 134.2, 129.1 121.7, 120.6, 48.3 (*C*H$_2$), 34.7 (*C*H$_2$), 30.5 (*C*H$_2$), 21.0 (*p*-*Me*), 17.9 (*o*-*Me*); Anal. calcd for $C_{19}H_{21}CuIN_3O_2$, C, 44.41; H, 4.36; N, 8.18; found: C, 44.02; H, 4.01; N, 7.75; ESIMS (+) *m*/*z* (%): calcd for $(C_{19}H_{21}CuN_3O_2)^+$ 388.092; found, 388.106 (100).

Synthesis of terpyridyl ligands **8** and **9**

A solution of terpyridine **5** (200 mg, 0.803 mmol, 1.00 equiv) in THF (10 mL) was treated with acid chloride **6** (165 mg, 0.884 mmol, 1.10 equiv) or **7** (177 mg, 0.884 mmol, 1.10 equiv) in THF (5 mL). Triethylamine (NEt_3) (222 μL, 1.61 mmol, 2.00 equiv) was added to the solution and the mixture was stirred for 16 h at 23 °C. The solution was filtered and all volatiles evaporated. The residue was dissolved in dichloromethane (50 mL), washed twice with water (50 mL), and once with brine (50 mL). The organic layer was dried over Na_2SO_4 and the solvent removed under vacuum affording the terpyridine ligand **8** (285 mg, 0.715 mmol, 89%) or **9** (280 mg, 0.699 mmol, 87%). ^{1}H NMR (**8**, 400 MHz, CD_2Cl_2) δ 8.69 (m, 2H, aryl C*H*), 8.60 (dt, $^{3}J_{HH}$ = 8.0 Hz, $^{3}J_{HH}$ = 1.0 Hz, 2H, aryl C*H*), 8.26 (s, 2H, aryl C*H*), 7.86 (m, 2H, aryl C*H*), 7.34 (ddd, $^{3}J_{HH}$ = 7.4 Hz, $^{3}J_{HH}$ = 4.8 Hz, $^{3}J_{HH}$ = 1.1 Hz, 2H, aryl C*H*), 6.75 (s, 2H, *H*C=C*H*), 4.00 (t, $^{3}J_{HH}$ = 7.0 Hz, 2H, CH_2), 2.99 (t, $^{3}J_{HH}$ = 7.0 Hz, 2H, CH_2) ppm; ^{1}H NMR (**9**, 400 MHz, CD_2Cl_2) δ 8.69 (m, 2H, aryl C*H*), 8.61 (dt, $^{3}J_{HH}$ = 7.8 Hz, $^{3}J_{HH}$ = 1.1 Hz, 2H, aryl C*H*), 8.25 (s, 2H, aryl C*H*), 7.85 (m, 2H, aryl C*H*), 7.34 (ddd, $^{3}J_{HH}$ = 7.4 Hz, $^{3}J_{HH}$ = 4.9 Hz, $^{3}J_{HH}$ = 1.0 Hz, 2H, aryl C*H*), 6.75 (s, 2H, *H*C=C*H*), 3.71 (t, $^{3}J_{HH}$ = 6.8 Hz, 2H, CH_2), 2.67 (t, $^{3}J_{HH}$ = 7.4 Hz, 2H, CH_2), 2.09 (pent, $^{3}J_{HH}$ = 7.2 Hz, 2H, CH_2) ppm.

Synthesis of Cu(II)-terpyridine complexes **10** and **11**

To a solution of terpyridine ligand **8** (200 mg, 0.500 mmol, 1.00 equiv) or **9** (207 mg, 0.500 mmol, 1.00 equiv) in ethanol (10 mL), $Cu(NO_3)_2{\cdot}3H_2O$ (120 mg, 0.500 mmol, 1.00 equiv) in ethanol was added. The solution was stirred for 2 h at 23 °C. The blue precipitate was collected and washed generously with cold THF (20 mL), cold ethanol (50 mL) and cold dichloromethane (10 mL). The residue was dried under vacuum, to give the copper complex **10** (214 mg, 0.365 mmol, 73%) or **11** (207 mg, 0.345 mmol, 69%). ESIMS (**10**) (+) *m*/*z* (%): calcd for

$(C_{22}H_{16}CuN_4O_4)^+$, 463.0468; found, 463.0459 (35); calcd for: $(C_{15}H_{10}CuN_3O)^+$, 311.0125; found, 311.0118 (43); ESIMS (**11**) (+) *m/z* (%): calcd for $(C_{23}H_{18}CuN_4O_4)^+$, 477.0624; found, 477.0624 (7); calcd for $(C_{15}H_{10}CuN_3O)^+$; 311.0125; found: 311.0114 (36).

General procedure: Conjugation of the catalysts to FhuAΔCVF^{tev} and refolding

To a degassed solution of FhuAΔCVF^{tev} in water (5 mg/mL, pH ≈ 8 ($NaHCO_3$)) containing 1% (w/w) SDS, 10 equiv of catalyst **4** in degassed THF (10% (v/v)) or 10 equiv of catalyst **10**, **11**, **12** in water (10% (v/v)) was added. The solution was allowed to stir 16 h.

In the case of catalyst **4**, water was removed in vacuum, and the residue was washed with degassed THF (4 × 15 mL) to remove excess of catalyst **4**. The residue was dried in vacuum and dissolved in water.

In the case of catalyst **10**–**12**, the solution was transferred into a dialysis tube and the solution was dialyzed for 3 days against 200 fold volume containing SDS (1% (w/w)) and water (pH ≈ 8 ($NaHCO_3$)). The dialysis solution was changed every 12 hours. Afterwards, the sample was dialyzed for 2 days against 200 fold volume containing the refolding detergent PE-PEG (0.125 mM, average M_n = 2250 g/mol), sodium phosphate buffer (10 mM, pH 7.4), and water. The dialysis solution was changed every 12 h.

The protein concentration was analyzed by BCA assay, the coupling efficiency was determined by ThioGlo fluorescence titration, and correct refolding was determined by CD spectroscopy, as previously reported [17,18]. Digestion of the proteins was performed as previously reported [17].

General procedure: Diels–Alder reaction

To the corresponding catalyst (1 mol %) in 2 mL of buffer solution (0.125 mM PE-PEG, sodium phosphate buffer (100 mM, pH 7.4), 1 mM EDTA) at 4 °C or 23 °C azachalcone **20** (4 mg, 0.02 mmol) in THF (10% (v/v)) and freshly distilled cyclopentadiene (40 µL, 50 µM, 33 equiv) was added subsequently. The reaction mixture was stirred for 72 h. Afterwards, the mixture was extracted with Et_2O (3 × 10 mL), the combined organic phases were dried over Na_2SO_4 and the solvent removed under reduced pressure. The residue was analyzed by ^1H NMR spectroscopy and chiral phase HPLC using heptane/isopropanol (98:2) as eluents. All reactions were carried out in triplicates.

Abbreviations

PE-PEG (polyethylene-polyethylene glycol), SDS (sodium dodecyl sulfate), TEV *(Tobacco Etch Virus),* MALDI–TOF–MS (matrix-assisted laser desorption/ionisation and time-of-flight mass spectrometry), FhuAΔCVF^{tev} (FhuA Δ1-159_C545_V548_F501_tev), CD (circular dichroism), ESI-MS (electrospray ionization-mass spectrometry), NaP_i (sodium phosphate buffer).

Supporting Information

Supporting Information File 1

Illustration of the catalyst **2** and NMR spectra of synthesized compounds.
[http://www.beilstein-journals.org/bjoc/content/supplementary/1860-5397-12-124-S1.pdf]

Acknowledgements

We gratefully acknowledge the financial support by the Deutsche Forschungsgemeinschaft (DFG) through the International Research Training Group “Selectivity in Chemo- and Biocatalysis” (SeleCa), the excellence cluster “Tailor-made Fuels from Biomass” (TMFB), the JSPS Japan-German Graduate Externship Program, and Grants-in-Aid for Scientific Research (JSPS KAKENHI Grant Number JP15H05804 in Precisely Designed Catalysts with Customized Scaffolding) from MEXT.

References

1. Lu, Y. *Angew. Chem., Int. Ed.* **2006,** *45,* 5588–5601. doi:10.1002/anie.200600168
2. Steinreiber, J.; Ward, T. R. *Coord. Chem. Rev.* **2008,** *252,* 751–766. doi:10.1016/j.ccr.2007.09.016
3. Reetz, M. T. *Chem. Rec.* **2012,** *12,* 391–406. doi:10.1002/tcr.201100043
4. Lewis, J. C. *ACS Catal.* **2013,** *3,* 2954–2975. doi:10.1021/cs400806a
5. Matsuo, T.; Hirota, S. *Bioorg. Med. Chem.* **2014,** *22,* 5638–5656. doi:10.1016/j.bmc.2014.06.021
6. Hayashi, T.; Sano, Y.; Onoda, A. *Isr. J. Chem.* **2015,** *55,* 76–84. doi:10.1002/ijch.201400123
7. Heinisch, T.; Ward, T. R. *Eur. J. Inorg. Chem.* **2015,** *2015,* 3406–3418. doi:10.1002/ejic.201500408
8. Lu, Y.; Yeung, N.; Sieracki, N.; Marshall, N. M. *Nature* **2009,** *460,* 855–862. doi:10.1038/nature08304
9. Yu, F.; Cangelosi, V. M.; Zastrow, M. L.; Tegoni, M.; Plegaria, J. S.; Tebo, A. G.; Mocny, C. S.; Ruckthong, L.; Qayyum, H.; Pecoraro, V. L. *Chem. Rev.* **2014,** *114,* 3495–3578. doi:10.1021/cr400458x
10. Letondor, C.; Pordea, A.; Humbert, N.; Ivanova, A.; Mazurek, S.; Novic, M.; Ward, T. R. *J. Am. Chem. Soc.* **2006,** *128,* 8320–8328. doi:10.1021/ja061580o
11. Zimbron, J. M.; Heinisch, T.; Schmid, M.; Hamels, D.; Nogueira, E. S.; Schirmer, T.; Ward, T. R. *J. Am. Chem. Soc.* **2013,** *135,* 5384–5388. doi:10.1021/ja309974s
12. Chatterjee, A.; Mallin, H.; Klehr, J.; Vallapurackal, J.; Finke, A. D.; Vera, L.; Marsh, M.; Ward, T. R. *Chem. Sci.* **2016,** *7,* 673–677. doi:10.1039/C5SC03116H

13. Lo, C.; Ringenberg, M. R.; Gnandt, D.; Wilson, Y.; Ward, T. R. *Chem. Commun.* **2011,** *47,* 12065–12067. doi:10.1039/c1cc15004a
14. Mayer, C.; Gillingham, D. G.; Ward, T. R.; Hilvert, D. *Chem. Commun.* **2011,** *47,* 12068–12070. doi:10.1039/c1cc15005g
15. Matsuo, T.; Imai, C.; Yoshida, T.; Saito, T.; Hayashi, T.; Hirota, S. *Chem. Commun.* **2012,** *48,* 1662–1664. doi:10.1039/c2cc16898g
16. Basauri-Molina, M.; Verhoeven, D. G. A.; van Schaik, A. J.; Kleijn, H.; Klein Gebbink, R. J. M. *Chem. – Eur. J.* **2015,** *21,* 15676–15685. doi:10.1002/chem.201502381
17. Philippart, F.; Arlt, M.; Gotzen, S.; Tenne, S.-J.; Bocola, M.; Chen, H.-H.; Zhu, L.; Schwaneberg, U.; Okuda, J. *Chem. – Eur. J.* **2013,** *19,* 13865–13871. doi:10.1002/chem.201301515
18. Sauer, D. F.; Bocola, M.; Broglia, C.; Arlt, M.; Zhu, L.-L.; Brocker, M.; Schwaneberg, U.; Okuda, J. *Chem. – Asian J.* **2015,** *10,* 177–182. doi:10.1002/asia.201403005
19. Sauer, D. F.; Himiyama, T.; Tachikawa, K.; Fukumoto, K.; Onoda, A.; Mizohata, E.; Inoue, T.; Bocola, M.; Schwaneberg, U.; Hayashi, T.; Okuda, J. *ACS Catal.* **2015,** *5,* 7519–7522. doi:10.1021/acscatal.5b01792
20. Zhao, J.; Kajetanowicz, A.; Ward, T. R. *Org. Biomol. Chem.* **2015,** *13,* 5652–5655. doi:10.1039/C5OB00428D
21. Zhang, C.; Srivastava, P.; Ellis-Guardiola, K.; Lewis, J. C. *Tetrahedron* **2014,** *70,* 4245–4249. doi:10.1016/j.tet.2014.03.008
22. Reetz, M. T.; Jiao, N. *Angew. Chem., Int. Ed.* **2006,** *45,* 2416–2419. doi:10.1002/anie.200504561
23. Podtetenieff, J.; Taglieber, A.; Bill, E.; Reijerse, E. J.; Reetz, M. T. *Angew. Chem., Int. Ed.* **2010,** *49,* 5151–5155. doi:10.1002/anie.201002106
24. Deuss, P. J.; Popa, G.; Slawin, A. M. Z.; Laan, W.; Kamer, P. C. J. *ChemCatChem* **2013,** *5,* 1184–1191. doi:10.1002/cctc.201200671
25. Bos, J.; Fusetti, F.; Driessen, A. J. M.; Roelfes, G. *Angew. Chem., Int. Ed.* **2012,** *51,* 7472–7475. doi:10.1002/anie.201202070
26. Himiyama, T.; Sauer, D. F.; Onoda, A.; Spaniol, T. P.; Okuda, J.; Hayashi, T. *J. Inorg. Biochem.* **2016,** *158,* 55–61. doi:10.1016/j.jinorgbio.2015.12.026
27. Ghattas, W.; Cotchico-Alonso, L.; Maréchal, J.-D.; Urvoas, A.; Rousseau, M.; Mahy, J.-P.; Ricoux, R. *ChemBioChem* **2016,** *17,* 433–440. doi:10.1002/cbic.201500445
28. Nicolaou, K. C.; Snyder, S. A.; Montagnon, T.; Vassilikogiannakis, G. *Angew. Chem., Int. Ed.* **2002,** *41,* 1668–1698. doi:10.1002/1521-3773(20020517)41:10<1668::AID-ANIE1668>3.0.CO;2-Z
29. Reymond, S.; Cossy, J. *Chem. Rev.* **2008,** *108,* 5359–5406. doi:10.1021/cr078346g
30. Kagan, H. B.; Riant, O. *Chem. Rev.* **1992,** *92,* 1007–1019. doi:10.1021/cr00013a013
31. Tenne, S.-J.; Schwaneberg, U. *Int. J. Mol. Sci.* **2012,** *13,* 2459–2471. doi:10.3390/ijms13022459
32. Otto, S.; Engberts, J. B. F. N.; Kwak, J. C. T. *J. Am. Chem. Soc.* **1998,** *120,* 9517–9525. doi:10.1021/ja9816537
33. Fulmer, G. R.; Miller, A. J. M.; Sherden, N. H.; Gottlieb, H. E.; Nudelman, A.; Stoltz, B. M.; Bercaw, J. E.; Goldberg, K. I. *Organometallics* **2010,** *29,* 2176–2179. doi:10.1021/om100106e
34. Occhipinti, G.; Jensen, V. R.; Törnroos, K. W.; Frøystein, N. Å.; Bjørsvik, H.-R. *Tetrahedron* **2009,** *65,* 7186–7194. doi:10.1016/j.tet.2009.05.095
35. Perera, A. S.; Subbaiyan, N. K.; Kalita, M.; Wendel, S. O.; Samarakoon, T. N.; D'Souza, F.; Bossmann, S. H. *J. Am. Chem. Soc.* **2013,** *135,* 6842–6845. doi:10.1021/ja403090x
36. Constable, E. C.; Ward, M. D. *Dalton Trans.* **1990,** 1405–1409. doi:10.1039/DT9900001405
37. de Figueiredo, R. M.; Oczipka, P.; Fröhlich, R.; Christmann, M. *Synthesis* **2008,** 1316–1318. doi:10.1055/s-2008-1032016

License and Terms

This is an Open Access article under the terms of the Creative Commons Attribution License (http://creativecommons.org/licenses/by/2.0), which permits unrestricted use, distribution, and reproduction in any medium, provided the original work is properly cited.

The license is subject to the *Beilstein Journal of Organic Chemistry* terms and conditions: (http://www.beilstein-journals.org/bjoc)

The definitive version of this article is the electronic one which can be found at: doi:10.3762/bjoc.12.124

BEILSTEIN JOURNAL OF ORGANIC CHEMISTRY

On the mechanism of imine elimination from Fischer tungsten carbene complexes

Philipp Veit, Christoph Förster* and Katja Heinze*

Full Research Paper

Open Access

Address:
Institute of Inorganic and Analytical Chemistry, Johannes Gutenberg-University, Duesbergweg 10-14, 55128 Mainz, Germany

Email:
Christoph Förster* - cfoerster@uni-mainz.de;
Katja Heinze* - katja.heinze@uni.mainz.de

* Corresponding author

Keywords:
carbene complexes; ferrocene; imine; mechanism; tungsten

Beilstein J. Org. Chem. **2016,** *12,* 1322–1333.
doi:10.3762/bjoc.12.125

Received: 15 April 2016
Accepted: 07 June 2016
Published: 27 June 2016

This article is part of the Thematic Series "Organometallic chemistry". In memoriam Prof. Dr. Peter Hofmann.

Guest Editor: B. F. Straub

© 2016 Veit et al.; licensee Beilstein-Institut.
License and terms: see end of document.

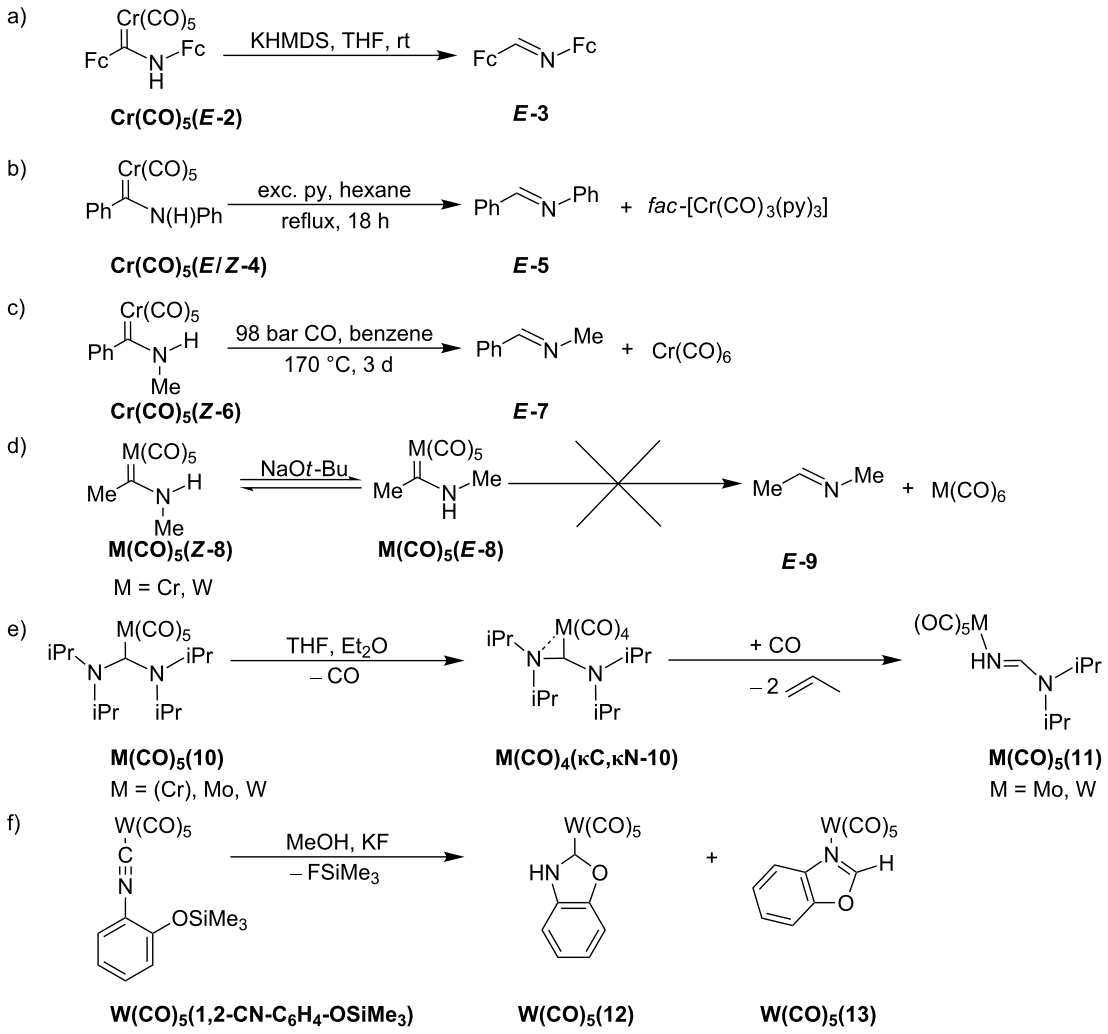
Abstract

(Aminoferrocenyl)(ferrocenyl)carbene(pentacarbonyl)tungsten(0) $(CO)_5W{=}C(NHFc)Fc$ (**W(CO)$_5$(*E*-2)**) is synthesized by nucleophilic substitution of the ethoxy group of $(CO)_5W{=}C(OEt)Fc$ (**M(CO)$_5$(1^{Et})**) by ferrocenyl amide Fc-NH$^-$ (Fc = ferrocenyl). **W(CO)$_5$(*E*-2)** thermally and photochemically eliminates bulky *E*-1,2-diferrocenylimine (***E*-3**) via a formal 1,2-H shift from the N to the carbene C atom. Kinetic and mechanistic studies to the formation of imine ***E*-3** are performed by NMR, IR and UV–vis spectroscopy and liquid injection field desorption ionization (LIFDI) mass spectrometry as well as by trapping experiments for low-coordinate tungsten complexes with triphenylphosphane. **W(CO)$_5$(*E*-2)** decays thermally in a first-order rate-law with a Gibbs free energy of activation of $\Delta G^{\ddagger}_{298K}$ = 112 kJ mol^{-1}. Three proposed mechanistic pathways are taken into account and supported by detailed (time-dependent) densitiy functional theory [(TD)-DFT] calculations. The preferred pathway is initiated by an irreversible CO dissociation, followed by an oxidative addition/pseudorotation/reductive elimination pathway with short-lived, elusive seven-coordinate hydrido tungsten(II) intermediates ***cis*(N,H)-W(CO)$_4$(H)(*Z*-15)** and ***cis*(C,H)-W(CO)$_4$(H)(*Z*-15)**.

Introduction

Since the first example of a Fischer carbene complex $(CO)_5W{=}C(OMe)Me$ [1] in 1964, these compounds have evolved into a huge substance class with versatile applications as chemical multitalents in organic synthesis [2-5] as well as in light-driven organic reactions [6-8]. Carbene complexes of pentacarbonyl metal fragments (M = Cr, Mo, W) have further proven to be effective carbene transfer agents to late transition metals in transmetalation reactions [9-15]. The manifold synthetic access routes to carbene complexes even allows the assembly of multicarbene and multimetal carbene complexes [16,17]. First representatives of multimetal carbene complexes **M(CO)$_5$(1^R)** bear α-ferrocenyl alkoxy carbenes :C(OR)Fc (**1^R**,

M = Cr, Mo, W; R = Me, Et; Fc = ferrocenyl) [18-22]. Nucleophilic substitution of the alkoxy substituent OR by amines gives access to α-ferrocenylamino Fischer carbene complexes [18,20,21,23-27], according to the classical Fischer route [28-31]. In contrast to conventional aromatic substituents, the Fc unit in **M(CO)$_5$(1^R)** is characterized by its redox activity and its large cylindrical steric bulk [32,33]. The electrochemical behaviour of ferrocenyl carbene complexes has been extensively investigated [25-27,34-39]. A second ferrocenyl unit can be incorporated by employing aminoferrocene (Fc-NH$_2$) [40,41] in a nucleophilic substitution reaction [27]. The trimetallic complex **Cr(CO)$_5$(*E*-2)** with the (aminoferrocenyl)ferrocenylcarbene ligand ***E*-2** is readily synthesized from **Cr(CO)$_5$(1^{Et})** by nucleophilic substitution of the ethoxy group with in situ generated ferrocenyl amide Fc-NH$^-$. Unlike the facile synthesis of the diphenyl derivative **Cr(CO)$_5$(*E*-4)** from **Cr(CO)$_5$(1^{Et})** and aniline [30,42], the preparation of the diferrocenyl derivative **Cr(CO)$_5$(*E*-2)** from bulky Fc-NH$_2$ [40,41] requires the presence of a base to increase the nucleophilicity of Fc-NH$_2$ by deprotonation. In the presence of base, **Cr(CO)$_5$(*E*-2)** decomposes readily in solution at room temperature releasing *E*-1,2-diferrocenylimine [43] ***E*-3** (Scheme 1a) [27]. Base assisted imine formation of NH carbene complexes typically occurs under rather harsh conditions. Thermal treatment of the significantly less encumbered complex **Cr(CO)$_5$(*E*/*Z*-4)** for 18 h in a 1:10 (v:v) pyridine (py)/hexane mixture yields imine ***E*-5** and *fac*-[Cr(CO)$_3$(py)$_3$] as side-product (Scheme 1b) [44]. Formation of the imine ***E*-7** and Cr(CO)$_6$ from the carbene complex **Cr(CO)$_5$(*Z*-6)** requires heating to 170 °C for 3 days under CO pressure (Scheme 1c) [42]. At room temperature and in the presence of base (KO*t*-Bu), **M(CO)$_5$(*Z*-8)** (M = Cr, W) simply isomerize to a mixture of *E*/*Z* isomers **M(CO)$_5$(*E*-8)**/



Scheme 1: Imine formation and isomerization reactions from NH carbene complexes **Cr(CO)$_5$(*E*-2)** (a) [27], **Cr(CO)$_5$(*E*/*Z*-4)** (b) [44], **Cr(CO)$_5$(*Z*-6)** (c) [42], **M(CO)$_5$(*Z*-8)** (d) [45,46], **M(CO)$_5$(10)** (e) [50-52] and during Si–O cleavage in the isonitrile complex **W(CO)$_5$(1,2-CN-C$_6$H$_4$-OSiMe$_3$)** (f) [53].

M(CO)$_5$(*Z*-8) without ligand loss or formation of imine ***E*-9** (Scheme 1d) [45,46]. It appears that the bulky diferrocenylcarbene ***E*-2** facilitates formation of imine ***E*-3**. Mechanistically, a base-assisted 1,2-H shift can be conceived either at the coordinated carbene or at the free carbene [47,48] after ligand exchange at chromium (by py or CO) for **Cr(CO)$_5$(*E*/*Z*-4)** and **Cr(CO)$_5$(*Z*-6)**. Both pathways are compatible with the formation of the metal-containing products *fac*-[Cr(CO)$_3$(py)$_3$] and Cr(CO)$_6$ by dissociation of the imines ***E*-5** or ***E*-7** or by dissociation of the carbenes ***E*-4** or ***E*-6**, respectively (Scheme 1b,c) [42,44].

The related pentacarbonyl complexes of bis[di(isopropyl)amino]carbene **10** [49] **M(CO)$_5$(10)** (M = Cr, Mo, W) readily decarbonylate at room temperature to give the tetracarbonyl complexes **M(CO)$_4$(κC,κN-10)** with a side-on coordinated carbene ligand (Scheme 1e) [50-52]. Under CO atmosphere, the molybdenum and tungsten complexes **M(CO)$_{4/5}$(10)**, (M = Mo, W) eliminate two equivalents of propene giving the imine complexes **M(CO)$_5$(11)**. Formation of the imine complex tungsten(benzoxazole)(pentacarbonyl) **W(CO)$_5$(13)** has been reported by Tamm and Hahn during the synthesis of the carbene complex tungsten(benzoxazolin-2-ylidene)(pentacarbonyl) **W(CO)$_5$(12)** (Scheme 1f) [53].

In principle, the formation of imines from NH carbene complexes can occur by three conceivable fundamental pathways. The first pathway starts with the dissociation of the carbene followed by a 1,2-H shift at the free carbene (elimination–migration). The second one operates via a hydrogen atom shift at the coordinated carbene followed by dissociation of the resulting imine (migration–elimination). A third conceivable pathway could start with CO loss, followed by H atom migration. To the best of our knowledge, the mechanism of the imine formation from NH carbene complexes is not yet established.

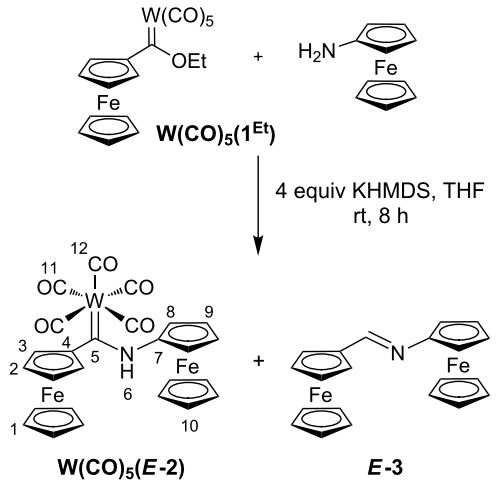
In the absence of a base, the bulky diferrocenylcarbene complex **Cr(CO)$_5$(*E*-2)** is stable even in refluxing toluene and hence, a simple migration–elimination or elimination–migration reaction is not anticipated in this case. We report here the heavier tungsten analogue **W(CO)$_5$(*E*-2)** which is thermally reactive and smoothly forms the imine ***E*-3** without the need of prior deprotonation. This apparently simpler reaction allows the investigation of the mechanism of imine formation from NH carbene complexes.

Herein, the synthesis and characterization of **W(CO)$_5$(*E*-2)** followed by detailed mechanistic studies regarding the formation of imine ***E*-3** are presented including mass spectrometric, NMR, IR and UV–vis spectroscopic kinetic studies in combination with (TD)-DFT methods.

Results and Discussion

Synthesis of W(CO)$_5$(*E*-2)

The diferrocenyl NH carbene complex **W(CO)$_5$(*E*-2)** is obtained by treating **W(CO)$_5$(1^{Et})** [20,21] with aminoferrocene (Fc-NH$_2$) [40,41] in the presence of potassium hexamethyldisilazide (KHMDS) in tetrahydrofuran at room temperature (Scheme 2). In an analogous reactivity to **Cr(CO)$_5$(*E*-2)** (Scheme 1a) [27], the formation of the imine ***E*-3** is observed as a side-reaction under the alkaline conditions. Due to this reactivity, **W(CO)$_5$(*E*-2)** is obtained in only 28% yield as a deep-red crystalline compound after purification via column chromatography.



Scheme 2: Synthesis of **W(CO)$_5$(*E*-2)** from **W(CO)$_5$(1^{Et})** [20,21] and aminoferrocene [40,41] with concomitant formation of *E*-1,2-diferrocenylimine ***E*-3** [43] as side-product and atom numbering of **W(CO)$_5$(*E*-2)** for NMR assignments.

Characterization of W(CO)$_5$(*E*-2)

The composition and purity of **W(CO)$_5$(*E*-2)** is ascertained by mass spectrometry, showing the expected molecular ion peak at m/z = 721 with appropriate isotopic pattern, and elemental analysis (Experimental section and Supporting Information File 1). At increasing temperature in the FD mass spectrometer, peaks at m/z = 397 appear which can be assigned to a molecular ion of the composition $C_{21}H_{19}NFe_2$. A tiny peak cluster at m/z = 693, assignable to the loss of CO from **W(CO)$_5$(*E*-2)**, and peaks at higher m/z ratios, assignable to tungsten clusters, are also observed when traces of oxygen/water were present. Using ^{1}H and ^{13}C NMR spectroscopy as well as 2D NMR (^{1}H,^{1}H COSY, ^{1}H,^{1}H NOESY, ^{13}C,^{1}H HSQC, ^{13}C,^{1}H HMBC techniques), all ^{1}H and ^{13}C NMR resonances of **W(CO)$_5$(*E*-2)** are assigned based on coupling patterns and NOE contacts (Experimental section and Supporting Information File 1). Only the resonances of the unsubstituted C_5H_5 ligands (H^1, H^{10} and C^1, C^{10}) could not be discriminated. The proton resonances are

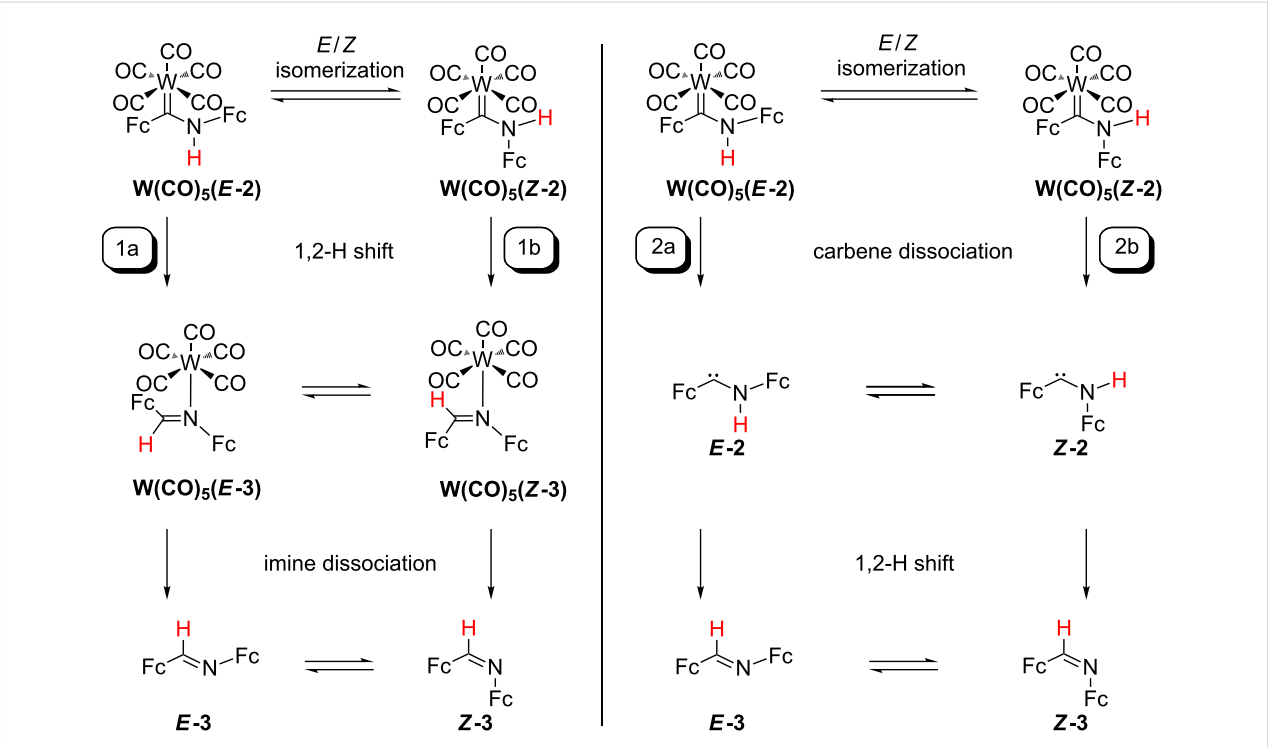
found in a similar region as for other (pentacarbonyl)tungsten complexes **W(CO)$_5$(*E*-14^R)** with the α-ferrocenyl NH carbene ligand :C(NHR)Fc ***E*-14^R** (R = Me, Et, *n*-Pr [23], *n*-Bu [25], *n*-Pent [21]). Due to additional ring-current effects and non-classical NH···Fe hydrogen bonding [54-59] of the NH-Fc moiety, the resonance for the amine proton NH[6] (δ = 10.50 ppm in CD_2Cl_2) is shifted to lower field as compared to that of alkylamine substituted NH carbene complexes **M(CO)$_5$(*E*-14^R)** (δ = 9.00–9.11 ppm in $CDCl_3$) [21,23]. The NH···Fe interaction is also supported by the low-energy NH stretching vibration of **W(CO)$_5$(*E*-2)** at 3240 cm^{-1} in CD_2Cl_2, which matches to that of **Cr(CO)$_5$(*E*-2)** (3233 cm^{-1}) [27] (Experimental section and Supporting Information File 1). A weak absorption band at 3439 cm^{-1} is tentatively assigned to some **W(CO)$_5$(*Z*-2)** isomer lacking the NH···Fe interaction. In the solid state (KBr) the NH stretching vibration appears at 3335 cm^{-1} (Experimental section and Supporting Information File 1). The C–N–H bending vibration is observed as a single sharp relatively strong band at 1508 cm^{-1}. These IR data reveal that the main isomer in solution as well in the solid state is the *E* isomer in accordance with the IR data of **W(CO)$_5$(*E*/*Z*-8)** [46]. The carbonyl region of IR spectra of **W(CO)$_5$(*E*-2)** are in accordance with those of **Cr(CO)$_5$(*E*-2)** [27] and related amino(ferrocenyl)carbene(pentacarbonyl)tungsten complexes **W(CO)$_5$(*E*-14^R)** (R = Me, Et, *n*-Pr [23], *n*-Bu [25], *n*-Pent [21]). The UV–vis spectrum of **W(CO)$_5$(*E*-2)** (Supporting Information File 1) is similar to that of **Cr(CO)$_5$(*E*-2)** [27] and to those of carbene(pentacarbonyl)metal complexes (Cr, W) [60,61].

Thermolysis of **W(CO)$_5$(*E*-2)** in refluxing toluene gives imine ***E*-3** [43] after ca. 24 h in almost quantitative yield, as monitored by ^{1}H NMR spectroscopy. Accordingly, **W(CO)$_5$(*E*-2)** is a suitable candidate to investigate the imine formation from NH carbene complexes in a simple one-component system under relatively mild conditions and, importantly, in the absence of a base.

DFT studies on the formation of imine *E*-3 from W(CO)$_5$(*E*-2)

Three conceivable reaction pathways for the formation of imine ***E*-3** have been considered. For each pathway, density functional theory (DFT) calculations on the B3LYP/LANL2DZ (IEF-PCM toluene) level of theory have been performed to localize minimum structures and energies of the intermediates which are connected by transition states. The Gibbs free energies are reported at 298 K.

The first pathway comprises the migration–elimination mechanism involving a 1,2-H shift at the coordinated carbene ligand ***E*-2** or ***Z*-2** in **W(CO)$_5$(*E*-2)** or **W(CO)$_5$(*Z*-2)** followed by dissociation of the respective imine ***E*-3** (pathway 1a, Scheme 3) or ***Z*-3** (pathway 1b, Scheme 3), respectively. In the

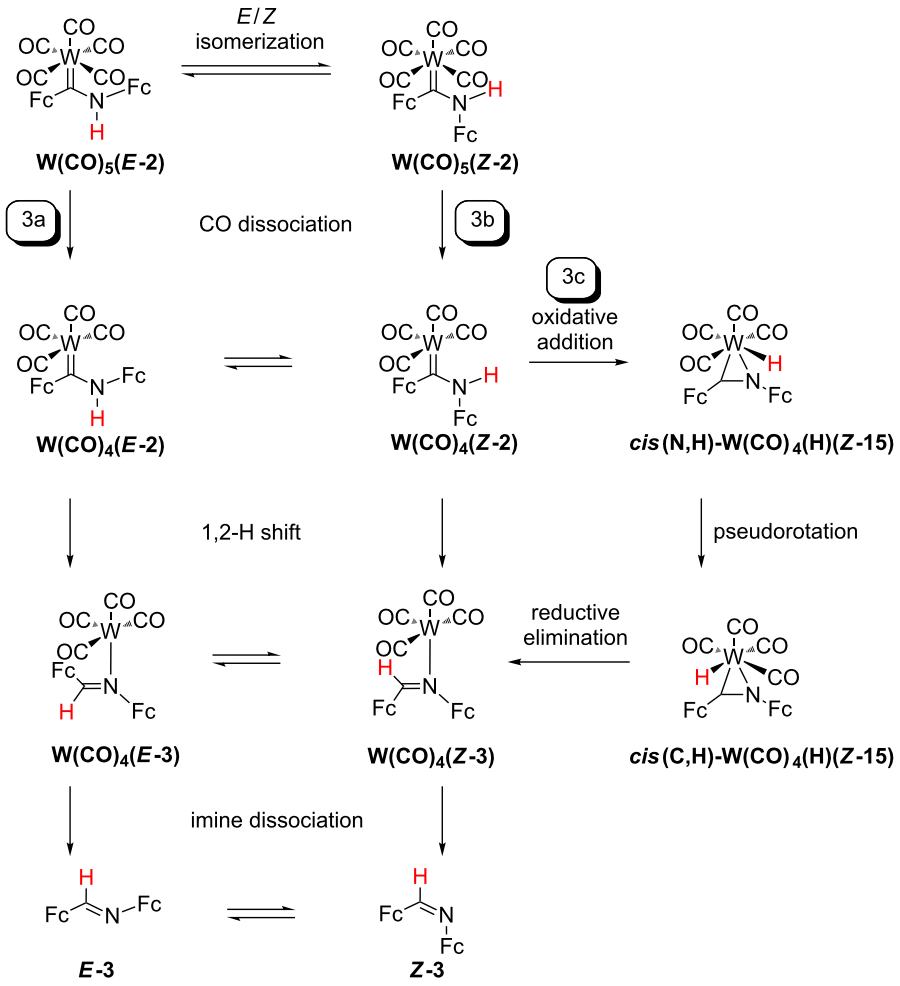


Scheme 3: Reaction pathways 1a/1b (migration–elimination) and 2a/2b (elimination–migration) for the formation of imine ***E*-3** from **W(CO)$_5$(*E*-2)**.

latter case, ***Z*-3** isomerizes to the thermodynamically preferred isomer ***E*-3**. The second pathway (carbene elimination–migration) starts with the elimination of the carbenes ***E*-2** or ***Z*-2** followed by an 1,2-H shift to give the imines ***E*-3** (pathway 2a, Scheme 3) or ***Z*-3** (pathway 2b, Scheme 3). In the latter case, a ***Z*-3** → ***E*-3** isomerization follows.

The initial step of the third pathway is a CO dissociation yielding the tetracarbonyl complexes **W(CO)$_4$(*E*-2)** or **W(CO)$_4$(*Z*-2)**. This elimination is followed by a hydrogen atom shift at the coordinated carbene ligands ***E*-2** or ***Z*-2** (pathway 3a and 3b, Scheme 4) giving **W(CO)$_4$(*E*-3)** or **W(CO)$_4$(*Z*-3)**, respectively. Furthermore, the free coordination site in **W(CO)$_4$(*E*-2)** or **W(CO)$_4$(*Z*-2)** offers an oxidative addition/pseudorotation/reductive elimination pathway via the hydrido tungsten(II) complexes **W(CO)$_4$(H)(*Z*-15)** with the formally anionic ligand [Fc-C=N-Fc]$^-$ (**15**$^-$) as further alternative (pathway 3c, Scheme 4).

The calculated Gibbs free energies for **W(CO)$_5$(*E*-2)** and **W(CO)$_5$(*Z*-2)** are basically identical (Supporting Information File 1, Figure S16, Scheme 3). The calculated barrier for the *E*/*Z* isomerization **W(CO)$_5$(*E*-2)** → **W(CO)$_5$(*Z*-2)** amounts to $\Delta G^{\ddagger}$ = 108 kJ mol^{-1}. This barrier is significantly higher than that reported for (methoxy)(methyl)carbene(pentacarbonyl)chromium(0) Cr(CO)$_5$(C(OMe)Me) (52 kJ mol^{-1} (experimental) and ca. 61 kJ mol^{-1} (theoretical)) due to the larger steric bulk of the (aminoferrocenyl)ferrocenylcarbene **2**, the higher π-donating character of the amino substituent vs the alkoxy substituent thus increasing the C(carbene)–X double bond character (X = N, O) [62-64] and the loss of some attractive NH···Fe interaction (H···Fe(Fc-C) = 2.98 Å) in **W(CO)$_5$(*E*-2)** [27,54-59]. The Gibbs free energy of activation for the 1,2-H shift in **W(CO)$_5$(*Z*-2)** to give the imine complex **W(CO)$_5$(*Z*-3)** amounts to $\Delta G^{\ddagger}$ = 333 kJ mol^{-1} which is prohibitively large. For **W(CO)$_5$(*E*-2)** → **W(CO)$_5$(*E*-3)**, this barrier is somewhat smaller ($\Delta G^{\ddagger}$ = 284 kJ mol^{-1}), yet this 1,2-



Scheme 4: Reaction pathways 3a/3b/3c (CO dissociation) for the formation of imine ***E*-3** from **W(CO)$_5$(*E*-2)**.

H shift initially only leads to a van-der-Waals adduct of the imine ***E*-3** [**W(CO)$_5$···*E*-3**]. Hence, this hydrogen atom shift is coupled with a W–C(carbene) bond dissociation.

The turn over frequency (TOF) of catalytic cycles can be estimated from the energies of the TOF-determining transition state (TDTS) and the TOF-determining intermediate (TDI) [65]. The given energy difference between TDTS and TDI is the maximum energy span between a given intermediate and all following transition states of the cycle and can be understood as the overall Gibbs free energy of activation of the whole catalytic cycle [65]. This procedure can be translated to competing reaction paths. For pathways 1a and 1b (Scheme 3), the rate-determining intermediate (RDI) is **W(CO)$_5$(*Z*-2)** and the rate-determining transition states (RDTS's) are TS(**W(CO)$_5$(*E*-2)** → **W(CO)$_5$···*E*-3**) (pathway 1a) and TS(**W(CO)$_5$(*Z*-2)** → **W(CO)$_5$(*Z*-3)** (pathway 1b) giving the overall Gibbs free energies of activation $\Delta G^{\ddagger}_{total}$ = 287 kJ mol^{-1} and $\Delta G^{\ddagger}_{total}$ = 333 kJ mol^{-1}, respectively. The lower energy pathway 1a is associated with the dissociation of the carbene ligand (Supporting Information File 1, Figure S16). Hence, the initial dissociation of the carbenes ***E*-2** and ***Z*-2** is considered in pathways 2a and 2b (Scheme 3).

Dissociation of the carbenes ***E*-2**/***Z*-2** from **W(CO)$_5$(*E*-2)**/**W(CO)$_5$(*Z*-2)** is calculated endergonic (ΔG = 141 kJ mol^{-1} and ΔG = 167 kJ mol^{-1}, respectively, Scheme 3). Transition states for the carbene dissociation could not be identified. Hence, this initial dissociative step is probably not the one with the lowest energy. Nonetheless, the 1,2-H shift in the free carbenes has been calculated as well (Scheme 3).

The carbene ***E*-2** is 23 kJ mol^{-1} more stable than the ***Z*-2** isomer (Supporting Information File 1, Figure S17). The interconversion between these isomers ***E*-2** → ***Z*-2** ($\Delta G^{\ddagger}$ = 130 kJ mol^{-1}) proceeds via a bending vibration of the Cp–C(carbene)–N moiety. This reaction coordinate is fully analogous to the proposed mechanism of the *E*/*Z* isomerization of imines [66,67]. During the 1,2-H-shift of ***E*-2** to ***E*-3**, the migrating hydrogen atom interacts with the empty p_π-type orbital of the carbene carbon atom ($\Delta G^{\ddagger}$ = 250 kJ mol^{-1}), which is in accordance with the established mechanism of 1,2-migration reactions of carbenes [47,48,68-71]. Interestingly, the 1,2-H-shift of ***Z*-2** (***Z*-2** → ***Z*-3**: $\Delta G^{\ddagger}$ = 179 kJ mol^{-1}) with a lower barrier occurs within the C–C(carbene)–N plane via a direct interaction of the n_σ orbital at the carbene carbon atom with the hydrogen 1s orbital. Because of the non-crossing rule, this path is symmetry forbidden for aromatic carbenes [47,72]. The calculated barrier of the *E*/*Z* isomerization ***Z*-3** → ***E*-3** ($\Delta G^{\ddagger}$ = 52 kJ mol^{-1}) is in good agreement with experimental data for other imines with similar steric bulk, e.g., (Fc)$_2$C=NAr, leading to the global minimum ***E*-3** of pathways 2a and 2b (Scheme 3) [66,67]. ***E*-2** is the RDI for pathways 2a and 2b. The transition states TS(***E*-2** → ***E*-3**) ($\Delta G^{\ddagger}_{total}$ = 250 kJ mol^{-1}, pathway 2a) and TS(***Z*-2** → ***Z*-3**) ($\Delta G^{\ddagger}_{total}$ = 202 kJ mol^{-1}, pathway 2b) are the RDTS's. The 1,2-H-shift of the free carbenes **2** preferably proceeds via pathway 2b (Supporting Information File 1, Figure S17).

Compared to the carbene dissociation, significantly smaller endergonicities are calculated for the dissociation of a carbonyl ligand (pathways 3a and 3b, Scheme 4) giving the tetracarbonyl complexes **W(CO)$_4$(*E*-2)** and **W(CO)$_4$(*Z*-2)** with ΔG = 86 kJ mol^{-1} and 115 kJ mol^{-1}, respectively (Scheme 4). The **W(CO)$_4$(*E*-2)** isomer is stabilized with respect to **W(CO)$_4$(*Z*-2)** by 26 kJ mol^{-1}. The *E*/*Z* isomerization of **W(CO)$_4$(2)** proceeds via an intermediate **W(CO)$_4$(κ*C*,κ*N*-2)** with a side-on coordination of the carbene ligand **2** exploiting the free coordination site at tungsten similar to **M(CO)$_4$(κC,κN-10)** [50-52] (Scheme 1, Supporting Information File 1, Figure S18). The barrier for this *E*/*Z* carbene isomerization amounts to only $\Delta G^{\ddagger}$ = 99 kJ mol^{-1}. This represents the lowest barrier for the ***E*-2**/***Z*-2** isomerization calculated in the systems **W(CO)$_5$(*E*-2**/***Z*-2)**, **W(CO)$_4$(*E*-2**/***Z*-2)** and ***E*-2**/***Z*-2** (vide supra). However, the following 1,2-H shifts have high barriers of 294 and 248 kJ mol^{-1} for **W(CO)$_4$(*E*-2)** → **W(CO)$_4$(*E*-3)** and **W(CO)$_4$(*Z*-2)** → **W(CO)$_4$(*Z*-3)**, respectively. For the former reaction and similar to the 1,2-H shift in **W(CO)$_5$(*E*-2)** (vide supra), the van-der-Waals adduct **[W(CO)$_4$···*E*-3]** is the initial product implying the dissociation of the W–C(carbene) bond. The RDI for pathways 3a and 3b is **W(CO)$_4$(*E*-2)**. The RDTS's are TS(**W(CO)$_4$(*E*-2)** → **[W(CO)$_4$···*E*-3]**) ($\Delta G^{\ddagger}_{total}$ = 294 kJ mol^{-1}, pathway 3a) and TS(**W(CO)$_4$(*Z*-2)** → **W(CO)$_4$(*Z*-3)**) ($\Delta G^{\ddagger}_{total}$ = 274 kJ mol^{-1}, pathway 3b). Both pathways 3a and 3b are quite energy demanding and require even more energy than the ***E*-2** → ***E*-3** and ***Z*-2** → ***Z*-3** hydrogen atom migrations in the free carbenes (vide supra). The free coordination site at tungsten in **W(CO)$_4$(*Z*-2)** provides a third sequence for the formation of imine ***E*-3** (Scheme 4, Figure 1). Oxidative addition of the NH bond to the unsaturated tungsten center ($\Delta G^{\ddagger}$ = 157 kJ mol^{-1}) gives the seven-coordinate hydrido tungsten(II) complex ***cis*(N,H)-W(CO)$_4$(H)(*Z*-15)** with formally anionic [Fc-C=N-Fc]$^-$ (**15**$^-$) and hydrido ligands (Scheme 4, Figure 1 and Figure 2).

A similar oxidative addition has been proposed in the literature for the iron (aminophenyl)phenylcarbene complex [Cp(CO)(S(SiEt$_3$))Fe(**4**)] leading to an intermediate hydrido species followed by the elimination of *E*-1,2-diphenylimine ***E*-5** [73]. Pseudorotation of ***cis*(N,H)-W(CO)$_4$(H)(*Z*-15)** to the isoenergetic rotamer ***cis*(C,H)-W(CO)$_4$(H)(*Z*-15)** ($\Delta G^{\ddagger}$ = 86 kJ mol^{-1}) enables a low-energy reductive elimination

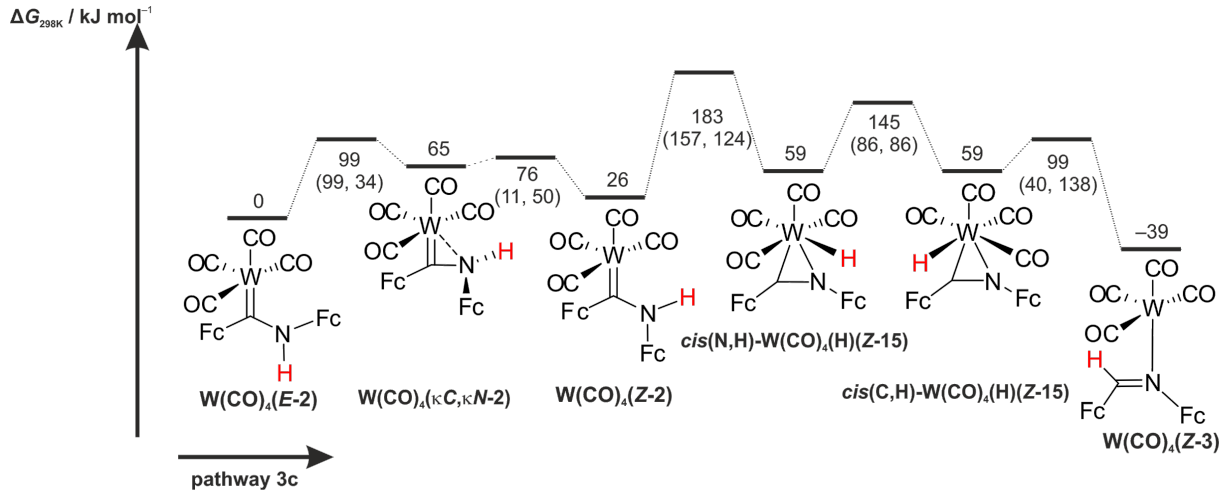


Figure 1: DFT calculated oxidative addition/pseudorotation/reductive elimination pathway 3c from **W(CO)$_4$(*E*-2)** to **W(CO)$_4$(*Z*-3)**.

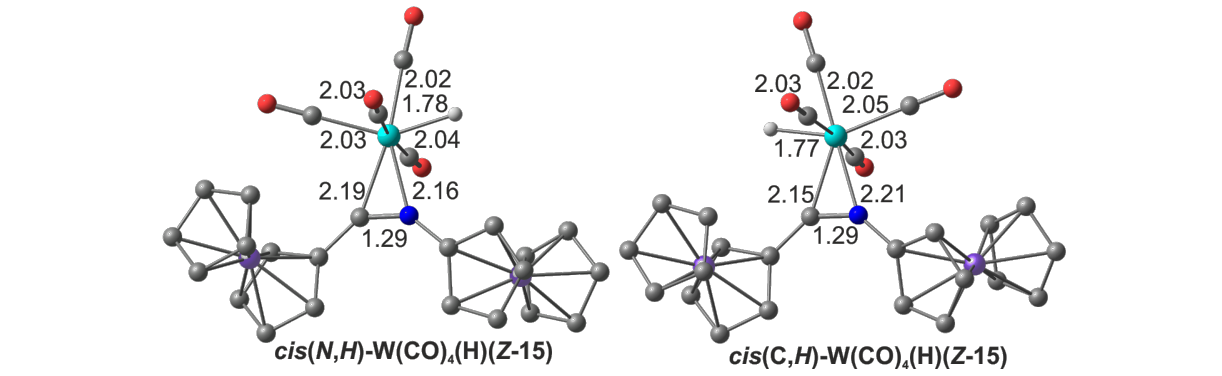


Figure 2: DFT calculated geometries of the two hydrido intermediates ***cis*(*N*,*H*)-W(CO)$_4$(H)(*Z*-15)** and ***cis*(*C*,*H*)-W(CO)$_4$(H)(*Z*-15)** and selected bond distances in Å.

($\Delta G^{\ddagger}$ = 40 kJ mol^{-1}) to give the imine complex **W(CO)$_4$(*Z*-3)** (Figure 1).

The overall Gibbs free energy of activation amounts to only $\Delta G^{\ddagger}_{total}$ = 183 kJ mol^{-1} with the RDI **W(CO)$_4$(*E*-2)** and the RDTS TS(**W(CO)$_4$(*Z*-2)** → ***cis*(*N*,*H*)-W(CO)$_4$(H)(*Z*-15)**) (pathway 3c) for this preferred reaction sequence (Figure 1 and Supporting Information File 1, Figure S19).

All overall Gibbs free energies of activation for the discussed pathways 1a/1b and 3a/3b in the coordination sphere of the metal center are higher than for the carbene → imine isomerization in the metal-free systems ***E*-2** → ***E*-3** and ***Z*-2** → ***Z*-3** (pathways 2a/2b). This suggests that W(CO)$_5$ or W(CO)$_4$ coordination to ***E*-2** or ***Z*-2** kinetically stabilizes the carbene ligand. All pathways 1a/1b, 2a/2b and 3a/3b have large overall Gibbs free energies of activation with $\Delta G^{\ddagger}_{total}$ > 200 kJ mol^{-1}. The alternative pathway 3c via CO dissociation, oxidative addition, pseudorotation and reductive elimination features the lowest overall Gibbs free energy of activation of $\Delta G^{\ddagger}_{total}$ = 183 kJ mol^{-1}. Although activation barriers for CO and carbene ligand dissociation steps could not be determined by DFT calculations, the formation of tetracarbonyl complexes is very probable, while the carbene dissociation is less likely. The experimentally determined barrier for CO dissociation from tungsten hexacarbonyl amounts to 193 kJ mol^{-1} [74]. According to the calculations, the **W(CO)$_4$(*Z*-2)** isomer is accessible from the thermodynamically preferred **W(CO)$_4$(*E*-2)** isomer. The following oxidative addition pathway 3c from **W(CO)$_4$(*Z*-2)** via the hydrido complexes ***cis*(*N*,*H*)-W(CO)$_4$(H)(*Z*-15)** and ***cis*(*C*,*H*)-W(CO)$_4$(H)(*Z*-15)** provides the lowest energy pathway for the formation of the imines ***Z*-3** and ***E*-3**. Important calculated bond distances in these key intermediates amount to W–C(carbene) = 2.19, 2.15 Å, W–N = 2.16, 2.21 Å, W–H = 1.78, 1.77 Å and C–N = 1.29, 1.29 Å for ***cis*(*N*,*H*)-W(CO)$_4$(H)(*Z*-15)** and ***cis*(*C*,*H*)-W(CO)$_4$(H)(*Z*-15)**, respec-

tively (Figure 2). These hydrido intermediates act as hydrogen atom shuttle from the nitrogen to the carbon atom in NH carbene tetracarbonyl tungsten complexes. Oxidative additions of XY bonds to low-coordinate $W(CO)_n$ fragments is a common reactivity pattern for tungsten carbonyl complexes [75-80] and appears to be operative in the present case as well.

Experimental studies on the formation of imine *E*-3 from W(CO)$_5$(*E*-2)

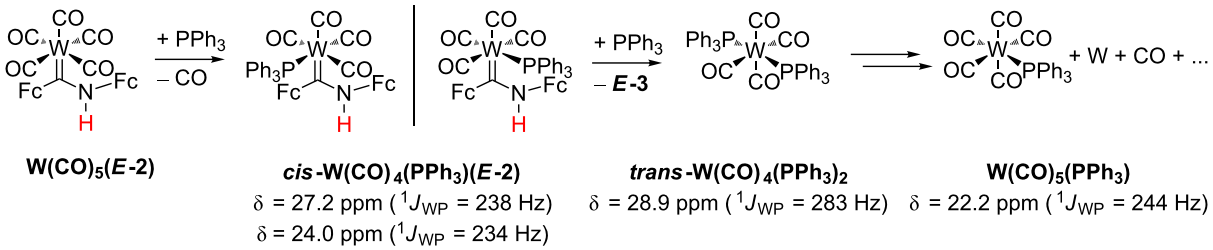
Heating of a toluene solution of **W(CO)$_5$(*E*-2)** results in the formation of the imine ***E*-3** according to ^{1}H NMR spectroscopy (monitored by the NH proton resonance of **W(CO)$_5$(*E*-2)** at δ = 10.16 ppm and the CH proton resonance of ***E*-3** at δ = 8.33 ppm; Supporting Information File 1, Figures S20–S24). The appearance of a resonance at δ = 9.68 ppm is assigned to a trace amount of **W(CO)$_5$(*Z*-2)**. A dark precipitate (possibly tungsten nanoparticles [81,82]) forms during the thermolysis. The half-lives at 60, 70, 80, 90 and 100 °C amount to 145.9, 39.4, 28.9, 16.2 and 12.2 h. The time traces fit to a first order kinetics as anticipated in the absence of a base. An Eyring–Polanyi plot gives an activation enthalpy of $\Delta H^{\ddagger}$ = 54.5 ± 10.4 kJ mol^{-1} and an activation entropy of $\Delta S^{\ddagger}$ = –193 ± 30 J mol^{-1} K^{-1} (Supporting Information File 1, Figure S25). These values give a Gibbs free energy of activation of $\Delta G^{\ddagger}_{298K}$ = 112 kJ mol^{-1}.

The ^{1}H NMR spectra during thermolysis provide no hint for a long-lived intermediate and the reaction cleanly proceeds from the starting material **W(CO)$_5$(*E*-2)** to the product ***E*-3**. No hydride resonances have been detected up to δ = −30 ppm in the ^{1}H NMR spectra. This suggests that subsequent reactions after ligand dissociation proceed faster and the irreversible ligand dissociation is the rate-determining step.

Attempts to intercept low-coordinate tungsten intermediates were conducted by thermolysis of **W(CO)$_5$(*E*-2)** in the presence of triphenylphosphane. In case of aminocarbenes, experiments on the synthesis and decomposition of carbene(tetracarbonyl)(phosphane) complexes of chromium and tungsten revealed the exclusive formation of ***cis*-M(CO)$_4$(PR$_3$)(carbene)** (R = *n*-Bu, Ph) [83-85]. **M(CO)$_5$(PR$_3$)** and ***trans*-M(CO)$_4$(PR$_3$)$_2$** (M = Cr, W) have been detected as side-products [83,84].

W(CO)$_5$(PPh$_3$) gives a ^{31}P resonance at δ = 20.9 ppm ($^1J_{WP}$ = 243 Hz) in $CDCl_3$ and ***trans*-W(CO)$_4$(PR$_3$)$_2$** at δ = 27.4 ppm ($^1J_{WP}$ = 282 Hz) [86], while reported $W(CO)_4(PPh_3)$(carbene) complexes resonate in CD_2Cl_2 at δ = 24–25 ppm ($^1J_{WP}$ = 232–236 Hz) (*cis*) and at δ = 23 ppm ($^1J_{WP}$ = 209 Hz) (*trans*) and exhibit significantly smaller $^1J_{WP}$ coupling constants [85]. A ^{31}P NMR resonance of a toluene-d_8 solution of **W(CO)$_5$(*E*-2)** with one equivalent PPh_3 heated to 100 °C for 1 h was observed at δ = 27.3 ppm with ^{183}W satellites ($^1J_{WP}$ = 238 Hz) fitting to the carbene tetracarbonyl phosphane complex ***cis*-W(CO)$_4$(PPh$_3$)(*E*-2)** (23%) in addition to residual PPh_3 (δ = −4.2 ppm, 73%) (Scheme 5, Supporting Information File 1, Figure S13). A less intense resonance (4%) at δ = 28.9 ppm ($^1J_{WP}$ = 283 Hz) is assigned to ***trans*-W(CO)$_4$(PPh$_3$)$_2$** [86]. At later stages of the reaction, isomerization to another *cis* isomer of ***cis*-W(CO)$_4$(PPh$_3$)(*E*-2)** with δ = 24.0 ppm ($^1J_{WP}$ = 234 Hz), according to the $^1J_{WP}$ coupling constant [85], probably occurs. After 4 h another ^{31}P resonance appears at δ = 22.2 ppm ($^1J_{WP}$ = 244 Hz). Comparison of $^1J_{WP}$ coupling constants confirms the presence of **W(CO)$_5$(PPh$_3$)** [86], with up to 67% spectroscopic yield after 25 h. Hence, the ^{31}P NMR data suggest the following sequence as a main pathway: The sequence starts with initial loss of a CO ligand from **W(CO)$_5$(*E*-2)**, followed by formation of ***cis*-W(CO)$_4$(PPh$_3$)(*E*-2)** complexes. Substitution of imine ***E*-3** by a second PPh_3 ligand gives ***trans*-W(CO)$_4$(PPh$_3$)$_2$**. Finally, **W(CO)$_5$(PPh$_3$)** is formed, presumably along with elemental tungsten (Scheme 5).

FD mass spectrometry confirms the most probable decomposition of **W(CO)$_4$(PPh$_3$)(*E*-2)** to ***trans*-W(CO)$_4$(PPh$_3$)$_2$** (*m*/*z* = 820), **W(CO)$_5$(PPh$_3$)** (*m*/*z* = 586) and imine ***E*-3** (*m*/*z* = 397) (Supporting Information File 1, Figure S14). The carbonyl and CN stretching frequencies (2072, 2018, 1982, 1938, 1889,



Scheme 5: Proposed reaction sequence from **W(CO)$_5$(*E*-2)** to **W(CO)$_5$(PPh$_3$)** in the presence of triphenylphosphane.

1614 cm^{-1}) and relative intensities of partially overlapping bands obtained by IR spectroscopy (Supporting Information File 1, Figure S15) fit to a mixture of **$W(CO)_5(PPh_3)$** ($\tilde{\nu}$ = 2072, 1982, 1938 cm^{-1}) [87,88], **$W(CO)_4(PPh_3)_2$** in *cis* ($\tilde{\nu}$ = 2018 cm^{-1}) and *trans* ($\tilde{\nu}$ = 1938, 1889 cm^{-1}) configuration [89,90] as well as imine ***E*-3** ($\tilde{\nu}$ = 1614 cm^{-1}). Hence, the initial thermally induced dissociation of a CO ligand is more favourable than carbene dissociation in agreement with the DFT calculations (vide supra).

Similarly, photochemical activation (400 nm LEDs) in toluene produces imine ***E*-3** in 31% yield after 120 h from **$W(CO)_5$(*E*-2)** already at room temperature, while only 1% ***E*-3** is formed in the dark at room temperature. This observation additionally supports the hypothesis that the key initial step is the dissociation of CO from **$W(CO)_5$(*E*-2)** to give **$W(CO)_4$(*E*-2)** (Scheme 4).

Attempts to observe the tetracarbonyl intermediates in the absence of PPh_3 by LIFDI mass spectrometry were unsuccessful. The mass spectra recorded at several time intervals during the heating procedure (reflux in toluene under strictly inert conditions) display the peak of the starting material at *m*/*z* = 721 and the peak of the imine product ***E*-3** at *m*/*z* = 397. The former peak decreases while the latter one increases during the heating process (Supporting Information File 1, Figure S26). No other intermediates appear in the FD mass spectra. Tentatively, the concomitantly formed tungsten species aggregate under these conditions and form the observed dark precipitate. This further supports the hypothesis that no intermediates accumulate during the reaction and that the rate-determining step is the CO ligand dissociation.

IR spectroscopic monitoring of a **$W(CO)_5$(*E*-2)** solution in 1,2-dichloroethane under reflux (ca. 84 °C) shows that **$W(CO)_5$(*E*-2)** simply decays to a carbonyl-free species (likely the dark precipitate) and no soluble CO-containing intermediates such as **$W(CO)_4$(*E*-2)**, **$W(CO)_4$(*Z*-2)** or hydrido carbonyl complexes are detected (Supporting Information File 1, Figure S27).

In full accordance with the above observations, UV–vis spectra recorded during the thermal treatment of **$W(CO)_5$(*E*-2)** in toluene (100 °C) show the clean decay of the characteristic bands of **$W(CO)_5$(*E*-2)** at 360 and 391 nm. The ferrocene based absorption band around 500 nm remains essentially constant indicating the stability of the Fc units. Isosbestic points are observed at 337 and 500 nm corroborating the clean conversion of **$W(CO)_5$(*E*-2)** to ***E*-3** without long-lived soluble intermediates (Supporting Information File 1, Figure S28). The final UV–vis spectrum after 6 h closely resembles that of the calculated TD-DFT spectrum of imine ***E*-3** (Supporting Information File 1, Figure S29). All spectroscopic and analytical data suggest that the imine formation is faster than the CO dissociation.

Conclusion

The thermally induced formation of *E*-1,2-diferrocenylimine ***E*-3** from the NH carbene pentacarbonyl tungsten complex **$W(CO)_5$(*E*-2)** was investigated by density functional theory methods and mechanistic experimental studies (NMR, IR, UV–vis spectroscopy, FD mass spectrometry, kinetic studies, trapping of intermediates). All available data support the initial dissociation of a CO ligand to give the tetracarbonyl complex **$W(CO)_4$(*E*-2)**. Isomerization to the **$W(CO)_4$(*Z*-2)** isomer allows for an oxidative addition of the NH bond to give the seven-coordinate hydrido tungsten(II) complex ***cis*(N,H)-$W(CO)_4$(H)(*Z*-15)**. After pseudorotation to the ***cis*(C,H)-$W(CO)_4$(H)(*Z*-15)** rotamer, a reductive elimination yields the imine complex **$W(CO)_4$(*Z*-3)**. All other conceivable pathways, namely 1,2-H shifts within the free carbene or within the carbonyl complexes **$W(CO)_5$(*E*-2)** or **$W(CO)_4$(*E*-2)**, are significantly more energy demanding. The possibility of a seven-coordinate tungsten(II) intermediate opens the oxidative addition/pseudorotation/reductive elimination pathway shuttling the hydrogen atom from the nitrogen atom via the W atom to the carbene carbon atom. This pathway is unfeasible for homologous chromium complexes and explains the resistance of **$Cr(CO)_5$(*E*-2)** towards thermal ***E*-3** formation. A base-assisted pathway for imine formation is operative both for **$Cr(CO)_5$(*E*-2)** and **$W(CO)_5$(*E*-2)**, but the thermal imine formation is only feasible for **$W(CO)_5$(*E*-2)**.

Experimental

General procedures: All reactions were performed under argon atmosphere unless otherwise noted. A glovebox of the type UniLab/MBraun (Ar 4.8, O_2 < 1 ppm, H_2O < 1 ppm) was used for storage and weighing of sensitive compounds. All analytical samples that required the absence of oxygen were prepared in the same glovebox. Dichloromethane and 1,2-dichloroethane were dried with CaH_2 and distilled prior to use. THF and toluene were distilled from potassium. All reagents were used as received from commercial suppliers (ABCR, Acros Organics, Alfa Aesar, Fischer Scientific, Fluka and Sigma-Aldrich). Deuterated solvents were purchased from euriso-top. (Ethoxy)(ferrocenyl)carbene(pentacarbonyl)tungsten(0) **$W(CO)_5(1^{Et})$** [21] and Fc–NH_2 [40,41] were prepared according to literature procedures.

NMR spectra were recorded on a Bruker Avance DRX 400 spectrometer at 400.31 MHz (^{1}H), 100.07 MHz ($^{13}C\{^1H\}$) and 162.05 MHz ($^{31}P\{^1H\}$). All resonances are reported in ppm vs the solvent signal as internal standard [CD_2Cl_2 (^{1}H: δ =

5.32 ppm; ^{13}C: δ = 53.8 ppm), toluene-d_8 (^{1}H: δ = 2.08 ppm)] [91] and versus external H_3PO_4 (85%) (^{31}P: δ = 0 ppm). IR spectra were recorded with a BioRad Excalibur FTS 3100 spectrometer as KBr disks or by using KBr cells in CH_2Cl_2 or in CD_2Cl_2. Electrochemical experiments were carried out on a BioLogic SP-50 voltammetric analyzer by using a platinum working electrode, a platinum wire as counter electrode and a 0.01 M Ag/$AgNO_3$ electrode as reference electrode. The measurements were carried out at a scan rate of 100 mV s^{-1} for cyclic voltammetry experiments and at 50 mV s^{-1} for square wave voltammetry experiments in 0.1 M [*n*-Bu_4N][$B(C_6F_5)_4$] as supporting electrolyte in THF. Potentials are referenced against the decamethylferrocene/decamethylferrocenium couple ($E_{½}$ = −525 ± 5 mV vs ferrocene/ferrocenium under our experimental conditions) and are given relative to the ferrocene/ferrocenium couple. UV–vis/NIR spectra were recorded on a Varian Cary 5000 spectrometer by using 1.0 cm cells (Hellma, suprasil). FD mass spectra were recorded on a Thermo Fisher DFS mass spectrometer with a LIFDI upgrade. Elemental analyses were performed by the microanalytical laboratory of the chemical institutes of the University of Mainz.

Density functional theory calculations were carried out with the Gaussian09/DFT series [92] of programs. The B3LYP [93] formulation of density functional theory was used employing the LANL2DZ [94-97] basis set. No symmetry constraints were imposed on the molecules. The presence of energy minima of the ground states was checked by analytical frequency calculations. The calculated transition states exhibit a single imaginary frequency and they were additionally verified by intrinsic reaction coordinate (IRC) calculations. Solvent modelling was done employing the integral equation formalism polarizable continuum model (IEFPCM, toluene). The approximate free energies at 298 K were obtained through thermochemical analysis of the frequency calculation, using the thermal correction to the Gibbs free energy as reported by Gaussian09.

(Aminoferrocenyl)(ferrocenyl)carbene(pentacarbonyl)tungsten(0) ($W(CO)_5$(*E*-2)): 402 mg (2.0 mmol) of Fc-NH_2 and 1132 mg (2.0 mmol) of **$W(CO)_5(1^{Et})$** where dissolved in dry THF (40 mL). 1595 mg (8.0 mmol) of potassium hexamethyldisilazide (KHMDS) in dry THF (40 mL) were added within 5.5 h while stirring at room temperature. The reaction was monitored by TLC to check the reaction progress and to stop the reaction before extensive imine formation occurs. After 8 h, the solvent was removed under reduced pressure and an aqueous saturated $NaHCO_3$ solution (100 mL) was added. The aqueous phase was extracted with dichloromethane (3 × 100 mL) and the combined organic phases were washed with aqueous saturated $NaHCO_3$ solution (2 × 100 mL) and brine (2 × 100 mL). The organic phase was dried over $MgSO_4$. After evaporation of the solvent under reduced pressure, a crude red product was obtained (1.04 mg). Purification by column chromatography (SiO_2; 40 cm × 5.5 cm; petroleum ether (40/60):CH_2Cl_2 1:1; R_f(Fc–NH_2) = 0.0, R_f(***E*-3**) = 0.5, R_f(**$W(CO)_5$(*E*-2)**) = 0.8) yielded 403 mg (0.56 mmol, 28%) of deep red crystalline needles. ^{1}H NMR (CD_2Cl_2): δ 10.50 (s, 1H, H6), 4.73 (pt, 2H, H8), 4.71 (pt, 2H, H3), 4.62 (pt, 2H, H2), 4.37 (s, 5H, H1/10), 4.33 (pt, 2H, H9), 4.32 (s, 5H, H1/10) ppm; ^{13}C NMR (CD_2Cl_2) δ 259.6 (C5), 204.4 (C12), 199.3 (C11, $^1J_{WC}$ = 127 Hz), 99.7 (C7), 97.7 (C4), 72.1 (C2), 70.7 (C3), 70.6 (C1/10), 70.2 (C1/10), 69.1 (C8), 67.8 (C9) ppm; MS (FD) *m/z* (int.): 721.0 (100, $[M]^+$); IR (KBr) $\tilde{\nu}$: 3335 (m, NH), 3107 (s, CH), 2058 (vs, CO), 1977 (vs, CO), 1899 (br, CO), 1508 (s), 1350 (m), 1238 (m), 1057 (m), 822 (m), 600 (s), 579 (m), 480 (m) cm^{-1}; IR (CH_2Cl_2) $\tilde{\nu}$: 2060 (vs, CO A_1), 1975 (s, CO B_1), 1921 (br, CO *E*, A_1), 1503 (m) cm^{-1}; IR (CD_2Cl_2) $\tilde{\nu}$: 3439 (w, NH($W(CO)_5$(*Z*-2))), 3240 (m, NH($W(CO)_5$(*E*-2))) cm^{-1}; UV–vis (CH_2Cl_2) λ_{max} (ε): 290 sh (15370), 355 (11020), 387 (11680), 468 sh (2570 M^{-1} cm^{-1}) nm; CV (THF, vs FcH/FcH^+): $E_{1/2}$ = −2.38 V (qrev.), $E_{p,ox}$ = 0.26, 0.48 V, $E_{p,red}$ = 0.17, –0.15, –0.76 V; Anal. calcd for $C_{26}H_{19}Fe_2NO_5W$ (720.95): C, 43.31; H, 2.66; N, 1.94; found: C, 43.30; H, 2.69; N, 1.91.

Supporting Information

Supporting Information File 1

Experimental spectra and DFT derived data.
[http://www.beilstein-journals.org/bjoc/content/supplementary/1860-5397-12-125-S1.pdf]

Acknowledgements

We are grateful to the Johannes Gutenberg University of Mainz (Germany) for financial support to C.F. (Internal University Research Funding). We thank Petra Auerbach and Dr. Mihail Mondeskhi for collecting the LIFDI mass spectra.

References

1. Fischer, E. O.; Maasböl, A. *Angew. Chem., Int. Ed. Engl.* **1964,** *3,* 580–581. doi:10.1002/anie.196405801
2. Dötz, K. H.; Stendel, J., Jr. *Chem. Rev.* **2009,** *109,* 3227–3274. doi:10.1021/cr900034e
3. de Meijere, A.; Schirmer, H.; Duetsch, M. *Angew. Chem., Int. Ed.* **2000,** *39,* 3964–4002. doi:10.1002/1521-3773(20001117)39:22<3964::AID-ANIE3964>3.0.CO;2-C
4. Barluenga, J.; Flórez, J.; Fañanás, F. J. *J. Organomet. Chem.* **2001,** *624,* 5–17. doi:10.1016/S0022-328X(00)00837-8
5. Barluenga, J.; Fernández-Rodríguez, M. A.; Aguilar, E. *J. Organomet. Chem.* **2005,** *690,* 539–587. doi:10.1016/j.jorganchem.2004.10.032

6. Hegedus, L. S. *Top. Organomet. Chem.* **2004,** 157–201. doi:10.1007/b98765
7. Hegedus, L. S. *Tetrahedron* **1997,** *53,* 4105–4128. doi:10.1016/S0040-4020(96)01186-6
8. Fernández, I.; Cossío, F. P.; Sierra, M. A. *Acc. Chem. Res.* **2011,** *44,* 479–490. doi:10.1021/ar100159h
9. Gómez-Gallego, M.; Mancheño, M. J.; Sierra, M. A. *Acc. Chem. Res.* **2005,** *38,* 44–53. doi:10.1021/ar040005r
10. Raubenheimer, H. G. *Dalton Trans.* **2014,** *43,* 16959–16973. doi:10.1039/c4dt01943a
11. Aumann, R.; Fischer, E. O. *Chem. Ber.* **1981,** *114,* 1853–1857. doi:10.1002/cber.19811140523
12. Bezuidenhout, D. I.; van der Westhuizen, B.; Rosenthal, A. J.; Wörle, M.; Liles, D. C.; Fernández, I. *Dalton Trans.* **2014,** *43,* 398–401. doi:10.1039/c3dt52961d
13. Ramollo, G. K.; López-Gómez, M. J.; Liles, D. C.; Matsinha, L. C.; Smith, G. S.; Bezuidenhout, D. I. *Organometallics* **2015,** *34,* 5745–5753. doi:10.1021/acs.organomet.5b00843
14. Seidel, G.; Gabor, B.; Goddard, R.; Heggen, B.; Thiel, W.; Fürstner, A. *Angew. Chem., Int. Ed.* **2014,** *53,* 879–882. doi:10.1002/anie.201308842
15. Seidel, G.; Fürstner, A. *Angew. Chem., Int. Ed.* **2014,** *53,* 4807–4811. doi:10.1002/anie.201402080
16. Sierra, M. A. *Chem. Rev.* **2000,** *100,* 3591–3638. doi:10.1021/cr9804137
17. Bezuidenhout, D. I.; Lotz, S.; Liles, D. C.; van der Westhuizen, B. *Coord. Chem. Rev.* **2012,** *256,* 479–524. doi:10.1016/j.ccr.2011.12.003
18. Connor, J. A.; Jones, E. M.; Lloyd, J. P. *J. Organomet. Chem.* **1970,** *24,* C20–C22. doi:10.1016/S0022-328X(00)80254-5
19. Mose, G. A.; Fischer, E. O.; Rausch, M. D. *J. Organomet. Chem.* **1971,** *27,* 379–382. doi:10.1016/S0022-328X(00)82169-5
20. Connor, J. A.; Lloyd, J. P. *J. Chem. Soc., Dalton Trans.* **1972,** 1470–1476. doi:10.1039/dt9720001470
21. López-Cortés, J. G.; Contreras de la Cruz, L. F.; Ortega-Alfaro, M. C.; Toscano, R. A.; Alvarez-Toledano, C.; Rudler, H. *J. Organomet. Chem.* **2005,** *690,* 2229–2237. doi:10.1016/j.jorganchem.2005.02.022
22. Schobert, R.; Kempe, R.; Schmalz, T.; Gmeiner, A. *J. Organomet. Chem.* **2006,** *691,* 859–868. doi:10.1016/j.jorganchem.2005.10.047
23. Sandoval-Chávez, C.; López-Cortés, J. G.; Gutiérrez-Hernández, A. I.; Ortega-Alfaro, M. C.; Toscano, A.; Alvarez-Toledano, C. *J. Organomet. Chem.* **2009,** *694,* 3692–3700. doi:10.1016/j.jorganchem.2009.07.044
24. Gutiérrez-Hernández, A. I.; López-Cortés, J. G.; Ortega-Alfaro, M. C.; Ramírez-Apan, M. T.; Cázares-Marinero, J. d. J.; Toscano, R. A. *J. Med. Chem.* **2012,** *55,* 4652–4663. doi:10.1021/jm300150t
25. Bezuidenhout, D. I.; Fernández, I.; van der Westhuizen, B.; Swarts, P. J.; Swarts, J. C. *Organometallics* **2013,** *32,* 7334–7344. doi:10.1021/om400865m
26. Bezuidenhout, D. I.; van der Westhuizen, B.; Strydom, I.; Swarts, P. J.; Swarts, J. C.; Fernández, I. *Inorg. Chim. Acta* **2014,** *423,* 184–192. doi:10.1016/j.ica.2014.07.068
27. Veit, P.; Förster, C.; Seibert, S.; Heinze, K. *Z. Anorg. Allg. Chem.* **2015,** *641,* 2083–2092. doi:10.1002/zaac.201500562
28. Klabunde, U.; Fischer, E. O. *J. Am. Chem. Soc.* **1967,** *89,* 7141–7142. doi:10.1021/ja01002a070
29. Connor, J. A.; Fischer, E. O. *J. Chem. Soc. A* **1969,** 578–584. doi:10.1039/J19690000578
30. Fischer, E. O.; Heckl, B.; Werner, H. *J. Organomet. Chem.* **1971,** *28,* 359–365. doi:10.1016/S0022-328X(00)88016-X
31. Grotjahn, D. B.; Dötz, K. H. *Synlett* **1991,** *1991,* 381–390. doi:10.1055/s-1991-20736
32. Togni, A.; Hayashi, T., Eds. *Ferrocenes;* Wiley-VCH: Weinheim, Germany, 1994.
33. Štěpnička, P., Ed. *Ferrocenes. Ligands, materials and biomolecules;* Wiley & Sons: Chichester, England, 2008.
34. van der Westhuizen, B.; Speck, J. M.; Korb, M.; Friedrich, J.; Bezuidenhout, D. I.; Lang, H. *Inorg. Chem.* **2013,** *52,* 14253–14263. doi:10.1021/ic402202w
35. Lloyd, M. K.; McCleverty, J. A.; Orchard, D. G.; Connor, J. A.; Hall, M. B.; Hillier, I. H.; Jones, E. M.; McEwen, G. K. *J. Chem. Soc., Dalton Trans.* **1973,** 1743–1747. doi:10.1039/dt9730001743
36. van der Westhuizen, B.; Swarts, P. J.; Strydom, I.; Liles, D. C.; Fernández, I.; Swarts, J. C.; Bezuidenhout, D. I. *Dalton Trans.* **2013,** *42,* 5367–5378. doi:10.1039/c3dt32913e
37. van der Westhuizen, B.; Swarts, P. J.; van Jaarsveld, L. M.; Liles, D. C.; Siegert, U.; Swarts, J. C.; Fernández, I.; Bezuidenhout, D. I. *Inorg. Chem.* **2013,** *52,* 6674–6684. doi:10.1021/ic4007422
38. van der Westhuizen, B.; Matthäus Speck, J.; Korb, M.; Bezuidenhout, D. I.; Lang, H. *J. Organomet. Chem.* **2014,** *772–773,* 18–26. doi:10.1016/j.jorganchem.2014.08.025
39. Bezuidenhout, D. I.; van der Westhuizen, B.; Swarts, P. J.; Chatturgoon, T.; Munro, O. Q.; Fernández, I.; Swarts, J. C. *Chem. – Eur. J.* **2014,** *20,* 4974–4985. doi:10.1002/chem.201304711
40. Bildstein, B.; Malaun, M.; Kopacka, H.; Wurst, K.; Mitterböck, M.; Ongania, K.-H.; Opromolla, G.; Zanello, P. *Organometallics* **1999,** *18,* 4325–4336. doi:10.1021/om990377h
41. Heinze, K.; Schlenker, M. *Eur. J. Inorg. Chem.* **2004,** 2974–2988. doi:10.1002/ejic.200300897
42. Fischer, E. O.; Leupold, M. *Chem. Ber.* **1972,** *105,* 599–608. doi:10.1002/cber.19721050225
43. Sierra, M. A.; Mancheño, M. J.; Vicente, R.; Gómez-Gallego, M. *J. Org. Chem.* **2001,** *66,* 8920–8925. doi:10.1021/jo015961q
44. Connor, J. A.; Rose, P. D. *J. Organomet. Chem.* **1972,** *46,* 329–334. doi:10.1016/S0022-328X(00)88335-7
45. Moser, E.; Fischer, E. O. *J. Organomet. Chem.* **1968,** *15,* 147–155. doi:10.1016/S0022-328X(00)86334-2
46. Moser, E.; Fischer, E. O. *J. Organomet. Chem.* **1969,** *16,* 274–282. doi:10.1016/S0022-328X(00)81115-8
47. Bourissou, D.; Guerret, O.; Gabbaï, F. P.; Bertrand, G. *Chem. Rev.* **2000,** *100,* 39–92. doi:10.1021/cr940472u
48. Vignolle, J.; Cattoën, X.; Bourissou, D. *Chem. Rev.* **2009,** *109,* 3333–3384. doi:10.1021/cr800549j
49. Alder, R. W.; Allen, P. R.; Murray, M.; Orpen, A. G. *Angew. Chem., Int. Ed. Engl.* **1996,** *35,* 1121–1123. doi:10.1002/anie.199611211
50. Tafipolsky, M.; Scherer, W.; Öfele, K.; Artus, G.; Pedersen, B.; Herrmann, W. A.; McGrady, G. S. *J. Am. Chem. Soc.* **2002,** *124,* 5865–5880. doi:10.1021/ja011761k
51. Herrmann, W. A.; Öfele, K.; von Preysing, D.; Herdtweck, E. *Organometallics* **2003,** *684,* 235–248. doi:10.1016/S0022-328X(03)00754-X
52. Frey, G. D.; Herdtweck, E.; Herrmann, W. A. *J. Organomet. Chem.* **2006,** *691,* 2465–2478. doi:10.1016/j.jorganchem.2006.01.033
53. Hahn, F. E.; Tamm, M. *J. Organomet. Chem.* **1993,** *456,* C11–C14. doi:10.1016/0022-328X(93)80442-E
54. Förster, C.; Veit, P.; Ksenofontov, V.; Heinze, K. *Chem. Commun.* **2015,** *51,* 1514–1516. doi:10.1039/C4CC08868A

55. Veit, P.; Prantl, E.; Förster, C.; Heinze, K. *Organometallics* **2016,** *35,* 249–257. doi:10.1021/acs.organomet.5b00963
56. Braga, D.; Grepioni, F.; Tedesco, E.; Biradha, K.; Desiraju, G. R. *Organometallics* **1997,** *16,* 1846–1856. doi:10.1021/om9608364
57. Braga, D.; Grepioni, F. *Acc. Chem. Res.* **2000,** *33,* 601–608. doi:10.1021/ar990143u
58. Epstein, L. M.; Shubina, E. S. *Coord. Chem. Rev.* **2002,** *231,* 165–181. doi:10.1016/S0010-8545(02)00118-2
59. Brammer, L. *Dalton Trans.* **2003,** 3145–3157. doi:10.1039/b303006g
60. Lage, M. L.; Fernández, I.; Mancheño, M. J.; Sierra, M. A. *Inorg. Chem.* **2008,** *47,* 5253–5258. doi:10.1021/ic800187r
61. Kvapilová, H.; Hoskovcová, I.; Kayanuma, M.; Daniel, C.; Záliš, S. *J. Phys. Chem. A* **2013,** *117,* 11456–11463. doi:10.1021/jp4074027
62. Kreiter, C. G.; Fischer, E. O. *Angew. Chem., Int. Ed. Engl.* **1969,** *8,* 761–762. doi:10.1002/anie.196907611
63. Cases, M.; Frenking, G.; Duran, M.; Solà, M. *Organometallics* **2002,** *21,* 4182–4191. doi:10.1021/om0203330
64. Fernández, I.; Cossío, F. P.; Arrieta, A.; Lecea, B.; Mancheño, M. J.; Sierra, M. A. *Organometallics* **2004,** *23,* 1065–1071. doi:10.1021/om0343263
65. Ananikov, V. P., Ed. *Understanding organometallic reaction mechanisms and catalysis. Computational and experimental tools;* Wiley-VCH: Weinheim, 2015.
66. Wurmb-Gerlich, D.; Vögtle, F.; Mannschreck, A.; Staab, H. A. *Justus Liebigs Ann. Chem.* **1967,** *708,* 36–50. doi:10.1002/jlac.19677080103
67. Saloman, S.; Hildebrandt, A.; Korb, M.; Schwind, M.; Lang, H. *Z. Anorg. Allg. Chem.* **2015,** *641,* 2282–2290. doi:10.1002/zaac.201500557
68. Heinemann, C.; Thiel, W. *Chem. Phys. Lett.* **1994,** *217,* 11–16. doi:10.1016/0009-2614(93)E1360-S
69. Sulzbach, H. M.; Platz, M. S.; Schaefer, H. F., III; Hadad, C. M. *J. Am. Chem. Soc.* **1997,** *119,* 5682–5689. doi:10.1021/ja970181d
70. McGibbon, G. A.; Heinemann, C.; Lavorato, D. J.; Schwarz, H. *Angew. Chem., Int. Ed. Engl.* **1997,** *36,* 1478–1481. doi:10.1002/anie.199714781
71. Shustov, G. V.; Liu, M. T. H.; Rauk, A. *J. Phys. Chem. A* **1997,** *101,* 2509–2513. doi:10.1021/jp963730v
72. Solé, S.; Gornitzka, H.; Guerret, O.; Bertrand, G. *J. Am. Chem. Soc.* **1998,** *120,* 9100–9101. doi:10.1021/ja980797i
73. Fukumoto, K.; Sakai, A.; Hayasaka, K.; Nakazawa, H. *Organometallics* **2013,** *32,* 2889–2892. doi:10.1021/om400304v
74. Lewis, K. E.; Golden, D. M.; Smith, G. P. *J. Am. Chem. Soc.* **1984,** *106,* 3905–3912. doi:10.1021/ja00326a004
75. Umland, P.; Vahrenkamp, H. *Chem. Ber.* **1982,** *115,* 3555–3564. doi:10.1002/cber.19821151108
76. Van der Sluys, L. S.; Kubat-Martin, K. A.; Kubas, G. J.; Caulton, K. G. *Inorg. Chem.* **1991,** *30,* 306–310. doi:10.1021/ic00002a028
77. Kubas, G. J.; Kiss, G.; Hoff, C. D. *Organometallics* **1991,** *10,* 2870–2876. doi:10.1021/om00054a062
78. Lang, R. F.; Ju, T. D.; Kiss, G.; Hoff, C. D.; Bryan, J. C.; Kubas, G. J. *J. Am. Chem. Soc.* **1994,** *116,* 7917–7918. doi:10.1021/ja00096a067
79. Butts, M. D.; Bryan, J. C.; Luo, X.-L.; Kubas, G. J. *Inorg. Chem.* **1997,** *36,* 3341–3353. doi:10.1021/ic960870a
80. Adrjan, B.; Szymańska-Buzar, T. *J. Organomet. Chem.* **2008,** *693,* 2163–2170. doi:10.1016/j.jorganchem.2008.03.017
81. Magnusson, M. H.; Deppert, K.; Malm, J.-O. *J. Mater. Res.* **2000,** *15,* 1564–1569. doi:10.1557/JMR.2000.0224
82. Sahoo, P. K.; Kalyan Kamal, S. S.; Premkumar, M.; Jagadeesh Kumar, T.; Sreedhar, B.; Singh, A. K.; Srivastava, S. K.; Chandra Sekhar, K. *Int. J. Refract. Met. Hard Mater.* **2009,** *27,* 784–791. doi:10.1016/j.ijrmhm.2009.01.005
83. Fischer, E. O.; Fischer, H. *Chem. Ber.* **1974,** *107,* 657–672. doi:10.1002/cber.19741070238
84. Fischer, H.; Fischer, E. O.; Kreissl, F. R. *J. Organomet. Chem.* **1974,** *64,* C41–C44. doi:10.1016/S0022-328X(00)92169-7
85. Landman, M.; Pretorius, R.; Fraser, R.; Buitendach, B. E.; Conradie, M. M.; van Rooyen, P. H.; Conradie, J. *Electrochim. Acta* **2014,** *130,* 104–118. doi:10.1016/j.electacta.2014.02.127
86. Schenk, W. A.; Buchner, W. *Inorg. Chim. Acta* **1983,** *70,* 189–196. doi:10.1016/S0020-1693(00)82801-7
87. Cotton, F. A.; Kraihanzel, C. S. *J. Am. Chem. Soc.* **1962,** *84,* 4432–4438. doi:10.1021/ja00882a012
88. Malosh, T. J.; Wilson, S. R.; Shapley, J. R. *Inorg. Chim. Acta* **2009,** *362,* 2849–2855. doi:10.1016/j.ica.2009.01.011
89. Graziani, M.; Zingales, F.; Belluco, U. *Inorg. Chem.* **1967,** *6,* 1582–1586. doi:10.1021/ic50054a034
90. Ardon, M.; Hogarth, G.; Oscroft, D. T. W. *J. Organomet. Chem.* **2004,** *689,* 2429–2435. doi:10.1016/j.jorganchem.2004.04.030
91. Fulmer, G. R.; Miller, A. J. M.; Sherden, N. H.; Gottlieb, H. E.; Nudelman, A.; Stoltz, B. M.; Bercaw, J. E.; Goldberg, K. I. *Organometallics* **2010,** *29,* 2176–2179. doi:10.1021/om100106e
92. *Gaussian 09,* Revision A.02; Gaussian, Inc.: Wallingford CT, 2009.
93. Becke, A. D. *J. Chem. Phys.* **1993,** *98,* 5648–5652. doi:10.1063/1.464913
94. Dykstra, C. E. *Chem. Phys. Lett.* **1977,** *45,* 466–469. doi:10.1016/0009-2614(77)80065-1
95. Hay, P. J.; Wadt, W. R. *J. Chem. Phys.* **1985,** *82,* 270–283. doi:10.1063/1.448799
96. Wadt, W. R.; Hay, P. J. *J. Chem. Phys.* **1985,** *82,* 284–298. doi:10.1063/1.448800
97. Hay, P. J.; Wadt, W. R. *J. Chem. Phys.* **1985,** *82,* 299–310. doi:10.1063/1.448975

License and Terms

This is an Open Access article under the terms of the Creative Commons Attribution License (http://creativecommons.org/licenses/by/2.0), which permits unrestricted use, distribution, and reproduction in any medium, provided the original work is properly cited.

The license is subject to the *Beilstein Journal of Organic Chemistry* terms and conditions: (http://www.beilstein-journals.org/bjoc)

The definitive version of this article is the electronic one which can be found at: doi:10.3762/bjoc.12.125

BEILSTEIN JOURNAL OF ORGANIC CHEMISTRY

Molecular weight control in organochromium olefin polymerization catalysis by hemilabile ligand–metal interactions

Stefan Mark, Hubert Wadepohl and Markus Enders*

Full Research Paper

Open Access

Address:
Anorganisch-Chemisches Institut, Heidelberg University, Im Neuenheimer Feld 270, D-69120 Heidelberg, Germany

Email:
Markus Enders* - markus.enders@uni-heidelberg.de

* Corresponding author

Keywords:
chromium single-site catalysts; olefin polymerization; ultra-high molecular weight polyethylene

Beilstein J. Org. Chem. **2016,** *12,* 1372–1379.
doi:10.3762/bjoc.12.131

Received: 04 March 2016
Accepted: 22 June 2016
Published: 04 July 2016

This article is part of the Thematic Series "Organometallic chemistry". In memory of Professor Dr. Peter Hofmann.

Guest Editor: B. F. Straub

© 2016 Mark et al.; licensee Beilstein-Institut.
License and terms: see end of document.

Abstract

A series of Cr(III) complexes based on quinoline-cyclopentadienyl ligands with additional hemilabile side arms were prepared and used as single-site catalyst precursors for ethylene polymerization. The additional donor functions interact with the metal centers only after activation with the co-catalyst. Evidence for this comes from DFT-calculations and from the differing behavior of the complexes in ethylene polymerization. All complexes investigated show very high catalytic activity and the additional side arm minimizes chain-transfer reactions, leading to increase of molecular weights of the resulting polymers.

Introduction

Chelate ligands with both, a strongly coordinating moiety and a weakly coordinating donor function allow the stabilization of vacant coordination sites at metal centers and may act as placeholders for external substrates. The concept of hemilabile ligands has been introduced in 1979 [1] and has been applied for the development of improved transition metal catalysts [2-7]. The donor–acceptor interaction of the hemilabile moiety with the metal center should be weak enough to allow the displacement by a substrate, which should itself be transformed during the catalytic reaction. The bonding ability of internal or external stabilizing ligands in relation to the substrate plays a crucial role. In contrast to external donors, a special feature of a hemilabile donor is the fact that only one stabilizing ligand per metal center is available. Consequently, a large excess of external donors (e.g., solvent molecules, substrates, additives, etc.) may displace a relatively strong intramolecular donor function. Several examples for olefin polymerization catalysts with hemilabile ligands are known and the impact of the hemilabile group on the polymerization behavior can be immense [8-12]. Examples are the switching from polymerization to trimerization selectivity [13] or the suppression of chain termination by weak interactions with fluorine substituents [14-17]. The inter-

action with fluorine atoms from fluorinated borate anions have also shown to play a role in olefin polymerization [18-24].

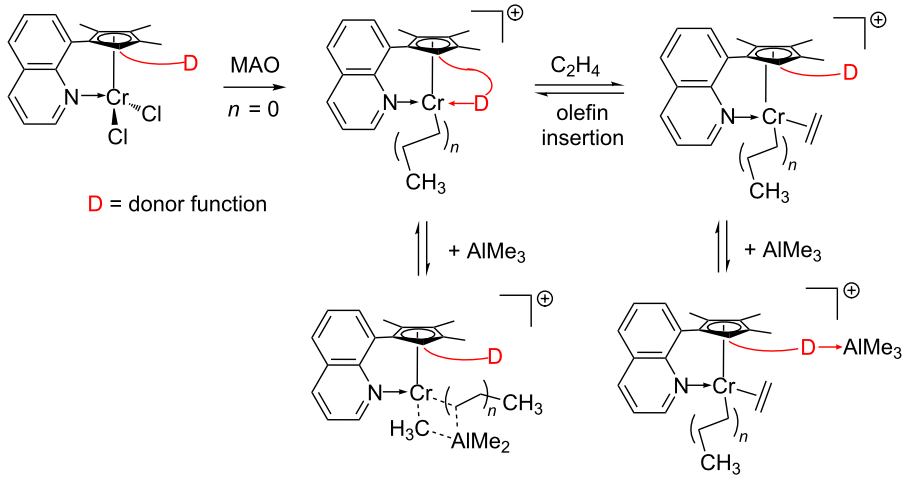
Cyclopentadienyl (Cp)-based chromium complexes exhibit very good ethylene polymerization properties, when the coordination sphere of the chromium center is completed by an additional ligand. Improved stability and hence polymer productivities are obtained when the donor is tethered to the Cp ring [25-36]. However, the tethered donor usually does not act as a hemilabile ligand as it remains coordinated during the catalytic process. Many cyclopentadienyl (Cp) ligands where an additional neutral donor function is covalently bonded have been reported [37-39]. Some of those donors bind strongly, others weakly, to a particular transition metal ion. Examples, which are related to the work described here, are Cp ligands with olefinic [40-52] or with a nitrile side arm [53,54].

We have recently described how external modifiers combined with Cp-chromium polymerization catalysts influence the chain-termination process and hence the molecular weight of the produced polyethylene [55]. This paper describes our results with covalently linked modifiers and their influence on the ethylene polymerization behavior. There is neither experimental nor theoretical evidence for a substantial beta-H elimination or beta-H transfer in such catalyst systems so that chain termination is dominated by chain-transfer reactions to the aluminum based co-catalysts [56,57]. Consequently, any component, which modulates the interaction of Al–alkyls with the catalyst center, can influence the molecular weight of the resulting polyethylene. The concept of the present investigation is sketched in Scheme 1. The pre-catalysts feature covalently bonded neutral donor functions (D) which do not interact with the coordinatively saturated chromium centers. The coordination ability of the chosen donors D range from very weak (organofluorine) to medium (olefinic or aryl, respectively) and strong (nitrile). Activation with methylaluminoxane (MAO) leads to the formation of monomethyl complexes and the active species is a cationic alkylchromium complex with one remaining „vacant“ coordination site. This site can bind one of the following donors: ethylene, internal labile donor D, alkylaluminium compound, etc. If the internal donor binds, the cationic chromium center is stabilized but ethylene can displace the donor and insert into the chromium alkyl bond leading to polyethylene. In the presence of aluminum alkyls like trimethylaluminum chain termination may occur by addition of $AlMe_3$ to the cationic chromium alkyl species. A simultaneous coordination of the internal donor D and alkylaluminum is not possible or at least very unlikely so that interaction of the hemilabile donor D can suppress chain transfer. Another possibility is that the donor D directly interacts with $AlMe_3$, which also reduces the chain-transfer rate. Both types of interaction lead to an increase in molecular weight of the polyethylene.

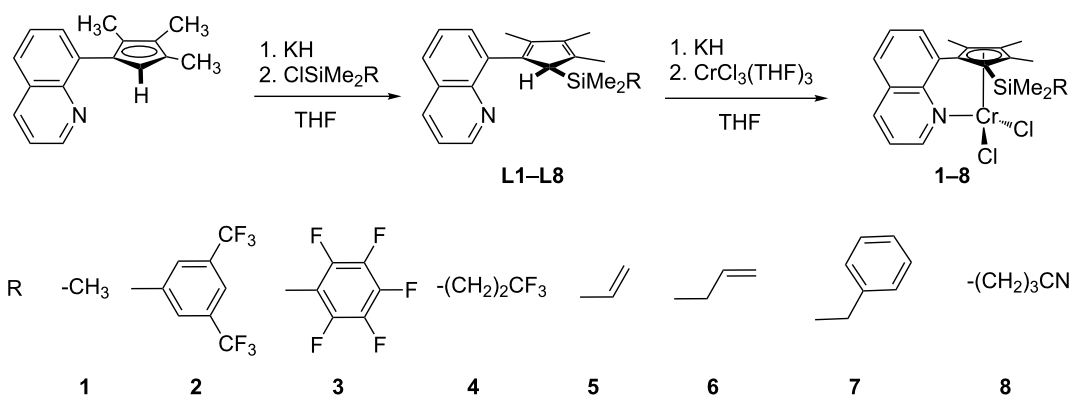
We have synthesized a number of ligands as presented in Scheme 2 and evaluated the interaction of the donor units with the Lewis acidic chromium center by DFT methods. The synthesized complexes where then tested in ethylene polymerization in order to evaluate the influence of the hemilabile donor in terms of catalyst activity and molecular weight of the polymer.

Results and Discussion

It is well known that early transition metal single-site polymerization catalysts can interact with organofluorine groups [15,17,20,22]. In FI-type catalysts the interaction of fluorine substituents with the catalyst center leads to a suppression of chain termination so that living olefin polymerization is



Scheme 1: Influencing catalyst stability, olefin coordination and chain-transfer reactions by hemilabile donor functions.



Scheme 2: Synthesis of ligands **L1**–**L8** and chromium complexes **1**–**8**.

possible [15]. The experimental verification of such an interaction was demonstrated by NMR of an MAO activated complex [17]. Consequently, we envisaged the synthesis of ligands where an organofluorine substituent is connected by a side arm with suitable length. In addition to that we choose side arms with olefinic groups, a benzyl unit and a stronger nitrile donor group, respectively. The synthesis of the new ligand derivatives and the corresponding Cr complexes follows known procedures (Scheme 2) [29,58]. The key step for the introduction of the hemilabile donor function is the electrophilic attack of a chlorosilane derivative at quinolyl-functionalized cyclopentadienides (Cp^Q). We used the trimethyl Cp^Q derivative as this leads to a single acidic proton in the ligands **L1**–**L8**. By this procedure we could introduce side arms with fluorine (**L2**–**L4**) or olefinic donor groups (**L5**, **L6**) as well as benzyl (**L7**) or nitrile (**L8**) moieties. Deprotonation with potassium hydride and subsequent reaction with chromium trichloride leads to the chromium complexes as green-blue solids in yields ranging from 21% (**3**) to 81% (**6**).

The ligand **L3** as well as the pre-catalysts **4**–**8** were studied by single crystal X-ray analysis. A selection of molecular structures is presented in Figure 1 and details of the structure determination are presented in Table S1 (see Supporting Information File 1). Due to the rigid and predefined geometry of the Cp^Q ligand, the coordination environment around the chromium centers is very similar in all cases and in line with previously published structures of such complexes [29,59,60].

As the metal center in the pre-catalysts **1**–**8** is coordinatively saturated, the additional side arm functionality cannot interact with the metal. However, after activation with a co-catalyst, the complexes become cationic with a vacant coordination site so that the side arms could interact with the metal centers. Crystals of an activated complex could not be obtained. Only very few examples are known where X-ray diffraction data could be obtained from the active form of chromium polymerization catalysts [61-63]. However, DFT calculation is well suitable for studying such interactions. By such methods it is not only

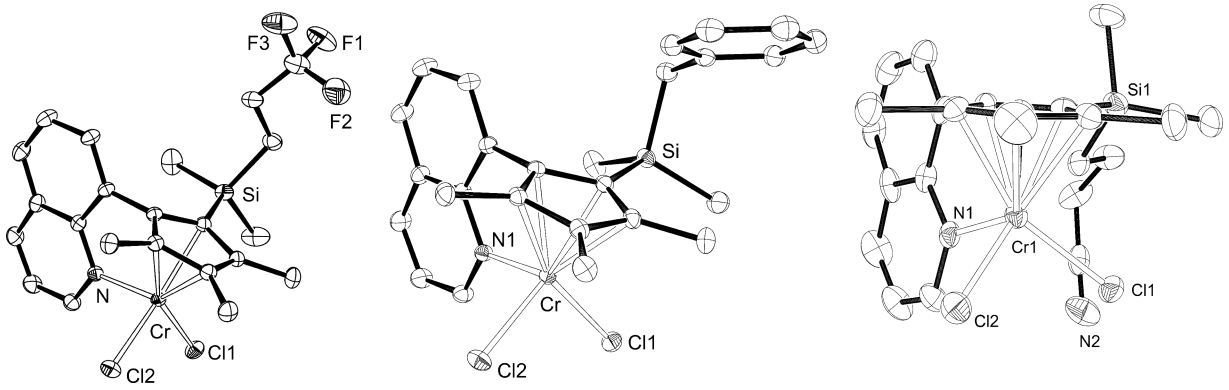


Figure 1: Solid-state molecular structures of selected complexes **4**, **7** and **8** (left, middle and right, respectively). Probability level: 50%. Hydrogen atoms and carbon labels are omitted for clarity.

possible to estimate the binding energy but also to compare it with that of ethylene or interaction with solvent molecules like toluene.

All DFT calculations were performed with the B3LYP functional and the 6-311g* basis set. This theoretical level has shown to reproduce well paramagnetic NMR shifts in such compounds [58,64,65]. As we compare only relative energies of the complexes, the errors in the absolute energy values will compensate considerably. As a model for the activated catalysts we calculated the cationic monomethyl complexes **1a**$^+$–**8a**$^+$. The complexes with ligands with a suitable geometry for intramolecular coordination indeed showed minima structures (as shown by the absence of imaginary frequencies) where the functionalized side-arms interact with the metal center (complexes **3a**$^+$–**8a**$^+$, see Figure 2, for the analogous complexes **1a**$^+$ and **2a**$^+$, respectively, no reasonable minima structures were obtained). We did not consider the conformers where the growing chain is on the "other" site (i.e., oriented in the direction of the Si substituent). From earlier theoretical work on related chromium complexes we know that the chain can move easily from one site to the other so that the hemilabile donor may interact easily [57].

The Cr–F distances in **3a**$^+$ and **4a**$^+$ are with 2.24 Å and 2.21 Å, respectively, in the range of non-covalent Cr–F interactions as exemplified by a cationic chromium complex with BF_4^- anion (2.37 Å) [66] and a typical covalent Cr–F bond (~1.95 Å) [67].

According to calculations the distances of the two carbon atoms of the coordinating unit to the Cr centers in **5a**$^+$, **6a**$^+$ and **7a**$^+$ are approximately 2.5 Å (shortest of the two Cr–C distances). No X-ray data are available for olefin complexes of chromium in oxidation state +3 whereas solid state molecular structures of

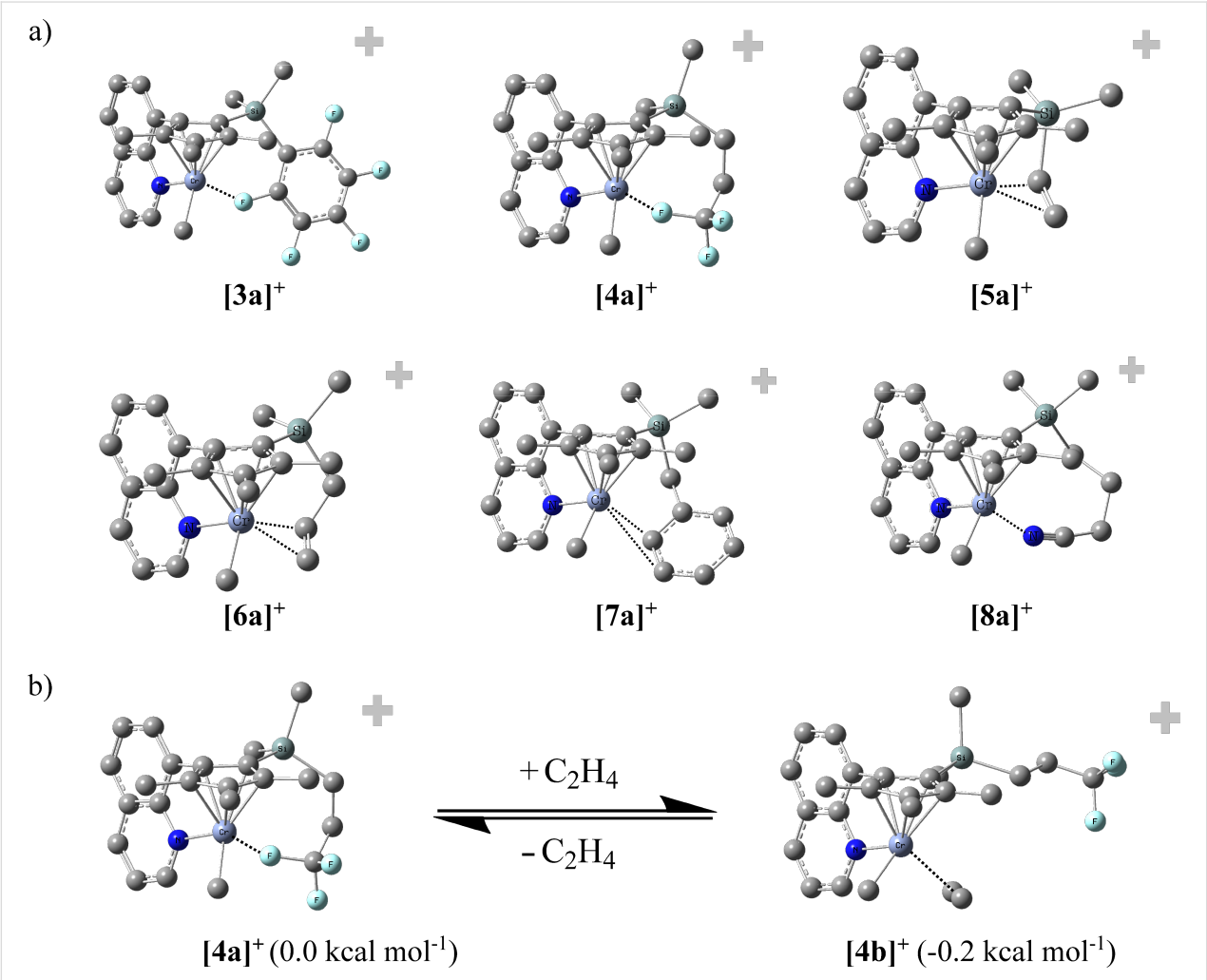


Figure 2: a) Calculated structures of cationic chromium complexes. Chromium–donor distances [Å]: **3a**$^+$ [2.21], **4a**$^+$ [2.24], **5a**$^+$ [2.53/2.51], **6a**$^+$ [2.75/2.46], **7a**$^+$ [2.58/3.17], **8a**$^+$ [2.06]. b) Displacement of hemilabile donor by ethylene under formation of the ethylene complex **4b**$^+$. (Energies for the formation of the analogous ethylene complexes **3b**$^+$ [−1.3], **5b**$^+$ [−4.5], **6b**$^+$ [+2.9], **7b**$^+$ [−2.9], **8b**$^+$ [+15.2].)

Cr^0 and Cr^{1+} complexes have been reported with C–Cr distances of 2.1 Å–2.2 Å (Cr^{1+}) [68,69] and 2.3 Å–2.4 Å (Cr^0) [70,71], respectively.

As an alternative to the intramolecular coordination of the hemilabile donor to the vacant coordination site at the chromium center, a dimerization of the cationic methylchromium fragment could occur and examples of such dicationic dimers have been reported [72-75]. We were able to identify local minimum structures of dimers of compounds **3a**$^+$–**8a**$^+$ but the calculated energies lie considerably higher compared to monomeric forms. Consequently, the saturation by the weak hemilabile donor is energetically preferred over dimerization. Another possible interaction is the coordination of Al–alkyls to the chromium centers. This has been addressed in detail in our previous work, where we could show that the energies of such adducts are similar compared to chromium complexes with olefin coordination [55,57]. For complex 8a$^+$, however, the situation is different: the interaction energy of the nitrile group with the chromium center leads to an energy gain which is 15.2 kcal mol^{-1} higher compared to the energy of the corresponding ethylene complex. Consequently, the ethylene can hardly displace the nitrile. However, addition of Al–alkyls leads to a strong interaction of the Al center with the nitrile group so that ethylene can coordinate. Related to this behavior is a report of an acetonitrile-stabilized chromium complex which upon activation with MAO leads to a highly active catalyst and even the addition of up to 4 equivalents of acetonitrile to the catalyst solution did not lead to lower catalyst activities [76].

Polymerization results

The ethylene polymerization behavior of all new chromium complexes has been evaluated and compared with the performance of the known derivative **1** as well as with zirconocene dichloride (Cp_2ZrCl_2). The results are summarized in Table 1 and the exact procedure is described in the experimental part (Supporting Information File 1). The pre-catalysts were activated with PMAO, which is a non-hydrolytically prepared variant of MAO from the company Akzo Nobel (also called PMAO-IP for "polymeric MAO-improved properties") [77]. All polymerizations were conducted at atmospheric ethylene pressure. The catalytic activities are very high for all derivatives ranging from 1400 to 3900 g polyethylene per mmol catalyst per hour. The lowest activities are obtained with the derivatives with fluorine substituents (complexes **2**–**4**, entries 2–4 in Table 1) whereas all other complexes show considerably higher activities in the range from 2800–3900 g (PE) mmol^{-1} (cat) h^{-1}. Polymerization under only 1 bar of ethylene pressure may lead to artifacts coming from limitations of ethylene transport into the solution and this may lead to biased turnover numbers. More interesting in terms of the concept of this work is the molecular weight of the polymers. The derivative **1** leads to a molecular weight of 530 000 g mol^{-1}. Introduction of the 3,5-bis(trifluoromethyl)phenyl group lowers the molecular weight drastically to 90 000 g mol^{-1}. In this derivative the electron-withdrawing CF_3 groups cannot coordinate to the cationic Cr center in the active catalyst form. Apparently the electron withdrawing $C_6H_3(CF_3)_2$ substituent leads to lower molecular weight. However, when the fluoro substituents are able to coordinate (complexes **3** and **4**, respectively) the polymer molecular weight is much higher compared to the results obtained with **2** and slightly higher compared to **1**. When the side-arm functionalities possess better donor properties the molecular weight increases considerably up to the UHMW-PE range (entries 5–8, Table 1). With pre-catalysts **5** or **6** it is also possible that the side arm (vinyl or allyl side arm, respectively) is incorporated into the polymer but we cannot verify this by our experimental data.

Table 1: Results of the ethylene-polymerization tests with complexes **1–8** and Cp_2ZrCl_2 as catalyst precursors.

entry[a]	catalyst	N_{cat} [µmol]	activity [g·mmol^{-1}·h^{-1}]	M_w[b] [10^3 g·mol^{-1}]	PE [g]	polym.-time [min]	[M_w/M_n]	degr. of cryst.[c] [%]	T_m[c] [°C]
1	**1**	4.42	3240	530	2.87	12	3.1	65	135.5
2	**2**	6.37	1590	90	3.37	20	3.2	–[d]	132.5
3	**3**	6.88	1450	660	2.32	14	2.2	62	133.0
4	**4**	7.82	1910	610	4.48	18	3.5	66	135.5
5	**5**	4.30	3130	900	3.37	15	3.5	59	135.5
6	**6**	7.68	2780	1 070	4.99	14	4.0	56	132.5
7	**7**	3.76	3940	1 140	2.96	12	3.0	54	133.5
8	**8**	4.14	3560	1 450	2.46	10	4.9	64	133.0
9	Cp_2ZrCl_2	10.30	2330	600	4.78	12	2.4	57	132.5

[a]Standard conditions: co-catalyst: PMAO (7% solution in toluene), Al:Cr = 1000:1, room temperature, 150 mL of toluene, atmospheric pressure, all reactions were performed with identical flasks and stirring bars. [b]GPC-measurements. [c]DSC measurements, for details see Supporting Information File 1. [d]The determined crystallinity was unexpectedly high which could be due to artifacts. Therefore, this value is not tabulated.

Figure 3 shows the effect on molecular weight of the produced polyethylene when comparing the known pre-catalyst derivative **1** with the new derivative **8**. As mentioned in the Introduction, the dominating chain termination pathway in olefin polymerization with Cp-chromium catalysts is chain transfer to aluminum alkyls and our results clearly show that this process can be suppressed efficiently by using the donor functions in the side arms of the silyl substituents. It has already been shown that external modifiers are also able to suppress chain termination. However, much higher amounts of such modifiers are necessary in order to give considerable effects [55,78].

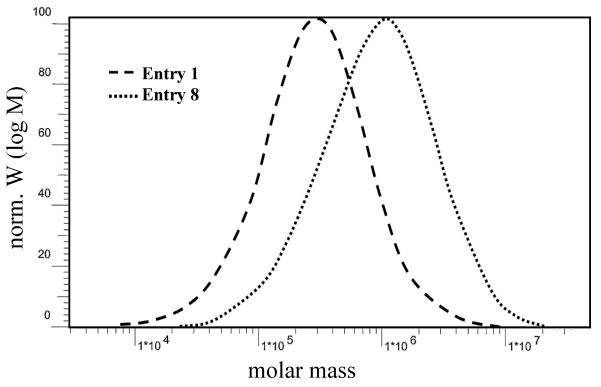


Figure 3: Comparison of GPC traces of polyethylene produced by **1**/PMAO and **8**/PMAO respectively (entries 1 and 8 in Table 1).

Conclusion

We have shown that weak donor groups, which are covalently bound to the metal complex can efficiently modulate chain termination processes in chromium-catalyzed ethylene polymerization catalysis. These hemilabile donors are able to protect coordinatively unsaturated metal centers against coordination of aluminum alkyls and hence reduce chain transfer to aluminum. On the other hand, the donors are weak enough in order to be displaced by ethylene monomers so that the insertion polymerization can proceed with high turnover numbers. With this concept, it is possible to tune the catalyst behavior in terms of the molecular weight they produce without lowering their very high catalytic activity.

Supporting Information

Supporting Information File 1

Experimental part.
[http://www.beilstein-journals.org/bjoc/content/supplementary/1860-5397-12-131-S1.pdf]

Acknowledgements

We thank the German Science Foundation (Sonderforschungsbereich 623) for funding and Basell Polyolefine GmbH (Germany) for ongoing support.

References

1. Jeffrey, J. C.; Rauchfuss, T. B. *Inorg. Chem.* **1979,** *18,* 2658–2666. doi:10.1021/ic50200a004
2. Slone, C. S.; Weinberger, D. A.; Mirkin, C. A. The Transition Metal Coordination Chemistry of Hemilabile Ligands. *Progress in Inorganic Chemistry;* John Wiley & Sons, Inc.: New York, 1999; Vol. 48, pp 233–350.
3. Lindner, E.; Speidel, R.; Fawzi, R.; Hiller, W. *Chem. Ber.* **1990,** *123,* 2255–2260. doi:10.1002/cber.19901231205
4. Bader, A.; Lindner, E. *Coord. Chem. Rev.* **1991,** *108,* 27–110. doi:10.1016/0010-8545(91)80013-4
5. Okuda, J. *Comments Inorg. Chem.* **1994,** *16,* 185–205. doi:10.1080/02603599408035859
6. Braunstein, P.; Naud, F. *Angew. Chem., Int. Ed.* **2001,** *40,* 680–699. doi:10.1002/1521-3773(20010216)40:4<680::AID-ANIE6800>3.0.CO;2-0
7. Weng, Z.; Teo, S.; Hor, T. S. A. *Acc. Chem. Res.* **2007,** *40,* 676–684. doi:10.1021/ar600003h
8. Wang, C.; Ma, Z.; Sun, X.-L.; Gao, Y.; Guo, Y.-H.; Tang, Y.; Shi, L.-P. *Organometallics* **2006,** *25,* 3259–3266. doi:10.1021/om060062j
9. Tshuva, E. Y.; Groysman, S.; Goldberg, I.; Kol, M.; Goldschmidt, Z. *Organometallics* **2002,** *21,* 662–670. doi:10.1021/om010493w
10. Qian, Y.; Huang, J.; Bala, M. D.; Lian, B.; Zhang, H.; Zhang, H. *Chem. Rev.* **2003,** *103,* 2633–2690. doi:10.1021/cr020002x
11. Flores, J. C.; Chien, J. C. W.; Rausch, M. D. *Organometallics* **1994,** *13,* 4140–4142. doi:10.1021/om00023a006
12. Müller, C.; Lilge, D.; Kristen, M. O.; Jutzi, P. *Angew. Chem., Int. Ed.* **2000,** *39,* 789–792. doi:10.1002/(SICI)1521-3773(20000218)39:4<789::AID-ANIE789>3.0.CO;2-F
13. Deckers, P. J. W.; Hessen, B.; Teuben, J. H. *Angew. Chem., Int. Ed.* **2001,** *40,* 2516–2519. doi:10.1002/1521-3773(20010702)40:13<2516::AID-ANIE2516>3.0.CO;2-V
14. Chan, M. C. W.; Kui, S. C. F.; Cole, J. M.; McIntyre, G. J.; Matsui, S.; Zhu, N.; Tam, K.-H. *Chem. – Eur. J.* **2006,** *12,* 2607–2619. doi:10.1002/chem.200501054
15. Mitani, M.; Mohri, J.-i.; Yoshida, Y.; Saito, J.; Ishii, S.; Tsuru, K.; Matsui, S.; Furuyama, R.; Nakano, T.; Tanaka, H.; Kojoh, S.-i.; Matsugi, T.; Kashiwa, N.; Fujita, T. *J. Am. Chem. Soc.* **2002,** *124,* 3327–3336. doi:10.1021/ja0117581
16. Chan, M. C. W. *Chem. – Asian J.* **2008,** *3,* 18–27. doi:10.1002/asia.200700226
17. Bryliakov, K. P.; Talsi, E. P.; Möller, H. M.; Baier, M. C.; Mecking, S. *Organometallics* **2010,** *29,* 4428–4430. doi:10.1021/om100729y
18. Ruwwe, J.; Erker, G.; Fröhlich, R. *Angew. Chem., Int. Ed. Engl.* **1996,** *35,* 80–82. doi:10.1002/anie.199600801
19. Sun, Y.; Spence, R. E. v. H.; Piers, W. E.; Parvez, M.; Yap, G. P. A. *J. Am. Chem. Soc.* **1997,** *119,* 5132–5143. doi:10.1021/ja970140h
20. Karl, J.; Erker, G.; Fröhlich, R. *J. Am. Chem. Soc.* **1997,** *119,* 11165–11173. doi:10.1021/ja971720h
21. Horton, A. D.; Orpen, A. G. *Organometallics* **1991,** *10,* 3910–3918. doi:10.1021/om00057a024

22. Siedle, A. R.; Newmark, R. A.; Lamanna, W. M.; Huffman, J. C. *Organometallics* **1993,** *12,* 1491–1492. doi:10.1021/om00029a002
23. Yang, X.; Stern, C. L.; Marks, T. J. *J. Am. Chem. Soc.* **1994,** *116,* 10015–10031. doi:10.1021/ja00101a022
24. Chen, E. Y.-X.; Marks, T. J. *Chem. Rev.* **2000,** *100,* 1391–1434. doi:10.1021/cr980462j
25. Thomas, B. J.; Noh, S. K.; Schulte, G. K.; Sendlinger, S. C.; Theopold, K. H. *J. Am. Chem. Soc.* **1991,** *113,* 893–902. doi:10.1021/ja00003a024
26. Liang, Y.; Yap, G. P. A.; Rheingold, A. L.; Theopold, K. H. *Organometallics* **1996,** *15,* 5284–5286. doi:10.1021/om960774h
27. White, P. A.; Calabrese, J.; Theopold, K. H. *Organometallics* **1996,** *15,* 5473–5475. doi:10.1021/om960697q
28. Döhring, A.; Göhre, J.; Jolly, P. W.; Kryger, B.; Rust, J.; Verhovnik, G. P. J. *Organometallics* **2000,** *19,* 388–402. doi:10.1021/om990643r
29. Enders, M.; Fernández, P.; Ludwig, G.; Pritzkow, H. *Organometallics* **2001,** *20,* 5005–5007. doi:10.1021/om010753+
30. Ikeda, H.; Monoi, T.; Ogata, K.; Yasuda, H. *Macromol. Chem. Phys.* **2001,** *202,* 1806–1811. doi:10.1002/1521-3935(20010601)202:9<1806::AID-MACP1806>3.0.CO;2-A
31. Mani, G.; Gabbaï, F. P. *Angew. Chem.* **2004,** *116,* 2313–2316. doi:10.1002/ange.200353040
32. Zhang, H.; Ma, J.; Qian, Y.; Huang, J. *Organometallics* **2004,** *23,* 5681–5688. doi:10.1021/om049731o
33. Randoll, S.; Jones, P. G.; Tamm, M. *Organometallics* **2008,** *27,* 3232–3239. doi:10.1021/om800145z
34. Zhang, L.; Gao, W.; Tao, X.; Wu, Q.; Mu, Y.; Ye, L. *Organometallics* **2011,** *30,* 433–440. doi:10.1021/om1005935
35. Sieb, D.; Baker, R. W.; Wadepohl, H.; Enders, M. *Organometallics* **2012,** *31,* 7368–7374. doi:10.1021/om300582j
36. Romano, D.; Ronca, S.; Rastogi, S. *Macromol. Rapid Commun.* **2015,** *36,* 327–331. doi:10.1002/marc.201400514
37. Siemeling, U. *Chem. Rev.* **2000,** *100,* 1495–1526. doi:10.1021/cr990287m
38. Butenschön, H. *Chem. Rev.* **2000,** *100,* 1527–1564. doi:10.1021/cr940265u
39. Müller, C.; Vos, D.; Jutzi, P. *J. Organomet. Chem.* **2000,** *600,* 127–143. doi:10.1016/S0022-328X(00)00060-7
40. Buzinkai, J. F.; Schrock, R. R. *Organometallics* **1987,** *6,* 1447–1452. doi:10.1021/om00150a014
41. Okuda, J.; Zimmermann, K. H. *J. Organomet. Chem.* **1988,** *344,* C1–C4. doi:10.1016/0022-328X(88)80219-5
42. Kohl, F. X.; Dickbreder, R.; Jutzi, P.; Müller, G.; Huber, B. *Chem. Ber.* **1989,** *122,* 871–878. doi:10.1002/cber.19891220513
43. Miguel-Garcia, J. A.; Maitlis, P. M. *J. Chem. Soc., Chem. Commun.* **1990,** 1472–1473. doi:10.1039/c39900001472
44. Lehmkuhl, H.; Näser, J.; Mehler, G.; Keil, T.; Danowski, F.; Benn, R.; Mynott, R.; Schroth, G.; Gabor, B.; Krüger, C.; Betz, P. *Chem. Ber.* **1991,** *124,* 441–452. doi:10.1002/cber.19911240306
45. Ogasa, M.; Mallin, D. T.; Macomber, D. W.; Rausch, M. D.; Rogers, R. D.; Rollins, A. N. *J. Organomet. Chem.* **1991,** *405,* 41–52. doi:10.1016/0022-328X(91)83154-V
46. Erker, G.; Aul, R. *Chem. Ber.* **1991,** *124,* 1301–1310. doi:10.1002/cber.19911240550
47. Zimmermann, K. H.; Pilato, R. S.; Horvath, I. T.; Okuda, J. *Organometallics* **1992,** *11,* 3935–3937. doi:10.1021/om00060a004
48. Okuda, J.; Zimmermann, K. H.; Herdtweck, E. *Angew. Chem., Int. Ed. Engl.* **1991,** *30,* 430–431. doi:10.1002/anie.199104301
49. Okuda, J.; Zimmermann, K. H. *Chem. Ber.* **1992,** *125,* 637–641. doi:10.1002/cber.19921250315
50. Alt, H. G.; Jung, S. H.; Thewalt, U. *J. Organomet. Chem.* **1993,** *456,* 89–95. doi:10.1016/0022-328X(93)83322-M
51. Spence, R. E. v. H.; Piers, W. E. *Organometallics* **1995,** *14,* 4617–4624. doi:10.1021/om00010a028
52. Galakhov, M. V. *Chem. Commun.* **1998,** 17–32. doi:10.1039/a704886f
53. Leong, W. L. J.; Garland, M. V.; Goh, L. Y.; Leong, W. K. *Inorg. Chim. Acta* **2009,** *362,* 2089–2092. doi:10.1016/j.ica.2008.09.026
54. Pinkas, J.; Gyepes, R.; Kubišta, J.; Horáček, M.; Lamač, M. *J. Organomet. Chem.* **2011,** *696,* 2364–2372. doi:10.1016/j.jorganchem.2011.02.032
55. Mark, S.; Kurek, A.; Mülhaupt, R.; Xu, R.; Klatt, G.; Köppel, H.; Enders, M. *Angew. Chem., Int. Ed.* **2010,** *49,* 8751–8754. doi:10.1002/anie.201003918
56. Döhring, A.; Jensen, V. R.; Jolly, P. W.; Thiel, W.; Weber, J. C. *Organometallics* **2001,** *20,* 2234–2245. doi:10.1021/om010146m
57. Xu, R.; Klatt, G.; Enders, M.; Köppel, H. *J. Phys. Chem. A* **2012,** *116,* 1077–1085. doi:10.1021/jp209451p
58. Fernández, P.; Pritzkow, H.; Carbó, J. J.; Hofmann, P.; Enders, M. *Organometallics* **2007,** *26,* 4402–4412. doi:10.1021/om070173y
59. Enders, M.; Fernández, P.; Mihan, S.; Pritzkow, H. *J. Organomet. Chem.* **2003,** *687,* 125–130. doi:10.1016/j.jorganchem.2003.07.017
60. Enders, M.; Kohl, G.; Pritzkow, H. *Organometallics* **2004,** *23,* 3832–3839. doi:10.1021/om030694v
61. Bazan, G. C.; Rogers, J. S.; Fang, C. C. *Organometallics* **2001,** *20,* 2059–2064. doi:10.1021/om001048o
62. MacAdams, L. A.; Buffone, G. P.; Incarvito, C. D.; Rheingold, A. L.; Theopold, K. H. *J. Am. Chem. Soc.* **2005,** *127,* 1082–1083. doi:10.1021/ja043877x
63. Theopold, K. H. *Eur. J. Inorg. Chem.* **1998,** 15–24. doi:10.1002/(SICI)1099-0682(199801)1998:1<15::AID-EJIC15>3.0.CO;2-M
64. Liimatainen, H.; Pennanen, T. O.; Vaara, J. *Can. J. Chem.* **2009,** *87,* 954–964. doi:10.1139/V09-045
65. Martin, B.; Autschbach, J. *Phys. Chem. Chem. Phys.* **2016**. doi:10.1039/c5cp07667f
66. Clérac, R.; Cotton, F. A.; Daniels, L. M.; Dunbar, K. R.; Murillo, C. A.; Pascual, I. *Inorg. Chem.* **2000,** *39,* 748–751. doi:10.1021/ic990793u
67. Thomas, B. J.; Mitchell, J. F.; Theopold, K. H.; Leafy, J. A. *J. Organomet. Chem.* **1988,** *348,* 333–342. doi:10.1016/0022-328X(88)80414-5
68. Emrich, R.; Heinemann, O.; Jolly, P. W.; Krüger, C.; Verhovnik, G. P. J. *Organometallics* **1997,** *16,* 1511–1513. doi:10.1021/om961044c
69. Monillas, W. H.; Yap, G. P. A.; MacAdams, L. A.; Theopold, K. H. *J. Am. Chem. Soc.* **2007,** *129,* 8090–8091. doi:10.1021/ja0725549
70. Wink, D. J.; Wang, N. F.; Creagan, B. T. *Organometallics* **1989,** *8,* 561–562. doi:10.1021/om00104a047
71. Fischer, H.; Hofmann, J. *Chem. Ber.* **1991,** *124,* 981–988. doi:10.1002/cber.19911240503
72. Noh, S. K.; Sendlinger, S. C.; Janiak, C.; Theopold, K. H. *J. Am. Chem. Soc.* **1989,** *111,* 9127–9129. doi:10.1021/ja00207a034
73. Richeson, D. S.; Mitchell, J. F.; Theopold, K. H. *Organometallics* **1989,** *8,* 2570–2577. doi:10.1021/om00113a009

74. Messere, R.; Spirlet, M.-R.; Jan, D.; Demonceau, A.; Noels, A. F. *Eur. J. Inorg. Chem.* **2000,** 1151–1153. doi:10.1002/(SICI)1099-0682(200006)2000:6<1151::AID-EJIC1151>3.3.CO;2-R
75. Nicoara, C. *Neue Cyclopentadienyl ~ N-Donor – Liganden für Chrom-basierte Single-Site-Katalysatoren zur Olefinpolymerisation*. Ph.D. Thesis, Universiät Heidelberg, Heidelberg, Germany, 2006.
76. Kirillov, E.; Roisnel, T.; Razavi, A.; Carpentier, J.-F. *Organometallics* **2009,** *28,* 2401–2409. doi:10.1021/om801196d
77. Smith, G. M.; Palmaka, S. W.; Rogers, J. S.; Malpass, D. B. Polyalkylaluminoxane compositions formed by non-hydrolytic means. U.S. Patent US5.831.109, Nov 3, 1998.
78. Busico, V.; Cipullo, R.; Cutillo, F.; Friederichs, N.; Ronca, S.; Wang, B. *J. Am. Chem. Soc.* **2003,** *125,* 12402–12403. doi:10.1021/ja0372412

License and Terms

This is an Open Access article under the terms of the Creative Commons Attribution License (http://creativecommons.org/licenses/by/2.0), which permits unrestricted use, distribution, and reproduction in any medium, provided the original work is properly cited.

The license is subject to the *Beilstein Journal of Organic Chemistry* terms and conditions: (http://www.beilstein-journals.org/bjoc)

The definitive version of this article is the electronic one which can be found at: doi:10.3762/bjoc.12.131

BEILSTEIN JOURNAL OF ORGANIC CHEMISTRY

Ring-whizzing in polyene-PtL_2 complexes revisited

Oluwakemi A. Oloba-Whenu[1], Thomas A. Albright[*2] and Chirine Soubra-Ghaoui[3]

Full Research Paper

Open Access

Address:
[1]Department of Chemistry, University of Lagos, Akoka, Yaba, Lagos, Nigeria, [2]Department of Chemistry, University of Houston, Houston, Texas 77204-5003, USA and [3]Department of Chemistry and Physics, University of St. Thomas, Houston, Texas 77006, USA

Email:
Oluwakemi A. Oloba-Whenu - ooloba-whenu@unilag.edu.ng;
Thomas A. Albright[*] - talbright@uh.edu;
Chirine Soubra-Ghaoui - ghaouic@stthom.edu

* Corresponding author

Keywords:
d^{10} metal complexes; density functional theory (DFT); hapototropic rearrangements; HOMO–LUMO interactions; polyene-ML_2 complexes; ring-whizzing

Beilstein J. Org. Chem. **2016,** *12,* 1410–1420.
doi:10.3762/bjoc.12.135

Received: 12 April 2016
Accepted: 23 June 2016
Published: 07 July 2016

This article is part of the Thematic Series "Organometallic chemistry".
In memorium: Peter Hofmann, a friend and colleague.

Guest Editor: B. F. Straub

© 2016 Oloba-Whenu et al.; licensee Beilstein-Institut.
License and terms: see end of document.

Abstract

Ring-whizzing was investigated by hybrid DFT methods in a number of polyene–Pt(diphosphinylethane) complexes. The polyenes included cyclopropenium$^+$, cyclobutadiene, cyclopentadienyl$^+$, hexafluorobenzene, cycloheptatrienyl$^+$, cyclooctatetraene, octafluorooctatetraene, 6-radialene, pentalene, phenalenium$^+$, naphthalene and octafluoronaphthalene. The HOMO of a d^{10} ML_2 group (with b_2 symmetry) interacting with the LUMO of the polyene was used as a model to explain the occurrence of minima and maxima on the potential energy surface.

Introduction

Polyene–transition metal complexes were found to undergo fluxional rearrangements as early as 1956 with the preparation of $Cp_2Fe(CO)_2$ [1]. The migration of an ML_n unit around the periphery of a cyclic polyene is commonly called ring-whizzing, purportedly ascribed to Rowland Pettit [2]. A more inclusive term is haptotropic rearrangement [3] wherein a metal atom changes its hapticity along the reaction path. Haptotropic rearrangements in ML_3 and MCp complexes are numerous [4-9] and have found use in synthetic strategies [10], switching devices [11-13] and energy storage [14,15]. Much less is known about the polyene–ML_2 analogs. There are two classes of compounds; one set consists of d^8 ML_2 compounds [16-19] and the other, which we will be concerned with, are the d^{10} ML_2 class. There is ample precedent for four basic coordination geometries exhibited by these compounds. These are shown in Figure 1. Notice that in each case the orientation of the ML_2 unit is tied to the coordination number of the polyene and total electron count. One of us undertook a theoretical survey of these compounds at the extended Hückel level a number of years ago [20,21]. In the present contribution we shall revisit some of these rearrangements using DFT theory, as well as, investigate some new compounds.

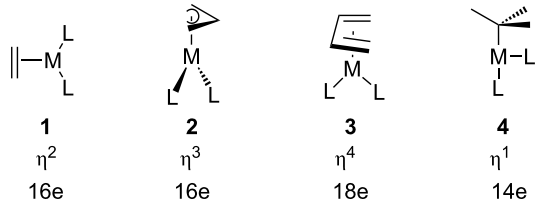


Figure 1: The four coordination geometries for d^{10} polyene-ML_2 complexes along with their hapto numbers and electron count.

A d^{10} ML_2 fragment possesses a high-lying HOMO, shown by **5** in Figure 2, which has b_2 symmetry and a low-lying LUMO, **6**, of a_1 symmetry [22]. An energetically favorable reaction path will be one that maximizes the interactions of these orbitals with the orbitals of a coordinated polyene. The lowest occupied polyene π level is fully symmetric and, therefore, **6** can always interact with it. On the other hand, the LUMO in the π system may not always have the correct symmetry to interact with the b_2 orbital on ML_2 and it is the evolution of this overlap that has an important impact on the reaction path and activation energy. We will also have an occasion to consider a lower lying filled orbital of b_1 symmetry, **7**.

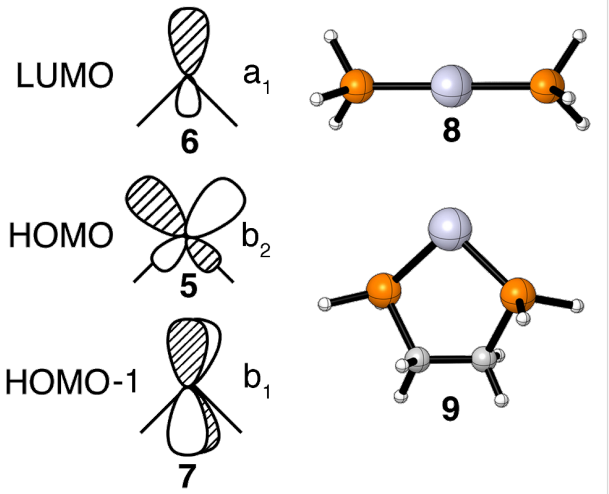


Figure 2: The important valence orbitals of a d^{10} ML_2 group, **5**–**7**, along with the computed structures of $Pt(PH_3)_2$ and Pt(dpe).

Polyene–ML_2 complexes are very fragile which in turn makes it somewhat difficult to compute the reaction path. The bond dissociation energy for ethylene–$Pt(PH_3)_2$ is only about 17 kcal/mol [23]. There are two ways in which the metal–polyene bond can be strengthened. The electron affinity for C_6F_6 is much larger than that for benzene [24]. Consequently interaction of the filled b_2 fragment orbital with the LUMO of C_6F_6 is expected to be larger and the binding energy larger than that for benzene. The M and L that we shall use in this work is Pt and a phosphine. The second method employs the use of a bidentate phosphine. In this regard we have chosen diphosphinylethane (dpe). This idea here is that the P–Pt–P angle is around 100° in polyene–ML_2 complexes. Upon dissociation the 14 electron PtL_2 complex strongly prefers to be linear [22]. So the computed ground state for $Pt(PH_3)_2$, shown in **8**, is calculated to be 29 kcal/mol more stable than one where the P–Pt–P bond angle was constrained to be 99°. This of course is not the case for Pt(dpe), **9**. The P–Pt–P angle remains at 98°. Thus, the bond dissociation energy in polyene–Pt(dpe) complexes rises along with the attendant barriers for haptotropic rearrangements. This has been analyzed and quantified in detail by Massera and Frenking [23] for olefin–ML_2 compounds.

Computational Details

All geometries for the L = PH_3 complexes were optimized without symmetry constraints within the DFT framework first using the B3LYP functional [25-27] in combination with the LANLDZ2 [28] basis sets. Single point calculations were carried out using the triple zeta d plus f polarization functions on Pt [29]. The geometry optimizations were then repeated using the M06 functional [30] along with the Def2-SV(P) basis set [31] for Pt, C, H and P except that the d functions on C were left off. Single point calculations used the Def2-TZVP basis [31] on Pt, P, C and H except for removing the f functions on C. F used a 6-31G basis [32] for the geometrical optimizations and 6-311G [33] in the single point calculations. Analytical frequencies were computed to determinate the nature of the stationary points. The Gaussian 09 software suite [34] was used in all of the calculations. The plots of the molecular structures utilized CYLview [35]. For brevity we will report the structures and Gibbs free energy differences in the standard state only for the polyene–Pt(dpe) complexes using frequencies from the Def2-SV(P) optimizations for the corrections to the Def2-TZVP energies. The geometries and total electronic energies are given as Supporting Information File 1.

Results and Discussion

A. Cyclic polyene–Pt(dpe) examples

The most simple of the cyclic polyenes is the cyclopropenium cation. Its LUMO is a degenerate par of π orbitals, labeled e”$_A$ and e”$_S$ in Figure 3. It is easy to see that e”$_A$ interacts with the b_2 orbital of ML_2 at an η^2 geometry. Indeed this is the computed group state for C_3H_3–$Pt(dpe)^+$ as shown from a side view, **10**, in Figure 3. The transition state for shifting Pt(dpe) from one C–C bond to another passes through a geometry very close to η^3, as shown by **11**. Here b_2 interacts with e”$_S$ and along the reaction path a combination of the e” degenerate set. The essential features can be found elsewhere [21]. The Gibbs free energy difference between the two structures is small: 4.1 kcal/mol

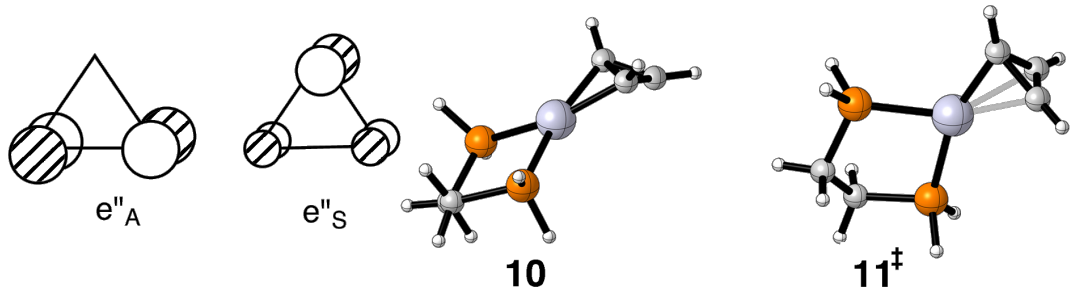


Figure 3: The empty degenerate set of π orbitals in the cyclopropenium cation is shown on the left side. On the right are the two optimized structures of C_3H_3–Pt(dpe)$^+$.

(2.4 kcal/mol for L = PH_3). This is in accord with four structures of $(Ph_3C_3)M(PPh_3)_2^+$ X^- where M = Ni, Pd, and Pt and X^- = ClO_4 and PF_6, which show a progressive movement of the ML_2 unit over the face of the cyclopropenium ring [36]. These structures serve to chart this reaction path and this is consistent with a small reaction barrier with the resultant structure being determined by crystal packing effects. The details have been reported previously [21,36]. The optimizations reveal that the coordinated C–C bond is much longer, 1.62 Å, than the other two, 1.38 Å. This compares favorably to the M = Pt, X^- = PF_6 structure [37] where the C–C distances are 1.58(2) and 1.39 Å, respectively.

The situation for Cp–Pt(dpe)$^+$ is very similar to the cyclopropenium case. Counting this as Cp^+ means that there are two unoccupied orbitals that the b_2 HOMO on ML_2 can interact with. Each is one member of a degenerate set and they are shown on the left side of Figure 4. The two stationary points on the potential energy surface are displayed from a top view on the right side of Figure 4. The e”$_2$ fragment orbital can interact with b_2 to form an η^3 complex as shown in **13**. An η^5 geometry, **14**, will be favored using the empty e”$_1$ orbital. The computed Gibbs free energy difference between the two is very small, namely 1.5 kcal/mol favoring η^3. A recent search of the Cambridge crystallographic database [38] reveals 29 structures of the Cp- and indenyl-$M(PR_3)_2^+$ type where M = Ni, Pd, Pt. For the more general $CpML_2$ case where M = Fe through Pt there are 1074 hits. The majority of these structures are close to the η^5 type although most have a significant range of M–C bond distances. For example, in cyclopentadienyl-platinum-bis(diphenylphosphinobiphenyl) [39] there are two Pt–C distances at 2.26(1) Å and one at 2.33(1) Å. The conformation of the PtL_2 unit with

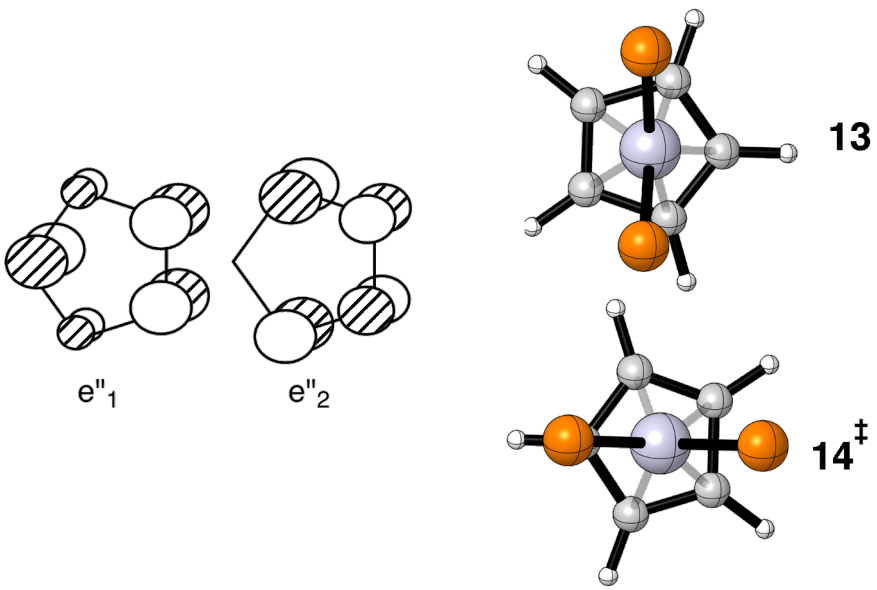


Figure 4: Two unoccupied MOs for Cp^+ are shown on the left side. The two stationary points for Cp–Pt(dpe)$^+$ are given by **13** and **14**. To conserve space the groups around the phosphorus atoms have been removed.

respect to the Cp ring is approximately that given by **13**. Accordingly, the remaining two Pt–C distances are 2.37(1) Å. For optimized **13** the corresponding set of distances is 2.29, 2.34 and 2.45 Å, respectively. The indenyl-M$(PR_3)_2^+$ examples are decidedly η^3 as a consequence of the perturbation generated by the benzo substituent. Normally one would do the electron counting in these molecules as Cp^- and d^8 ML_2 yielding an 18-electron complex. The b_2 fragment orbital is now formally empty and the e"$_1$ set is filled. A full discussion of the bonding in these compounds may be found elsewhere [22].

Another polyene with two coordination geometries is cyclobutadiene. The e_g set shown on the left side of Figure 5 is half-filled. It is easy to see that one member has the correct symmetry to interact with b_2 ML_2 at both the η^2 and η^4 geometries. We found for cyclobutadiene–Pt(dpe) that the η^2 geometry, **15**, is 6.5 kcal/mol more stable than the η^4 geometry, **16**. For L = PH_3 the energy difference is even larger, 10.5 kcal/mol. These results are a little surprising in that the energy difference is larger than what we expected. We are aware of only one structure at this electron count, Ph_4C_4–Ni$(PEt_3)_2$ [40], and it is clearly η^4. As we shall see later, the difference between Ni and Pt can be significant but for the time being, experiment and theory are not in agreement with each other.

Benzene–Ni$(PR_3)_2$ compounds have been known for some time [41]. An η^2 geometry has been observed to be the precursor to C–F bond insertion for F_6C_6 complexes [42] and a number of theoretical studies have been carried out [43-46] which address this reaction. There are two arene–Pt$(PR_3)_2$ structures in the literature [47,48] and both have η^2 geometries. The barrier for ring whizzing in $(CF_3)_6C_6$–Pt$(PEt_3)_2$ has been measured to be ≈11 kcal/mol [41]. One member of the LUMO e_{1g} set in benzene has a large overlap with the b_2 ML_2 MO. The computed ground state structure for η^2 F_6C_6–Pt(dpe), **17** in Figure 6 agrees well with the experiment. The issue is whether the transition state for ring whizzing favors the interaction between e_{1g} and b_2 shown from a top view in **18** or **19**. Extended Hückel

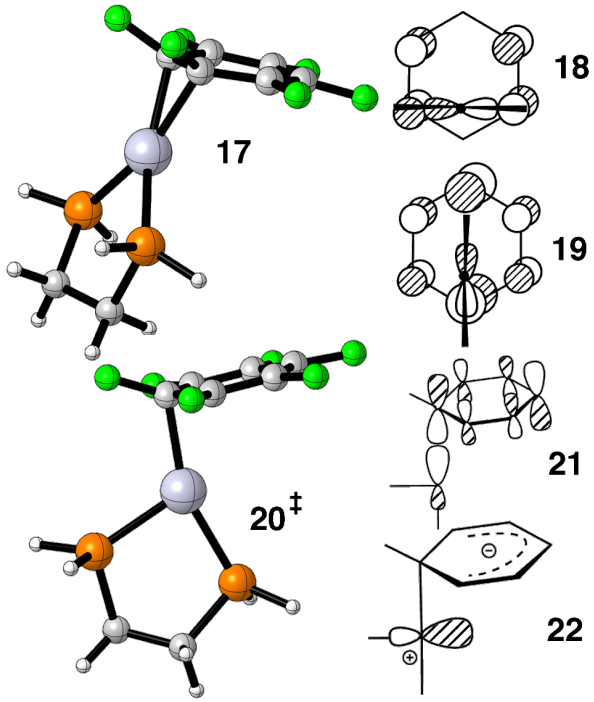


Figure 6: The ground and transition state for ring whizzing in F_6C_6–Pt(dpe), **17** and **20**, respectively. The dominant bonding interaction for two possible transition states, **18** and **19** along with the HOMO, **21** and LUMO, **22**, in the η^1 transition state.

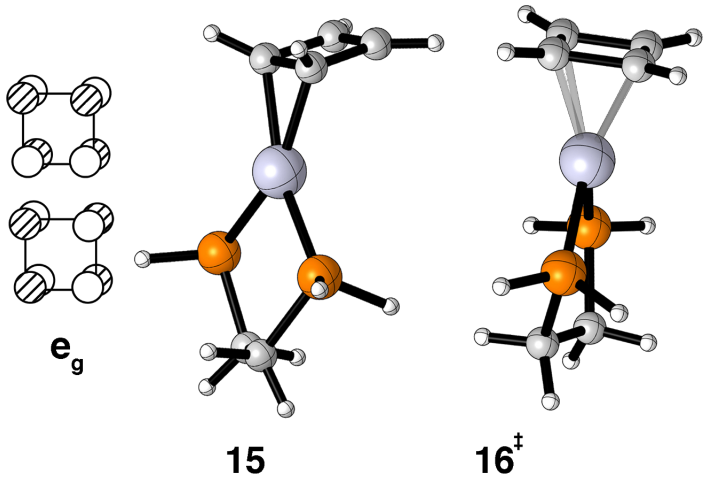


Figure 5: The half-filled degenerate π orbitals in cyclobutadiene. The computed ground state (**15**) and transition state (**16**) for cyclobutadiene–Pt(dpe) on the right.

calculations favored the former [20,21]. Our present day calculations, however, favor **19**. The structure is shown in **20**. Special care was taken to search for a transition state where the Pt(dpe) group was rotated by 90° but none was found. The activation barrier was computed to be 7.4 kcal/mol. Reinhold, McGrady and Perutz [46] obtained a barrier of 6.4 kcal/mol for the same molecule using the B3LYP hybrid functional and a different basis set. The computed geometric parameters for the molecules are very close to each other. One Pt–C bond is short (2.10 Å) while the other two flanking bonds are 2.52 Å. Thus, **20** strongly resembles an η^1 14 electron complex with a "T" shaped geometry. An easy way to view these results is to take a linear combination of b_2 (**5**) and a_1 (**6**). This will generate two equivalent dsp hybrids. One will be filled and can interact with one component of the e_{1g} LUMO, **21**, in Figure 6 and the other will remain empty, **22**.

Another highly fluxional molecule is cycloheptatrienyl–Pt(dpe)$^+$ which exhibits a situation similar to that described for Cp–Pt(dpe)$^+$. The ground state is again an η^3 structure. This is in agreement with several substituted cyclohepatrieneyl–PdL_2 complexes [49]. We looked hard for an η^5 species but instead found an η^2 structure which serves as a transition state for ring whizzing. The activation barrier was computed to be 3.2 kcal/mol. Barriers from 10.5 to 7.6 kcal/mol were found for the Pd complexes [49]. Interestingly an η^1 transition structure with one imaginary frequency was also discovered. It was found to be 7.2 kcal/mol above the ground state.

We thought that radialenes would be an attractive candidate as a ligand and would exhibit a facile haptotropic rearrangement when coordinated to Pt(dpe). The LUMO is all-in phase combination of olefinic π* as shown for 6-radialene by **23** in Figure 7. Therefore, the ML_2 b_2 fragment would retain a sizable portion of its overlap on going from an η^2 to η^4 geometry. For some time 6-radialene and many alkyl derivatives have been known [50]. It is extraordinarily reactive and a bis-$Fe(CO)_3$ derivative of 5-radialene has recently been prepared [51]. The structure of 6-radialene is strongly distorted into a chair form with a boat conformation slightly higher in energy [51]. The D_{6h} structure lies higher in energy by 17.1 kcal/mol [51]. Our optimization of the η^2 ground state shows a twisted boat conformation to be the most stable, **24**, in Figure 7. The activation barrier was found to be 13.7 kcal/mol. We thought that by tying the ends of the olefins together via a CH_2 group would force the ligand to be flat. In fact there are compounds analogous to this having O, S and Se as the linker that are in fact flat [52]. Our calculations reveal that the η^2 ground state, **25**, and the η^4 transition state, **26**, are essentially flat, but the energy difference is only lowered to 13.0 kcal/mol. In **25** the two Pt–C bond distances are 2.17 Å, however, in **26** they are considerably lengthened. The inner Pt–C distances are 2.36 Å and the ones adjacent to the CH_2 group are 2.61 Å! The principal destabilization in **26** is due to the interaction between b_1 (**7**) and the HOMO on 6-radialene, which is the totally antibonding combination of π orbitals, **27**.

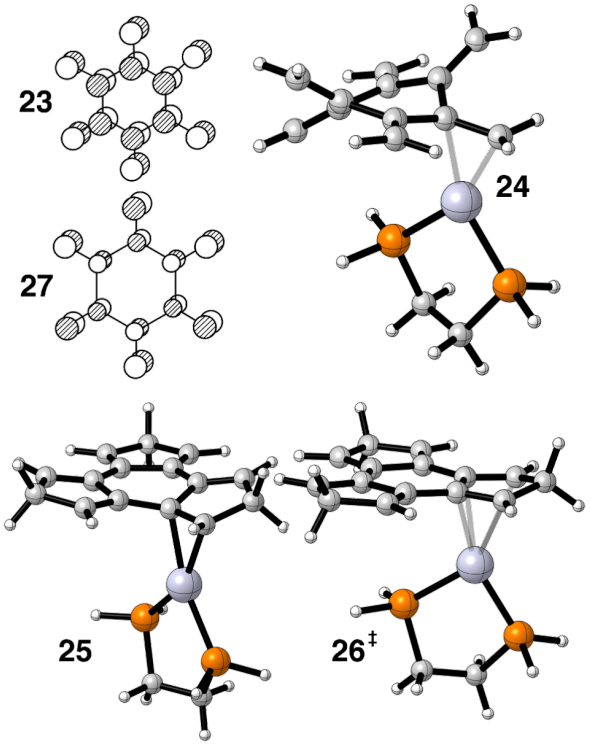


Figure 7: The LUMO, **23**, and HOMO, **27**, in 6-radialene. The optimized η^2 ground states are shown in **24** and **25** while **26** shows the geometry for one η^4 transition state.

B. The strange case of cyclooctatetraene

Cyclooctatetraene (COT) has been a favorite ligand since the dawn of organometallic chemistry [2]. Figure 8 shows two representations for the half-filled e_{2u} set of π orbitals in the flat D_{8h} geometry. One can see from the representation in a) that an η^2 or η^4 conformation are possibilities. In b) one can envision η^1 or η^3 as potential structures. The optimized structures for C_8F_8–Pt(dpe) are illustrated in Figure 9. To conserve space the groups around the phosphorus atoms have been removed. COT and C_8F_8 have a tub shaped structure with D_{2d} symmetry [53,54]. As expected an η^2 structure, **28**, was found to be a minimum. A 1,4-diyl minimum was also found where there are two Pt–C σ bonds, **30**. This structure has also been suggested by means of the low temperature ^{31}P and ^{13}C NMR of COT-Pt($R_2PCH_2CH_2PR_2$), R = iPr [55]. The transition state that interconnects **28** to **30** is shown in **29**. The coordination geometry around Pt is typical of that in η^2 olefin complexes. What is novel is that the COT (and C_8F_8) ring is essentially flat with the uncoordinated portion of the polyene having alternating C–C

bond lengths of ≈1.45 and 1.35 Å. This is in fact the structure of an analogous Ni complex as determined by X-ray crystallography [56]. The haptotropic rearrangement of **28** to **30** does not permute all of the carbon atoms in the COT ring. There is a mirror plane in the plane of the paper for all of the structures in Figure 9. This equivalences the carbons on the front side of the paper with those on the back side. Compounds **28**–**30** do not have a mirror plane perpendicular to this and, therefore, C2 (see **28**) does not become equivalent to C3, etc. As we shall see, a structure akin to **35** would accomplish this. In searching for another structure that accomplishes this we discovered tricyclic **32**. The transition state that converts **28** into **32** is **31**. For the C_8F_8 complex, **28**, the Pt–C distances are 2.08 Å. In **31** the corresponding distances are 2.11 and 2.26 Å with the dashed green bond being formed measuring at 2.32 Å. In COT–Pt(dpe) the transition state **31** is akin to an η^3 complex with the three Pt–C bond lengths calculated to be 2.22–2.26 Å. Since **32** has C_s symmetry (discounting the dpe ligand), it serves as a way-point for ring-whizzing. It is easy to see the electronic basis for ring folding and construction of the tricyclic molecule. Consider that in **28** the filled ML_2 b_2 orbital coordinates to the two lower p AOs in the upper component of e_{2u} in Figure 8a. Then empty a_1 interacts with the lower component in Figure 8a. As ML_2 slips over the polyene in a clockwise motion the appropriate e_{2u} representations become those in Figure 8b. The empty orbital at the top right in Figure 8 interacts with the filled b_2 ML_2 orbital and a_1 interacts with the filled e_{2u}. This is explicitly drawn in **33** and **34**, respectively, of Figure 10. The important consequence of this motion is that the p AO on the opposite side of the ring in **34** has the correct phase to generate a C–C σ bond and this collapses to bicyclic **32**.

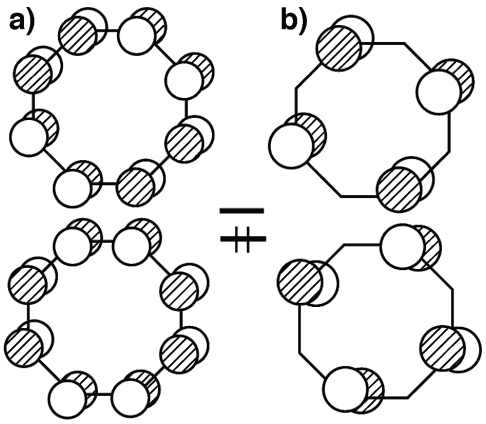


Figure 8: Two representations for the half-filled e_{2u} set of π orbitals in cyclooctatetraene.

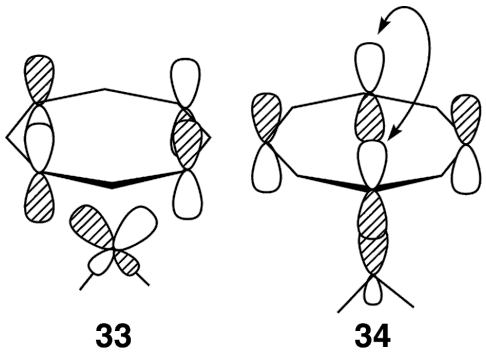


Figure 10: The two important bonding interactions for transition state **31** are drawn in **33** and **34**.

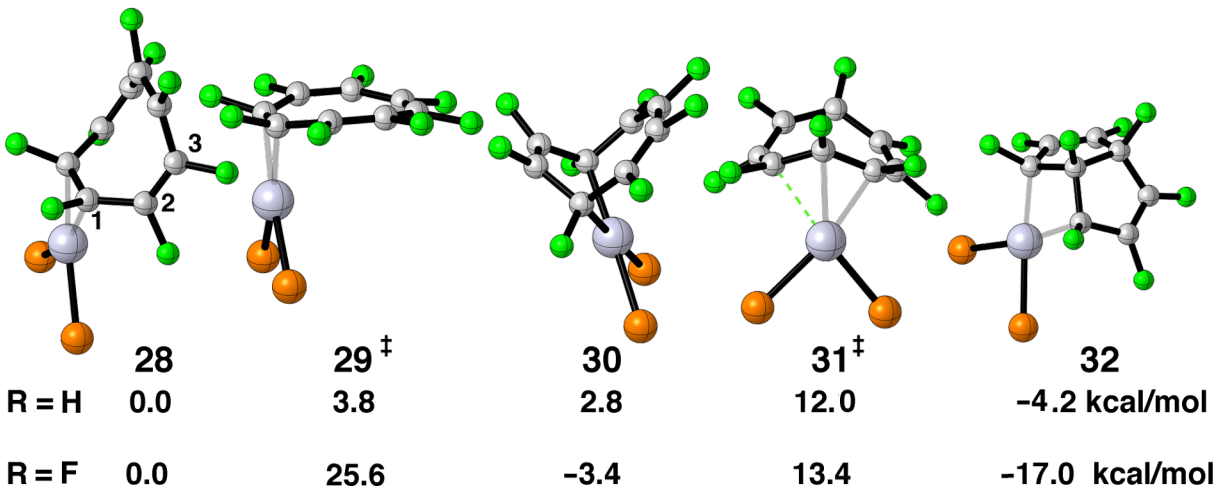


Figure 9: The stationary points found on the potential energy surface of C_8F_8–Pt(dpe). For clarity the groups around the phosphines have been removed. The relative energies for this compound, as well as COT–Pt(dpe) are given below each structure.

Our calculations find that C_8F_8–Pt(dpe) will be caught in the deep potential energy well of the tricyclic isomer, **32**. Hughes and co-workers have shown that experimentally this is indeed the case [57,58]. With PPh_3 and $AsPh_3$ ligands compounds analogous to **30** are initially formed from the reaction of C_8F_8 and a Pt(0) precursor. **30** then irreversibly rearranges in solution to **32** overnight at room temperature. This is also in accord with our calculations. Notice that going from **30** to **32** requires the passage through transition state **29**, which requires 29 kcal/mol. We think that the reason why **29** lies much higher in energy than the COT analog is due to the energy cost associated with flattening the ligand to a D_{4h} type of geometry. For COT itself this entails an energy cost of 10–13 kcal/mol [59]. We find that the conversion for C_8F_8 is nearly triple this amount, namely 29.9 kcal/mol [60].

The picture for COT–Pt(dpe) is not so clear. Our calculations would have **28**, **30** and **32** in rapid equilibrium with the overwhelming majority of the equilibrium shifted to the tricyclic compound. The low temperature ^{31}P and ^{13}C NMR of COT–Pt($R_2PCH_2CH_2PR_2$), R = iPr [55], clearly shows that either **28** or **31** (the authors prefer **31**) is in rapid equilibrium with **30**. There is no spectroscopic evidence consistent with the existence of **32**. It may well be the case that bulky iPr groups in place of hydrogens alter the relative energetics. Perhaps computations with a different functional and/or a larger basis set might bring theory and experiment into agreement. Furthermore, moving from Pt to the isoelectronic Ni also can have a significant impact. An X-ray of the COT–Ni complex [56] reveals the structure is analogous to that for **29**. An X-ray of another Ni complex [60] produces a bis-η^2 isomer, **35**. This is also true for C_8F_8–Ni complexes with certain ligand sets [57,58]. We carried out a number of potential energy minimizations as shown in Figure 11 starting from **35**, as well as, η^1, **36**, and η^3, **37**. Unfortunately none of these produced new stationary points. We will return to this Ni versus Pt issue later.

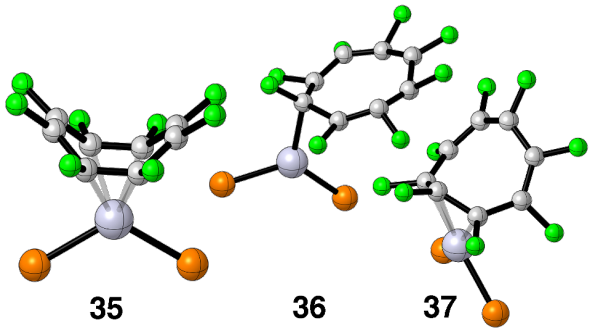


Figure 11: Three other coordination geometries that did not lead to new stationary points are shown in **35**–**37**.

C. Polycyclic examples

Pentalene metal complexes have been the subject of a number of investigations [61], as well as, theoretical explorations of haptotropic rearrangements with ML_3 and MCp [62,63]. However, we are not aware of any complexes with a d^{10} ML_2 group. Pentalene has an energetically low-lying LUMO and close to it another empty orbital. These are shown in **38** and **39**, respectively, in Figure 12. It is easy to see that in **38** the b_2 ML_2 fragment orbital can interact in an η^3 mode both within the five-membered ring, as well as, between the two. **39** has the correct topology to interact with b_2 in η^2 and η^3 modes. We were able to locate four stationary points on the potential energy surface of pentalene–Pt(dpe). These are shown from a top view along with their relative energies in Figure 12. Here again the hydrogens and ethano-bridge connected to the phosphorus atoms has

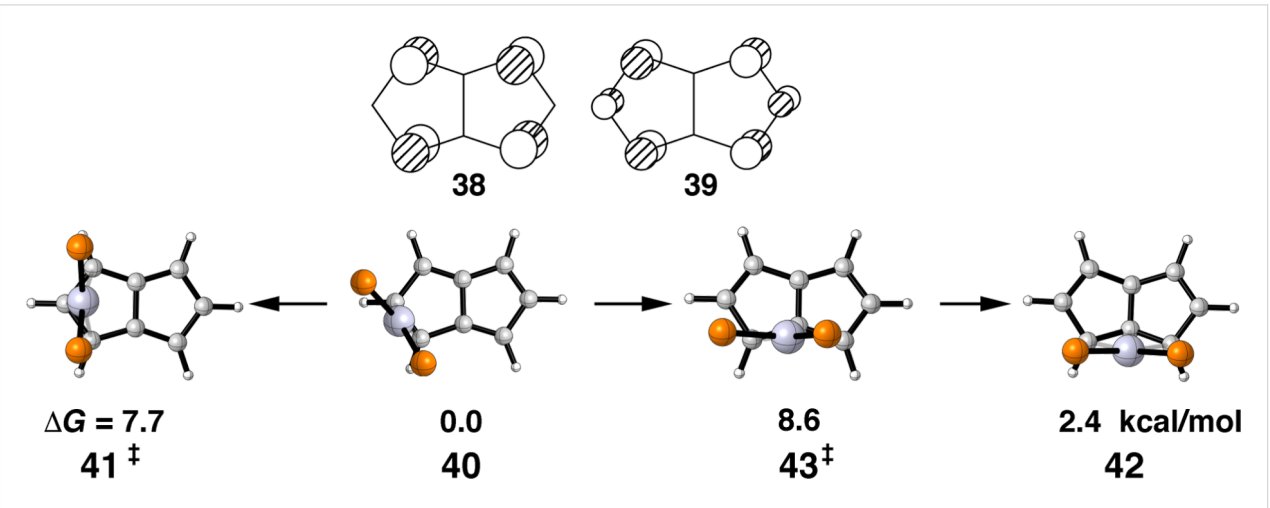


Figure 12: The LUMO and LUMO+1 shown in **38** and **39**, respectively. The four stationary points found for pentalene–Pt(dpe) are displayed in **40**–**43** along with their relative energies. The groups connected to the phosphorus atoms are not shown.

been removed for clarity. We find that the η^2 structure, **40**, to be the ground state. A low energy η^3 transition state, **41**, at 7.7 kcal/mol serves to equivalence the top and bottom halves of the pentalene ligand. The Pt(dpe) group can migrate from one ring to the other via the η^3 structure, **42**. Again the activation energy associated with the transition state **43** is predicted to be small at 8.6 kcal/mol. We anticipate that pentalene–$Pt(PR_3)_2$ will be a highly fluxional molecule.

The situation for phenalenium–$Pt(dpe)^+$ is very similar. The LUMO for phenalenium$^+$ is a rigorously non-bonding MO, **44** in Figure 13. One expects and finds η^3 structures both within and between rings as given by **45** and **46**, respectively, with essentially identical relative energies. Experimentally, all known complexes [64-67] are akin to **45**. Our calculated barrier of 14.7 kcal/mol via **47** seems a bit too low. The measured barrier in two Pd(tmeda) complexes was 21.4 and 21.6 kcal/mol [66]. No signs of fluxionality was found in a substituted phenalenium–$Pt(PPh_3)_2^+$ complex [67].

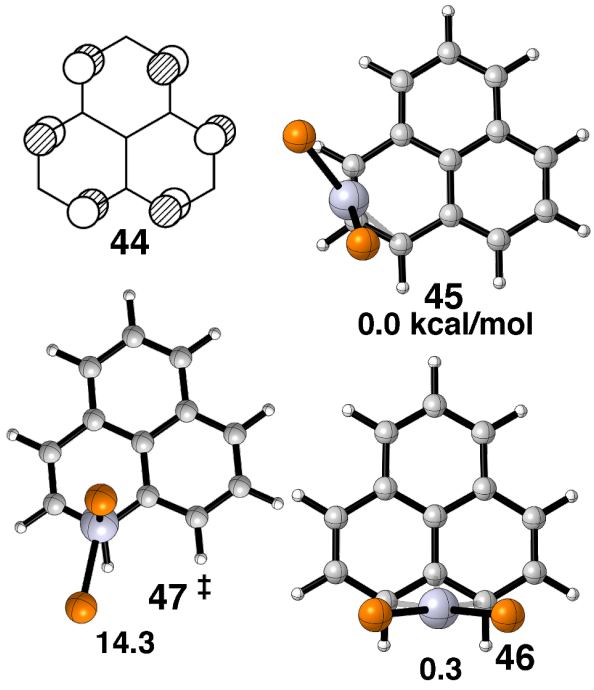


Figure 13: The LUMO of the phenalenium cation is given in **44**. The structures of the three stationary points found for phenalenium–Pt(dpe)$^+$ along with their relative energies are shown from a top view in **45**–**47**. Again the groups connected to the phosphorus atoms are not shown.

Naphthalene and anthracene–$Ni(PR_3)_2$ compounds have been known and studied for some time [45,46,68-75]. We are, however, unaware of any $Pt(PR_3)_2$ examples. The ground state structures of the Ni compounds possess an η^2 geometry where the Ni is coordinated to a carbon–carbon bond adjacent to the ring fusion. Our calculations on octafluoronaphthalene–Ni(dpe) and –Pt(dpe) (as well as naphthalene–Pt(dpe) itself) are in good agreement with experiment. A top view of the structure is shown by **48** in Figure 14. This offers a good overlap between the LUMO in $C_{10}F_8$, **49**, and the b_2 HOMO, **5**, in Pt(dpe). It was thought [20] that migration of an ML_2 unit from one ring to another would involve an η^3 structure where Pt would bond to C(1), C(9) and C(8). For the carbon numbering system please see **48**. Bonding between b_2 ML_2 and the b_{1g} MO would be retained. Unfortunately this is not quite the entire story. One of the stationary points is shown by **50**. The a_u HOMO, **51**, in $C_{10}F_8$ also has a significant overlap with b_2 at this geometry. Since these two fragment orbitals are both filled, there is also considerable destabilization. What we find is that this expanse of the potential energy surface is a twixtyl intermediate [76]. At the stationary point given by **50** there is one imaginary frequency of 17i cm^{-1}; at another closer to η^3 the computed frequencies are all positive but one is tiny, 15 cm^{-1}. So this region of the coordinate space is analogous to a plateau; the potential energy is essentially flat. The activation energy to attain **50** in $C_{10}F_8$–Pt(dpe) was computed to be 13.7 kcal/mol; in $C_{10}H_8$–Pt(dpe) the barrier was 14.8 kcal/mol. This is in line with an NMR derived barrier of about 15 kcal/mol for $C_{10}H_8NiL_2$ [74] and 15–20 kcal/mol for anthracene–$Ni(PR_3)_2$ [69,70]. Oprunenko and Gloriozov [75] have calculated the η^3 tranisition state to lie at a relative energy of 12.2 kcal/mol for naphthalene–$Ni(PEt_3)_2$ using the PBE functional and a different basis set than that employed here. Jones and co-workers [45] have undertaken an exhaustive study of ring whizzing and oxidative addition in a series of cyano and methyl substituted naphthalene–Ni(dmpe) complexes at the B3LYP level. Structures analogous to **50** were reported at relative energies of 12–17.5 kcal/mol. We do find in $C_{10}F_8$–Pt(dpe) that there is a second path for the haptotropic rearrangement from one ring to the other. Here the Pt(dpe) group migrates further in towards the ring junction with a weakly bound transition state of 21.9 kcal/mol and ending at an η^2 minimium where the C(9) and C(10) atoms are coordinated to Pt at a relative energy of 17.9 kcal/mol. The latter structures were also computed to lie at high energies by Jones and co-workers [45]. So, at this point theory and experiment appear to be in agreement for the NiL_2 and PtL_2 cases.

But the story does not end here. Experimentally there is a low energy process that converts, **48**, to the equivalent η^2 complex where the ML_2 group is coordinated to C(3) and C(4). This is also the case for anthracene–NiL_2. The experimental barriers range ≈5–6 kcal/mol [69,70,74]. The aforementioned calculations [45,75] yield barriers of 4.2–9.5 kcal/mol in reasonable agreement with the experiment. The structures of these

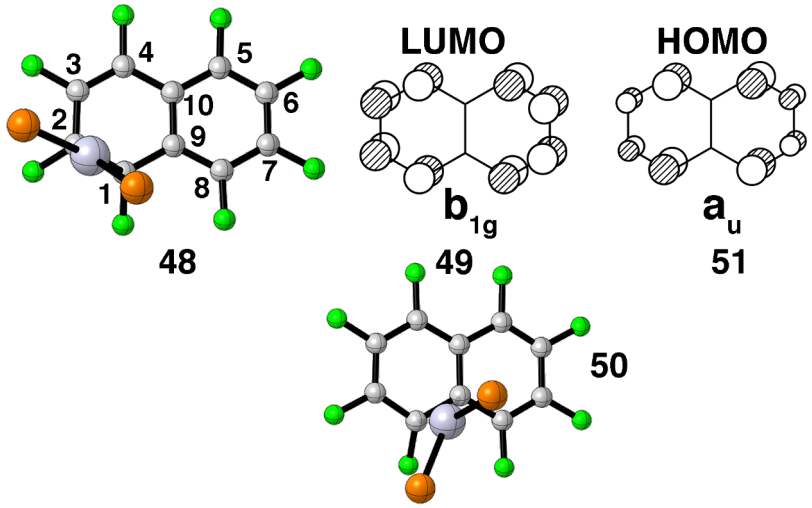


Figure 14: A top view of two stationary points found for F_8C_{10}–Pt(dpe); **48** is the ground state and **50**, represents one point on the plateau. The LUMO and HOMO in naphthalene are drawn in **49** and **51**, respectively.

transition states resemble η^4 species with the geometry akin to **52** in Figure 15. This is not the case for $C_{10}F_8$–Pt(dpe) or $C_{10}H_8$–Pt(dpe). The barriers are calculated to be 17.1 and 17.4 kcal/mol, respectively. Furthermore, the barrier for $C_{10}H_8$–Pt(dpe) using the B3LYP function generates a barrier of 17.8 kcal/mol. Using the M06 functional for $C_{10}F_8$–Ni(dpe) yields a barrier of 6.1 kcal/mol which is in line with the calculations by others. Therefore, the discrepancy must lie in the difference between Pt and Ni. There is also a difference in the metrical details of these transition states. For the Ni examples the Ni–C(1) and Ni–C(4) distances are ≈0.3 Å longer than the Ni–C(2) and Ni–(3) ones (see **48** for the numbering scheme). For the Pt complexes we find this difference to be about twice as large. In other words, the Pt cases are closer to η^2 complexes where the olefinic portion of the ligand is rotated by 90° from the minimum energy conformation given in **1**. We will return to this point shortly. One might think that the overlap between b_2 ML_2 and the LUMO, **49**, from the η^2 ground state to η^4 will be retained and, thus, the activation energy will be small. However, note that at η^4 the overlap between the filled b_1 fragment orbital, **7**, and the a_u HOMO on $C_{10}F_8$ is turned on and this is repulsive. With this in mind it is tempting to put forward the hypothesis that the 3d AOs in Ni are very contracted and their overlap at **52** is not so large. Hence the $a_u - b_1$ repulsion is not so large and it is the mixing of 4p character in the Ni b_2 orbital that retains reasonable overlap with b_{1g}. On the other hand, the Pt 5d AO is more diffuse and consequently more bonding is lost at η^4 than its Ni congener. But this cannot be the whole story. Massera and Frenking [23] have shown that there is essentially no energy difference between the bond dissociation energy (BDE) in ethylene–Ni(dpe) and the Pt analog. Furthermore, their calculated BDE for ethylene–$Pt(PH_3)_2$ is in very good agreement with that found [23] at the CCSD(T) level with a large basis set. On the other hand, Reinhold, McGrady and Perutz have reported [46] that C_6H_6 and C_6F_6–Pt(dpe) BDEs are about 8 kcal/mol less than that for the Ni(dpe) analogs.

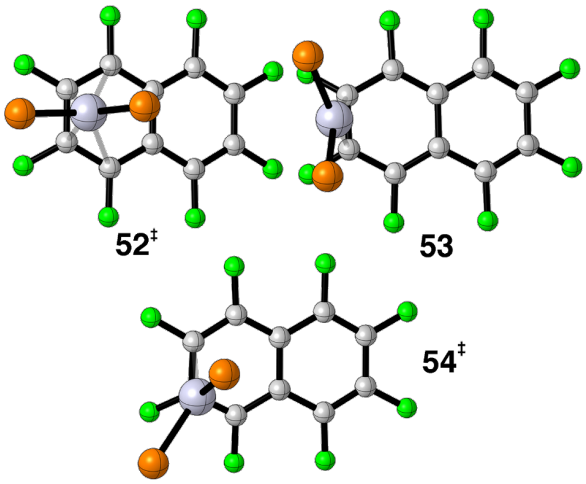


Figure 15: At top view of the η^4, **52**, and η^4, **54**, transition states along with the η^2, **53**, intermediate.

A close examination of the potential energy surface in $C_{10}F_8$–Pt(dpe) revealed the existence of another η^2 minimum, **53**, in Figure 15. It lies 13.7 kcal/mol above the ground state. This is in line with the corresponding minima found by Jones and co-workers [45] in the substituted naphthalene–Ni(dmpe) compounds (≈13 kcal/mol). So our calculations put the η^2 minimum, **53**, to be 3.4 kcal/mol more stable than the η^4 transition state, **52**. However, the latter does not serve as the

waypoint for the former. An η^1 structure, **54**, was found to be the transition state for the haptotropic rearrangement of **48** to **53**. Notice that passage through the η^2 intermediate causes the phosphines to become equivalent. Benn and co-workers [74] in fact observe phosphine equivalence with a barrier of approximately 13 kcal/mol for the naphthalene–Ni$(PR_3)_2$ compounds. Our calculations put **54** to be 14.9 kcal/mol above the ground state, **48**. This is in reasonable agreement with the NMR results [74]. The reaction path and associated electronic details for the **48** to **54** to **53** haptotropic shift is precisely analogous to ring-whizzing in C_6F_6–Pt(dpe) that was covered previously. In summary we find the potential energy surface for naphthalene–Pt and –Ni complexes to be quite different. In $C_{10}F_8$–Pt(dpe), haptotropic rearrangement from one ring to another is energetically similar to that within one ring, whereas, in the Ni analog the former is much slower than the latter.

Conclusion

Our original thesis that the ML_2 b_2 interaction with the LUMO of the polyene dictated the reaction path was largely fulfilled. Often this guided our exploration of the potential energy surfaces. But molecules, like life, sometimes yield unexpected conclusions. We miss you, Peter Hofmann.

Supporting Information

Supporting Information File 1

The molecular geometry and total electronic energy for the molecules in this work are given in .xyz format. The file may be opened as a text file to read the coordinates, or opened directly by a molecular modeling program such as Mercury (http://www.ccdc.cam.ac.uk/pages/Home.aspx). Molecular geometry and total electronic energy data.
[http://www.beilstein-journals.org/bjoc/content/supplementary/1860-5397-12-135-S1.xyz]

References

1. Piper, T. S.; Wilkinson, G. *J. Inorg. Nucl. Chem.* **1956,** *3,* 104. doi:10.1016/0022-1902(56)80073-0
2. Cotton, F. A. *Inorg. Chem.* **2002,** *41,* 643. doi:10.1021/ic010972n and references therein.
3. Anh, N. T.; Elian, M.; Hoffmann, R. *J. Am. Chem. Soc.* **1978,** *100,* 110. doi:10.1021/ja00469a019
4. Gloriozov, I. P.; Marchal, R.; Saillard, J.-Y.; Oprunenko, Y. F. *Eur. J. Inorg. Chem.* **2015,** 250. doi:10.1002/ejic.201402879
5. Jiménez-Halla, J. O. C.; Robles, J.; Solá, M. *Organometallics* **2008,** *27,* 5230. doi:10.1021/om800505j
6. Czerwinski, C. J.; Fetisov, E. O.; Gloriozov, I. P.; Oprunenko, Y. F. *Dalton Trans.* **2013,** *42,* 10487. doi:10.1039/c3dt50655j
7. Fetisov, E. O.; Gloriozov, I. P.; Oprunenko, Yu. F.; Saillard, J.-Y.; Kahlal, S. *Organometallics* **2013,** *32,* 3512. doi:10.1021/om4003335
8. Gridnev, I. D. *Coord. Chem. Rev.* **2008,** *252,* 1798. doi:10.1016/j.ccr.2007.10.021
9. Oprunenko, Yu. F. *Russ. Chem. Rev.* **2000,** *69,* 683. doi:10.1070/RC2000v069n08ABEH000589
10. Kündig, E. P.; Pape, A. *Top. Organomet. Chem.* **2004,** *7,* 71. doi:10.1007/b12823
11. Hülsen, M.; Norman, P.; Dolg, M. *J. Organomet. Chem.* **2011,** *696,* 3861. doi:10.1016/j.jorganchem.2011.08.039
12. Nakai, H.; Isobe, K. *Coord. Chem. Rev.* **2010,** *254,* 2652. doi:10.1016/j.ccr.2009.12.025
13. Dötz, K. H.; Jahr, H. C. *Chem. Rec.* **2004,** *4,* 61. doi:10.1002/tcr.20007
14. Albright, T. A.; Dosa, P. I.; Grossmann, T. N.; Khrustalev, V. N.; Oloba, O. A.; Padilla, R.; Paubelle, R.; Stanger, A.; Timofeeva, T. V.; Vollhardt, K. P. C. *Angew. Chem., Int. Ed.* **2009,** *48,* 9853. doi:10.1002/anie.200905088
15. Albright, T. A.; Drissi, R.; Gandon, V.; Oldenhof, S.; Oloba-Whenu, O. A.; Padilla, R.; Shen, H.; Vollhardt, K. P. C.; Vreeken, V. *Chem. – Eur. J.* **2015,** *21,* 4546. doi:10.1002/chem.201406211
16. Crabtree, R. H.; Parnell, C. P. *Organometallics* **1984,** *3,* 1727. doi:10.1021/om00089a022
17. Woolf, A.; Chaplin, A. B.; McGrady, J. E.; Alibadi, M. A. M.; Rees, N.; Draper, S.; Murphy, F.; Weller, A. S. *Eur. J. Inorg. Chem.* **2011,** 1614. doi:10.1002/ejic.201001263
18. Woolf, A.; Alibadi, M. A. M.; Chaplin, A. B.; McGrady, J. E.; Weller, A. S. *Eur. J. Inorg. Chem.* **2011,** 1626. doi:10.1002/ejic.201001264
19. Oprunenko, Yu. F.; Gloriozov, I. P. *Russ. Chem. Bull.* **2010,** *59,* 2061. doi:10.1007/s11172-010-0355-1
20. Silvestre, J.; Albright, T. A. *J. Am. Chem. Soc.* **1985,** *107,* 6829. doi:10.1021/ja00310a015
21. Silvestre, J.; Albright, T. A. *Nouv. J. Chim.* **1985,** 9659.
22. Albright, T. A.; Burdett, J.; Whangbo, M.-H. *Orbital Interactions in Chemistry,* 2nd ed.; Wiley: Hoboken, 2013; pp 537–544; 549–552. doi:10.1002/9781118558409
23. Massera, C.; Frenking, G. *Organometallics* **2003,** *22,* 2758. doi:10.1021/om0301637
24. Voora, V. K.; Jordan, K. D. *J. Phys. Chem. A* **2014,** *118,* 7201. doi:10.1021/jp408386f and references therein.
25. Becke, A. D. *J. Chem. Phys.* **1993,** *98,* 5648. doi:10.1063/1.464913
26. Stephens, P. J.; Devlin, F. J.; Chabalowski, C. F.; Frisch, M. J. *J. Phys. Chem.* **1994,** *98,* 11623. doi:10.1021/j100096a001
27. Lee, C.; Yang, W.; Parr, R. G. *Phys. Rev. B* **1988,** *37,* 785. doi:10.1103/PhysRevB.37.785
28. Hay, J. R.; Wadt, W. R. *J. Chem. Phys.* **1985,** *82,* 299. doi:10.1063/1.448975
29. Roy, L. E.; Hay, J. P.; Martin, R. L. *J. Chem. Theory Comput.* **2008,** *4,* 1029. doi:10.1021/ct8000409
30. Zhao, Y.; Truhlar, D. G. *Theor. Chem. Acc.* **2008,** *120,* 215. doi:10.1007/s00214-007-0310-x
31. Weigend, F.; Ahlrichs, R. *Phys. Chem. Chem. Phys.* **2005,** *7,* 3297. doi:10.1039/b508541a
32. Ditchfield, R.; Hehre, W. J.; Pople, J. A. *J. Chem. Phys.* **1971,** *54,* 724. doi:10.1063/1.1674902
33. Krishnan, R.; Binkley, J. S.; Seeger, R.; Pople, J. A. *J. Chem. Phys.* **1980,** *72,* 650. doi:10.1063/1.438955
34. *Gaussian 09,* Revision B.01; Gaussian, Inc.: Wallingford CT, 2010.
35. *CYLview,* 1.0b; Legault, C. Y., Université de Sherbrooke, 2009, http://www.cylview.org.

36. Mealli, C.; Midollini, S.; Moneti, S.; Sacconi, L.; Silvestre, J.; Albright, T. A. *J. Am. Chem. Soc.* **1982,** *104,* 95. doi:10.1021/ja00365a020
37. McClure, M. D.; Weaver, D. L. *J. Organomet. Chem.* **1973,** *54,* C59. doi:10.1016/S0022-328X(00)84983-9
38. CSD version 5.37 (Nov.2015 plus 1 update).
39. Becker, J. J.; White, P. S.; Gagné, M. R. *J. Am. Chem. Soc.* **2001,** *123,* 9478. doi:10.1021/ja016167p
40. Eisch, J. J.; Piotrowski, A. M.; Aradi, A. A.; Krüger, C.; Romão, M. J. *Z. Naturforsch., B* **1985,** *40,* 624. doi:10.1515/znb-1985-0511
41. Browning, J.; Green, M.; Penfold, B. R.; Spencer, J. L.; Stone, F. G. A. *J. Chem. Soc., Chem. Commun.* **1973,** 31. doi:10.1039/c39730000031
42. Clot, E.; Eisenstein, O.; Jasim, N.; Macgregor, S. A.; McGrady, J. E.; Perutz, R. N. *Acc. Chem. Res.* **2011,** *44,* 333. doi:10.1021/ar100136x see for a review.
43. Hatnean, J. A.; Johnson, S. A. *Organometallics* **2012,** *31,* 1361. doi:10.1021/om200990g
44. Johnson, S. A.; Mroz, N. M.; Valdizon, R.; Murray, S. *Organometallics* **2011,** *30,* 441. doi:10.1021/om100699d
45. Li, T.; García, J. J.; Brennessel, W. W.; Jones, W. D. *Organometallics* **2010,** *29,* 2430. doi:10.1021/om100001m
46. Reinhold, M.; McGrady, J. E.; Perutz, R. N. *J. Am. Chem. Soc.* **2004,** *126,* 5268. doi:10.1021/ja0396908
47. Cobbledick, R. E.; Einstein, F. W. B. *Acta Crystallogr., Sect. B: Struct. Crystallogr. Cryst. Chem.* **1978,** *34,* 1849. doi:10.1107/S0567740878006822
48. Browning, J.; Penfold, B. R. *J. Cryst. Mol. Struct.* **1974,** *4,* 335. doi:10.1007/BF01636047
49. Jandl, C.; Öfele, K.; Kühn, F. E.; Herrmann, W. A.; Pöthig, A. *Organometallics* **2014,** *33,* 6398. doi:10.1021/om500738d
50. Barkovich, A. J.; Strauss, E. S.; Vollhardt, K. P. C. *J. Am. Chem. Soc.* **1977,** *99,* 8321. doi:10.1021/ja00467a036
51. Mackay, E. G.; Newton, C. G.; Toombs-Ruane, H.; Lindeboom, E. J.; Fallon, T.; Willis, A. C.; Paddon-Row, M. N.; Sherburn, M. S. *J. Am. Chem. Soc.* **2015,** *137,* 14653. doi:10.1021/jacs.5b07445
52. Fallon, T.; Willis, A. C.; Rae, A. D.; Paddon-Row, M. N.; Sherburn, M. S. *Chem. Sci.* **2012,** *3,* 2133. doi:10.1039/c2sc20130e and references therein.
53. Claus, K. H.; Krüger, C. *Acta Crystallogr., Sect. C: Cryst. Struct. Commun.* **1988,** *C44,* 1632. doi:10.1107/S0108270188005840
54. Laird, B. B.; Davis, R. E. *Acta Crystallogr., Sect. B: Struct. Crystallogr. Cryst. Chem.* **1982,** *B38,* 678. doi:10.1107/S0567740882003781
55. Schager, F.; Haack, K.-J.; Mynott, R.; Rufińska, A.; Pörschke, K.-R. *Organometallics* **1998,** *17,* 807. doi:10.1021/om970762b and references therein.
56. Bach, I.; Pörschke, K.-R.; Proft, B.; Goddard, R.; Kopiske, C.; Krüger, C.; Rufińska, A.; Seevogel, K. *J. Am. Chem. Soc.* **1997,** *119,* 3773. doi:10.1021/ja964210g
57. Carl, R. T.; Corcoran, E. W., Jr.; Hughes, R. P.; Samkoff, D. E. *Organometallics* **1990,** *9,* 838. doi:10.1021/om00117a046
58. Hughes, R. P. *J. Fluorine Chem.* **2010,** *131,* 1059. doi:10.1016/j.jfluchem.2010.06.014
59. Klärner, F.-G. *Angew. Chem., Int. Ed.* **2001,** *40,* 3977. doi:10.1002/1521-3773(20011105)40:21<3977::AID-ANIE3977>3.0.CO;2-N and references therein.
60. Sánchez-Sanz, G.; Trujillo, C.; Rozas, I.; Alkorta, I. *Phys. Chem. Chem. Phys.* **2015,** *17,* 14961. doi:10.1039/C5CP00876J
61. Summerscales, O. T.; Cloke, F. G. N. *Coord. Chem. Rev.* **2006,** *250,* 1122. doi:10.1016/j.ccr.2005.11.020
62. Deramchi, K.; Maouche, B.; Kahlal, S.; Saillard, J.-Y. *Inorg. Chim. Acta* **2011,** *370,* 499. doi:10.1016/j.ica.2011.02.059
63. Li, H.; Feng, H.; Sun, W.; Xie, Y.; King, R. B.; Schaefer, H. F., III. *New J. Chem.* **2011,** *35,* 1718. doi:10.1039/c1nj20144a
64. Nakasuji, K.; Yamaguschi, M.; Murata, I.; Tatsumi, K.; Nakamura, A. *Chem. Lett.* **1983,** *12,* 1489. doi:10.1246/cl.1983.1489
65. Nakasuji, K.; Yamaguschi, M.; Murata, I.; Tatsumi, K.; Nakamura, A. *Organometallics* **1984,** *3,* 1257. doi:10.1021/om00086a018
66. Nakasuji, K.; Yamaguschi, M.; Murata, I.; Nakanishi, H. *J. Am. Chem. Soc.* **1986,** *108,* 325. doi:10.1021/ja00262a039
67. Keasey, A.; Bailey, P. M.; Maitlis, P. M. *J. Chem. Soc., Chem. Commun.* **1978,** 142. doi:10.1039/C39780000142
68. Stanger, A. *Organometallics* **1991,** *10,* 2979. doi:10.1021/om00054a082
69. Stanger, A.; Vollhardt, K. P. C. *Organometallics* **1992,** *11,* 317. doi:10.1021/om00037a054
70. Stanger, A.; Weisman, H. *J. Organomet. Chem.* **1996,** *515,* 183. doi:10.1016/0022-328X(95)06104-5
71. Braun, Y.; Cronin, L.; Higgitt, C. L.; McGrady, J. E.; Perutz, R. N.; Reinhold, M. *New J. Chem.* **2001,** *25,* 19. doi:10.1039/B006368L
72. Hatnean, J. A.; Beck, R.; Borrelli, J. D.; Johnson, S. A. *Organometallics* **2010,** *29,* 6077. doi:10.1021/om1008499
73. Schaub, T.; Fischer, P.; Steffen, A.; Braun, T.; Radius, U.; Mix, A. *J. Am. Chem. Soc.* **2008,** *130,* 9304. doi:10.1021/ja074640e
74. Benn, R.; Mynott, R.; Topalovic, I.; Scott, F. *Organometallics* **1989,** *8,* 2299. doi:10.1021/om00112a002
75. Oprunenko, Yu. F.; Gloriozov, I. P. *Russ. Chem. Bull.* **2011,** *60,* 213. doi:10.1007/s11172-011-0036-8
76. Hoffmann, R.; Swaminathan, S.; Odell, B. G.; Gleiter, R. *J. Am. Chem. Soc.* **1970,** *92,* 7091. doi:10.1021/ja00727a013

License and Terms

This is an Open Access article under the terms of the Creative Commons Attribution License (http://creativecommons.org/licenses/by/2.0), which permits unrestricted use, distribution, and reproduction in any medium, provided the original work is properly cited.

The license is subject to the *Beilstein Journal of Organic Chemistry* terms and conditions: (http://www.beilstein-journals.org/bjoc)

The definitive version of this article is the electronic one which can be found at: doi:10.3762/bjoc.12.135

BEILSTEIN JOURNAL OF ORGANIC CHEMISTRY

Stereodynamic tetrahydrobiisoindole “NU-BIPHEP(O)”s: functionalization, rotational barriers and non-covalent interactions

Golo Storch, Sebastian Pallmann, Frank Rominger and Oliver Trapp*

Full Research Paper

Open Access

Address:
Organisch-Chemisches Institut, Ruprecht-Karls Universität Heidelberg, Im Neuenheimer Feld 270, 69120 Heidelberg, Germany

Email:
Oliver Trapp* - trapp@oci.uni-heidelberg.de

* Corresponding author

Keywords:
atropisomer; enantioselective DHPLC; ligand design; non-covalent interactions; Okamoto phases; phosphine ligand; stereodynamic ligands

Beilstein J. Org. Chem. **2016,** *12,* 1453–1458.
doi:10.3762/bjoc.12.141

Received: 08 April 2016
Accepted: 28 June 2016
Published: 14 July 2016

This article is part of the Thematic Series "Organometallic chemistry".

Guest Editor: B. F. Straub

© 2016 Storch et al.; licensee Beilstein-Institut.
License and terms: see end of document.

Abstract

Stereodynamic ligands offer intriguing possibilities in enantioselective catalysis. “NU-BIPHEPs” are a class of stereodynamic diphosphine ligands which are easily accessible via rhodium-catalyzed double [2 + 2 + 2] cycloadditions. This study explores the preparation of differently functionalized “NU-BIPHEP(O)” compounds, the characterization of non-covalent adduct formation and the quantification of enantiomerization barriers. In order to explore the possibilities of functionalization, we studied modifications of the ligand backbone, e.g., with 3,5-dichlorobenzoyl chloride. Diastereomeric adducts with Okamoto-type cellulose derivatives and on-column deracemization were realized on the basis of non-covalent interactions. Enantioselective dynamic HPLC (DHPLC) allowed for the determination of rotational barriers of $\Delta G^{\ddagger}_{298K}$ = 92.2 ± 0.3 kJ mol^{-1} and 99.5 ± 0.1 kJ mol^{-1} underlining the stereodynamic properties of “NU-BIPHEPs” and “NU-BIPHEP(O)s”, respectively. These results make the preparation of tailor-made functionalized stereodynamic ligands possible and give an outline for possible applications in enantioselective catalysis.

Introduction

Axially chiral biaryl compounds such as BINAP (2,2’-bis(diphenylphosphino)-1,1’-binaphthyl) represent widely used and highly efficient ligands that can be applied in a variety of enantioselective catalytic transformations. Unlike BINAP, the related stereodynamic BIPHEP (2,2’-bis(diphenylphosphino)-1,1’-biphenyl) ligands have a significantly lower barrier of rotation around the central C–C bond regarding the conversion of the enantiomers into one another. This enables fast enantiomerization at room temperature.

This, however, does not conflict with their usage in enantioselective catalysis. Noyori and Mikami reported the stereochemi-

cal alignment of BIPHEP ligands in ruthenium complexes upon addition of chiral diamine co-ligands [1,2]. The resulting complexes were successfully employed in enantioselective ketone hydrogenation. Further examples of such systems are BIPHEP complexes of rhodium [3-6], palladium [7,8], platinum [9,10] and gold [11-13] in combination with chiral co-ligands or counter ions that are used after alignment of the ligand's axial chirality.

One major advantage of stereodynamic ligands is that there is no need for separate preparation of one ligand enantiomer as long as their chirality can be controlled by chiral additives or auxiliaries. In addition, the simultaneous presence of both axially chiral BIPHEP enantiomers can be beneficial as this allows bidirectional control of enantioselectivity depending on temperature [14,15]. In this approach, both product enantiomers of an enantioselective transformation can be addressed selectively by fine tuning of the conditions prior to and during catalysis.

The rotational barrier around the central C–C bond of BIPHEP ligands is a key property of stereodynamic ligands that determines the temperature required for ligand enantiomerization as well as the half-life of isolated enantiomers. The latter are of particular importance if chiral co-ligands are cleaved off prior to catalysis and if the remaining stereochemically aligned BIPHEP complex fragment serves as the active species. Therefore, detailed knowledge of the interconversion barriers of stereodynamic ligands is crucial for the choice of conditions used for stereochemical alignment and subsequent application in catalysis. A rotational barrier of 92 kJ mol^{-1} for the unsubstituted BIPHEP was determined by NMR coalescence of a partially deuterated derivative [16]. However, this method does not fulfil the requirements for a reliable rapid screening of novel stereodynamic ligands due to harsh conditions such as isotope exchange. We recently reported the rotational barriers of 3,3' and 5,5' substituted BIPHEP and BIPHEP(O) compounds based on enantioselective DHPLC by evaluation of elution profiles using the unified equation [17-20]. Rotational barriers were found to be between $\Delta G^{\ddagger}_{298K}$ = 86.8 kJ mol^{-1} (unsubstituted BIPHEP) and $\Delta G^{\ddagger}_{298K}$ = 100.4 kJ mol^{-1}. BIPHEP(O) derivatives (unsubstituted BIPHEP(O): $\Delta G^{\ddagger}_{298K}$ = 88.6 kJ mol^{-1}) were observed to exhibit slightly increased (approximately 2 kJ mol^{-1}) barriers.

Functionalization of stereodynamic BIPHEP ligands at the biaryl core offers multiple possibilities. The introduction of achiral, non-covalent interaction sites allows for ee determination of chiral analytes via NMR spectroscopy [21] as well as deracemization of the BIPHEPs with HPLC stationary phases [22].

However, introduction of functional groups which enable a modular derivatization approach is often hampered by long and tedious synthetic procedures. Doherty et al. reported a rhodium catalyzed double [2 + 2 + 2] cycloaddition strategy for a convergent synthesis of "NU-BIPHEP"s [23].

In this paper, we describe the application of Doherty's synthetic strategy for the synthesis of stereodynamic tetrahydrobiisoindole "NU-BIPHEP(O)" compounds bearing secondary amino groups for functionalization. The attachment of a 3,5-dichlorobenzoyl binding site is reported and non-covalent interactions as well as rotational barriers are studied in solution by (D)HPLC techniques.

Results and Discussion

Synthesis of tetrahydrobiisoindole "NU-BIPHEP(O)s"

The rhodium catalyzed double [2 + 2 + 2] cycloaddition of 1,4-bis(diphenylphosphinoyl)buta-1,3-diyne and a variable diyne compound is the key step in the preparation of "NU-BIPHEPs" [23] and related biaryls [24]. Doherty et al. reported the use of various diynes yielding for instance tetrahydrobiindene **1a** and *N*-tosyl-protected tetrahydrobiisoindole **1b** as the only *N*-heterocyclic compound (Figure 1A).

Aiming at facile deprotection and enabling subsequent functionalization at the secondary amine position, we changed the strategy and used *N*-Boc dipropargylamine as the diyne compound (Figure 1A). The double cycloaddition product **1c** was obtained in 77% yield. In accordance with the report of Doherty et al., very slow addition of the diyne compound via syringe pump was crucial.

In contrast to **1a** and **1b**, three coexisting isomeric species were observed with NMR spectroscopy in $CDCl_3$ for tetrahydrobiisoindole "NU-BIPHEP(O)" **1c**. This behaviour originates from an increased interconversion barrier between the *E*/*Z* isomers of the carbamate N–C(O) unit that is derived from a secondary amine. Deprotection of **1c** proceeds smoothly with 5–6 M HCl in 2-propanol and the tetrahydrobiisoindole "NU-BIPHEP(O)" **2** can be isolated as hydrogen chloride salt in 93% yield (Figure 1B).

Tetrahydrobiisoindole "NU-BIPHEP(O)" **2** offers various possibilities for functionalization with chiral and achiral auxiliaries or binding sites. In this study, we chose amide bond formation with 3,5-dichlorobenzoyl chloride (Figure 2B) in connection with our recent report [21] on non-covalent interaction properties of stereodynamic BIPHEP ligands with this binding site that is well known in HPLC stationary phase design. The "NU-BIPHEP(O)" **3** was isolated in 49% yield and again three

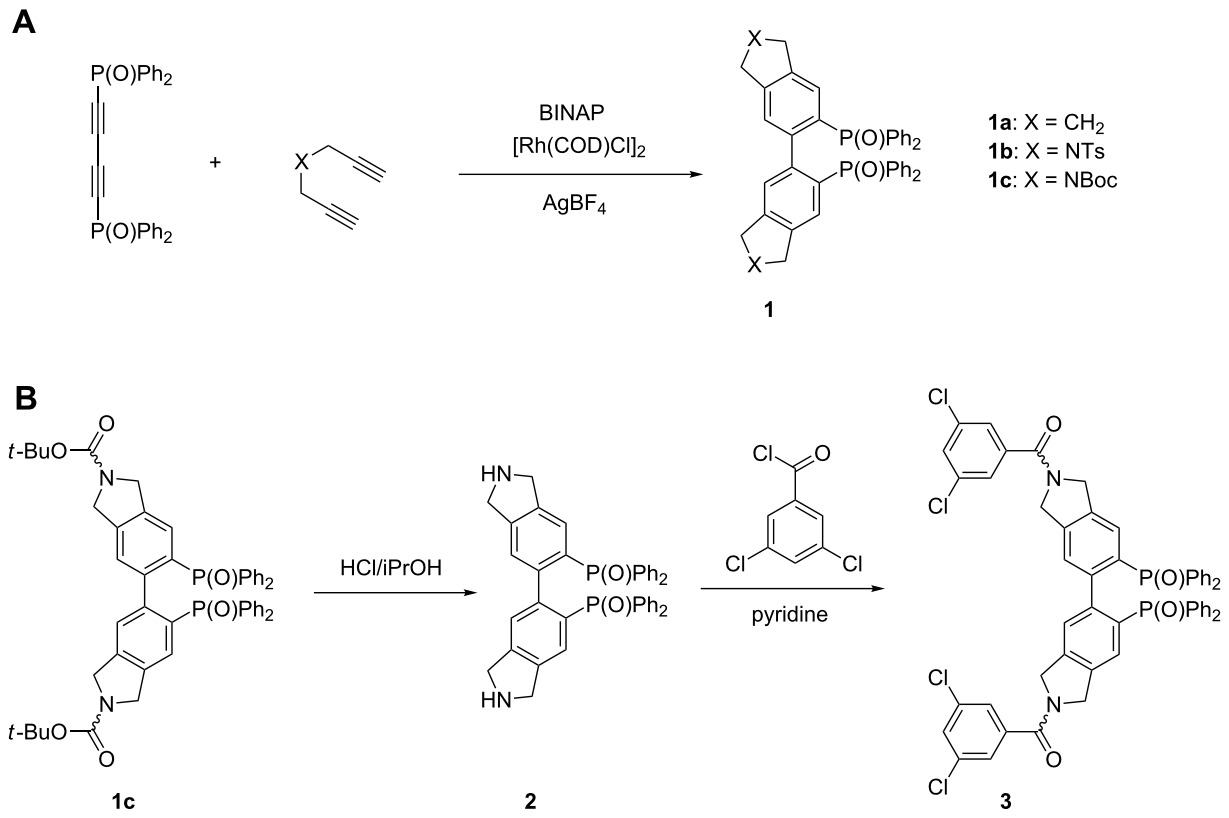


Figure 1: Synthetic overview of "NU-BIPHEP(O)s". A) Rhodium catalyzed double [2 + 2 + 2] cycloaddition. B) Acidic deprotection of tetrahydrobiisoindole "NU-BIPHEP(O)" **1c** and subsequent amide bond formation with 3,5-dichlorobenzoyl chloride.

isomeric species were observed by NMR spectroscopy in $CDCl_3$ due to hindered rotation of the tertiary amide bond (Figure 2A).

Intriguingly, only two peaks were observed upon investigation of **3** by enantioselective HPLC applying *n*-hexane/2-propanol as mobile phase and a normal phase Okamoto-type stationary phase (CHIRALPAK® IA-3). Opposing signals in HPLC–CD coupling corroborated the assumption that the peaks correspond to two axially chiral enantiomers (Figure 2B).

When left on the chiral stationary phase (*n*-hexane/2-propanol 50:50, CHIRALPAK® IA) for seven days in a stopped-flow experiment, partial deracemization of **3** was observed. The final enantiomeric ratio (absolute configurations were not determined) was observed to reach approximately 72:28.

Non-covalent interactions in solution

Non-covalent interactions are not only a key step in deracemization of stereodynamic compounds but they also allow ee determination in solution by NMR spectroscopy. However, the formation of diastereomeric adducts between chiral compounds and BIPHEP(O) [25] or BINAP(O) [26] has so far rarely been investigated. In a subsequent part of our study, we explored the non-covalent interactions of tetrahydrobiisoindole "NU-BIPHEP(O)s" in solution since they exhibit very strong interactions with Okamoto-type chiral stationary phases (CSPs) in HPLC.

Okamoto et al. reported the preparation of short CSP-analogue cellulose and amylose compounds with carbamate selector units that are soluble in organic solvents [27-30]. We prepared cellulose derivative **4** which bears 5-fluoro-2-methylphenylcarbamate binding sites [27] and investigated the formation of diastereomeric adducts with **1b** and **3** by $^{31}P\{^{1}H\}$ NMR spectroscopy in anhydrous $CDCl_3$. Significant signal splitting was observed for both "NU-BIPHEP(O)s" due to strong non-covalent interactions. However, detailed analysis of **3** was hampered due to overlaying multiple signal sets caused by *E*/*Z* isomerism of the tertiary amide unit.

Adding **4** to a solution of **1b** (Figure 3A, solid-state structure) in $CDCl_3$ resulted in significant signal splitting of $\Delta\delta = 0.30$ ppm ($^{31}P\{^{1}H\}$ NMR). This effect could be intensified by adding *n*-pentane which increased the splitting to $\Delta\delta = 0.41$ ppm although signal broadening rose simultaneously (Figure 3B).

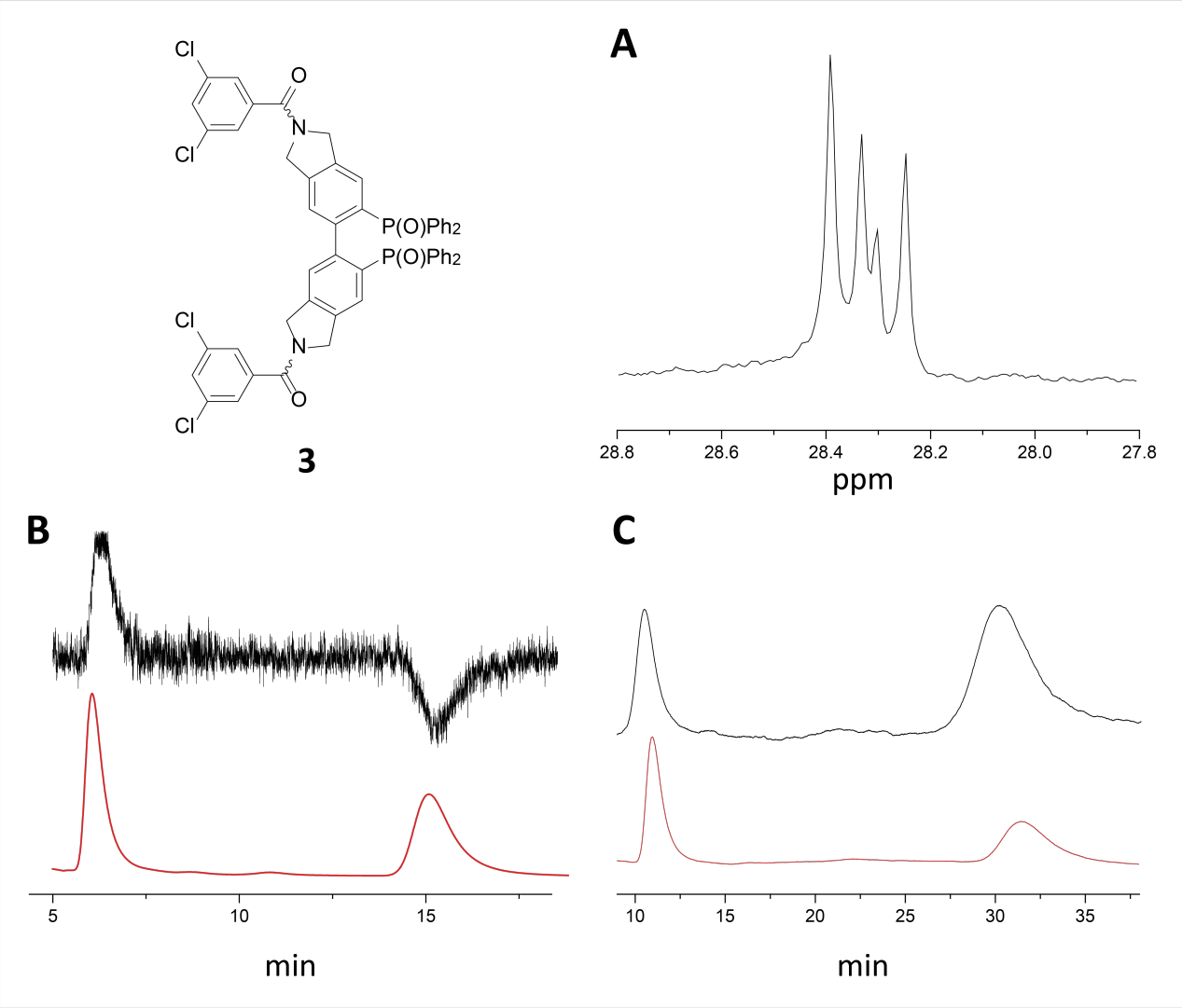


Figure 2: Investigation of 3,5-dichlorobenzoyl modified tetrahydrobiisoindole "NU-BIPHEP(O)" **3**. A) Three signal sets are observed in $^{31}P\{^{1}H\}$ NMR spectroscopy ($CDCl_3$). B) HPLC–CD chromatogram (*n*-hexane/2-propanol 50:50, CHIRALPAK® IA-3, 1 mL/min, 20 °C). Red: UV trace, black: CD trace. C) On-column deracemization of **3** (*n*-hexane/2-propanol 50:50, CHIRALPAK® IA). Chromatogram with (black) and without (red) the analyte after being kept on the stationary phase for seven days.

Determination of rotational barriers by enantioselective DHPLC

To the best of our knowledge the enantiomerization properties of "NU-BIPHEP(O)s" have not yet been studied. Therefore, we investigated the rotational barriers of **1a** and **3** by enantioselective DHPLC. Elution profiles of **3** were obtained in a temperature range between 50.0 °C and 80.0 °C (CHIRALPAK® IA-3, t_{ret} (50 °C) = 4.25 and 8.87 min, α = 2.42, Figure 4A). All rate constants and corresponding Gibbs free energies of activation were directly calculated using the unified equation and the Eyring equation. This elution profile evaluation was done using the DCXplorer software which can be obtained from the corresponding author upon request. A rotational barrier of $\Delta G^{\ddagger}_{298K}$ = 99.5 ± 0.1 kJ mol^{-1} was determined for the interconversion of **3**. This is a significant increase compared to unsubstituted BIPHEP(O) ($\Delta G^{\ddagger}_{298K}$ = 88.6 kJ mol^{-1}). Eyring plot analysis allowed the determination of the activation parameters $\Delta H^{\ddagger}$ = 96.3 ± 1.2 kJ mol^{-1} and $\Delta S^{\ddagger}$ = −10.9 ± 0.2 J (K mol)$^{-1}$ (Figure 4B). The increased rotational barrier of **3** can be rationalized according to additional interactions and steric repulsion of the large 3,5-dichlorobenzoyl amide binding sites. It has to be noted that the entropic contribution to the enantiomerization barrier is exceptionally low.

For comparison, we investigated tetrahydrobiindene "NU-BIPHEP(O)" **1a** in a similar way (see Supporting Information File 1 for details). The elution profiles were evaluated in a temperature range between 20.0 °C and 45.0 °C (CHIRALPAK® IE-3, t_{ret} (20 °C) = 14.2 and 26.6 min, α = 1.94). A rotational barrier of $\Delta G^{\ddagger}_{298K}$ = 92.2 ± 0.3 kJ mol^{-1} was determined and

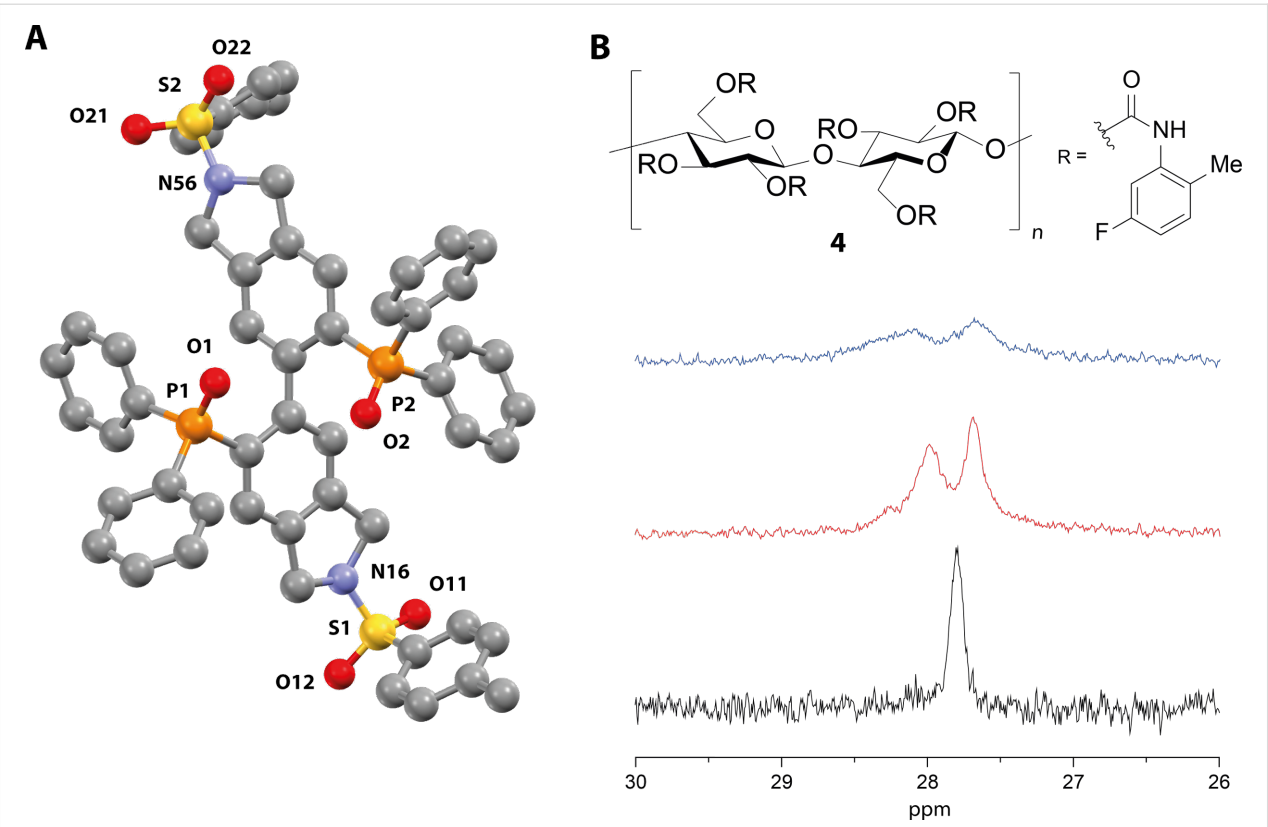


Figure 3: Investigation of "NU-BIPHEP(O)" **1b**. A) Solid-state structure determined by X-ray crystallography. Hydrogen atoms and methanol solvent molecules are omitted for clarity. B) Interaction studies in solution with soluble Okamoto phase **4** by $^{31}P\{^{1}H\}$ NMR spectroscopy. Black: spectrum of 4.7 mg (5 μmol) **1b** in 0.5 mL anhydrous $CDCl_3$ (filtered through basic alumina). Red: spectrum after addition of 20 mg **4**. Blue: spectrum after addition of 0.1 mL anhydrous *n*-pentane. All NMR samples were completely dissolved.

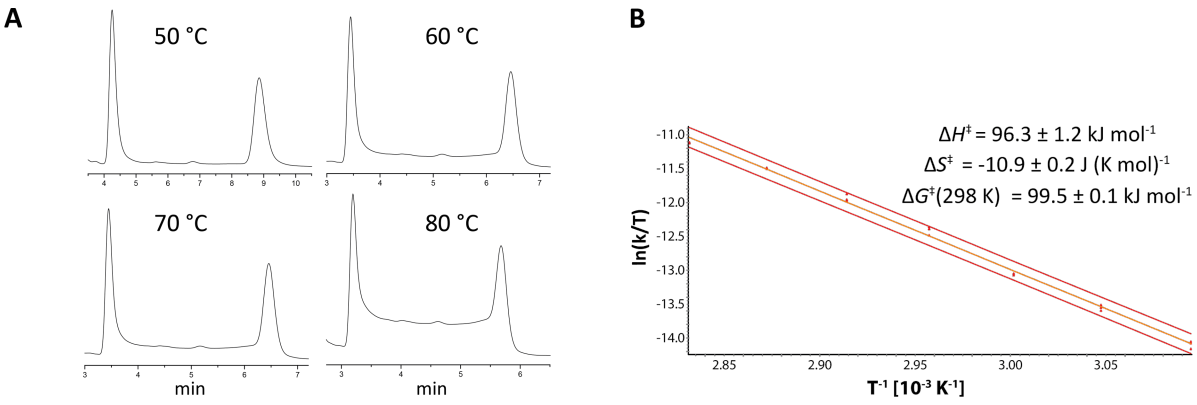


Figure 4: Enantioselective DHPLC investigation of tetrahydrobiisoindole "NU-BIPHEP(O)" **3**. A) Elution profiles at various temperatures with increasing plateau formation. B) Eyring plot analysis for the determination of the activation parameters $\Delta H^{‡}$ and $\Delta S^{‡}$.

subsequent Eyring plot analysis gave the activation parameters $\Delta H^{‡}$ = 68.4 ± 1.9 kJ mol^{-1} and $\Delta S^{‡}$ = −79.9 ± 4.5 J (K mol)$^{-1}$. Interestingly, the activation parameters of **1a** are similar to those reported for 5,5'-dimethoxy BIPHEP(O) ($\Delta G^{‡}_{298K}$ = 93.0 kJ mol^{-1}) [20] which is in accordance with a barrier increase caused by small substituents in the 5,5' positions.

Conclusion

We report a strategy to use unprotected tetrahydrobiisoindole "NU-BIPHEP(O)" for functionalization with substituents at the secondary amine position, in this study namely by formation of tertiary amide binding sites with 3,5-dichlorobenzoyl chloride. Non-covalent interactions of "NU-BIPHEP(O)s" with

Okamoto-type cellulose derivatives resulted in the formation of diastereomeric adducts which led to significant NMR signal splitting in solution and additionally enabled successful on-column deracemization. Furthermore, interconversion barriers of $\Delta G^{\ddagger}_{298K}$ = 92.2 ± 0.3 kJ mol^{-1} and $\Delta G^{\ddagger}_{298K}$ = 99.5 ± 0.1 kJ mol^{-1} were determined by evaluation of enantioselective DHPLC elution profiles quantifying the stereodynamic properties of "NU-BIPHEP(O)" compounds. These results help understanding the influence of substitution patterns on the enantiomerization barrier of BIPHEP ligands and open up new possibilities towards designing tailor-made stereodynamic compounds used as smart ligands in enantioselective catalysis.

Supporting Information

Supporting Information File 1

Experimental procedures, data for the determination of rotational barriers and copies of NMR spectra.
[http://www.beilstein-journals.org/bjoc/content/supplementary/1860-5397-12-141-S1.pdf]

Acknowledgements

Generous financial support by the European Research Council (ERC) for a Starting Grant (No. 258740, AMPCAT) is gratefully acknowledged. G.S. acknowledges the Fonds der Chemischen Industrie for a Ph.D. fellowship.

References

1. Mikami, K.; Korenaga, T.; Terada, M.; Ohkuma, T.; Pham, T.; Noyori, R. *Angew. Chem., Int. Ed.* **1999,** *38,* 495. doi:10.1002/(SICI)1521-3773(19990215)38:4<495::AID-ANIE495>3.0.CO;2-O
2. Mikami, K.; Aikawa, K.; Korenaga, T. *Org. Lett.* **2001,** *3,* 243. doi:10.1021/ol0068896
3. Mikami, K.; Kataoka, S.; Yusa, Y.; Aikawa, K. *Org. Lett.* **2004,** *6,* 3699. doi:10.1021/ol048604l
4. Mikami, K.; Kataoka, S.; Wakabayashi, K.; Aikawa, K. *Tetrahedron Lett.* **2006,** *47,* 6361. doi:10.1016/j.tetlet.2006.06.179
5. Aikawa, K.; Takabayashi, Y.; Kawauchi, S.; Mikami, K. *Chem. Commun.* **2008,** 5095. doi:10.1039/b809683j
6. Punniyamurthy, T.; Mayr, M.; Dorofeev, A. S.; Bataille, C. J. R.; Gosiewska, S.; Nguyen, B.; Cowley, A. R.; Brown, J. M. *Chem. Commun.* **2008,** 5092. doi:10.1039/b807669c
7. Mikami, K.; Aikawa, K.; Yusa, Y. *Org. Lett.* **2002,** *4,* 95. doi:10.1021/ol0169675
8. Mikami, K.; Aikawa, K.; Yusa, Y.; Hatano, M. *Org. Lett.* **2002,** *4,* 91. doi:10.1021/ol016969p
9. Becker, J. J.; White, P. S.; Gagné, M. R. *J. Am. Chem. Soc.* **2001,** *123,* 9478. doi:10.1021/ja016167p
10. Mikami, K.; Kakuno, H.; Aikawa, K. *Angew. Chem., Int. Ed.* **2005,** *44,* 7257. doi:10.1002/anie.200502682
11. Aikawa, K.; Kojima, M.; Mikami, K. *Angew. Chem., Int. Ed.* **2009,** *48,* 6073. doi:10.1002/anie.200902084
12. Kojima, M.; Mikami, K. *Chem. – Eur. J.* **2011,** *17,* 13950. doi:10.1002/chem.201103023
13. Kojima, M.; Mikami, K. *Synlett* **2012,** 57. doi:10.1055/s-0031-1289875
14. Storch, G.; Trapp, O. *Angew. Chem., Int. Ed.* **2015,** *54,* 3580. doi:10.1002/anie.201412098
15. Oczipka, P.; Müller, D.; Leitner, W.; Franció, G. *Chem. Sci.* **2016,** *7,* 678. doi:10.1039/C5SC03465E
16. Desponds, O.; Schlosser, M. *Tetrahedron Lett.* **1996,** *37,* 47. doi:10.1016/0040-4039(95)02080-2
17. Trapp, O. *J. Chromatogr., B* **2008,** *875,* 42. doi:10.1016/j.jchromb.2008.07.047
18. Trapp, O. *Anal. Chem.* **2006,** *78,* 189. doi:10.1021/ac051655r
19. Maier, F.; Trapp, O. *Angew. Chem., Int. Ed.* **2012,** *51,* 2985. doi:10.1002/anie.201107907
20. Maier, F.; Trapp, O. *Chirality* **2012,** *25,* 126. doi:10.1002/chir.22125
21. Storch, G.; Siebert, M.; Rominger, F.; Trapp, O. *Chem. Commun.* **2015,** *51,* 15665. doi:10.1039/C5CC06306J
22. Maier, F.; Trapp, O. *Angew. Chem., Int. Ed.* **2014,** *53,* 8756. doi:10.1002/anie.201402293
23. Doherty, S.; Knight, J. G.; Smyth, C. H.; Harrington, R. W.; Clegg, W. *Org. Lett.* **2007,** *9,* 4925. doi:10.1021/ol702390p
24. Mori, F.; Fukawa, N.; Noguchi, K.; Tanaka, K. *Org. Lett.* **2010,** *13,* 362. doi:10.1021/ol102927y
25. Demchuk, O. M.; Świerczynska, W.; Michał Pietrusiewicz, K.; Woźnica, M.; Wójcik, D.; Frelek, J. *Tetrahedron: Asymmetry* **2008,** *19,* 2339. doi:10.1016/j.tetasy.2008.10.001
26. Hatano, B.; Hashimoto, K.; Katagiri, H.; Kijima, T.; Murakami, S.; Matsuba, S.; Kusakari, M. *J. Org. Chem.* **2012,** *77,* 3595. doi:10.1021/jo202630p
27. Yashima, E.; Yamamoto, C.; Okamoto, Y. *J. Am. Chem. Soc.* **1996,** *118,* 4036. doi:10.1021/ja960050x
28. Yamamoto, C.; Yashima, E.; Okamoto, Y. *J. Am. Chem. Soc.* **2002,** *124,* 12583. doi:10.1021/ja020828g
29. Ye, Y. K.; Bai, S.; Vyas, S.; Wirth, M. J. *J. Phys. Chem. B* **2007,** *111,* 1189. doi:10.1021/jp0637173
30. Ikai, T.; Okamoto, Y. *Chem. Rev.* **2009,** *109,* 6077. doi:10.1021/cr8005558

License and Terms

This is an Open Access article under the terms of the Creative Commons Attribution License (http://creativecommons.org/licenses/by/2.0), which permits unrestricted use, distribution, and reproduction in any medium, provided the original work is properly cited.

The license is subject to the *Beilstein Journal of Organic Chemistry* terms and conditions: (http://www.beilstein-journals.org/bjoc)

The definitive version of this article is the electronic one which can be found at:
doi:10.3762/bjoc.12.141

BEILSTEIN JOURNAL OF ORGANIC CHEMISTRY

Methylpalladium complexes with pyrimidine-functionalized N-heterocyclic carbene ligands

Dirk Meyer and Thomas Strassner*§

Full Research Paper

Open Access

Address:
Physikalische Organische Chemie, TU Dresden, Bergstraße 66, 01062 Dresden, Germany

Email:
Thomas Strassner* - thomas.strassner@chemie.tu-dresden.de

* Corresponding author
§ Tel.: +49 351 4633 8571; Fax: +49 351 4633 9679

Keywords:
alkane activation; alkyl complex; NHC; palladium; solid state structure

Beilstein J. Org. Chem. **2016,** *12,* 1557–1565.
doi:10.3762/bjoc.12.150

Received: 27 April 2016
Accepted: 29 June 2016
Published: 21 July 2016

This article is part of the Thematic Series "Organometallic chemistry".

Guest Editor: B. F. Straub

© 2016 Meyer and Strassner; licensee Beilstein-Institut.
License and terms: see end of document.

Abstract

A series of methylpalladium(II) complexes with pyrimidine-NHC ligands carrying different aryl- and alkyl substituents R ([((pym)^(NHC-R))$Pd^{II}(CH_3)X$] with X = Cl, CF_3COO, CH_3) has been prepared by transmetalation reactions from the corresponding silver complexes and chloro(methyl)(cyclooctadiene)palladium(II). The dimethyl(1-(2-pyrimidyl)-3-(2,6-diisopropylphenyl)imidazolin-2-ylidene)palladium(II) complex was synthesized via the free carbene route. All complexes were fully characterized by standard methods and in three cases also by a solid state structure.

Introduction

Palladium complexes have been shown to be versatile homogeneous catalysts in a variety of reactions [1]. One of the most prominent examples are the palladium catalyzed cross-coupling reactions [2], but in addition palladium complexes recently received much attention also in the field of selective CH oxidations [3-6]. The catalytic conversion of alkanes and especially of methane into a value-added products while avoiding over-oxidation to carbon dioxide is still one of the most difficult tasks and considered to be one of the "Holy Grails" of chemistry [7]. Early work by Bergman [8,9] and Graham [10,11] showed that the activation of methane is possible, but their systems provided only stoichiometric reactions. The Shilov system [12-17], had the disadvantage of using stoichiometric amounts of platinum for the reoxidation of the active catalyst and the platinum bispyrimidine system [18-20] was not successful because of the large amounts of diluted sulfuric acids as the byproduct of the methanol synthesis. Sen reported the activity of palladium(II) catalysts for the oxidation of methane [21] and several groups contributed to the progress in the field which is summarized in recent reviews [22,23]. The system based on N-heterocyclic carbene (NHC) ligands developed in our group uses a mixture of trifluoroacetic acid (TFA) and its anhydride (TFAA) as solvents. It has the advantage that the formed ester can be separated and hydrolyzed, followed by recycling of the free acid which potentially can be reused in the process [24-30]. Contrary to the "Catalytica" bispyrimidine system, for the

biscarbene system the palladium complexes turned out to be more stable than the corresponding platinum complexes under the reaction conditions [31,32], although Peter Hofmann had recently shown the stability and reactivity of the platinum-alkyl complexes with bis-NHC ligand [33]. To study the differences between both systems we synthesized palladium [34] and platinum [35] "hybrid complexes" with ligands combining both structural elements the pyrimidine as well as the NHC fragment. We also used density functional theory (DFT) calculations to investigate the mechanism and potential intermediates.

Quantum chemical (QC) investigations have been very helpful during the last years in elucidating the mechanisms of palladium-catalyzed reactions [26,36]. According to our QC calculations the catalytic cycle for the alkane activation by bis(NHC) palladium complexes like the bis(1,1'-dimethyl-3,3'-methylenediimidazoline-2,2'-diylidene)palladium(II) dibromide [L_2PdBr_2] consists of three steps: electrophilic substitution, oxidation and reductive elimination involving a palladium(IV) intermediate [26]. But we also experimentally set out to investigate potential intermediates of the catalytic cycle [37]. One of the proposed intermediates in the catalytic cycle is a monomethyl complex which is formed from the starting material after methane activation and which could either carry a bromo [$L_2PdBr(CH_3)$] or a trifluoroacetato [$L_2Pd(CF_3COO)(CH_3)$] ligand. These intermediates should be active according to the proposed catalytic cycle, which starts with an electrophilic substitution reaction. We therefore set out to synthesize the corresponding methyl complexes for the "hybrid ligand" with chloro- and trifluoroacetato ligands.

Results and Discussion

Synthesis

Some time ago we reported the synthesis of the imidazolium salts **1**–**4** and their corresponding silver complexes **5**–**8**. The reaction with dichloro(cyclooctadiene)-palladium(II) [(COD)$Pd^{II}Cl_2$] allowed for the isolation and characterization of the [((pym)^(NHC-R))$Pd^{II}Cl_2$]-complexes [34]. For the synthesis of the corresponding monomethyl complexes we could rely on earlier work by Byers and Canty which reported the synthesis of methyl- and dimethylpalladium(II) complexes with various nitrogen donor systems [38]. The palladium complexes [(pym)^(NHC-R)$Pd^{II}(CH_3)Cl$] **9**–**12** have been synthesized in good yields from the corresponding silver complexes **5**–**8** by transmetalation with chloro(methyl)(cyclooctadiene)palladium(II) [(COD)$Pd^{II}(CH_3)Cl$] either in dichloromethane (A) or acetonitrile (B, Scheme 1).

Although two isomers could be formed we only observed the isomer **B**, where the methyl group is located *cis* to the carbene carbon atom (Figure 1). This can be explained by the strong donor character of the carbene which makes the *trans* isomer less favorable. NMR analysis of the reaction products confirms that only one complex is formed. Additional proof comes from density functional theory (DFT) calculations which predict isomer **B** to be more stable for all complexes **9**–**12**. At the B3LYP/6-311+G** level of theory the isomer with the methyl group coordinated *cis* to the carbene carbon atom the **B** isomers are thermodynamically favored by 5–11 kcal/mol (Table 1).

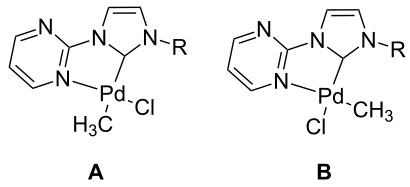
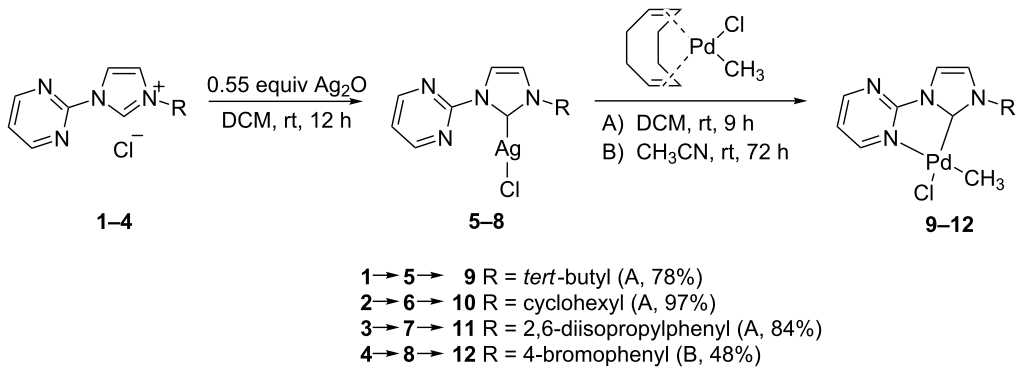


Figure 1: Possible isomers.

For complexes **9** and **12** (Figure 2 and Figure 3) we were able to obtain solid state structures, which show the predicted geometry and confirm that the **B** isomers are formed.



Scheme 1: Synthesis of the monomethylpalladium(II) complexes **9**–**11** (in DCM) and **12** (in CH_3CN).

Table 1: Calculated free energy differences (Δ*G* in kcal/mol) between the *trans*- (**A**) and *cis*- (**B**) isomers (B3LYP/6-311+*G*(d,p)).

Complex	Substituent R	Δ*G*
9	*tert*-butyl	4.7
10	cyclohexyl	7.3
11	diisopropylphenyl	10.7
12	4-bromophenyl	10.0

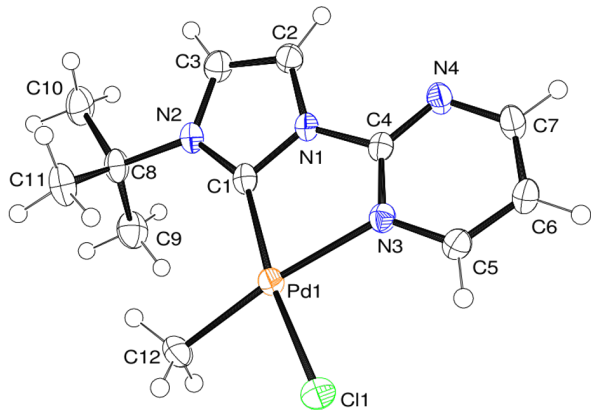


Figure 2: ORTEP [39] style plot of complex **9** in the solid state. Thermal ellipsoids are given at the 50% probability level. Selected bond lengths in angstrom and angles in degrees: Pd–C1 2.031(4), Pd–N3 2.137(2), Pd–C12 2.030(2), Pd–Cl1 2.342(1), C1–Pd–N3 80.1(1), C1–N1–C4–N3 −9.7(3).

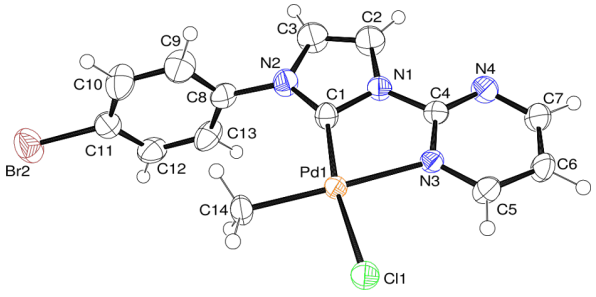
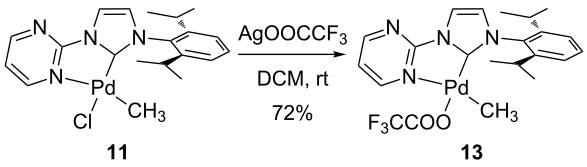


Figure 3: ORTEP [39] style plot of complex **12** in the solid state. Thermal ellipsoids are drawn at the 50% probability level. Selected bond lengths in angstrom and angles in degrees: Pd–C1 1.966(4), Pd–N3 2.145(3), Pd–C14 2.035(3), Pd–Cl1 2.341(1), C1–Pd–N3 79.0(1), C1–N1–C4–N3 −5.9(5).

It is interesting to note that the two structures show very similar bond lengths and angles with the exception of the palladium–carbene bond lengths (**9**: 2.03 Å; **12**: 1.97 Å), which might be an indication of the different donor character. The experimentally determined geometrical parameters are in good agreement with the computed results.

Interestingly, complexes **9**, **10** and **12** show only one discrete doublet for the *m*-pyrimidine proton signals in the ^{1}H NMR spectrum in DMSO-d_6 indicating that the pyrimidine ring might rotate at room temperature and therefore a weak coordination of the pyrimidine nitrogen atom to the palladium center. The broader signal in case of complex **11** indicates a stronger coordination of the nitrogen and a hindered rotation of the pyrimidine ring. Within some hours, complexes **9** and **12** decompose in DMSO-d_6 by reductive *cis*-elimination [40] leading to imidazolium salts with the methyl group on the former carbene carbon atom and palladium black. The weaker coordination is most probably caused by the stronger *trans* effect of the methyl group. The decomposition is significantly slower in $CDCl_3$, where two different signals for the *m*-pyrimidine protons are observed.

We recently reported that the dihalogenato complexes are active catalysts of the methane CH activation in trifluoroacetic acid [34]. Under the reaction conditions it seems likely, that an exchange of the chloro against a trifluoroacetato ligands occurs [29], which is present in the solution in large excess. This potential intermediate of the catalytic cycle, the [(pym)^(NHC-R)Pd^{II}(CH_3)(CF_3COO)]-complex **13** (with R = 2,6-diisopropylphenyl), could be synthesized by the reaction of complex **11** with silver trifluoroacetate (Scheme 2). We could also confirm the formation of the desired product by a solid state structure (Figure 4).



Scheme 2: Synthesis of complex **13**.

Typical reaction conditions of the catalytic CH activation are 30 atmospheres of methane under strongly oxidizing conditions (potassium peroxodisulfate, trifluoroacetic acid and its anhydride), where methane is converted into methyl trifluoroacetate catalyzed by a Pd(II) complex. To examine if a methylated Pd(II) complex like **13** can be an intermediate of this reaction, potassium peroxodisulfate and sodium trifluoroacetate were added to a solution of **13** in DMSO-d_6 or $CDCl_3$. Analyzing the solution we could confirm the formation of methyl trifluoroacetate and a 'methyl free' Pd(II) complex. This complex showed similar NMR spectra like the bistrifluoroacetate complex **14** (Scheme 3), which was prepared by the reaction of the corresponding dichloro complex [34] with silver trifluoroacetate for comparison (see experimental details). The

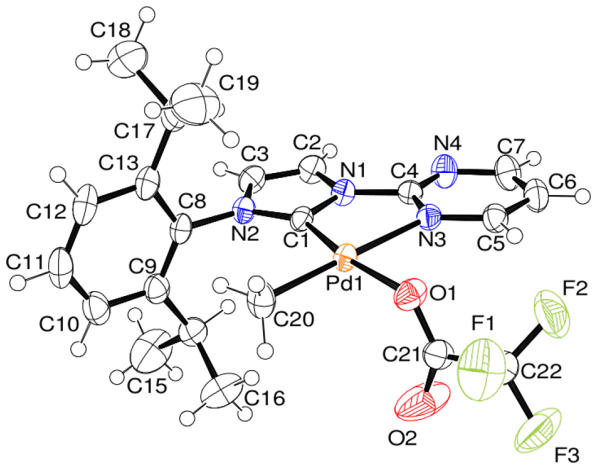
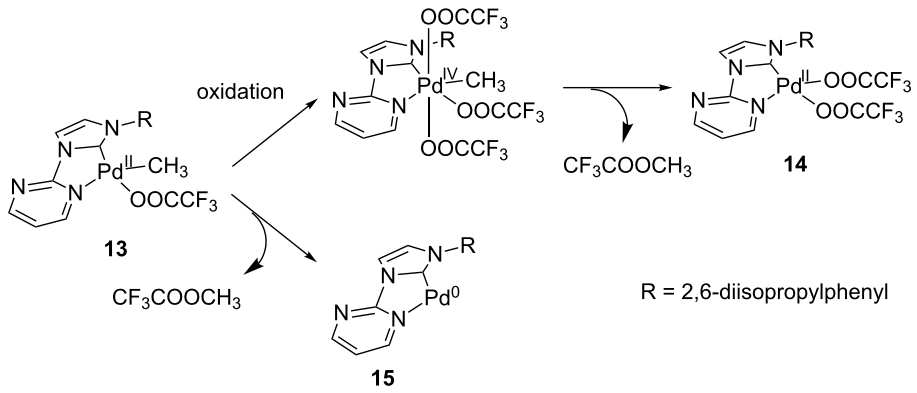


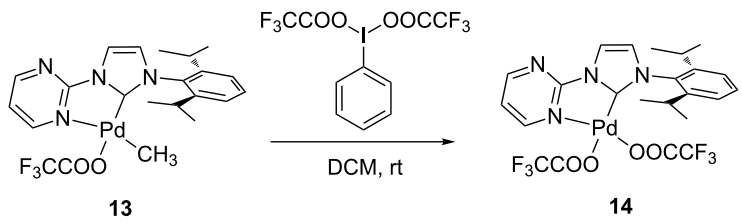
Figure 4: ORTEP [39] style plot of complex **13** in the solid state. Thermal ellipsoids are drawn at the 50% probability level. Selected bond lengths in angstrom and angles in degrees: Pd–C1 1.956(2), Pd–N3 2.151(2), Pd–C20 2.015(2), Pd–O1 2.098(2), C1–Pd–N3 79.6(1), C1–N1–C4–N3 −3.3(3).

result indicates that an oxidation/reductive elimination cycle took place (Scheme 3, upper pathway). The direct reductive elimination of methyl trifluoroacetate from complex **13** by heating complex **13** in DMSO-d_6 up to 90 °C in the presence of sodium trifluoroacetate [30,34], yielding complex **15**, could not be observed (Scheme 3). This indicates that a P(II)/Pd(0)-mechanism is unfavorable. A more representative simulation of the reaction conditions of the catalytic methane activation by using trifluoroacetic acid as solvent was not possible as the protonation and dissociation of the methyl group occurs very quickly and quantitatively. The results obtained are in agreement with the computational results [41] that for this ligand system a Pd(II)/Pd(IV)-mechanism might be more favorable than a Pd(II)/Pd(0)-pathway for the formation of methyl trifluoroacetate from methylpalladium(II) complexes like **13** (Scheme 3).

It has previously been shown that the oxidation of palladium(II) complexes is feasible [42]. Several papers reported the successful oxidation of Pd(II) complexes by hypervalent iodo reagents [43-48]. Sanford, Arnold and co-workers could also show, that the Pd(IV)(NHC) complexes prepared by this reaction tend to reductively eliminate at temperatures around −35 °C [49]. As we also consider a Pd(IV) intermediate, the corresponding complex [(pym)^(NHC-R)Pd$^{(IV)}$(CH_3)(CF_3COO)$_3$] was synthesized by reaction of **13** with iodobenzene bistrifluoroacetate at room temperature. We observed the formation of complex **14** as the only product (Scheme 4), while at a temperature of −78 °C no reaction was observed and complex **13** was reisolated from the reaction mixture.



Scheme 3: Possible pathways of methyl trifluoroacetate formation starting from complex **13**.



Scheme 4: Synthesis of complex **14** by conversion of complex **13** with iodobenzene bistrifluoroacetate.

We followed the reaction by NMR by mixing the reagents at −78 °C while measuring the ^{1}H NMR spectra at −10 °C. After 5 minutes we observed a 1:1 mixture of complexes **13** and **14**. When the mixture warmed up to room temperature, the formation of complex **14** and methyl trifluoroacetate was detected. We believe that the reaction mechanism is similar to what was observed before by Sanford, Arnold and co-workers [49].

After we could successfully synthesize all the monomethyl complexes we were curious whether also the corresponding dimethyl complex is accessible. For this synthesis we decided to use the reaction of the free carbene with dimethyl(*N,N,N′,N′*-tetramethyl-1,2-diaminoethylene)palladium(II), [(tmeda)Pd(CH_3)$_2$], an approach which is frequently used to synthesize dimethyl Pd complexes [50-53]. Deprotonation of the imidazolium salt **3** and subsequent conversion of the free carbene with [(tmeda)Pd(CH_3)$_2$] gave the desired dimethylpalladium(II) complex **15** (Scheme 5) in 47% yield.

Conclusion

Methylpalladium(II) complexes are discussed as possible intermediates of the methane activation reaction. Herein, we present the synthesis of the potential intermediates ([((pym)^(NHC-R))Pd^{II}(CH_3)Cl] **9**–**12** with different substituents R (*t*-Bu, Cy, DIPP, 4-bromophenyl) of the corresponding catalytically active palladium dichloro complexes [(pym)^(NHC)Pd^{II}(Cl)$_2$] [34]. As the methane activation is carried out in a mixture of trifluoroacetic acid and its anhydride, another potential intermediate could be the [((pym)^(NHC-DIPP))Pd^{II}(CH_3)(CF_3COO)] complex **13**. Formation of methyl trifluoroacetate and the bistrifluoroacetate complex **14** from this complex under oxidizing reaction conditions points to a Pd(II)/Pd(IV)-mechanism for the reductive elimination of the observed product methyl trifluoroacetate. The dimethyl complex [((pym)^(NHC-DIPP))Pd^{II}(CH_3)$_2$] **15** could be synthesized to demonstrate the accessibility of these complexes as well.

Experimental

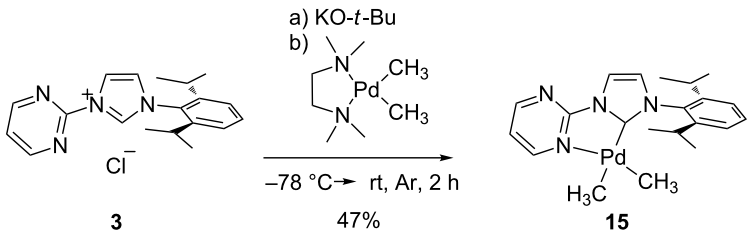
^{1}H and ^{13}C NMR spectra were obtained on a Bruker AC 300 P (^{1}H: 300.1 MHz, ^{13}C: 75.5 MHz, ^{19}F: 282.4 MHz) or a Bruker DRX 500 (^{1}H: 500.1 MHz, ^{13}C: 125.8 MHz, ^{19}F: 470.3 MHz) spectrometer at 298 K. Elemental analyses were performed by the microanalytical laboratory of our institute using an EuroVektor Euro EA-300 Elemental Analyzer. Chemicals were supplied by Acros, Fluka and Aldrich and used as received; solvents were dried by standard procedures before use. Imidazolium salts **1**–**4** [34], silver complexes **5**–**8** [27], chloro(methyl)(cyclooctadiene)palladium(II) [54] and dimethyl(*N,N,N′,N′*-tetramethyl-1,2-ethylendiamine)palladium(II) [38] were prepared according to literature procedures.

Chloro(methyl)(1-(2-pyrimidyl)-3-(*tert*-butyl)imidazolin-2-ylidene)palladium(II) (**9**)

0.20 g (0.6 mmol) of the silver complex **5** and 0.16 g (0.6 mmol) chloro(methyl)(cyclooctadiene)palladium(II) are dissolved in 30 mL dichloromethane. Under exclusion of light in an argon atmosphere the reaction mixture is stirred for 9 h at room temperature. The resulting suspension is filtrated over a celite pad and concentrated in vacuo. The product is precipitated by the addition of diethyl ether, filtrated, washed with diethyl ether and dried in vacuo. The product is obtained as a yellow solid (0.16 g, 78%). Mp 165 °C (dec); ^{1}H NMR ($CDCl_3$, 300 MHz, ppm) δ 1.27 (s, 3H, Pd-CH_3), 1.81 (s, 9H, CH_3 *t*-Bu), 7.26 (d, *J* = 2.2 Hz, 1H, NC*H*), 7.43 (t, *J* = 5.1 Hz, 1H, *p*-*H* pym), 7.91 (d, *J* = 2.2 Hz, 1H, NC*H*), 9.21 (bs, 2H, *m*-*H* pym); ^{13}C NMR (DMSO-d_6, 75.5 MHz, ppm) δ −1.5 (Pd-*C*H_3), 31.2 (*C*H_3), 59.9 (*ipso*-*C* *t*-Bu), 116.0 (*p*-*C*H pym), 120.1 (N*C*H), 120.9 (N*C*H), 156.4 (*ipso*-*C* pym), 159.4 (*m*-*C*H pym), 170.0 (carbene-*C*); anal. calcd for $C_{12}H_{17}ClN_4Pd{\cdot}0.2CH_2Cl_2$: C, 39.34%; H, 4.63%; N, 14.80%; found: C, 39.68%; H, 4.46%; N, 15.32%.

Chloro(methyl)(1-(2-pyrimidyl)-3-(cyclohexyl)imidazolin-2-ylidene)palladium(II) (**10**)

0.10 g (0.3 mmol) of the silver complex **6** and 0.08 g (0.3 mmol) chloro(methyl)(cyclooctadiene)palladium(II) are dissolved in 30 mL dichloromethane. Under exclusion of light in an argon atmosphere the reaction mixture is stirred for 9 h at room temperature. The resulting suspension is filtrated over a celite pad and concentrated in vacuo. The product is precipitated by the addition of diethyl ether, filtrated, washed with diethyl



Scheme 5: Synthesis of the [((pym)^(NHC-R))Pd^{II}(CH_3)$_2$] complex **15**.

ether and dried in vacuo. The product is obtained as a yellow solid (0.10 g, 97%). Mp 167 °C (dec); ^{1}H NMR (DMSO-d_6, 300 MHz, ppm) δ 0.87 (s, 3H, Pd-CH_3), 1.23–1.96 (2m, 10H, cyc), 4.45 (m, 1H, NC*H* cyc), 7.70 (t, *J* = 5.1 Hz, 1H, *p*-*H* pym), 7.80 (d, *J* = 2.3 Hz, 1H, NC*H*), 8.16 (d, *J* = 2.3 Hz, 1H, NC*H*), 9.07 (d, 5.1 Hz, 2H, *m*-*H* pym); ^{13}C NMR (DMSO-d_6, 75.5 MHz, ppm) δ −11.6 (Pd-*C*H$_3$), 24.4 (*p*-*C*H$_2$ cyc), 25.0 (*m*-*C*H$_2$ cyc), 32.5 (*o*-*C*H$_2$ cyc), 57.7 (N*C*H cyc), 117.2 (*p*-*C*H pym), 120.2 (N*C*H), 120.7 (N*C*H), 155.4 (*ipso*-*C* pym), 158.4 (*m*-*C*H pym), 159.6 (*m*-*C*H pym), 167.3 (carbene-*C*); anal. calcd for $C_{14}H_{19}ClN_4Pd{\cdot}0.1AgCl$: C, 42.09%; H, 4.79%; N, 14.02%; found: C, 42.27%; H, 4.71%; N, 13.70%.

Chloro(methyl)(1-(2-pyrimidyl)-3-(2,6-diisopropylphenyl)imidazolin-2-ylidene)palladium(II) (**11**)

0.04 g (0.1 mmol) of the silver complex **7** and 0.03 g (0.1 mmol) chloro(methyl)(cyclooctadiene)palladium(II) are dissolved in 30 mL dichloromethane. Under exclusion of light in an argon atmosphere the reaction mixture is stirred for 9 h at room temperature. The resulting suspension is filtrated over a celite pad and concentrated in vacuo. The product is precipitated by the addition of diethyl ether, filtrated, washed with diethyl ether and dried in vacuo. The product is obtained as a white solid (0.04 g, 84%). Mp 158 °C (dec); ^{1}H NMR (DMSO-d_6, 300 MHz, ppm) δ 0.04 (s, 3H, Pd-CH_3), 1.12 (d, *J* = 6.8 Hz, 6H, CH_3), 1.22 (d, *J* = 6.8 Hz, 6H, CH_3), 2.59 (m, 2H, C*H*), 7.36 (d, *J* = 7.7 Hz, 2H, *o*-*H* ph), 7.53 (t, *J* = 7.7 Hz, 1H, *p*-*H* ph), 7.75 (t, *J* = 5.1 Hz, 1H, *p*-*H* pym), 7.77 (d, *J* = 2.3 Hz, 1H, NC*H*), 8.33 (d, *J* = 2.2 Hz, 1H, NC*H*), 9.09 (bs, 2H, *m*-*C*H pym); ^{13}C NMR (DMSO-d_6, 75.5 MHz, ppm) δ −10.7 (Pd-*C*H$_3$), 22.8, 24.3 (*C*H$_3$ iPr), 27.9 (*C*H), 117.1 (*p*-*C*H pym), 120.7 (N*C*H), 123.7 (*m*-*C*H ph), 126.8 (N*C*H), 130.3 (*p*-*C*H ph), 134.4 (*ipso*-*C* ph), 144.5 (*o*-*C* ph), 155.3 (*ipso*-*C* pym), 156.7 (*m*-*C*H pym), 160.4 (*m*-*C*H pym), 170.7 (carbene-*C*); anal. calcd for $C_{20}H_{25}ClN_4Pd$: C, 51.85%; H, 5.44%; N, 12.09%; found: C, 51.66%; H, 5.73%; N 11.65%.

Chloro(methyl)(1-(2-pyrimidyl)-3-(4-bromophenyl)imidazolin-2-ylidene)palladium(II) (**12**)

0.05 g (0.1 mmol) of silver complex **8** and 0.03 g (0.1 mmol) chloro(methyl)(cyclooctadiene)palladium(II) are dissolved in 30 mL acetonitrile. Under exclusion of light the reaction mixture is stirred in an argon atmosphere for 72 h at room temperature. The resulting suspension is filtrated over a celite pad and the solvent is removed in vacuo. The product is recrystallized from acetonitrile and dried in vacuo. The product is obtained as a white solid 0.02 g (48%). Mp 202 °C (dec); ^{1}H NMR ($CDCl_3$, 300 MHz, ppm) δ 0.04 (s, 3H, Pd-CH_3), 7.01 (d, *J* = 2.2 Hz, 1H, NC*H*), 7.37 (d, *J* = 8.7 Hz, 2H, *o*-*H* ph), 7.48 (t, *J* = 5.1 Hz, 1H, *p*-*H* pym), 7.66 (d, *J* = 8.7 Hz, 2H, *m*-*H* ph), 7.99 (d, *J* = 2.2 Hz, 1H, NC*H*), 8.83 (bs, 1H, *m*-*H* pym), 9.39 (bs, 1H, *m*-*H* pym); ^{13}C NMR ($CDCl_3$, 75.5 MHz, ppm) δ −7.4 (Pd-*C*H$_3$), 116.8 (*p*-*C*H pym), 120.2 (N*C*H), 124.2 (*p*-C ph), 124.8 (N*C*H), 125.9 (*ipso*-*C* ph), 128.0 (*o*-*C*H ph), 132.8 (*m*-*C*H ph), 154.9 (*m*-*C*H pym), 155.6 (*ipso*-*C* pym); anal. calcd for $C_{14}H_{12}BrClN_4Pd{\cdot}0.1AgCl$: C, 35.60%; H, 2.56%; N, 11.86%; found: C, 35.98%; H, 2.14%; N, 12.16%.

Methyl(trifluoroacetato)(1-(2-pyrimidyl)-3-(2,6-diisopropylphenyl)imidazolin-2-ylidene)palladium(II) (**13**)

0.10 g (0.2 mmol) of **11** and 0.05 g (0.2 mmol) silver trifluoroacetate are dissolved in 100 mL dichloromethane. Under exclusion of light the reaction mixture is stirred under an argon atmosphere for 9 h at room temperature. The resulting suspension is filtrated over a celite pad and concentrated in vacuo. The product is precipitated by the addition of diethyl ether, filtrated, washed with diethyl ether and dried in vacuo. The product is obtained as a white solid (0.08 g, 82%). Mp 232 °C (dec); ^{1}H NMR (DMSO-d_6, 300 MHz, ppm) δ 0.09 (s, 3H, Pd-CH_3), 1.13 (d, *J* = 6.8 Hz, 6H, CH_3), 1.23 (d, *J* = 6.8 Hz, 6H, CH_3), 2.55 (sept, *J* = 6.8 Hz, 2H, C*H*), 7.39 (d, *J* = 7.8 Hz, 2H, *o*-*H* ph), 7.56 (t, *J* = 7.8 Hz, 1H, *p*-*H* ph), 7.79 (t, *J* = 5.2 Hz, 1H, *p*-*H* pym), 7.89 (d, *J* = 2.1 Hz, 1H, NC*H*), 8.43 (d, *J* = 2.1 Hz, 1H, NC*H*), 8.99 (bs, 2H, *m*-*C*H pym); ^{13}C NMR (DMSO-d_6, 75.5 MHz, ppm) δ −6.9 (Pd-*C*H$_3$), 23.0 (*C*H$_3$ iPr), 24.3 (*C*H$_3$ iPr), 28.0 (*C*H), 118.1 (*p*-*C*H pym), 121.1 (N*C*H), 124.0 (*m*-*C*H ph), 127.4 (N*C*H), 130.7 (*p*-*C*H ph), 134.2 (*ipso*-*C* ph), 144.6 (*o*-*C* ph), 155.0 (*ipso*-*C* pym), *m*-*C*H pym and carben-*C* not observed in DMSO-d_6.

Bis(trifluoroacetato)(1-(2-pyrimidyl)-3-(2,6-diisopropylphenyl)imidazolin-2-ylidene)palladium(II) (**14**)

Synthetic pathway 1: 0.05 g (0.1 mmol) of **13** and 0.08 g (0.2 mmol) iodobenzene bis(trifluoroacetate) are dissolved in 10 mL dichloromethane. The reaction mixture is stirred for 12 h at room temperature. The solvent is removed in vacuo, the resulting solid is washed with THF. The product is obtained as a white solid (quant.). Mp 259 °C (dec).

Synthetic pathway 2, starting from dichloro(1-(2-pyrimidyl)-3-(2,6-diisopropylphenyl)imidazolin-2-ylidene)palladium(II) [34]: 0.03 g (0.1 mmol) dichloro(1-(2-pyrimidyl)-3-(2,6-diisopropylphenyl)imidazolin-2-ylidene)palladium(II) and 0.05 g (0.2 mmol) silver trifluoroacetate are dissolved in 10 mL dichloromethane at 0 °C. The reaction mixture is allowed to warm up to room temperature and stirred for another 4 h. The resulting suspension is filtrated over a celite pad, the solvent is removed in vacuo and the resulting solid washed with THF. The product is obtained as a white solid (quant.). Mp 259 °C (dec);

^{1}H NMR (DMSO-d_6, 300 MHz, ppm) δ 1.08 (d, J = 6.6 Hz, 6H, CH_3), 1.28 (d, J = 6.6 Hz, 6H, CH_3), 2.62 (sept, J = 6.6 Hz, 2H, CH), 7.29 (d, J = 7.8 Hz, 2H, *o*-H ph), 7.46 (t, J = 7.7 Hz, 1H, *p*-H ph), 7.79 (t, J = 5.2 Hz, 1H, *p*-H pym), 7.93 (s, 1H, NCH), 8.50 (d, J = 1.3 Hz, 1H, NCH), 8.68 (m, 1H, *m*-CH pym), 9.19 (m, 1H, *m*-CH pym); ^{13}C NMR (DMSO-d_6, 75.5 MHz, ppm) δ 22.4 (*C*H$_3$ iPr), 24.8 (*C*H$_3$ iPr), 27.9 (*C*H iPr), 118.1 (*p*-*C*H pym), 120.4 (N*C*H), 123.7 (*m*-*C*H ph), 127.2 (N*C*H), 130.4 (*p*-*C*H ph), 131.7 (*ipso*-*C* ph), 144.3 (*o*-*C* ph), 156.2 (*ipso*-*C* pym), 162.1 (*m*-*C*H pym), carbene-*C* not observed; ^{19}F NMR (DMSO-d_6, 75.5 MHz, ppm) δ −72.54 (CF_3), −73.47 (CF_3); anal. calcd for $C_{23}H_{22}F_6N_4O_4Pd$: C, 43.24%; H, 3.47%; N, 8.77%; found: C, 42.73%; H, 3.67%; N, 8.38%.

Dimethyl(1-(2-pyrimidyl)-3-(2,6-diisopropylphenyl)imidazolin-2-ylidene)palladium(II) (**15**)

0.18 g (0.6 mmol) of the imidazolium salt **3** and 0.07 g (0.6 mmol) potassium *tert*-butanolat are suspended in dry THF at −78 °C under an atmosphere of argon. Over a period of 2 h, the reaction mixture is allowed to warm up to 0 °C. Afterwards the solution is again cooled to −78 °C. A cold solution (−78 °C) of 0.10 g (0.4 mmol) dimethyl(*N,N,N′,N′*-tetramethyl-1,2-diaminoethylene)palladium(II) in 20 mL THF is added. The reaction mixture is allowed to warm up to 0 °C over a period of 2 h, the solvent is removed in vacuo and the resulting precipitate is extracted with dry toluene (2 × 10 mL). The solvent is concentrated in vacuo again and the product is precipitated by the addition of 20 mL pentane. The solid is filtrated, washed with cold pentane and dried in vacuo. Yield: 0.13 g (47%). ^{1}H NMR (C_6D_6, 300 MHz, ppm) δ 0.68 (s, 3H, Pd-CH_3), 0.94 (s, 3H, Pd-CH_3), 1.04 (d, J = 6.9 Hz, 6H, CH_3), 1.41 (d, J = 6.9 Hz, 6H, CH_3), 2.85 (sept, J = 6.8 Hz, 2H, CH), 5.94 (t, J = 5.9 Hz, 1H, *p*-H pym), 6.17 (d, J = 2.0 Hz, 1H, NCH), 7.12 (d, J = 7.6 Hz, 2H, *m*-H ph), 7.26 (t, J = 7.3 Hz, 1H, *p*-H ph), 7.49 (d, J = 2.0 Hz, 1H, NCH), 7.67 (m, 1H, *m*-CH pym), 8.53 (m, 1H, *m*-CH pym); ^{13}C NMR (C_6D_6, 75.5 MHz, ppm) δ = −10.9 (Pd-*C*H$_3$), 1.7 (Pd-*C*H$_3$), 23.9 (*C*H$_3$ iPr), 24.3 (*C*H$_3$ iPr), 28.9 (*C*H iPr), 115.3 (*p*-*C*H pym), 118.9 (N*C*H), 124.0 (*m*-*C*H ph), 124.5 (N*C*H), 130.4 (*p*-*C*H ph), 135.8 (*ipso*-*C* ph), 145.6 (*o*-*C* ph), 155.3 (*ipso*-*C* pym), 156.1 (*m*-*C*H pym), 157.0 (*m*-*C*H pym), 194.7 (carbene-*C*). ESIMS: 444.1 $[M + H]^+$.

Computational details

All calculations were performed with the Gaussian 09 software [55]. The geometries were optimized using the density functional hybrid model B3LYP [56-60] together with the split valence double-ζ 6-31G(d) [61-66] and triple-ζ 6-311+G(d,p) [67-74] basis sets. All reported structures were verified as true minima by the absence of negative eigenvalues in the vibrational frequency analysis. All energies reported are Gibbs free energies at standard conditions (T = 298 K, p = 1 atm) using unscaled frequencies. For visualization GaussView [75] was used.

Solid-state structure determination of **9**, **12** and **13**

Preliminary examination and data collection were carried out on an area detecting system (Kappa-CCD; Nonius) at the window of a sealed X-ray tube (Nonius, FR590) and graphite monochromated Mo Kα radiation (λ = 0.72073 Å). The reflections were integrated. Raw data were corrected for Lorentz and polarization and, arising from the scaling procedure, for latent decay. An absorption correction was applied using SADABS [76]. After merging, the independent reflections were all used to refine the structures, which were solved by a combination of direct methods and difference Fourier synthesis. All non-hydrogen atoms were refined with anisotropic displacement parameters. All hydrogen atoms were placed in calculated positions and refined using the riding model. Full-matrix least-squares refinements were carried out by minimizing $\Sigma w(F_o^2 - F_c^2)^2$. Details of the structure determinations are given in Table S1 (Supporting Information File 1). Neutral atom scattering factors for all atoms and anomalous dispersion corrections for the non-hydrogen atoms were taken from the International Tables for Crystallography [77]. All calculations were performed with the SHELXL-97 [78] package and the programs COLLECT [79], DIRAX [80], EVALCCD [81], SIR-92 [82], SADABS [76], ORTEP III [83] and PLATON [84].

Supporting Information

Supplementary crystallographic data can be obtained free of charge from The Cambridge Crystallographic Data Centre via http://www.ccdc.cam.ac.uk/data_request/cif.

Supporting Information File 1

Details of the DFT calculations and additional crystallographic data for **9** (CCDC 1484282), **12** (CCDC 1484281) and **13** (CCDC 1484283).
[http://www.beilstein-journals.org/bjoc/content/supplementary/1860-5397-12-150-S1.pdf]

Supporting Information File 2

CIF file for compound **9**.
[http://www.beilstein-journals.org/bjoc/content/supplementary/1860-5397-12-150-S2.cif]

Supporting Information File 3

CIF file for compound **12**.
[http://www.beilstein-journals.org/bjoc/content/supplementary/1860-5397-12-150-S3.cif]

Supporting Information File 4
CIF file for compound **13**.
[http://www.beilstein-journals.org/bjoc/content/supplementary/1860-5397-12-150-S4.cif]

Acknowledgements

D.M. thanks the 'Evonik-foundation' for financial support. We are grateful for the generous allocation of compute time by the ZIH (TU Dresden) on their high-performance computing facility. We thank P. Pinter (TU Dresden) for helpful discussions.

References

1. Tsuji, J. *Tetrahedron* **2015,** *71,* 6330–6348. doi:10.1016/j.tet.2015.06.010
2. Johansson Seechurn, C. C. C.; Kitching, M. O.; Colacot, T. J.; Snieckus, V. *Angew. Chem., Int. Ed.* **2012,** *51,* 5062–5085. doi:10.1002/anie.201107017
3. Hartwig, J. F. *J. Am. Chem. Soc.* **2016,** *138,* 2–24. doi:10.1021/jacs.5b08707
4. Campbell, A. N.; Stahl, S. S. *Acc. Chem. Res.* **2012,** *45,* 851–863. doi:10.1021/ar2002045
5. Labinger, J. A. Alkane Functionalization via Electrophilic Activation. *Alkane C-H Activation by Single-Site Metal Catalysis;* Catalysis by Metal Complexes, Vol. 38; Springer: Netherlands, 2012; pp 17–71. doi:10.1007/978-90-481-3698-8_2
6. Lyons, T. W.; Sanford, M. S. *Chem. Rev.* **2010,** *110,* 1147–1169. doi:10.1021/cr900184e
7. Arndtsen, B. A.; Bergman, R. G.; Mobley, T. A.; Peterson, T. H. *Acc. Chem. Res.* **1995,** *28,* 154–162. doi:10.1021/ar00051a009
8. Janowicz, A. H.; Bergman, R. G. *J. Am. Chem. Soc.* **1982,** *104,* 352–354. doi:10.1021/ja00365a091
9. Janowicz, A. H.; Bergman, R. G. *J. Am. Chem. Soc.* **1983,** *105,* 3929–3939. doi:10.1021/ja00350a031
10. Hoyano, J. K.; Graham, W. A. G. *J. Am. Chem. Soc.* **1982,** *104,* 3723–3725. doi:10.1021/ja00377a032
11. Hoyano, J. K.; McMaster, A. D.; Graham, W. A. G. *J. Am. Chem. Soc.* **1983,** *105,* 7190–7191. doi:10.1021/ja00362a039
12. Shteinman, A. A. *J. Organomet. Chem.* **2015,** *793,* 34–40. doi:10.1016/j.jorganchem.2015.03.020
13. Crabtree, R. H. *J. Organomet. Chem.* **2015,** *793,* 41–46. doi:10.1016/j.jorganchem.2015.02.031
14. Shestakov, A. F.; Goldshleger, N. F. *J. Organomet. Chem.* **2015,** *793,* 17–33. doi:10.1016/j.jorganchem.2015.04.040
15. Stahl, S. S.; Labinger, J. A.; Bercaw, J. E. *Angew. Chem., Int. Ed.* **1998,** *37,* 2180–2192. doi:10.1002/(SICI)1521-3773(19980904)37:16<2180::AID-ANIE2180>3.0.CO;2-A
16. Gol'dshleger, N. F.; Es'kova, V. V.; Shilov, A. E.; Shteinman, A. A. *Zh. Fiz. Khim.* **1972,** *46,* 1353–1354.
17. Gol'dshleger, N. F.; Tyabin, M. B.; Shilov, A. E.; Shteinman, A. A. *Zh. Fiz. Khim.* **1969,** *43,* 2174–2175.
18. Periana, R. A.; Taube, D. J.; Gamble, S.; Taube, H.; Satoh, T.; Fujii, H. *Science* **1998,** *280,* 560–564. doi:10.1126/science.280.5363.560
19. Kua, J.; Xu, X.; Periana, R. A.; Goddard, W. A., III. *Organometallics* **2002,** *21,* 511–525. doi:10.1021/om0101691
20. Ahlquist, M.; Nielsen, R. J.; Periana, R. A.; Goddard, W. A., III. *J. Am. Chem. Soc.* **2009,** *131,* 17110–17115. doi:10.1021/ja903930e
21. Sen, A. *Platinum Met. Rev.* **1991,** *35,* 126–132.
22. Balcer, S. *Pol. J. Chem. Technol.* **2015,** *17* (3), 52–61. doi:10.1515/pjct-2015-0050
23. Caballero, A.; Pérez, P. J. *Chem. Soc. Rev.* **2013,** *42,* 8809–8820. doi:10.1039/c3cs60120j
24. Munz, D.; Strassner, T. *Inorg. Chem.* **2015,** *54,* 5043–5052. doi:10.1021/ic502515x
25. Munz, D.; Strassner, T. *Top. Catal.* **2014,** *57,* 1372–1376. doi:10.1007/s11244-014-0305-5
26. Munz, D.; Meyer, D.; Strassner, T. *Organometallics* **2013,** *32,* 3469–3480. doi:10.1021/om400232u
27. Ahrens, S.; Zeller, A.; Taige, M.; Strassner, T. *Organometallics* **2006,** *25,* 5409–5415. doi:10.1021/om060577a
28. Strassner, T.; Ahrens, S.; Zeller, A. N-heterocyclische Carbenkomplexe des Platins und des Palladiums, deren Herstellung und Verwendung zur partiellen Oxidation von Kohlenwasserstoffen. WO 2006058535 A3, Feb 8, 2007.
29. Strassner, T.; Muehlhofer, M.; Zeller, A.; Herdtweck, E.; Herrmann, W. A. *J. Organomet. Chem.* **2004,** *689,* 1418–1424. doi:10.1016/j.jorganchem.2004.02.013
30. Muehlhofer, M.; Strassner, T.; Herrmann, W. A. *Angew. Chem., Int. Ed.* **2002,** *41,* 1745–1747. doi:10.1002/1521-3773(20020517)41:10<1745::AID-ANIE1745>3.0.CO;2-E
31. Ahrens, S.; Strassner, T. *Inorg. Chim. Acta* **2006,** *359,* 4789–4796. doi:10.1016/j.ica.2006.05.042
32. Maletz, G.; Schmidt, F.; Reimer, A.; Strassner, T.; Muehlhofer, M.; Mihalios, D.; Herrmann, W. Katalysator und Verfahren zur partiellen Oxidation von Alkanen. DE 10151660 B4, Feb 9, 2006.
33. Brendel, M.; Engelke, R.; Desai, V. G.; Rominger, F.; Hofmann, P. *Organometallics* **2015,** *34,* 2870–2878. doi:10.1021/acs.organomet.5b00204
34. Meyer, D.; Taige, M. A.; Zeller, A.; Hohlfeld, K.; Ahrens, S.; Strassner, T. *Organometallics* **2009,** *28,* 2142–2149. doi:10.1021/om8009238
35. Meyer, D.; Zeller, A.; Strassner, T. *J. Organomet. Chem.* **2012,** *701,* 56–61. doi:10.1016/j.jorganchem.2011.12.014
36. Sperger, T.; Sanhueza, I. A.; Kalvet, I.; Schoenebeck, F. *Chem. Rev.* **2015,** *115,* 9532–9586. doi:10.1021/acs.chemrev.5b00163
37. Meyer, D.; Strassner, T. *J. Organomet. Chem.* **2015,** *784,* 84–87. doi:10.1016/j.jorganchem.2014.09.022
38. Byers, P. K.; Canty, A. J. *Organometallics* **1990,** *9,* 210–220. doi:10.1021/om00115a033
39. Farrugia, L. J. *J. Appl. Crystallogr.* **1997,** *30,* 565. doi:10.1107/S0021889897003117
40. Magill, A. M.; McGuinness, D. S.; Cavell, K. J.; Britovsek, G. J. P.; Gibson, V. C.; White, A. J. P.; Williams, D. J.; White, A. H.; Skelton, B. W. *J. Organomet. Chem.* **2001,** *617–618,* 546–560. doi:10.1016/S0022-328X(00)00720-8
41. Meyer, D. Azoliumsalze als NHC-Precursoren fur Katalysatoren (Pd, Pt) zur Methanaktivierung sowie als ionische Flussigkeiten – Synthese, DFT Rechnungen und mechanistische Studien. Dissertation, TU Dresden, 2011.
42. McCall, A. S.; Wang, H.; Desper, J. M.; Kraft, S. *J. Am. Chem. Soc.* **2011,** *133,* 1832–1848. doi:10.1021/ja107342b

43. Pérez-Temprano, M. H.; Racowski, J. M.; Kampf, J. W.; Sanford, M. S. *J. Am. Chem. Soc.* **2014,** *136,* 4097–4100. doi:10.1021/ja411433f
44. Racowski, J. M.; Ball, N. D.; Sanford, M. S. *J. Am. Chem. Soc.* **2011,** *133,* 18022–18025. doi:10.1021/ja2051099
45. Racowski, J. M.; Dick, A. R.; Sanford, M. S. *J. Am. Chem. Soc.* **2009,** *131,* 10974–10983. doi:10.1021/ja9014474
46. Powers, D. C.; Ritter, T. *Nat. Chem.* **2009,** *1,* 302–309. doi:10.1038/nchem.246
47. Whitfield, S. R.; Sanford, M. S. *J. Am. Chem. Soc.* **2007,** *129,* 15142–15143. doi:10.1021/ja077866q
48. Dick, A. R.; Kampf, J. W.; Sanford, M. S. *J. Am. Chem. Soc.* **2005,** *127,* 12790–12791. doi:10.1021/ja0541940
49. Arnold, P. L.; Sanford, M. S.; Pearson, S. M. *J. Am. Chem. Soc.* **2009,** *131,* 13912–13913. doi:10.1021/ja905713t
50. Danopoulos, A. A.; Tsoureas, N.; Macgregor, S. A.; Smith, C. *Organometallics* **2007,** *26,* 253–263. doi:10.1021/om0608408
51. Subramanium, S. S.; Slaughter, L. M. *Dalton Trans.* **2009,** 6930–6933. doi:10.1039/b908689g
52. Douthwaite, R. E.; Green, M. L. H.; Silcock, P. J.; Gomes, P. T. *J. Chem. Soc., Dalton Trans.* **2002,** 1386–1390. doi:10.1039/b110261n
53. Tsoureas, N.; Danopoulos, A. A.; Tulloch, A. A. D.; Light, M. E. *Organometallics* **2003,** *22,* 4750–4758. doi:10.1021/om034061s
54. Salo, E. V.; Guan, Z. *Organometallics* **2003,** *22,* 5033–5046. doi:10.1021/om034051r
55. *Gaussian 09,* Rev. B 0.1; Gaussian, Inc.: Wallingford CT, 2009.
56. Stephens, P. J.; Devlin, F. J.; Chabalowski, C. F.; Frisch, M. J. *J. Phys. Chem.* **1994,** *98,* 11623–11627. doi:10.1021/j100096a001
57. Miehlich, B.; Savin, A.; Stoll, H.; Preuss, H. *Chem. Phys. Lett.* **1989,** *157,* 200–206. doi:10.1016/0009-2614(89)87234-3
58. Becke, A. D. *Phys. Rev. A* **1988,** *38,* 3098–3100. doi:10.1103/PhysRevA.38.3098
59. Vosko, S. H.; Wilk, L.; Nusair, M. *Can. J. Phys.* **1980,** *58,* 1200–1211. doi:10.1139/p80-159
60. Lee, C.; Yang, W.; Parr, R. G. *Phys. Rev. B* **1988,** *37,* 785–789. doi:10.1103/PhysRevB.37.785
61. Rassolov, V. A.; Pople, J. A.; Ratner, M. A.; Windus, T. L. *J. Chem. Phys.* **1998,** *109,* 1223–1229. doi:10.1063/1.476673
62. Hehre, W. J.; Ditchfield, R.; Pople, J. A. *J. Chem. Phys.* **1972,** *56,* 2257–2261. doi:10.1063/1.1677527
63. Hariharan, P. C.; Pople, J. A. *Mol. Phys.* **1974,** *27,* 209–214. doi:10.1080/00268977400100171
64. Hariharan, P. C.; Pople, J. A. *Chem. Phys. Lett.* **1972,** *16,* 217–219. doi:10.1016/0009-2614(72)80259-8
65. Hariharan, P. C.; Pople, J. A. *Theor. Chim. Acta* **1973,** *28,* 213–222. doi:10.1007/BF00533485
66. Ditchfield, R.; Hehre, W. J.; Pople, J. A. *J. Chem. Phys.* **1971,** *54,* 724–728. doi:10.1063/1.1674902
67. Binning, R. C., Jr.; Curtiss, L. A. *J. Comput. Chem.* **1990,** *11,* 1206–1216. doi:10.1002/jcc.540111013
68. Clark, T.; Chandrasekhar, J.; Spitznagel, G. W.; Von Ragué Schleyer, P. *J. Comput. Chem.* **1983,** *4,* 294–301. doi:10.1002/jcc.540040303
69. Frisch, M. J.; Pople, J. A.; Binkley, J. S. *J. Chem. Phys.* **1984,** *80,* 3265–3269. doi:10.1063/1.447079
70. Hay, P. J. *J. Chem. Phys.* **1977,** *66,* 4377–4384. doi:10.1063/1.433731
71. Krishnan, R.; Binkley, J. S.; Seeger, R.; Pople, J. A. *J. Chem. Phys.* **1980,** *72,* 650–654. doi:10.1063/1.438955
72. McGrath, M. P.; Radom, L. *J. Chem. Phys.* **1991,** *94,* 511–516. doi:10.1063/1.460367
73. Raghavachari, K.; Trucks, G. W. *J. Chem. Phys.* **1989,** *91,* 2457–2460. doi:10.1063/1.457005
74. Wachters, A. J. H. *J. Chem. Phys.* **1970,** *52,* 1033–1036. doi:10.1063/1.1673095
75. Dennington, R. I.; Keith, T.; Millam, J. M.; Eppinnett, W.; Hovell, W. L.; Gilliland, R. *GaussView*, 3.09; Gaussian, Inc.: Wallingford, CT, 2003.
76. Sheldrick, G. M., *SADABS, Version 2.10.* University of Goettingen, Goettingen, Germany, 2003.
77. Wilson, A. J. C. *International Tables for Crystallography;* Kluwer Academic Publisher: Dodrecht, The Netherlands, 1992.
78. Sheldrick, G. M., *SHELXL-97, Program for the Refinement of Structures.* University of Goettingen, Goettingen, Germany, 1997.
79. Nonius, *Data Collection Software for Nonius-kappa CCD devices.* Delft, The Netherlands, 1997–2000.
80. Duisenberg, A. J. M. *J. Appl. Crystallogr.* **1992,** *25,* 92–96. doi:10.1107/S0021889891010634
81. Duisenberg, A. J. M.; Hooft, R. W. W.; Schreurs, A. M. M.; Kroon, J. *J. Appl. Crystallogr.* **2000,** *33,* 893–898. doi:10.1107/S0021889800002363
82. Altomare, A.; Cascarano, G.; Giacovazzo, C.; Guagliardi, A.; Burla, M. C.; Polidori, G.; Camalli, M. *J. Appl. Crystallogr.* **1994,** *27,* 435–436.
83. Burnett, M. N.; Johnson, C. K. *ORTEPIII;* Oak Ridge National Laboratory: Tennessee, USA, 1996.
84. Spek, A. L. *PLATON;* Utrecht University: Utrecht, The Netherlands, 2001.

License and Terms

This is an Open Access article under the terms of the Creative Commons Attribution License (http://creativecommons.org/licenses/by/2.0), which permits unrestricted use, distribution, and reproduction in any medium, provided the original work is properly cited.

The license is subject to the *Beilstein Journal of Organic Chemistry* terms and conditions: (http://www.beilstein-journals.org/bjoc)

The definitive version of this article is the electronic one which can be found at: doi:10.3762/bjoc.12.150

BEILSTEIN JOURNAL OF ORGANIC CHEMISTRY

Dinuclear thiazolylidene copper complex as highly active catalyst for azid–alkyne cycloadditions

Anne L. Schöffler, Ata Makarem, Frank Rominger and Bernd F. Straub*

Full Research Paper

Open Access

Address:
Organisch-Chemisches Institut, Universität Heidelberg, Im Neuenheimer Feld 270, D-69120 Heidelberg, Germany

Email:
Bernd F. Straub* - straub@oci.uni-heidelberg.de

* Corresponding author

Keywords:
catalysis; click; copper; CuAAC; *N*-heterocyclic carbene; thiazole

Beilstein J. Org. Chem. **2016,** *12,* 1566–1572.
doi:10.3762/bjoc.12.151

Received: 02 April 2016
Accepted: 28 June 2016
Published: 21 July 2016

This article is part of the Thematic Series "Organometallic chemistry". In memoriam Prof. Dr. Peter Hofmann.

Guest Editor: L. Gade

© 2016 Schöffler et al.; licensee Beilstein-Institut.
License and terms: see end of document.

Abstract

A dinuclear *N*-heterocyclic carbene (NHC) copper complex efficiently catalyzes azide–alkyne cycloaddition (CuAAC) "click" reactions. The ancillary ligand comprises two 4,5-dimethyl-1,3-thiazol-2-ylidene units and an ethylene linker. The three-step preparation of the complex from commercially available starting compounds is more straightforward and cost-efficient than that of the previously described 1,2,4-triazol-5-ylidene derivatives. Kinetic experiments revealed its high catalytic CuAAC activity in organic solvents at room temperature. The activity increases upon addition of acetic acid, particularly for more acidic alkyne substrates. The modular catalyst design renders possible the exchange of *N*-heterocyclic carbene, linker, sacrificial ligand, and counter ion.

Introduction

The copper-catalyzed azide–alkyne cycloaddition (CuAAC) is one of the most important "click" reactions for the facile covalent linking of two molecules [1-3]. In 2002, the research groups of Meldal and Sharpless independently discovered the strongly rate-enhancing effect of copper(I) salts for azide–alkyne cycloadditions. The 1,4-disubstituted 1,2,3-triazoles are formed exclusively with essentially quantitative conversion and under mild reaction conditions [4-6]. The CuAAC reaction has found broad application in the preparation of peptide-conjugates [7,8], multicomponent syntheses [9], preparation of hydrogels, microgels and nanogels [10], (anion) supramolecular chemistry [11,12], in medicinal chemistry [13], therapeutics, biomaterials and bioactive surfaces [8,14], imaging of biochemical processes [15], localization of bioactive compounds inside living cells [16], syntheses of small-molecule screening libraries [17], catenane and rotaxane syntheses [18], in reactions under continuous flow processing [19], polymer and surface science [20-26], nucleoside, nucleotide, and oligonucleotide chemistry [27-29], in fluorogenic reactions [30], and in the syntheses of dendrimers [25,31]. The detailed mechanism of this reaction and the exact role of copper(I) and the species involved in the catalytic cycle had remained unclear for many years. The first proposals for the mechanism suggested the participation of only one copper(I) atom in the key

elementary steps. In 2005, Fokin and Finn determined the reaction rate of a CuAAC reaction to be second order in the concentration of copper [32]. Since then, the understanding of the mandatory role of dinuclear copper complexes as catalyst intermediates has vastly improved (Scheme 1) [33-37]. In 2013, the Fokin group provided evidence for the dicopper pathway of CuAAC reactions by a series of kinetic and isotopic labeling studies [34]. In 2015, the Bertrand group prepared, isolated, and structurally characterized molecular dicopper acetylide complexes, and investigated their reactivity towards azide substrates [36].

For standard CuAAC reactions, copper(I) carboxylates [5,38], mononuclear copper(I) phosphine carboxylate complexes [39] or copper(I) salts are an ideal compromise of low catalyst cost and high catalyst activity. However, CuAAC reactions of some substrates are not compatible with heterogeneous catalysis at the surface of insoluble copper(I) compounds. Instead, they depend on highly active molecular catalysts under homogeneous reaction conditions. Our research group has already established molecularly defined dicopper catalysts with unprecedented activity under diluted conditions with low catalyst loading [37,40]. Thus, we aimed at an even more facile synthesis of dicopper complexes with bis-*N*-heterocyclic carbene ancillary ligands.

Results and Discussion

We herein report the synthesis of an ethylene-linked bisthiazol-2-ylidene dicopper(I) complex **2** that features high catalytic activity in CuAAC reactions. The advantage of this new complex **2** in comparison to dicopper complexes previously described by our research group [40] is its less time-consuming and more cost-efficient synthesis. Commercially available, inexpensive 4,5-dimethylthiazole is used as azole starting material instead of 4-aryl-1,2,4-triazoles. The precursor **1a** for the NHC ancillary ligand is synthesized via a double S_N2-reaction of two equivalents of thiazole derivative with 1,2-dibromoethane. In order to avoid the presence of halide ions as inhibitory ligands for copper(I) [2,41], bisthiazolium hexafluorophosphate **1b** was obtained by a salt metathesis from bromide salt **1a** with aqueous hexafluorophosphoric acid (Figure 1).

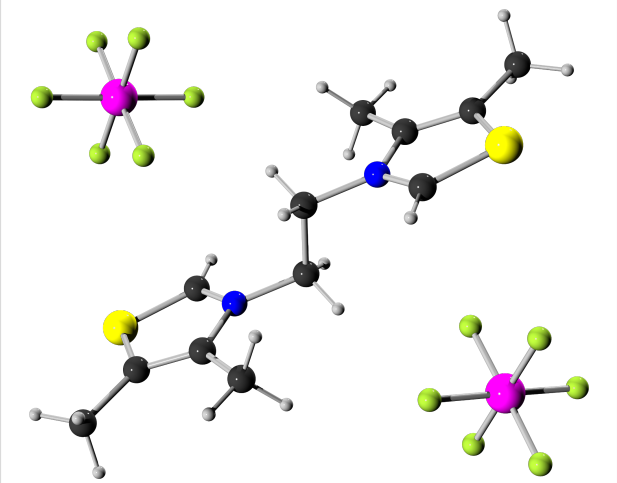
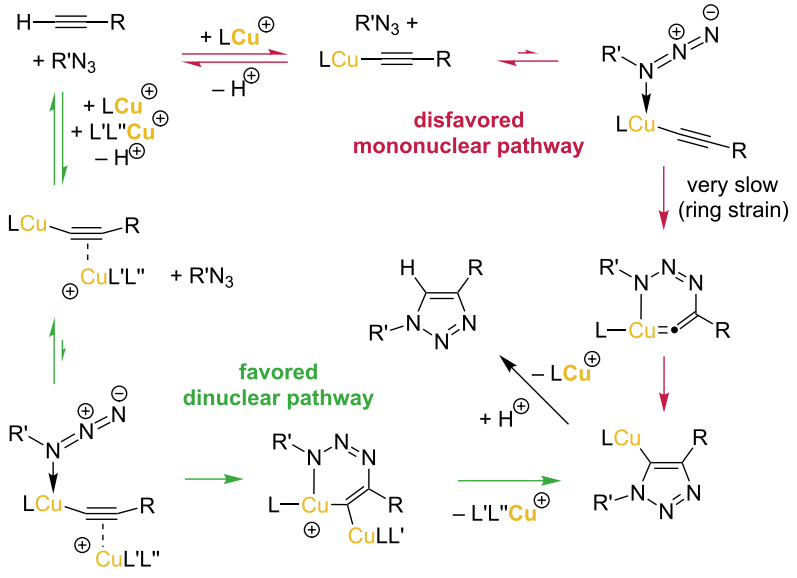
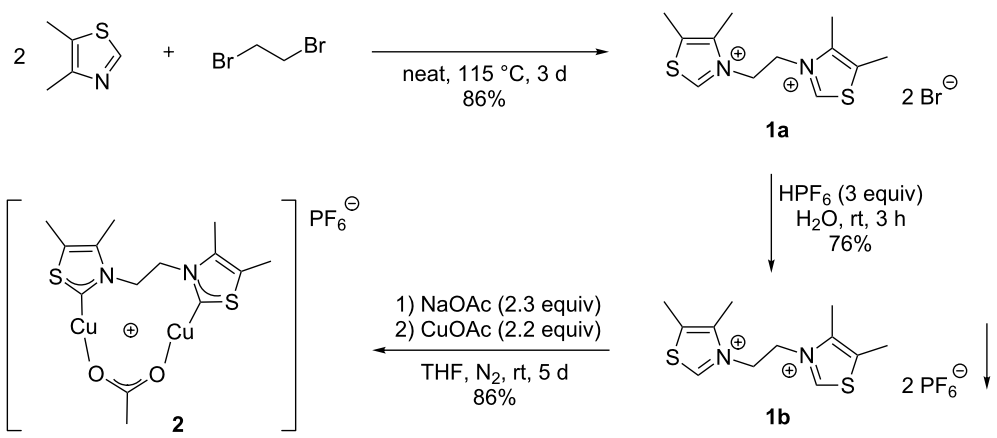


Figure 1: Ball-and-stick model [42,43] of a single crystal X-ray structure of hexafluorophosphate salt **1b** (CCDC 1472789). Color code: black carbon, grey hydrogen, yellow sulfur, blue nitrogen, magenta phosphorus, green fluorine.



Scheme 1: Disfavored mononuclear pathway and favored dinuclear pathway in the CuAAC click reaction, according to the mechanistic proposal of reference [37]. R, R' = alkyl, aryl, silyl, carbonyl groups; L = NHC; L' = NHC or solvent; L'' = solvent, acetylide, carboxylate, halide.

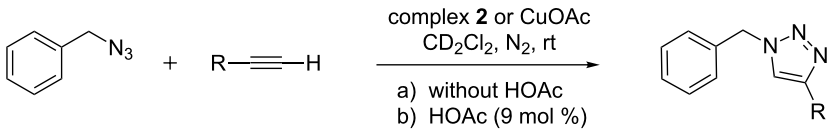


Scheme 2: Synthesis of dinuclear copper complex **2**.

The final step is the reaction with copper(I) acetate and sodium acetate as additional base in order to deprotonate the thiazolium salt **1b** and to form the bisthiazolylidene copper(I) complex **2**. Due to the relatively high acidity of the thiazolium precursor ($pK_a \approx 18$ [44]), a weak base such as sodium acetate yields small equilibrium concentrations of thiazol-2-ylidene. The latter then irreversibly binds to copper(I) ions (Scheme 2). The structure of the resulting complex **2** is presumably similar to the previously reported dinuclear bis(1,2,4-triazol-5-ylidene)copper(I) complexes that had been synthesized, characterized, and structurally characterized in our group [40]. The similarity of NMR-spectroscopic data of the 1,2,4-triazol-5-ylidene and the 1,3-thiazol-2-ylidene dicopper complex indicate that the complexes of both NHC ligand types consist of a bis-NHC ligand, two copper(I) ions and a labile acetate ligand that bridges the metal centers. The thiazolylidene complex **2** is air-stable in the solid state for at least several days. Stability tests in solution were taken under an atmosphere of nitrogen. Small amounts of a brown precipitate were formed in solution after one day. However, the NMR spectra showed no changes even after one week and in the presence of acetic acid. Therefore, we assume that complex **2** is quite robust against oxidization.

To test the catalytic performance of complex **2** with the help of continuous NMR spectroscopy, the reaction of benzyl azide with either phenylacetylene or ethyl propiolate in deuterated dichloromethane at room temperature was used (Table 1 and Figure 2). Due to the highly exothermic nature of the triazole formation, a high dilution of the reaction mixture and low catalyst loadings are necessary to prevent a thermal runaway. In order to compare the catalytic activity of complex **2** with conventional catalysts a kinetic study with copper(I) acetate was performed. All kinetic experiments were carried out under an atmosphere of nitrogen because of the air-sensitivity of complex **2** in solution (see Supporting Information File 1 for the detailed procedure).

Table 1: CuAAC reaction of benzyl azide and terminal alkynes with complex **2** or CuOAc as catalyst in absence or presence of added acetic acid.



Entry	Alkyne	Catalyst	Additional HOAc	Half conversion time
1	phenylacetylene	1.8 mol % complex **2**	–	37 min
2	phenylacetylene	1.8 mol % complex **2**	9 mol %	22 min
3	phenylacetylene	CuOAc (homogeneous solution)	–	166 min
4	ethyl propiolate	0.9 mol % complex **2**	–	≈ 15 h*
5	ethyl propiolate	0.9 mol % complex **2**	9 mol %	6 min
6	ethyl propiolate	CuOAc (homogeneous solution)	–	≈ 19 h*

*extrapolated half conversion time.

The reaction with phenylacetylene and 1.8 mol % copper complex **2** (Table 1, entries 1 and 2) reaches 50% conversion within 37 min (without acetic acid, green triangles in Figure 2) and is slightly accelerated by addition of acetic acid (half conversion within 22 min, blue dots). In contrast, the half conversion time for this reaction catalyzed by a saturated homogeneous solution of copper(I) acetate in deuterated dichloromethane is about 3 h (Table 1, entry 3, black dots in Figure 2). Therefore, the reaction with complex **2** is about 4.5 times (without HOAc) to 7.5 times (with HOAc) more effective compared to the homogeneous reaction with copper acetate. Under heterogeneous catalytic conditions, however, larger amounts of commercially available CuOAc powder with vivid stirring or shaking of the reaction mixture give rise to rapid CuAAC conversion. Thus, the molecular NHC dicopper catalyst complexes excel in homogeneous CuAAC reactions [40], while CuOAc excels in heterogeneous catalysis and in cost-effectiveness [38].

The reaction with ethyl propiolate in the presence of 0.9 mol % catalyst is very slow with a half conversion time of more than nine hours (Table 1, entry 4, yellow diamonds). We attribute this poor catalytic activity to the formation of copper acetylide clusters or even coordination polymers. Analogous dicopper complexes of more sterically demanding bis-1,2,4-triazolylidene ancillary ligands are quantitatively converted to octacopper hexaacetylide clusters under the same conditions [37]. To date, we have not been able to characterize thiazolylidene copper acetylides. Addition of acetic acid greatly increases the rate of the CuAAC reaction with ethyl propiolate, so that half-conversion is reached after 6 min (Table 1, entry 5, red squares). These observations are again consistent with the formation of a thermodynamically stable copper acetylide species [37], which are regenerated in the presence of acid to catalytically active dicopper acetylide intermediates [36]. The reaction catalyzed by copper acetate proceeds very slow. The extrapolated half-conversion is reached within approximately one day (Table 1, entry 6, grey triangles).

Conclusion

In summary, we have presented a molecularly defined bisthiazolylidene dicopper(I) complex that features high catalytic activity in CuAAC reactions. Its three-step synthesis is straightforward and cost-efficient. The modular design of this class of catalysts renders possible the tuning of the complex's properties and its features according to specific demands. Dicopper complexes with thiazolylidene ancillary ligands provide for improved availability, air-stability and convenience for the growing community of CuAAC users.

Experimental

General methodology

All reactions were carried out, unless described otherwise, under normal laboratory conditions under air. Reactions involving air-sensitive reagents were carried out in an atmosphere of argon using standard Schlenk techniques or in an MBraun LABmaster 130 glove box operated with nitrogen. Chemicals and solvents used in this work were supplied by the Department of Chemistry at the Ruprecht-Karls-University Heidel-

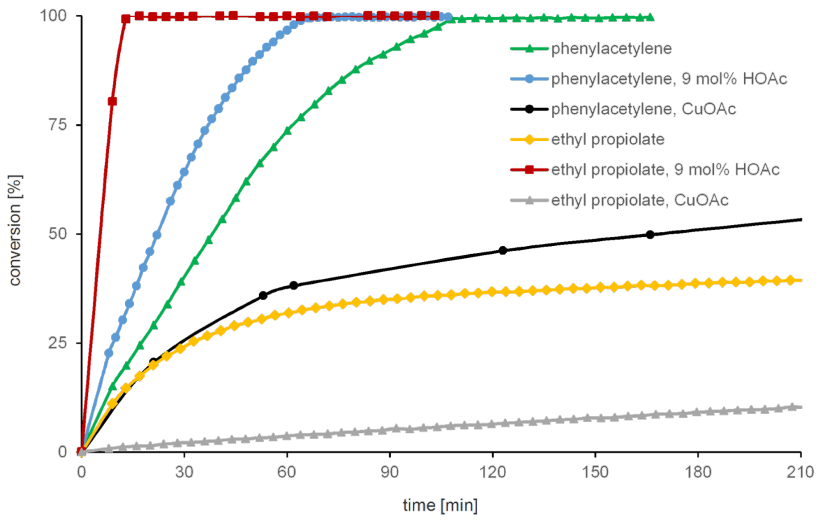


Figure 2: Time-conversion-diagram of the CuAAC reaction of benzyl azide with either phenylacetylene or ethyl propiolate in the presence of copper complex **2** (1.8 mol % for reaction with phenylacetylene, 0.9 mol % for reaction with ethyl propiolate) or in presence of CuOAc (saturated homogeneous solution) under an atmosphere of nitrogen in CD_2Cl_2 at rt (conversion referred to benzyl azide); reaction with phenylacetylene: green triangles (complex **2** without additional HOAc), blue dots (complex **2** in presence of 9 mol % additional HOAc) and black dots (CuOAc solution); reaction with ethyl propiolate: yellow diamonds (complex **2** without additional HOAc), red squares (complex **2** in presence of 9 mol % additional HOAc) and grey triangles (CuOAc solution).

berg or bought directly from Acros Organics, Fisher Scientific, Sigma Aldrich, Strem Chemicals, and TCI. Anhydrous solvents were taken from an MBraun MB SCS-800 solvent purification system containing appropriate drying agents. Deuterated solvents for the use of NMR spectroscopy were obtained from Deutero GmbH and Euriso-Top.

^{1}H NMR spectra were recorded at room temperature and the following instruments were employed: Bruker ARX-250 (250 MHz), Bruker Avance 300 (300 MHz), Bruker Avance 400 (400 MHz), Bruker Avance 500 (500 MHz). Chemical shifts δ are indicated in ppm and were determined by reference to the residual ^{1}H solvent peaks (acetone: 2.05 ppm; chloroform: 7.26 ppm; dichloromethane: 5.32 ppm; DMSO: 2.50 ppm). Coupling constants *J* are given in Hz. The following abbreviations describe the observed multiplicities: s = singlet, d = doublet, t = triplet, q = quartet, quin = quintet, sext = sextet, sept = septet, m = multiplet (composed abbreviations refer to multiple coupling patterns with the first letter indicating the greater coupling constant). ^{13}C{^{1}H} NMR spectra were recorded at room temperature with the following spectrometers: Bruker Avance 300 (75 MHz) and Bruker Avance 500 (125 MHz). The spectra were calibrated with respect to the solvent (acetone: 29.84 ppm, 206.26 ppm; chloroform: 77.16 ppm; dichloromethane: 53.84 ppm; DMSO: 39.52 ppm). For processing, analysis and interpretation of NMR spectra, the program TopSpin 3.2 by Bruker was used. All observed signals are singlets. Elemental analyses were carried out in the Department of Chemistry at the University of Heidelberg on the instruments vario EL and vario MICRO cube by Elementar Analysensysteme GmbH. Infrared spectra were recorded on a Bruker Lumos instrument with a Germanium ATR-crystal. The positions of the peaks are indicated in wavenumbers ν in cm^{-1}. The following abbreviations were used to describe both the intensity and profile of the signals: w (weak), m (medium), s (strong), br (broad). Mass spectra were recorded by the Mass Spectrometry Service Facility of the Organic-Chemical Department of the University of Heidelberg using the following instruments: Vacuum Generators ZAB-2F, Finnigan MAT TSQ 700, JEOL JMS-700, Bruker ICR Apex-Qe hybrid 9.4 T FT-ICR. In general the ionization method was specified. Apart from the method of ionization and the peak of the molecular ion, the base peak and characteristic fragmentation peaks with their relative intensities are reported.

Syntheses

3,3'-(Ethane-1,2-diyl)bis(4,5-dimethylthiazolium) dibromide (**1a**)

A Schlenk flask was charged with 3.00 equiv 4,5-dimethylthiazole (1.00 g, 8.84 mmol) and 1.00 equiv 1,2-dibromoethane (0.55 g, 2.95 mmol). The mixture was stirred at 115 °C for 3 d. After cooling to room temperature, the resulting solid was suspended in ethanol (2 mL) and the mixture was filtered. The solid residue was washed with ethanol (3 × 2 mL) and diethyl ether (3 × 3 mL) and dried in vacuo to give the beige product **1a** (1.05 g, 2.53 mmol, 86%). ^{1}H NMR (400.33 MHz, DMSO-d_6, 300.0 K) δ 9.90 (s, 2H, NC*H*S), 5.04 (s, 4H, CH_2), 2.52 (s, 6H, NCCH_3), 2.47 (s, 6H, SCCH_3) ppm; ^{13}C{^{1}H} NMR (100.66 MHz, DMSO-d_6, 295.0 K) δ 157.1 (N*C*HS), 141.9 (N*C*CH$_3$), 133.7 (S*C*CH$_3$), 50.6 (*C*H$_2$), 12.1 (NC*C*H$_3$), 11.1 (SC*C*H$_3$) ppm; elemental analysis calculated: C, 34.80; H, 4.38; N, 6.76; found: C, 34.69; H, 4.63; N, 6.64; HRMS (ESI$^+$, DMSO/MeOH) *m*/*z* (%): 253.0827 (100.0) [M − H − 2Br]$^+$, 352.9222 (41.3), 746.9344 (35.0) [2 M(^{79}Br) − Br]$^+$, calculated for [M − H − 2Br]$^+$: 253.0833, found: 253.0827; IR (ATR) ν = 3400 (w, br), 3070 (s), 2970 (s), 1738 (m), 1583 (s), 1443 (s), 1405 (s), 1189 (s), 798 (s) cm^{-1}; mp 255 °C dec.

3,3'-(Ethane-1,2-diyl)bis(4,5-dimethylthiazolium) bis(hexafluorophosphate) (**1b**)

1.00 equiv 3,3'-(ethane-1,2-diyl)bis(4,5-dimethylthiazolium) dibromide (**1a**, 1.50 g, 3.62 mmol) was dissolved in 75 mL H_2O. The solution was added slowly to aqueous 55% hexafluorophosphoric acid (3.00 equiv, 2.88 g, 10.9 mmol) in 50 mL H_2O. The mixture was stirred at room temperature for 3 h. The formed precipitate was filtered and washed with water (3 × 25 mL) and diethyl ether (5 × 20 mL). It was dried in vacuo to give the colourless product **1b** (1.50 g, 2.75 mmol, 76%). Single crystals of salt **1b** that were suitable for an X-ray structure analysis were obtained from acetone/diethyl ether. ^{1}H NMR (400.33 MHz, acetone-d_6, 295.0 K) δ 9.88 (s, 2H, NC*H*S), 5.42 (s, 4H, CH_2), 2.68 (s, 6H, NCCH_3), 2.66 (s, 6H, SCCH_3) ppm; ^{13}C{^{1}H} NMR (100.66 MHz, acetone-d_6, 295.0 K) δ 157.1 (N*C*HS), 143.7 (N*C*CH$_3$), 136.1 (S*C*CH$_3$), 52.4 (*C*H$_2$), 12.6 (NC*C*H$_3$), 11.6 (SC*C*H$_3$) ppm; elemental analysis calculated: C, 26.48; H, 3.33; N, 5.15; found: C, 26.50; H, 3.34; N, 5.37; HRMS (ESI$^+$, CH_2Cl_2/MeOH) *m*/*z* (%): 253.0828 (14.0) [M − H − 2PF$_6$]$^+$, 399.0548 (100.0) [M − PF$_6$]$^+$, 683.1201 (15.7), 943.0741 (73.0) [2 M − PF$_6$]$^+$; calculated for [M − PF$_6$]$^+$: 399.0548, found: 399.0548; IR (ATR) ν = 3132 (w), 1739 (w), 1595 (w), 1453 (w), 1211 (w), 828 (s), 740 (w) cm^{-1}; mp 220 °C dec.

μ-Acetato-κ*O*,κ*O*'-μ-[3,3'-(ethane-1,2-diyl)bis(4,5-dimethylthiazol-2-ylidene)]-κ*C*,κ*C*'-dicopper(I) hexafluorophosphate (**2**)

A Schlenk flask flushed with argon was charged with 3,3'-(ethane-1,2-diyl)bis(4,5-dimethylthiazolium) bis(hexafluorophosphate) (**1b**, 0,10 g, 0.18 mmol, 1.00 equiv) and anhydrous sodium acetate (0.04 g, 0.42 mmol, 2.30 equiv). The reaction mixture was stirred under reduced pressure overnight. In a glove box, copper(I) acetate (0.05 g, 0.40 mmol, 2.20 equiv)

and dichloromethane or tetrahydrofuran (3 mL) were added. The suspension was stirred at room temperature for 5 d.

a) Procedure for the reaction in dichloromethane: The suspension was filtered over a frit and the solution was concentrated by reducing the solvent in vacuo to 2 mL. Diethyl ether (4 mL) was added and the formed precipitate was filtered, washed with diethyl ether (3 × 2 mL) and dried in vacuo to give the light beige product **2** (0.06 g, 0.10 mmol, 56%).

b) Procedure for reaction in tetrahydrofuran: The solvent was removed under reduced pressure and dichloromethane (4 mL) was added in the glove box. The suspension was filtered over a frit and the solution was concentrated by reducing the solvent in vacuo to 2 mL. Diethyl ether (4 mL) was added and the formed precipitate was filtered, washed with diethyl ether (3 × 2 mL) and dried in vacuo to give the light beige product **2** (0.09 g, 0.16 mmol, 86%). ^{1}H NMR (600.24 MHz, CD_2Cl_2, 295.0 K) δ 4.85 (s, 4H, CH_2), 2.47 (s, 6H, NCCH_3), 2.38 (s, 6H, SCCH_3), 2.13 (s, 3H, H_3CCOO) ppm; ^{13}C{^{1}H} NMR (150.95 MHz, CD_2Cl_2, 295.0 K) δ 197.7 (N*C*CuS), 182.7 (H_3C*C*OO), 141.2 (N*C*CH_3), 133.6 (S*C*CH_3), 55.3 (*C*H_2), 22.9 (H_3*C*COO), 12.7 (NC*C*H_3), 12.1 (SC*C*H_3) ppm; elemental analysis calculated: C, 28.82; H, 3.28; N, 4.80; found: C, 28.70; H, 3.61; N, 4.84; HRMS (ESI$^+$, DMSO/MeOH) *m/z* (%): 251.0672 (42.3) $[M - 2Cu - H - Oac - PF_6]^+$, 283.0935 (100.0) $[M - 2Cu - Oac - PF_6 + CH_3O]^+$, 397.0392 (17.7), 599.0698 (69.9); calculated for $[M - 2Cu - Oac - PF_6 + CH_3O]^+$: 283.0949, found: 283.0935. IR (ATR) ν = 1594 (w), 1555 (m), 1447 (m), 1397 (w), 1328 (w), 835 (s), 691 (m) cm^{-1}; mp 175 °C dec.

Supporting Information

Supporting Information File 1

Author contributions, details of the procedures for the kinetic measurements, and figures of NMR spectra.
[http://www.beilstein-journals.org/bjoc/content/supplementary/1860-5397-12-151-S1.pdf]

Acknowledgements

Financial support by the Ruprecht-Karls-Universität Heidelberg is gratefully acknowledged.

References

1. Kolb, H. C.; Finn, M. G.; Sharpless, K. B. *Angew. Chem., Int. Ed.* **2001,** *40,* 2004–2021. doi:10.1002/1521-3773(20010601)40:11<2004::AID-ANIE2004>3.0.CO;2-5
2. Hein, J. E.; Fokin, V. V. *Chem. Soc. Rev.* **2010,** *39,* 1302–1315. doi:10.1039/b904091a
3. Meldal, M.; Tornøe, C. W. *Chem. Rev.* **2008,** *108,* 2952–3015. doi:10.1021/cr0783479
4. Tornøe, C. W.; Christensen, C.; Meldal, M. *J. Org. Chem.* **2002,** *67,* 3057–3064. doi:10.1021/jo011148j
5. Rostovtsev, V. V.; Green, L. G.; Fokin, V. V.; Sharpless, K. B. *Angew. Chem., Int. Ed.* **2002,** *41,* 2596–2599. doi:10.1002/1521-3773(20020715)41:14<2596::AID-ANIE2596>3.0.CO;2-4
6. Tornøe, C. W.; Meldal, M. In *Peptides: The Wave of the Future: Proceedings of the Second International and the Seventeenth American Peptide Symposium,* San Diego, CA, U.S.A., June 9–14, 2001; Lebl, M.; Houghen, R. A., Eds.; Springer: Dordrecht, Netherlands, 2001; pp 263–264.
7. Tang, W.; Becker, M. L. *Chem. Soc. Rev.* **2014,** *43,* 7013–7039. doi:10.1039/C4CS00139G
8. Lutz, J.-F.; Zarafshani, Z. *Adv. Drug Delivery Rev.* **2008,** *60,* 958–970. doi:10.1016/j.addr.2008.02.004
9. Hassan, S.; Müller, T. J. J. *Adv. Synth. Catal.* **2015,** *357,* 617–666. doi:10.1002/adsc.201400904
10. Jiang, Y.; Chen, J.; Deng, C.; Suuronen, E. J.; Zhong, Z. *Biomaterials* **2014,** *35,* 4969–4985. doi:10.1016/j.biomaterials.2014.03.001
11. Schulze, B.; Schubert, U. S. *Chem. Soc. Rev.* **2014,** *43,* 2522–2571. doi:10.1039/C3CS60386E
12. Hua, Y.; Flood, A. H. *Chem. Soc. Rev.* **2010,** *39,* 1262–1271. doi:10.1039/b818033b
13. Tron, G. C.; Pirali, T.; Billington, R. A.; Canonico, P. L.; Sorba, G.; Genazzani, A. A. *Med. Res. Rev.* **2008,** *28,* 278–308. doi:10.1002/med.20107
14. Mamidyala, S. K.; Finn, M. G. *Chem. Soc. Rev.* **2010,** *39,* 1252–1261. doi:10.1039/B901969N
15. Fokin, V. V. *ACS Chem. Biol.* **2007,** *2,* 775–778. doi:10.1021/cb700254v
16. Bevilacqua, V.; King, M.; Chaumontet, M.; Nothisen, M.; Gabillet, S.; Buisson, D.; Puente, C.; Wagner, A.; Taran, F. *Angew. Chem., Int. Ed.* **2014,** *53,* 5872–5876. doi:10.1002/anie.201310671
17. Wu, P.; Fokin, V. V. *Aldrichimica Acta* **2007,** *40,* 7–17.
18. Hänni, K. D.; Leigh, D. A. *Chem. Soc. Rev.* **2010,** *39,* 1240–1251. doi:10.1039/B901974J
19. Kappe, C. O.; Van der Eycken, E. *Chem. Soc. Rev.* **2010,** *39,* 1280–1290. doi:10.1039/b901973c
20. Golas, P. L.; Matyjaszewski, K. *Chem. Soc. Rev.* **2010,** *39,* 1338–1354. doi:10.1039/b901978m
21. Evans, R. A. *Aust. J. Chem.* **2007,** *60,* 384–395. doi:10.1071/CH06457
22. Binder, W. H.; Sachsenhofer, R. *Macromol. Rapid Commun.* **2008,** *29,* 952–981. doi:10.1002/marc.200800089
23. Meldal, M. *Macromol. Rapid Commun.* **2008,** *29,* 1016–1051. doi:10.1002/marc.200800159
24. Johnson, J. A.; Finn, M. G.; Koberstein, J. T.; Turro, N. J. *Macromol. Rapid Commun.* **2008,** *29,* 1052–1072. doi:10.1002/marc.200800208
25. Liang, L.; Astruc, D. *Coord. Chem. Rev.* **2011,** *255,* 2933–2945. doi:10.1016/j.ccr.2011.06.028
26. Fournier, D.; Hoogenboom, R.; Schubert, U. S. *Chem. Soc. Rev.* **2007,** *36,* 1369–1380. doi:10.1039/B700809K
27. Presolski, S. I.; Hong, V. P.; Finn, M. G. Copper-Catalyzed Azide–Alkyne Click Chemistry for Bioconjugation. *Current Protocols in Chemical Biology;* 2011; Vol. 3, pp 153–162. doi:10.1002/9780470559277.ch110148
28. El-Sagheer, A. H.; Brown, T. *Chem. Soc. Rev.* **2010,** *39,* 1388–1405. doi:10.1039/b901971p

29. Amblard, F.; Cho, J. H.; Schinazi, R. F. *Chem. Rev.* **2009,** *109,* 4207–4220. doi:10.1021/cr9001462
30. Le Droumaguet, C.; Wang, C.; Wang, Q. *Chem. Soc. Rev.* **2010,** *39,* 1233–1239. doi:10.1039/B901975H
31. Arseneault, M.; Wafer, C.; Morin, J.-F. *Molecules* **2015,** *20,* 9263. doi:10.3390/molecules20059263
32. Rodionov, V. O.; Fokin, V. V.; Finn, M. G. *Angew. Chem.* **2005,** *117,* 2250–2255. doi:10.1002/ange.200461496
33. Berg, R.; Straub, B. F. *Beilstein J. Org. Chem.* **2013,** *9,* 2715–2750. doi:10.3762/bjoc.9.308
34. Worrell, B. T.; Malik, J. A.; Fokin, V. V. *Science* **2013,** *340,* 457–460. doi:10.1126/science.1229506
35. Schoffelen, S.; Meldal, M. *Modern Alkyne Chemistry;* Wiley-VCH: Weinheim, Germany, 2014; pp 113–142.
36. Jin, L.; Tolentino, D. R.; Melaimi, M.; Bertrand, G. *Sci. Adv.* **2015,** *1,* e1500304. doi:10.1126/sciadv.1500304
37. Makarem, A.; Berg, R.; Rominger, F.; Straub, B. F. *Angew. Chem., Int. Ed.* **2015,** *54,* 7431–7435. doi:10.1002/anie.201502368
38. Shao, C.; Cheng, G.; Su, D.; Xu, J.; Wang, X.; Hu, Y. *Adv. Synth. Catal.* **2010,** *352,* 1587–1592. doi:10.1002/adsc.200900768
39. Gonda, Z.; Novák, Z. *Dalton Trans.* **2010,** *39,* 726–729. doi:10.1039/b920790m
40. Berg, R.; Straub, J.; Schreiner, E.; Mader, S.; Rominger, F.; Straub, B. F. *Adv. Synth. Catal.* **2012,** *354,* 3445–3450. doi:10.1002/adsc.201200734
41. Bessel, M. Rationales Design von Katalysatoren für die Kupfer-katalysierte Azid-Alkin-Cycloaddition. Ph.D. Thesis, Ruprecht-Karls-Universität Heidelberg, Germany, 2010.
42. Farrugia, L. J. *J. Appl. Crystallogr.* **2012,** *45,* 849–854. doi:10.1107/S0021889812029111
43. *Persistence of Vision Raytracer POV-Ray,* Version 3.7; , http://www.povray.org.
44. Dewick, P. M. *Essentials of Organic Chemistry: For Students of Pharmacy, Medicinal Chemistry and Biological Chemistry;* John Wiley & Sons: Hoboken, NJ, U.S.A., 2006.

License and Terms

This is an Open Access article under the terms of the Creative Commons Attribution License (http://creativecommons.org/licenses/by/2.0), which permits unrestricted use, distribution, and reproduction in any medium, provided the original work is properly cited.

The license is subject to the *Beilstein Journal of Organic Chemistry* terms and conditions: (http://www.beilstein-journals.org/bjoc)

The definitive version of this article is the electronic one which can be found at: doi:10.3762/bjoc.12.151

BEILSTEIN JOURNAL OF ORGANIC CHEMISTRY

A T-shape diphosphinoborane palladium(0) complex

Patrick Steinhoff and Michael E. Tauchert*

Letter

Open Access

Address:
Institute of Inorganic Chemistry, RWTH Aachen University, Landoltweg 1, D-52074 Aachen, Germany

Email:
Michael E. Tauchert* - Michael.Tauchert@ac.rwth-aachen.de

* Corresponding author

Keywords:
ambiphilic ligand; coordination chemistry; diphosphinoborane; organometallics; palladium

Beilstein J. Org. Chem. **2016,** *12,* 1573–1576.
doi:10.3762/bjoc.12.152

Received: 18 April 2016
Accepted: 04 July 2016
Published: 22 July 2016

This article is part of the Thematic Series "Organometallic chemistry".

Guest Editor: B. F. Straub

© 2016 Steinhoff and Tauchert; licensee Beilstein-Institut.
License and terms: see end of document.

Abstract

The reaction of CpPd(η^3-C_3H_5) with the new diphosphinoborane ligand derivative (o-PCy_2-C_6H_4)$_2$BPh ^{Cy}**DPB**^{Ph} affords the T-shape complex (^{Cy}**DPB**^{Ph})Pd(0) **9**, which was characterized by X-ray analysis.

Introduction

The amplification of traditional bidentate chelating L_2-type ligands with a tethered borane functionality (e.g., Bourissou's diphospinoborane (o-PR_2-C_6H_4)$_2$BR' ligand ^{R}**DPB**$^{R'}$) has received considerable attention [1-3], with first catalytic applications emerging [4]. The acyclic boron group in these ligands can adopt a variety of coordination modes (Figure 1) [5].

The borane can act as a σ-acceptor ligand in case of η^1-B coordination (e.g., **1** [6] and **2** [7]), or as a boron containing π-ligand adopting η^2-B,C (**3**) [8] or η^3-B,C,C coordination (**4** and **5**) [5,9,10]. Changes of the hapticity appear to have significant influence onto the reactivity of the coordinated transition metal towards substrates [8]. For zerovalent palladium complexes only few examples featuring a η^1-type Pd→B interaction have been reported [6,7]. However, these complexes require phosphines or pyridines as a stabilizing co-ligand, which can act as an inhibitor in catalytic transformations [7]. Similarly, monometallic 14 VE palladium complexes featuring a chelating diphosphine, such as in Hofmanns Rucaphos complexes **6**, are very scarce [11]. While the dative Pd→B bond is strong in zerovalent Pd(0) **DPB** complexes such as **2**, only weak Pd→B interactions have been observed for the respective Pd(II) complexes [7,12]. Discrimination by the borane functionality between the oxidations states Pd(0)/Pd(II) is of potential interest for organometallic transformations involved in homogeneous catalysis, such as the reductive elimination. Here we report the synthesis of the diphosphinoborane (o-PCy_2-C_6H_4)$_2$BPh ligand ^{Cy}**DPB**^{Ph}. ^{Cy}**DPB**^{Ph} reacts with CpPd(η^3-C_3H_5) yielding monometallic zerovalent palladium complex **9** featuring a distinct η^1-B coordination mode, without the need of a stabilizing co-ligand.

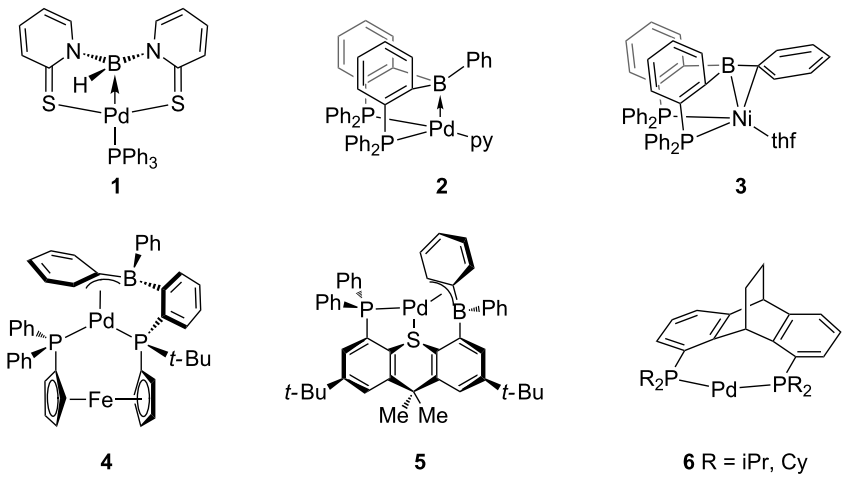


Figure 1: Selected M→B coordination modes **1**–**5** [6-10] and Hofmann's Rucaphos complex **6** [11].

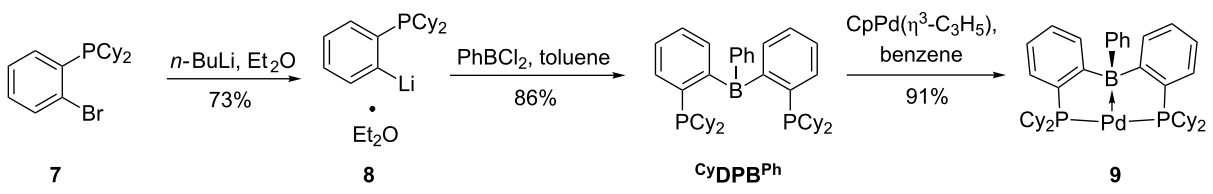
Findings

For the synthesis of ^{Cy}**DPB**^{Ph} we adapted the known reaction sequence for the production of Bourissou's (o-PPh_2-C_6H_4)$_2$BPh ligand ^{Ph}**DPB**^{Ph} (Scheme 1) [13,14].

Starting material (2-bromophenyl)dicyclohexylphosphine (**7**) was produced by palladium catalyzed coupling of dicyclohexylphosphine with 1-iodo-2-bromobenzene [15]. Phosphine **7** was lithiated in diethyl ether with *n*-BuLi [16,17], affording the diethyl ether adduct **8**. Reaction of **8** with 0.5 equiv of $PhBCl_2$ in toluene at −78 °C produced the desired ligand ^{Cy}**DBP**^{Ph} in 86% isolated yield. Typical resonances for a DPB ligand were observed in the ^{31}P NMR spectrum at δ 1.70 and in the ^{11}B NMR spectrum at δ 41 ($w_{1/2}$ = 1300 ± 120 Hz), which are indicative for a dynamic P→B bond in solution [18].

^{Cy}**DPB**^{Ph} was reacted with 1 equiv of CpPd(η^3-C_3H_5) in benzene. Complete conversion towards complex **9** with equimolar formation of 5-allylcyclopenta-1,3-diene was reached within 18 h at 50 °C. Complex **9** showed a singlet resonance at δ 41.0 in the ^{31}P NMR spectrum and a broad resonance at δ 22 ($w_{1/2}$ = 800 ± 50 Hz) in the ^{11}B NMR spectrum. High field shift and narrowing of the ^{11}B NMR with respect to the free ^{Cy}**DPB**^{Ph} ligand indicated the presence of a strong dative Pd(0)→B bond [7]. Despite the absence of a stabilizing co-ligand, we found complex **9** to be very stable in solution. The coordinating properties of ^{Cy}**DPB**^{Ph} deviate from those observed for its aryl derivatives (^{Ph}**DPB**^{Ph} ((o-PPh_2-C_6H_4)$_2$BPh) and ^{Ph}**DPB**^{Mes} ((o-PPh_2-C_6H_4)$_2$B(Mes))). For these ligands the reaction with one equivalent of CpPd(η^3-C_3H_5) leads to 50% consumption of CpPd(η^3-C_3H_5) with simultaneous formation of 5-allylcyclopenta-1,3-diene, but complete conversion of the ligand pointing towards the formation of a bisligand complex (DPB)$_2$Pd [7]. Unlike complex **2** we were unable to form a pyridine adduct complex by treatment of **9** with 10 equiv of pyridine. Single crystals of complex **9** suitable for X-ray diffraction analysis were grown from hexane (Figure 2).

The solid-state structure of **9** displayed a slightly distorted T-shape geometry around the palladium center. A short Pd1–B1 distance of 2.243(2) Å (cf. complex **2**: 2.194(3) Å) and a significant pyramidalization at the boron center (ΣB_α = 341°) is observed, indicating a strong Pd(0)→B bond. The distance between C20 and Pd1 was found to be 3.0805(22) Å. The η^1-B coordination mode was well reproduced by DFT calculations (Supporting Information File 1). DFT calculations predict



Scheme 1: Synthesis of diphosphinoborane ^{Cy}**DPB**^{Ph} and complex **9**.

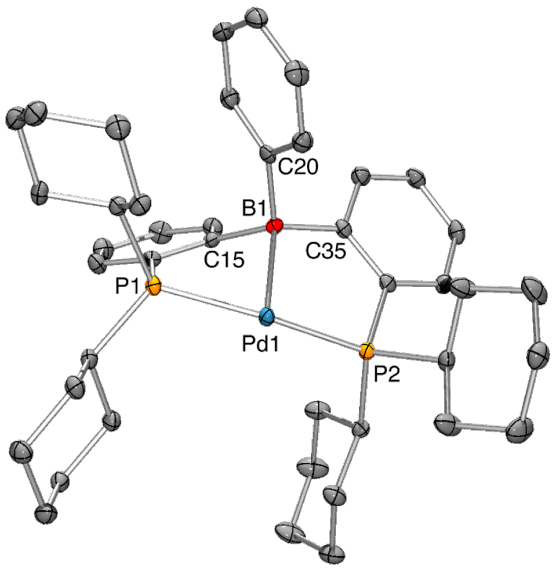


Figure 2: Thermal ellipsoid plots of complex **9** at the 50% probability level. H atoms and one molecule of hexane have been omitted for clarity. Selected interatomic distances (Å) and angles (°): Pd1–B1 2.243(2), Pd1–P1 2.2761(6), Pd1–P2 2.3084(6), B1–Pd1–P1 85.82(6), B1–Pd1–P2 82.49(6), P1–Pd1–P2 157.72(2), C15–B1–C20 110.94(18), C15–B1–C35 116.58(18), C20–B1–C35 112.56(18).

T-shape complexes with an almost linear P–Pd–P angle for model complexes $(PMe_3)_2Pd \rightarrow EX_3$ (E = B; X = H, F, Cl, Br, I) [17]. In complex **9** the *trans*-coordinated palladium center featured an obtuse P1–Pd1–P2 angle of 157.72(2)°.

Conclusion

In conclusion we synthesized the zerovalent palladium complex [{(*o*-PCy_2-C_6H_4)$_2$BPh}Pd(0)] **9**. Complex **9** supplements the few known examples (e.g., **6** [11]) of 14 VE palladium complexes bearing a chelating diphosphine ligand by introduction of a borane acceptor functionality.

Supporting Information

Supporting Information File 1

Experimental procedures and characterization data; crystallographic information for **9**; ^{1}H, ^{11}B, ^{13}C and ^{31}P NMR spectra.
[http://www.beilstein-journals.org/bjoc/content/supplementary/1860-5397-12-152-S1.pdf]

Supporting Information File 2

CIF file of **9**, CCDC 1471929.
[http://www.beilstein-journals.org/bjoc/content/supplementary/1860-5397-12-152-S2.cif]

Acknowledgements

We are grateful for financial support of this research by the Funds of the Chemical Industry (fellowships to PS and MET). We thank Q. Guo for collection of X-ray diffraction data and J. Wiesenthal for experimental assistance. We thank Prof. Dr. J. Okuda for his continuous and generous support.

References

1. Fontaine, F.-G.; Boudreau, J.; Thibault, M.-H. *Eur. J. Inorg. Chem.* **2008,** 5439–5454. doi:10.1002/ejic.200800784
2. Amgoune, A.; Bourissou, D. *Chem. Commun.* **2011,** *47,* 859–871. doi:10.1039/C0CC04109B
3. Kameo, H.; Nakazawa, H. *Chem. – Asian J.* **2013,** *8,* 1720–1734. doi:10.1002/asia.201300184
4. Bouhadir, G.; Bourissou, D. *Chem. Soc. Rev.* **2016,** *45,* 1065–1079. doi:10.1039/C5CS00697J
5. Emslie, D. J. H.; Cowie, B. E.; Kolpin, K. B. *Dalton Trans.* **2012,** *41,* 1101–1117. doi:10.1039/C1DT11271F
6. Zech, A.; Haddow, M. F.; Othman, H.; Owen, G. R. *Organometallics* **2012,** *31,* 6753–6760. doi:10.1021/om300482m
7. Schindler, T.; Lux, M.; Peters, M.; Scharf, L. T.; Osseili, H.; Maron, L.; Tauchert, M. E. *Organometallics* **2015,** *34,* 1978–1984. doi:10.1021/acs.organomet.5b00217
8. Harman, W. H.; Peters, J. C. *J. Am. Chem. Soc.* **2012,** *134,* 5080–5082. doi:10.1021/ja211419t
9. Emslie, D. J. H.; Harrington, L. E.; Jenkins, H. A.; Robertson, C. M.; Britten, J. F. *Organometallics* **2008,** *27,* 5317–5325. doi:10.1021/om800670e
10. Cowie, B. E.; Emslie, D. J. H. *Organometallics* **2015,** *34,* 4093–4101. doi:10.1021/acs.organomet.5b00539
11. Schnetz, T.; Röder, M.; Rominger, F.; Hofmann, P. *Dalton Trans.* **2008,** 2238–2240. doi:10.1039/b802684j
12. Bontemps, S.; Sircoglou, M.; Bouhadir, G.; Puschmann, H.; Howard, J. A. K.; Dyer, P. W.; Miqueu, K.; Bourissou, D. *Chem. – Eur. J.* **2008,** *14,* 731–740. doi:10.1002/chem.200701027
13. Sircoglou, M.; Bontemps, S.; Mercy, M.; Saffon, N.; Takahashi, M.; Bouhadir, G.; Maron, L.; Bourissou, D. *Angew. Chem., Int. Ed.* **2007,** *46,* 8583–8586. doi:10.1002/anie.200703518
14. Conifer, C. M.; Law, D. J.; Sunley, G. J.; White, A. J. P.; Britovsek, G. J. P. *Organometallics* **2011,** *30,* 4060–4066. doi:10.1021/om200341t
15. Murata, M.; Buchwald, S. L. *Tetrahedron* **2004,** *60,* 7397–7403. doi:10.1016/j.tet.2004.05.044
16. Harder, S.; Brandsma, L.; Kanters, J. A.; Duisenberg, A.; van Lenthe, J. H. *J. Organomet. Chem.* **1991,** *420,* 143–154. doi:10.1016/0022-328X(91)80257-K
17. Goedecke, C.; Hillebrecht, P.; Uhlemann, T.; Haunschild, R.; Frenking, G. *Can. J. Chem.* **2009,** *87,* 1470–1479. doi:10.1139/V09-099
18. Bontemps, S.; Bouhadir, G.; Dyer, P. W.; Miqueu, K.; Bourissou, D. *Inorg. Chem.* **2007,** *46,* 5149–5151. doi:10.1021/ic7006556

License and Terms

This is an Open Access article under the terms of the Creative Commons Attribution License (http://creativecommons.org/licenses/by/2.0), which permits unrestricted use, distribution, and reproduction in any medium, provided the original work is properly cited.

The license is subject to the *Beilstein Journal of Organic Chemistry* terms and conditions: (http://www.beilstein-journals.org/bjoc)

The definitive version of this article is the electronic one which can be found at: doi:10.3762/bjoc.12.152

BEILSTEIN JOURNAL OF ORGANIC CHEMISTRY

Experimental and theoretical investigations on the high-electron donor character of pyrido-annelated N-heterocyclic carbenes

Michael Nonnenmacher[1], Dominik M. Buck[2] and Doris Kunz[*1,2]

Full Research Paper

Open Access

Address:
[1]Organisch-Chemisches Institut, Ruprecht-Karls Universität Heidelberg, Im Neuenheimer Feld 250, D-69120 Heidelberg, Germany and [2]Institut für Anorganische Chemie, Eberhard Karls Universität Tübingen, Auf der Morgenstelle 18, D-72076 Tübingen, Germany (current address of corresponding author)

Email:
Doris Kunz[*] - Doris.Kunz@uni-tuebingen.de

* Corresponding author

Keywords:
carbonyl complexes; electron donor character; N-heterocyclic carbene; rhodium

Beilstein J. Org. Chem. **2016,** *12,* 1884–1896.
doi:10.3762/bjoc.12.178

Received: 17 May 2016
Accepted: 04 August 2016
Published: 23 August 2016

This article is part of the Thematic Series "Organometallic chemistry". In memoriam Professor Peter Hofmann.

Guest Editor: B. F. Straub

© 2016 Nonnenmacher et al.; licensee Beilstein-Institut.
License and terms: see end of document.

Abstract

$Rh(CO)_2Cl(NHC)$ complexes of dipyrido-annelated N-heterocyclic carbenes were prepared. From the C–H coupling constant of the respective imidazolium salts and the N–C–N angle of the N-heterocyclic carbene (NHC), a weaker σ-donor character than that of typical unsaturated NHCs is expected. However, the IR stretching frequencies of their $Rh(CO)_2Cl$ complexes suggest an electron-donor character even stronger than that of saturated NHCs. We ascribe this to the extremely weak π-acceptor character of the dipyrido-annelated NHCs caused by the conjugated 14 πe^- system that thus allows for an enhanced Rh–CO backbonding. This extremely low π-acceptor ability is also corroborated by the ^{77}Se NMR chemical shift of −55.8 ppm for the respective selenourea, the lowest value ever measured for imidazole derived selenoureas. DFT-calculations of the free carbene confirm the low σ-donor character by the fact that the σ-orbital of the carbene is the HOMO−1 that lies 0.58 eV below the HOMO which is located at the π-system. Natural population analysis reveals the lowest occupation of the p_π-orbital for the saturated carbene carbon atom and the highest for the pyrido-annelated carbene. Going from the free carbene to the $Rh(CO)_2Cl(NHC)$ complexes, the increase in occupancy of the complete π-system of the carbene ligand upon coordination is lowest for the pyrido-annelated carbene and highest for the saturated carbene.

Introduction

N-Heterocyclic carbenes form a ligand class that is typically characterized by a strong σ-donor and a weak or even negligible π-acceptor effect [1-3], although Meyer has shown pronounced π-acceptor ability in Cu complexes [4-6]. In recent years many varieties of N-heterocyclic carbenes have been synthesized [7,8], focusing mainly on a strong σ-donor character, for example by increasing the ring-size [9-15], substituting one nitrogen atom by carbon [16,17] or using diamido backbones

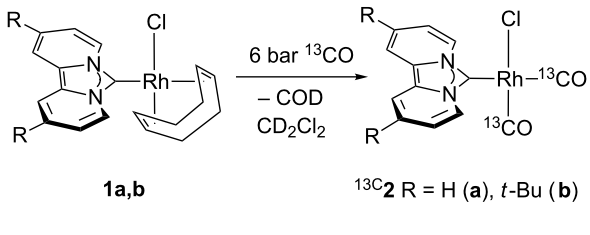
[18,19] and only rarely on enhancing the π-donor character by using π-electron donating backbones [20]. Many efforts have been made to determine and compare the donor abilities of N-heterocyclic carbenes including DFT calculations [2-6,21-24], among which are the most prominent examples: the Tolman-parameter [25-28], the ^{13}C NMR chemical shift of special Pd(NHC)$_2$ complexes [29,30], and electrochemical properties [31-33] (see [34,35] for reviews). In all these cases, only the overall donor-abilities of the NHC ligand are obtained. In the case of the Tolman parameter, not only the electronic properties of the carbene influence the CO stretching modes, but also steric effects and the coupling of stretching modes. The latter two drawbacks have recently been overcome by calculating the metal–ligand electronic parameter (MLEP) [36]. Separating the influence of the σ-donor and π-acceptor abilities was limited to determining the overall donor character and taking into account the σ-donor character. The latter is dependant on the s-character of the σ-orbital and thus can be obtained directly from the $^1J_{CH}$ coupling constant of the imidazolium salt [37-39] (which can be regarded as the H^+ complex of the carbene and therefore π-influences are avoided) or by the N–C–N angle at the carbene [40], which also correlates with the ^{13}C NMR chemical shift [41]. In 2013, Ganter presented the ^{77}Se NMR chemical shift of the respective selenoureas as a suitable probe to determine directly the π-influence of the carbene [42,43], as the paramagnetic shift tensor has the largest influence on the ^{77}Se NMR chemical shift. This method is so far redundant [44] to the method of determining the ^{31}P NMR chemical shifts of the respective NHC–phosphinidene adducts [45,46].

For some years we have worked with pyrido-annelated N-heterocyclic carbenes, an NHC class that was introduced by Weiss and co-workers (Figure 1) [39,47]. They pointed out the unusual high s-character of that carbene σ-orbital by a $^1J_{CH}$ coupling constant of 232.6 Hz, which corresponds to a hybridization of only sp$^{1.15}$. Although they had prepared the respective selenourea, the ^{77}Se NMR chemical shift was not reported [39,47,48]. We showed that the *tert*-butyl substituted dipyridocarbene dipiy^{tBu} exhibits an unusual high thermal stability and proofed the alternating bond lengths in the conjugated π-system of this carbene (similar to heptafulvalene) as well as the very low N–C–N angle by X-ray structure analysis [41]. Weiss proposed this carbene to have a "built-in umpolung" [39] ability which means that there could be a participation of the dicationic bisylidene resonance form as it is usually described for carbodiphosphoranes [49] and carbodicarbenes [50,51], in which the carbon atom has a formal oxidation state of ±0 (Figure 1) [52-54]. Earlier, we had prepared their tungsten and chromium carbonyl complexes, but could not find deviations of the CO stretching frequencies from those of analogous NHC complexes [55]. As this might be due to the distribution of the effect on five carbonyl ligands, we now prepared the [Rh(CO)$_2$Cl(dipiy)] complex to obtain a more sensitive probe. In the following we will provide the experimental evidence that dipyrido-annelated carbenes are indeed not only weak σ-donors but also the weakest π-accepting carbenes derived from imidazole so far. This overcompensates even the lower σ-donor character, so that their overall electron-donating ability lies in between that of acyclic diaminocarbenes and saturated NHCs.

Results and Discussion

Synthesis of the rhodium CO and ^{13}CO complexes **2a** and **2b**

We generated the desired carbonyl complexes **2a** and **2b** from the respective COD complex **1** [56] by ligand exchange under a ^{13}CO atmosphere of 6 bar in CD_2Cl_2 in a pressure-NMR tube according to Scheme 1.



Scheme 1: Preparation of the ^{13}CO substituted rhodium complexes **2** bearing the dipyrido-annelated carbenes dipiy (**a**) and dipiy^{tBu} (**b**).

At first, a precipitate forms which is redissolved shortly after and a color change of the solution from light yellow to greenish

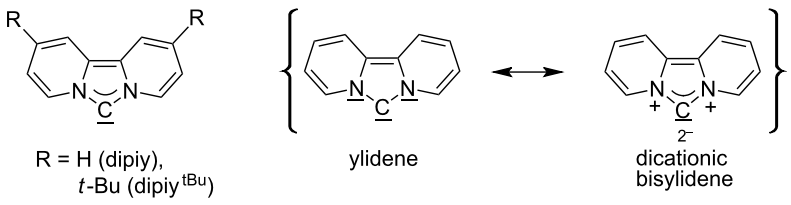


Figure 1: Left: resonance hybrid of the dipyrido carbenes dipiy and dipiy^{tBu}. Right: two canonical forms of the dipyridocarbene according to Weiss and co-workers.

yellow occurs. The ^{1}H NMR spectrum confirms full conversion and release of the COD ligand. Due to a fast exchange with the ^{13}CO atmosphere, the respective ^{13}C NMR carbonyl signals were not detected. Therefore, we measured the ^{13}C{^{1}H} NMR spectra at −30 °C. The doublet at 185.9 ppm with a $^{1}J_{RhC}$ coupling constant of 53.6 Hz refers to one ^{13}CO ligand, while a broad peak at 183.0 ppm indicates fast exchange of the second ^{13}CO ligand with non-coordinated ^{13}CO (Figure 2). Neither cooling down the sample to −50 °C nor the release of the ^{13}CO pressure to 1 bar changed the spectrum qualitatively. The sample was then shaken in an open atmosphere of nitrogen to remove the non-coordinated ^{13}CO. This led to a substantial decrease of the intensity of the broad peak, but only after three freeze-pump-thaw cycles to fully remove residual ^{13}CO the former broad signal turned into a sharp doublet of doublets at 183.2 ppm with a $^{1}J_{RhC}$ coupling of 72.8 Hz and a $^{2}J_{CC}$ coupling to the second ^{13}CO ligand of 6.1 Hz. Consequently, the former doublet at 186.3 ppm for the second ^{13}CO ligand appears now as a doublet of doublets ($^{1}J_{RhC}$ = 54.5 Hz and $^{2}J_{CC}$ = 6.1 Hz).

A comparison of the $^{1}J_{RhC}$ coupling constants with those of *cis*- and *trans*-CO Rh-NHC complexes bearing an additional P donor reveals a smaller $^{1}J_{RhC}$ coupling constant for the *trans*-CO ligand and a larger coupling constant for the *cis*-CO ligand (relative to the NHC ligand) [57]. This trend is also observed for the $^{1}J_{RhC}$ coupling constants of carbonyl complexes with phosphine ligands [58,59]. Consequently, the signal at 186.3 ppm can be assigned to the *trans*-CO ligand and that at 183.2 ppm to the *cis*-CO ligand (relative to NHC). Thus, it is the *cis*-CO ligand that undergoes a fast CO exchange. The same dynamic behavior is observed for complex ^{13C}**2b** containing the *tert*-butyl substituted dipyridocarbene ligand dipiy^{tBu}. For iridium complexes [Ir(CO)$_2$Cl(NHC)] (NHC = imidazolidin-2-ylidene) a preferred *cis*-CO exchange was reported and an activation energy of 12.7–12.9 kcal/mol was determined by NMR

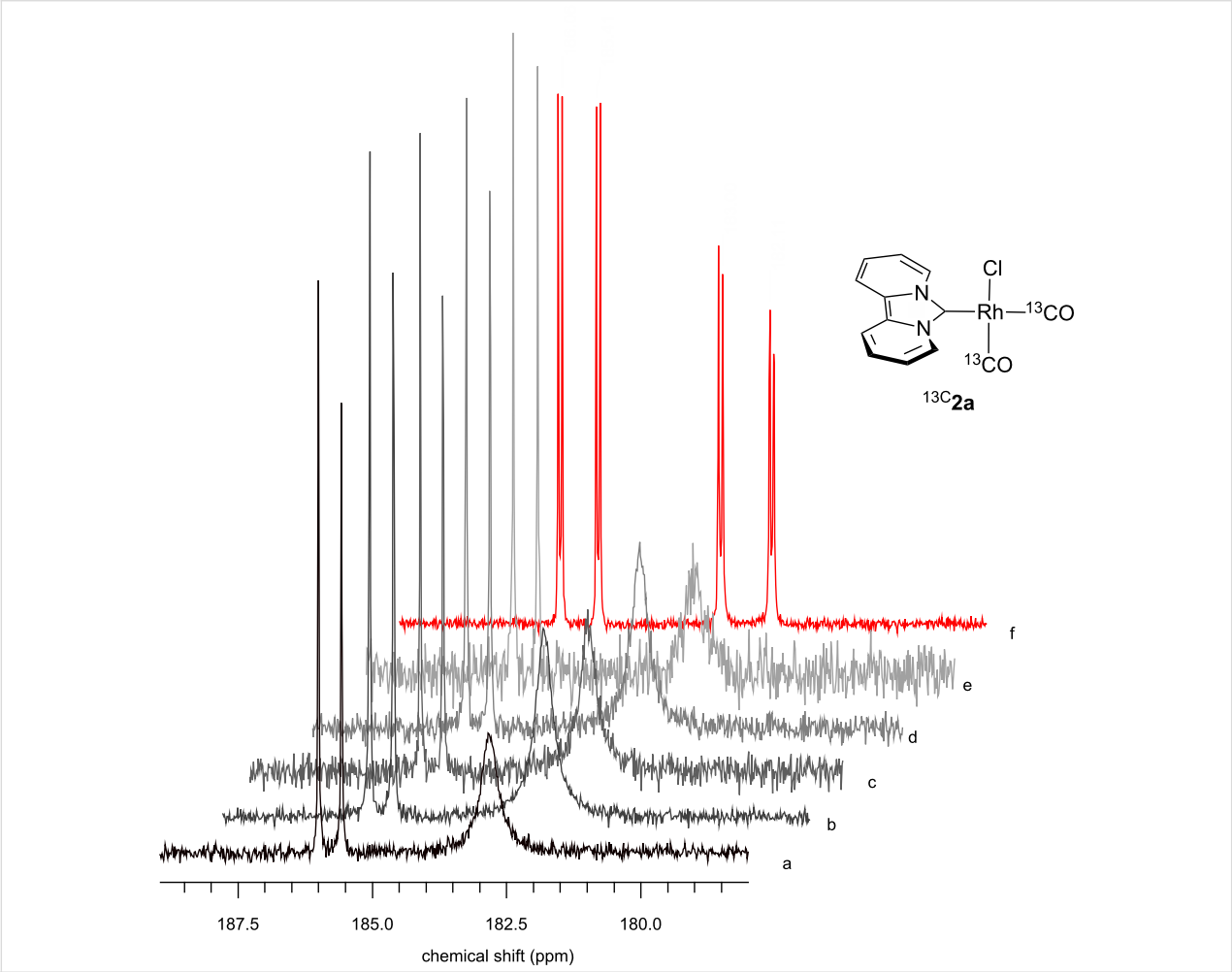


Figure 2: ^{13}C NMR spectra (carbonyl region, 125 MHz) of the reaction of **1a** with ^{13}CO under variable pressure and temperature: left: a) 6 bar ^{13}CO, −30 °C; b) 6 bar ^{13}CO, −50 °C; c) 1 bar ^{13}CO, −30 °C; d) 1 bar ^{13}CO, −50 °C; e) grey: 1 bar N_2 and residual ^{13}CO, rt; f) red: ^{13}CO-free solution, rt, 75 MHz.

spectroscopy for this process [60]. However, an exchange of the CO ligand by phosphines in $[M(CO)_2Cl(NHC)]$ complexes (M = Rh, Ir) or even by DMSO [60-62] occurs at the *trans*-CO ligand. In some cases, loss of CO upon formation of dimers can be observed for rhodium NHC complexes [63-65].

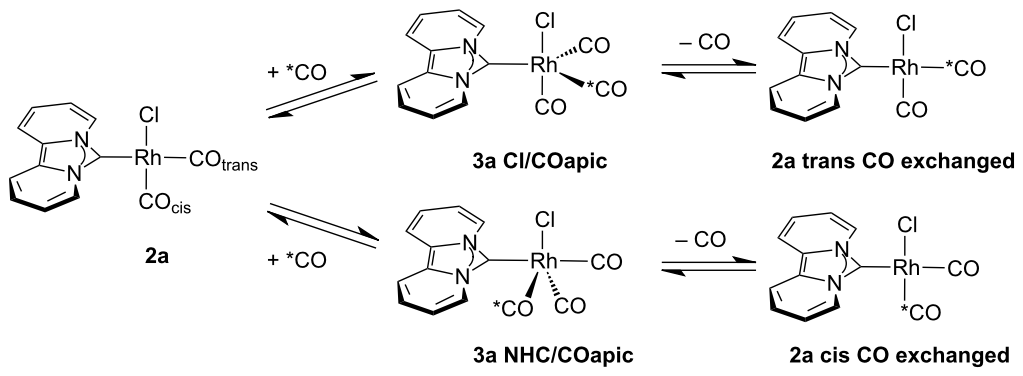
Ligand exchange in square planar Rh(I) carbonyl complexes was shown to occur by an associative mechanism via a trigonal bipyramidal intermediate [66,67], which was also crystallographically characterized in the case of a cationic Rh complex bearing a bidentate phosphine ligand [68]. Our DFT-calculations for the tricarbonyl complex **3a** bearing the dipiy ligand show that the pentacoordinated intermediate **3a NHC/COapic,** in which the NHC and the former *trans*-CO ligand take in the apical positions, is energetically favored over that with Cl^- and the former *cis*-CO ligand in the apical positions (**3a Cl/COapic**) by 16.9 kJ/mol (Scheme 2). The calculated data is similar for complexes with the unsaturated NHC ligand **III**, which favors the respective NHC/COapic intermediate by 14.9 kJ/mol. Assuming similar low activation barriers for the CO association and the dissociation, release of the CO ligand from the trigonal plane in the intermediate **3a NHC/COapic** leads to the preferred exchange of the *cis*-CO ligand (Scheme 2). This is in accordance with the experimental observation of the ^{13}CO exchange. Although the formation of **3a NHC/COapic** from **2a** and CO is exothermic ($\Delta H_{298K,1bar}$ = −11.4 kJ/mol), considering the entropy leads to an endergonic reaction ($\Delta G_{298K,1bar}$ = 29.4 kJ/mol), even at −50 °C and 6 bar ($\Delta G_{223K,6bar}$ = 15.7 kJ/mol).

On a preparative scale, complexes **2a** and **2b** were synthesized in a glass autoclave with a CO pressure of 8 bar. In both cases the carbene ^{13}C NMR signals (−30 °C, CD_2Cl_2) could be detected at 152.2 ppm ($^1J_{RhC}$ = 43.6 Hz) (**2a**) and at 150.3 ppm ($^1J_{RhC}$ = 44.4 Hz) (**2b**). The carbonyl signals are detected at 182.5 ($^1J_{RhC}$ = 72.7 Hz; *cis*-CO) and 185.9 ppm ($^1J_{RhC}$ = 54.0 Hz; *trans*-CO) for complex **2a** and at 182.8 ($^1J_{RhC}$ = 75.8 Hz; *cis*-CO) and 186.1 ppm ($^1J_{RhC}$ = 53.6 Hz; *trans*-CO) for complex **2b**.

To compare the IR stretching frequencies with other Rh-complexes in literature, we determined the symmetric and asymmetric CO stretching modes of complex **2a** in dichloromethane ($\tilde{\nu}$ = 2082 and 2003 cm^{-1}), dimethyl sulfoxide ($\tilde{\nu}$ = 2064 and 1984 cm^{-1}) and as a KBr pellet ($\tilde{\nu}$ = 2073 and 1993 cm^{-1}). This large medium dependence shows that it is mandatory to compare the stretching frequencies analyzed in the same medium. As the difference of the symmetric and the asymmetric CO stretching frequencies is not constant, it is common to compare the average value of these two bands. Table 1 gives an overview of the CO stretching frequencies of $[Rh(CO)_2Cl(L)]$ complexes with the most common types of NHC ligands L.

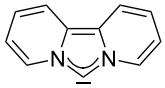
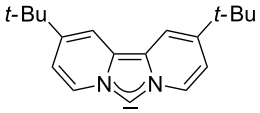
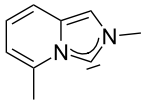
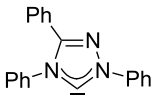
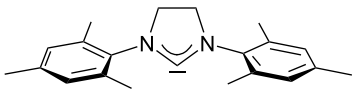
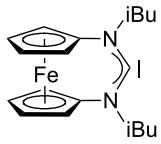
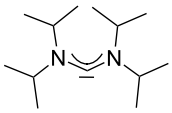
A graphical illustration of these values is depicted in Figure 3. It shows that the dipyrido-annelated carbenes have an overall donor capacity that lies in between that of acyclic (**Ia**) or ferrocene bridged (**Ib**) diaminocarbenes and saturated imidazolidin-2-ylidenes (**II**). This is surprising, as the σ-donor character of dipyridocarbenes is lower than that of the unsaturated imidazolin-2-ylidenes (**III**) and triazolinylidenes (**IV**), as it can be derived from the low N–C–N angle (99.6°) which enhances the s-character of the carbene σ-orbital and thus reduces the σ-donor character (deduced directly from the larger $^1J_{CH}$ coupling constant of the respective imidazolium salts that correlates with the higher s-character in the C–H bond). Therefore, we expected the average CO stretching frequencies to lie about 15 cm^{-1} higher at around 2050 cm^{-1} for complexes **2a** and **2b**.

This discrepancy can be explained by a substantial lower π-acceptor character than the generally low π-acceptor char-



Scheme 2: Proposed mechanism for the preferred exchange of the *cis*-CO ligand based on DFT-calculations (BP86 / def2-TZVP) with the dipiy ligand. Intermediate **3a NHC/COapic** is lower in energy by 16.9 kJ/mol compared to intermediate **3a Cl/COapic**.

Table 1: IR carbonyl stretching frequencies of $[Rh(CO)_2Cl(L)]$ complexes bearing various diaminocarbenes (L).

L in $[Rh(CO)_2Cl(L)]$	L	$\tilde{\nu}$ cm^{-1}	ν_{av} cm^{-1} Ø	method
	dipiy [39]	2072.8 1993.2	2033.0	KBr, rt
		2082.1 2003.1	2042.6	CH_2Cl_2, rt
		2064 1984	2024	DMSO, rt
	dipiy^{tBu} [41]	2074.5 1996.6	2035.6	KBr, rt
	**V** [69]	2079.0 2000.0	2039.5	CH_2Cl_2, rt
	**IV** [70]	2089.0 2009.0 [71]	2049.0	KBr, rt
	**III** [72]	2076 2006 [73]	2041.0	KBr, rt
	**IIa** [74]	2081.0 1997.0 [75]	2039.0	KBr, rt
	**Ib** [14]	2072 1994	2033	KBr, rt
		2075 1995	2035	CH_2Cl_2, rt
	**Ia** [76]	2056.0 1985.0 [75]	2020.5	KBr, rt

acter of carbenes. This may even be considered as a π-donor character – as proposed by Weiss and co-workers – to overcompensate the reduced σ-donor property. The description of Weiss and co-workers that dipyridocarbenes had a structural relationship "with "true" bis(ylides) such as carbodiphosphoranes" [39] illustrates very nicely the experimentally determined high overall donor effect of the dipyridocarbene reported herein.

The reason for this behavior seems to be the cross-conjugated 14 πe^- system into which the "empty" p_π-orbital of the carbene is embedded and therefore, could also act as a π-electron donor. To obtain further experimental evidence for this unusually weak π-acceptor (or already weak π-donor character), we determined the ^{77}Se NMR chemical shift of the respective selenourea **4b** to be −55.8 ppm [77]. This value is the most negative reported so far for imidazole derived selenoureas and therefore, is another hint for the unusually low π-accepting quality of the dipyridocarbene family dipiy.

To rationalize these strong overall donating properties we performed DFT calculations of the free dipyridocarbene dipiy and its $Rh(CO)_2Cl$ complex **2a**, as well as the acyclic (**I**, **I-Rh**, **Ia**, **Ia-Rh**), saturated (**II**, **II-Rh**) and unsaturated (**III**, **III-Rh**) diaminocarbenes and their rhodium complexes.

Firstly, we could confirm the trend of the IR stretching frequencies for the calculated complexes although the differences are smaller between **Ia-Rh, 2a**, **II-Rh** and **III-Rh** (Table 2) than observed experimentally. The complex with the isopropyl acyclic carbene **Ia-Rh** shows its unique electron donating effect also in the calculations. The smaller differences found for the calculated CO stretching frequencies are independent of the used functionals (BP86 and B3LYP). Both functionals lead to

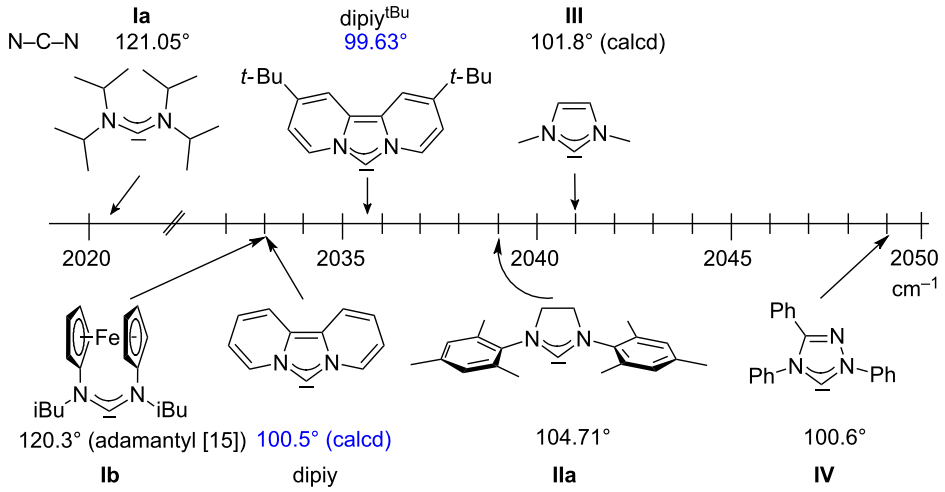
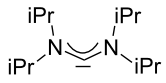
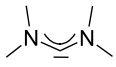
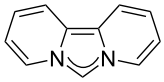


Figure 3: IR scale (cm^{-1}) to determine the overall electron-donor capacity of various N-heterocyclic carbenes based on the average wavenumber $\tilde{\nu}_{av}$ of the CO stretching frequencies of their respective $Rh(CO)_2Cl$ complexes. The strongest donating NHCs are found on the left side (lower $\tilde{\nu}_{av}$), the weakest on the right side (higher $\tilde{\nu}_{av}$). In addition the N–C–N angles are given (from X-ray, if not marked otherwise. For **Ib** the mean value for the *N*-adamantyl substituted species is given).

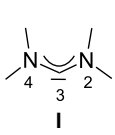
Table 2: Calculated values $\tilde{\nu}$ for the symmetric and asymmetric CO stretching frequencies as well as the average $\tilde{\nu}_{av}$ of various $Rh(CO)_2Cl$(Carbene) complexes (BP86/def2-TZVP or B3LYP/def2-TZVP) and numbering scheme for the DFT-calculations of the respective carbene.

L	 **Ia**	 **I**	 dipiy	 **II**	 **III**
$Rh(CO)_2Cl(L)$	**Ia-Rh**	**I-Rh**	**2a**	**II-Rh**	**III-Rh**
$\tilde{\nu}_{asym}/cm^{-1}$ $\tilde{\nu}_{sym}/cm^{-1}$ (BP86)	1972.4 2047.3	1979.7 2052.6	1983.8 2055.4	1984.1 2056.5	1984.1 2056.8
$\tilde{\nu}_{av}/cm^{-1}$ (BP86)	2009.8	2016.1	2019.6	2020.3	2020.5
$\tilde{\nu}_{asym}/cm^{-1}$ $\tilde{\nu}_{sym}/cm^{-1}$ (B3LYP)	–	2057.2 2138.9	2062.4 2141.5	2062.2 2142.5	2062.3 2143.2
$\tilde{\nu}_{av}/cm^{-1}$ (B3LYP)	–	2098.0	2102.0	2102.4	2102.7

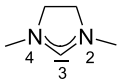
comparable results with respect to the experimental values when calibrated to free CO (2125 cm^{-1} (BP86), 2208 cm^{-1} (B3LYP), exp. 2143 cm^{-1}).

To obtain information to which extent the carbene ligands act as an overall π-electron acceptor (or π-donor), we analyzed the electron occupation of the respective p_π-orbital at the carbene performing a natural population analysis [78] (Table 3). As expected the stronger stabilization of the p_π orbital within the conjugated 14 πe^- system results in a higher occupation for the carbene dipiy (0.738) at C3, which decreases in the order 6 πe^- carbene **III** (0.687), 4 πe^- carbene **II** (0.592) and the acyclic 4πe^- carbene **I** (0.618) (Table 3). For the rhodium complexes these values are higher, so that an overall π-electron-withdrawing character of the carbene ligand can be concluded. It is surprising that the largest increase in electron occupancy (ΔRh-NHC e^- (C3)) is found for the dipyridocarbene dipiy (0.16) and the weakest for the acyclic carbene (**I**) (0.12). However, the increase must not necessarily stem from electron density of the metal center. It could also originate from the π-system of the respective carbene. Therefore, we also calculated the sum of the p_π-electron occupancy for the free carbene as well as for the complex (which should sum up to 4 e^- (**I** and **II**), 6 e^- (**III**) or 14 e^- (dipiy), respectively). It now becomes clear that the overall gain in π-electron occupancy $\Delta_{Rh\text{-}NHC}$ e^- is highest in the case of the saturated carbene **II** (0.08) and

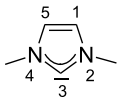
Table 3: Electron occupation (e^-) of the p_π orbital at the carbene atom C3 and at the other atoms of the π-system in the free carbenes **I–III** and dipiy and in their Rh carbonyl complexes.



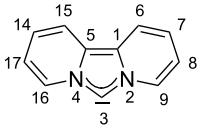
I



II



III



dipiy

	I	I-Rh	II	II-Rh	III	III-Rh	dipiy	2a
C1					1.09029	1.07851	1.08021	1.07529
N2	1.63207	1.60438	1.64093	1.61073	1.54167	1.51623	1.47370	1.45994
C3	0.61791	0.73749	0.59200	0.72812	0.68712	0.82047	0.73731	0.89882
N4	1.63228	1.60384	1.64069	1.61126	1.54169	1.51738	1.47369	1.46334
C5					1.09032	1.07994	1.08021	1.08121
C6							1.00124	1.00100
C7							1.03216	1.00947
C8							1.03375	1.01227
C9							0.98590	0.97578
C14							1.03216	1.01769
C15							1.00123	0.99519
C16							0.98589	0.99538
C17							1.03375	1.01041
Σ πe^-	3.88226	3.94571	3.87362	3.95011	5.95109	6.01253	13.95120	13.99579
$\Delta_{Rh\text{-}NHC}$ e^- (C3)		0.11958		0.13612		0.13335		0.16151
$\Delta_{Rh\text{-}NHC}$ e^- (π)		0.06345		0.07649		0.06144		0.04459

smallest for the dipyridocarbene dipiy (0.04). It may therefore be concluded that dipiy is the carbene with the weakest π-acceptor character. In addition, the role of a potential net π-donor character of the dipyridocarbene dipiy can be ruled out in the Rh complex **2a**. A less electron-rich metal center might induce a net π-donor property in this carbene.

It is known from theoretical studies that a reduction of the N–C–N angle leads to a stabilization of the carbene σ-orbital [40]. At the same time the extended conjugated π-system leads to an energy increase of the highest occupied π-orbital and a smaller HOMO–LUMO gap. Analyzing the molecular orbitals of the free carbenes **I**–**III** and dipiy reveals that in dipiy the carbene σ-orbital is no longer the highest occupied orbital, but it is found stabilized by 0.58 eV as the HOMO−1 (−5.18 eV). The HOMO at −4.60 eV is located at the π-system (see Figure 4). This has only been observed for the bisoxazoline-derived IBioxMe4 carbene before, whose calculated N–C–N angle of 98.6° is even more acute than that of dipiy [79]. For dipiy the other 6 occupied MOs of the 14 πe^- system are found between −6.28 eV and −11.7 eV (HOMO−2 to HOMO−5, HOMO−10 and HOMO−14, see Supporting Information File 1 for a graphi-

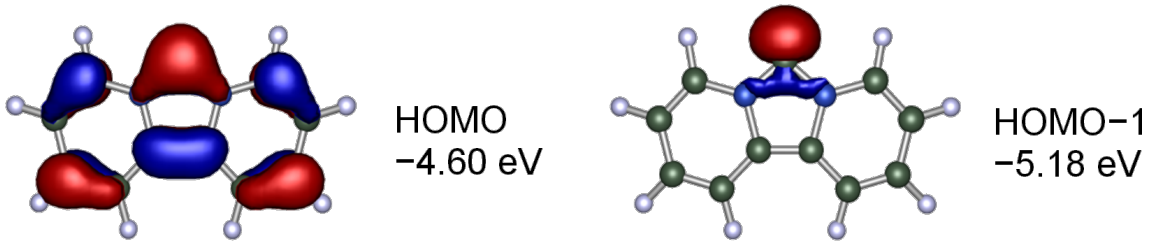


Figure 4: Highest occupied molecular orbitals for the dipyrido-annelated carbene dipiy. The σ-type carbene lone pair is not the HOMO but the HOMO−1.

cal comparison of the highest occupied MOs of **I–III** and dipiy).

The energy gain (ΔE_σ) of the σ-orbitals upon coordination to the rhodium fragment is by far highest for the acyclic carbene **I** (4.14 eV) and lowest for the dipyridocarbene carbene dipiy (3.30 eV) (**II**: 3.57 eV; **III**: 3.66 eV) which displays the order of decreasing σ-donor character (and the decreasing N–C–N angle) of these carbenes.

For the Rh-complexes **I-Rh**–**III-Rh** two type of orbitals that indicate a ligand to metal π-donor bond are revealed. One is found for the **II-Rh** complex between the HOMO−2 of the ligand and the d_{xy} orbital of Rh (plus contributions of the chlorido and the antibonding π-orbital of the *cis*-CO ligand) at −9.07 eV (HOMO−9) (Figure 5). The other is found between the HOMO−1 of the carbene ligand and the d_{xy} orbital of Rh in complex **III-Rh** (plus contributions of the chlorido and the antibonding π-orbital of the *cis*- and *trans*-CO ligands) at −7.85 eV. In the case of the dipiy ligand both of these orbital types are recognized at −7.61 eV (HOMO−8) and −9.13 eV (HOMO−12). Tentatively, this could indicate an overall stronger π-donor contribution of this ligand. A molecular orbital that shows an in plane metal-to-ligand π-interaction with the carbene σ*(C–N) orbitals [79] was not observed.

Explaining the observed CO stretching frequencies

The CO stretching frequencies of imidazolium-derived carbene complexes of Rh are influenced by the sum of σ and π-donor as well as the π-acceptor character of the carbenes. In acyclic diaminocarbene complexes of type **I** the strong σ-donor character dominates as evidenced by the large N–C–N angles and the high lying σ-orbital (HOMO). In the case of complex **Ia-Rh** bearing the isopropyl substituted carbene **Ia**, the steric hindrance of the *N*-isopropyl substituents causes an even larger N–C–N angle. This leads to a further reduction of the s-character and thus an increased σ-donor character that explains the pronounced shift to smaller wavenumbers. According to our DFT calculations, the saturated and unsaturated carbenes have an almost similar donor character so that the weaker σ-donor character is almost compensated by a reduced π-acceptor character. In complexes **2a** and **2b** bearing the pyrido-annelated carbenes dipiy and dipiy^{tBu}, the extremely weak π-acceptor character overcompensates the weaker σ-donor effect, so that the overall donor property of the carbene increases and results in CO stretching frequencies that lie in between those of the acyclic (**I-Rh**) and the saturated carbene complex (**II-Rh**).

Conclusion

We prepared and analyzed both experimentally and theoretically the dipyridocarbene rhodium carbonyl complexes **2a** and **2b**. We showed that the CO exchange of the *cis*-CO ligand is enhanced over that of the *trans*-CO ligand. The unusually high overall donating property of the dipyridocarbenes dipiy exceeds that of imidazolidinylidenes (**II**) and was revealed by IR spectroscopy. The unusually weak π-acceptor character of the dipyridocarbenes was evidenced by the so far lowest ^{77}Se NMR chemical shift for imidazole-derived carbenes. Comparing the

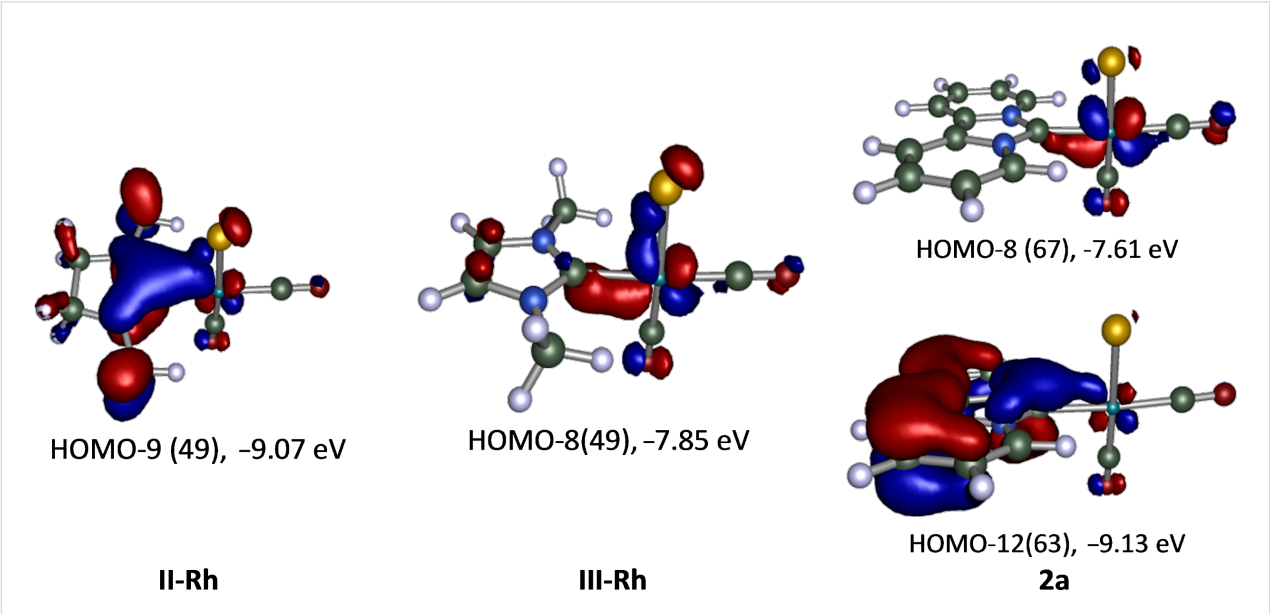


Figure 5: Molecular orbitals of the Rh complexes **II-Rh**, **III-Rh** and **2a** that show ligand-metal π-bonds.

electron occupancy in the π-system of the free and the coordinated carbene revealed still a, although very low, net π-acceptor character of the dipyridocarbene. We are convinced that less electron-rich metal fragments could induce an overall π-donor character in dipyridocarbenes and could thus proof the "built-in umpolung" [39] ability proposed by Weiss and co-workers. This property might be advantageous to stabilize low coordinated metal fragments in higher oxidation states, for example intermediates of catalytic reactions.

Experimental

General information. All reactions were carried out under an inert argon atmosphere in dried and degassed solvents using standard Schlenk techniques. All metal complexes were handled in an MBraun glovebox with a nitrogen atmosphere. Solvents were dried according to standard procedures. [Rh(dipiy)Cl(cod)] (**1a**), [Rh(dipiy^{tBu})Cl(cod)] (**1b**) [56] and the dipyridoimidazolium salt dipiy^{tBu}*HBF_4 [41] were prepared according to literature procedures. NMR spectra were recorded using Bruker instruments (DRX-250, 300 or 500). ^{1}H and ^{13}C NMR spectra were referenced to TMS on the basis of the (residual) signal of the deuterated solvent. ^{77}Se NMR shifts were calibrated towards Ph_2Se_2 (463 ppm) in $CDCl_3$ as an external standard [80]. Medium-wall NMR tubes with a PTFE valve from Wilmad were used for the NMR experiments under CO pressure. IR spectra were recorded on a Bruker Equinox 55 FTIR spectrometer as a KBr pellet or in solution. Mass spectra were recorded on a Jeol JMS-700 and the melting point was determined with a Büchi Melting Point B 540 apparatus. The elemental analysis was carried out at Mikroanalytisches Laboratorium der Chemischen Institute of Heidelberg University. All experiments except for the synthesis and the analysis of the selenourea **4** (Institut für Anorganische Chemie of the University of Tübingen) were carried out at the Organisch-Chemisches Institut of Heidelberg University.

Calculations. All calculations were performed based on density functional theory at the BP86/def2-TZVP [81-85] or B3LYP/def2-TZVP [86-88] level implemented in Turbomole [89-97]. The RI-approximation [98-103] and def2-ecp [104] for Rh were used all over (in case of compounds **3a** also the D3-correction [105]). All structures were verified to be minimum structures by calculating Hessian matrices and ensuring that they have no imaginary frequency. Graphics of the MOs were prepared using POV-Ray^{TM} [106].

NMR experiment for the in situ generation of [Rh(^{13}CO)$_2$Cl(dipyrido[1,2-*c*;2',1'-*e*]imidazolin-6-ylidene)] (^{13C}2a). A medium wall NMR tube was charged with a yellow solution of 6.0 mg (15 μmol) [RhCl(COD)(dipiy)] (**1a**) in 0.4 mL CD_2Cl_2 and pressurized with 6 bar of ^{13}CO upon which a yellow precipitate formed that dissolved immediately and the solution turned greenish yellow. The signals of non-coordinated COD were observed as the only side product. ^{1}H NMR (300.13 MHz, CD_2Cl_2) δ 7.07–7.13 (m, 4H, 2-H, 3-H, 9-H, 10-H), 7.92–7.97 (m, 2H, 1-H, 11-H), 8.92–8.97 (m, 2H, 4-H, 8-H); Contains free COD: δ = 2.31–2.36 (m, 8H, CH_2), 5.54–5.57 (m, 4H, CH); ^{13}C{^{1}H} NMR (75.5 MHz, CD_2Cl_2) δ 117.6 (C3, C9), 118.2 (C1, C11), 120.7 (C2, C10), 127.3 (C4, C8), 184.3 (free CO), 186.3 (d, $^1J_{RhC}$ = 54.6 Hz, *trans*-^{13}CO). The signals of C6 and C11a/11b were not detected; contains free COD (δ 28.6 (CH_2), 184.3 (CH)).

NMR experiment of in situ generated (^{13C}2a) at variable temperature. The experiment was repeated with a sample containing 7.0 mg (17 μmol) [RhCl(COD)(dipiy)] (**1a**) in 0.4 mL CD_2Cl_2 at 6 bar ^{13}CO. NMR spectra were recorded at −30 °C and −50 °C. Then the pressure was released and NMR spectra were recorded at −50 °C and −30 °C. Afterward the sample was opened under nitrogen atmosphere and shaken to release free ^{13}CO. NMR spectra were recorded at room temperature. Finally the solution was transferred to a regular J. Young® NMR tube and any residual ^{13}CO removed by three freeze-thaw cycles using liquid nitrogen. The NMR spectra of the sample were then recorded at room temperature. All spectra ^{13}C{^{1}H} NMR (125.8 MHz, CD_2Cl_2, only carbonyl region) 243 K, 6 bar ^{13}CO: δ 183.0 (broad peak, free and *cis*-^{13}CO), 185.9 (d, $^1J_{RhC}$ = 53.6 Hz, *trans*-^{13}CO); 223 K, 6 bar ^{13}CO: δ 182.8 (broad peak, free and *cis*-^{13}CO), 185.7 (d, $^1J_{RhC}$ = 53.6 Hz, *trans*-^{13}CO); 223 K, 1 bar ^{13}CO: δ 182.8 (free and *cis*-^{13}CO), 185.7 (d, $^1J_{RhC}$ = 53.6 Hz, *trans*-^{13}CO); 243 K, 1 bar ^{13}CO: δ 182.9 (free and *cis*-^{13}CO), 185.9 (d, $^1J_{RhC}$ = 53.6 Hz, *trans*-^{13}CO); 298 K, 1 bar N_2: δ 183.5 (free and *cis*-^{13}CO), 186.3 (d, $^1J_{RhC}$ = 55.5 Hz, *trans*-^{13}CO); 298 K, 1 bar N_2, after freeze-thaw cycles: δ 183.2 (dd, $^1J_{RhC}$ = 72.8 Hz, $^2J_{CC}$ = 6.1 Hz, *cis*-^{13}CO), 186.3 (dd, $^1J_{RhC}$ = 54.5 Hz, $^2J_{CC}$ = 6.1 Hz, *trans*-^{13}CO).

NMR experiment for the in situ generation of [Rh(^{13}CO)$_2$Cl(2,10-di-*tert*-butyldipyrido[1,2-*c*;2',1'-*e*]imidazolin-6-ylidene)] (^{13C}2b). A medium-wall NMR tube was charged with a yellow solution of 10.0 mg (20.0 μmol) [RhCl(COD)(dipiy^{tBu})] (**1b**) in 0.4 mL CD_2Cl_2 and pressurized with 6 bar of ^{13}CO. The signals of non-coordinated COD were observed as the only side product. ^{1}H NMR (300.13 MHz, CD_2Cl_2) δ 1.39 (s, 18H, C(CH_3)$_3$), 7.13 (dd, $^3J_{HH}$ = 7.5 Hz, $^4J_{HH}$ = 1.9 Hz, 2H, 3-H, 9-H,), 7.76 (bs, 2H, 1-H, 11-H), 8.82 (d, $^3J_{HH}$ = 7.5 Hz, 2H, 4-H, 8-H). Contains free COD (δ 2.35 (br m, 8H, CH_2), 5.55 (br m, 4H, CH); ^{13}C{^{1}H} NMR (75.5 MHz, CD_2Cl_2) δ 30.6 (C(CH_3)$_3$), 35.4 (C(CH_3)$_3$), 112.0 (C1, C11), 117.2 (C3, C9), 123.9 (C11a, C11b), 126.7 (C4, C8), 143.9 (C2, C10), 184.1 (broad peak, free and *cis*-^{13}CO) 186.6

(d, $^1J_{RhC}$ = 55.4 Hz, *trans*-^{13}CO). The carbene signal C6 was not detected; contains free COD (δ 28.6 (CH_2), 129.2 (CH)).

Synthesis of [Rh(CO)$_2$Cl(dipyrido[1,2-*c*;2',1'-*e*]imidazolin-6-ylidene)] (2a). In a 25 mL-size glass autoclave was dissolved [RhCl(COD)(dipiy)] (**1a**) (60.0 mg, 150 μmol) in 5 mL dichloromethane and pressurized with CO (8 bar) upon which an immediate color change to green was observed. Afterwards the pressure was released and all volatiles removed in vacuo. The light yellow residue was washed two times with pentane (1 mL each) and dried in vacuo to obtain the carbonyl complex **2a** in 93% yield (47.0 mg, 130 μmol). Mp 259–262 °C (dec); ^{1}H NMR (300.13 MHz, CD_2Cl_2) δ 7.07–7.14 (m, 4H, 2-H, 3-H, 9-H, 10-H), 7.93–7.96 (m, 2H, 1-H, 11-H), 8.93–8.96 (m, 2H, 4-H, 8-H); ^{13}C{^{1}H} NMR (−30 °C, 75.5 MHz, CD_2Cl_2) δ 117.3 (C3, C9), 117.8 (C1, C11), 120.2 (C2, C10), 123.4 (C11a, C11b), 126.4 (C4, C8), 152.2 (d, $^1J_{RhC}$ = 43.6 Hz, C6), 182.5 (d, C_{CO}, $^1J_{RhC}$ = 72.7 Hz, *cis*-CO), 185.9 (d, $^1J_{RhC}$ = 54.0 Hz, *trans*-CO); IR (KBr, cm^{-1}) $\tilde{\nu}$: 3105 (w), 3058 (w), 2963 (w), 2073 (s, CO), 1993 (s, CO), 1622 (w), 1355 (w), 1331 (w), 739 (m), 704 (w); (CH_2Cl_2, cm^{-1}) $\tilde{\nu}$: 2082 (m, CO), 2003 (m, CO); (DMSO, cm^{-1}) $\tilde{\nu}$: 2064 (m, CO), 1984 (m, CO); MS (FD$^+$, LIFDI$^+$ in CH_2Cl_2) *m*/*z*: 362.0 [M$^+$]; anal. calcd for $C_{13}H_8ClN_2O_2Rh$: C, 43.06; H, 2.39; N, 7.73; found: C, 42.88; H, 2.22; N, 7.65.

Synthesis of [Rh(CO)$_2$Cl(2,10-di-*tert*-butyldipyrido[1,2-*c*;2',1'-*e*]imidazolin-6-ylidene)] (2b). [RhCl(COD)(dipiy^{tBu})] (**1b**) (15.0 mg, 30.0 μmol) was dissolved in 2.5 mL dichloromethane and pressurized with CO (8 bar) in a 10 mL-size glass autoclave. After 10 min the pressure was released and all volatiles were removed in vacuo. The residue was washed with pentane (1 mL) and dried in vacuo to obtain about 50% (7.0 mg, 15 μmol) of the carbonyl complex **2b** as a yellow solid. ^{13}C{^{1}H} NMR (243 K, 125.8 MHz, CD_2Cl_2) δ 30.0 (C(CH$_3$)$_3$), 35.0 (C(CH$_3$)$_3$), 111.5 (C1, C11), 116.9 (C3, C9), 123.2 (C11a, C11b), 126.1 (C4, C8), 143.2 (C2, C10), 150.3 (d, $^1J_{RhC}$ = 44.4 Hz, C6), 182.8 (d, $^1J_{RhC}$ = 75.8 Hz, *cis*-CO), 186.1 (d, $^1J_{RhC}$ = 53.6 Hz, *trans*-CO); IR (KBr, cm^{-1}) $\tilde{\nu}$: 2962 (s), 2868 (m), 2075 (s, CO), 1997 (s, CO), 1659 (w), 1533 (w), 1475 (w), 1366 (w), 1335 (w), 1300 (w), 1267 (m), 964 (m), 873 (w), 789 (m), 638 (m), 590 (m); HRMS (FAB$^+$ in NBA) *m*/*z*: 446.0612 [M(^{35}Cl) − CO$^+$] (calcd 446.0632), 448.0596 [M(^{37}Cl) − CO$^+$] (calcd 448.0603), 474.0584 [M(^{35}Cl)$^+$] (calcd 474.0581), 476.0581 [M(^{37}Cl)$^+$] (calcd 476.0552).

Synthesis of 2,10-di-*tert*-butyldipyrido[1,2-*c*:2′,1′-*e*]imidazolin-6-selenone (4b). A suspension of 2,10-di-*tert*-butyldipyrido[1,2-*c*:2′,1′-*e*]imidazolium tetrafluoroborate [41] (40.5 mg, 110 μmol) and selenium (32.1 mg, 407 μmol) in 3 mL of tetrahydrofuran was cooled to −35 °C and a solution of potassium *tert*-butoxide (14.9 mg, 133 μmol) in 1 mL tetraydrofuran was added. After 30 min the deep red suspension was warmed up to room temperature and stirred overnight. The solvent was removed in vacuo and the residue suspended in 7 mL of dichloromethane. After filtration through a pipette containing glass wool and 3 cm of Celite®, the red solution was concentrated to dryness in vacuo to yield 33.2 mg (84%) of the product as a red solid. ^{1}H NMR (250.13 MHz, $CDCl_3$) δ 1.38 (s, 18H, *t*-Bu), 7.19 (dd, $^3J_{HH}$ = 7.7 Hz, $^4J_{HH}$ = 1.9 Hz, 2H, 3-H, 9-H), 7.65 (dd, $^4J_{HH}$ = 1.9 Hz, $^5J_{HH}$ = 1.0 Hz, 2H, 1-H, 11-H), 8.73 (dd, $^3J_{HH}$ = 7.7 Hz, $^5J_{HH}$ = 1.0 Hz, 2H, 4-H, 8-H); ^{13}C{^{1}H} NMR (62.9 MHz, $CDCl_3$) δ 30.2 (C(CH$_3$)$_3$), 34.8 (C(CH$_3$)$_3$), 111.0 (C1, C11), 116.2 (C3, C9), 120.6 (C11a, C11b), 124.2 (C4, C8), 131.9 (C6), 142.6 (C2, C10); ^{77}Se NMR (47.70 MHz, $CDCl_3$) δ −55.8 (s, Se); HRMS (ESI$^+$) *m*/*z*: 360.11023 [M$^+$] (calcd 360.10992).

Supporting Information

Supporting Information File 1

NMR spectra of compounds **2a**, **2b** and **4b** as well as details of the DFT calculations.
[http://www.beilstein-journals.org/bjoc/content/supplementary/1860-5397-12-178-S1.pdf]

Acknowledgements

Financial help from the Deutsche Forschungsgemeinschaft (Emmy Noether-Programm (Ku 1437/2-3); Graduiertenkolleg 850 fellowship for M.N.) is gratefully acknowledged. We are thankful for continuous and generous support from Professor Peter Hofmann and we thank Professor Reinhold Fink for helpful discussions.

References

1. Öfele, K.; Herrmann, W. A.; Mihalios, D.; Elison, M.; Herdtweck, E.; Scherer, W.; Mink, J. *J. Organomet. Chem.* **1993,** *459,* 177. doi:10.1016/0022-328X(93)86070-X
2. Boehme, C.; Frenking, G. *Organometallics* **1998,** *17,* 5801. doi:10.1021/om980394r
3. Tafipolsky, M.; Scherer, W.; Öfele, K.; Artus, G.; Pedersen, B.; Herrmann, W. A.; McGrady, S. G. *J. Am. Chem. Soc.* **2002,** *124,* 5865. doi:10.1021/ja011761k
4. Hu, X.; Tang, Y.; Gantzel, P.; Meyer, K. *Organometallics* **2003,** *22,* 612–614. doi:10.1021/om020935j
5. Hu, X.; Castro-Rodrigues, I.; Olsen, K.; Meyer, K. *Organometallics* **2004,** *23,* 755–764. doi:10.1021/om0341855
6. Nemcsok, D.; Wichmann, K.; Frenking, G. *Organometallics* **2004,** *23,* 3640–3646. doi:10.1021/om049802j
7. Hahn, F. E.; Jahnke, M. C. *Angew. Chem., Int. Ed.* **2008,** *47,* 3122–3172. doi:10.1002/anie.200703883
8. Benhamou, L.; Chardon, E.; Lavigne, G.; Bellemin-Laponnaz, S.; César, V. *Chem. Rev.* **2011,** *111,* 2705–2733. doi:10.1021/cr100328e

9. Mayr, M.; Wurst, K.; Ongania, K.-H.; Buchmeiser, M. R. *Chem. – Eur. J.* **2004,** *10,* 1256–1266. doi:10.1002/chem.200305437
10. Bazinet, P.; Yap, G. P. A.; Richeson, D. S. *J. Am. Chem. Soc.* **2003,** *125,* 13314–13315. doi:10.1021/ja0372661
11. Iglesias, M.; Beetstra, D. J.; Knight, J. C.; Ooi, L.-L.; Stasch, A.; Coles, S.; Male, L.; Hursthouse, M. B.; Cavell, K. J.; Dervisi, A.; Fallis, I. A. *Organometallics* **2008,** *27,* 3279–3289. doi:10.1021/om800179t
12. Iglesias, M.; Beetstra, D. J.; Stasch, A.; Horton, P. N.; Hursthouse, M. B.; Coles, S. J.; Cavell, K. J.; Dervisi, A.; Fallis, I. A. *Organometallics* **2007,** *26,* 4800–4809. doi:10.1021/om7004904
13. Scarborough, C. C.; Guzei, I. A.; Stahl, S. S. *Dalton Trans.* **2009,** 2284–2286. doi:10.1039/b902460c
14. Khramov, D. M.; Rosen, E. L.; Lynch, V. M.; Bielawski, C. W. *Angew. Chem., Int. Ed.* **2008,** *47,* 2267–2270. doi:10.1002/anie.200704978
15. Siemeling, U.; Färber, C.; Bruhn, C. *Chem. Commun.* **2009,** 98–100. doi:10.1039/B813809E
16. Lavallo, V.; Canac, Y.; Präsang, C.; Donnadieu, B.; Bertrand, G. *Angew. Chem., Int. Ed.* **2005,** *44,* 5705–5709. doi:10.1002/anie.200501841
17. Soleilhavoup, M.; Bertrand, G. *Acc. Chem. Res.* **2015,** *48,* 256–266. doi:10.1021/ar5003494
18. Hudnall, T. W.; Bielawski, C. W. *J. Am. Chem. Soc.* **2009,** *131,* 16039–16041. doi:10.1021/ja907481w
19. Braun, M.; Frank, W.; Reiss, G. J.; Ganter, G. *Organometallics* **2010,** *29,* 4418–4420. doi:10.1021/om100728n
20. César, V.; Lugan, N.; Lavigne, G. *J. Am. Chem. Soc.* **2008,** *130,* 11286–11287. doi:10.1021/ja804296t
21. Cavallo, L.; Correa, A.; Costabile, C.; Jacobsen, H. *J. Organomet. Chem.* **2005,** *690,* 5407–5413. doi:10.1016/j.jorganchem.2005.07.012
22. Jacobsen, H.; Correa, A.; Costabile, C.; Cavallo, L. *J. Organomet. Chem.* **2006,** *691,* 4350–4358. doi:10.1016/j.jorganchem.2006.01.026
23. Jacobsen, H.; Correa, A.; Poater, A.; Costabile, C.; Cavallo, L. *Coord. Chem. Rev.* **2009,** *253,* 687–703. doi:10.1016/j.ccr.2008.06.006
24. Huynh, H. V.; Frison, G. *J. Org. Chem.* **2013,** *78,* 328–338. doi:10.1021/jo302080c
25. Tolman, C. A. *Chem. Rev.* **1977,** *77,* 313–348. doi:10.1021/cr60307a002
26. Chianese, A. R.; Li, X.; Janzen, M. C.; Faller, J. W.; Crabtree, R. H. *Organometallics* **2003,** *22,* 1663–1667. doi:10.1021/om021029+
27. Wolf, S.; Plenio, H. *J. Organomet. Chem.* **2009,** *694,* 1487–1492. doi:10.1016/j.jorganchem.2008.12.047
28. Dorta, R.; Stevens, E. D.; Scott, N. M.; Costabile, C.; Cavallo, L.; Hoff, C. D.; Nolan, S. P. *J. Am. Chem. Soc.* **2005,** *127,* 2485–2495. doi:10.1021/ja0438821
29. Huynh, H. V.; Han, Y.; Jothibasu, R.; Yang, J. A. *Organometallics* **2009,** *28,* 5395–5404. doi:10.1021/om900667d
30. Teng, Q.; Huynh, H. V. *Inorg. Chem.* **2014,** *53,* 10964–10973. doi:10.1021/ic501325j
31. Lever, A. B. P. *Inorg. Chem.* **1990,** *29,* 1271–1285. doi:10.1021/ic00331a030
32. Koizumi, T.-a.; Tomon, T.; Tanaka, K. *Organometallics* **2003,** *22,* 970–975. doi:10.1021/om020637m
33. Ghattas, W.; Müller-Bunz, H.; Albrecht, M. *Organometallics* **2010,** *29,* 6782–6789. doi:10.1021/om100925j
34. Dröge, T.; Glorius, F. *Angew. Chem., Int. Ed.* **2010,** *49,* 6940–6952. doi:10.1002/anie.201001865
35. Nelson, D. J.; Nolan, S. P. *Chem. Soc. Rev.* **2013,** *42,* 6723–6753. doi:10.1039/c3cs60146c
36. Setiawan, D.; Kalescky, R.; Kraka, E.; Cremer, D. *Inorg. Chem.* **2016,** *55,* 2332–2344. doi:10.1021/acs.inorgchem.5b02711
37. Bent, H. A. *Chem. Rev.* **1961,** *61,* 275–311. doi:10.1021/cr60211a005
38. Muller, N.; Pritchard, D. E. *J. Chem. Phys.* **1959,** *31,* 768–771. doi:10.1063/1.1730460
39. Weiss, R.; Reichel, S.; Handke, M.; Hampel, F. *Angew. Chem., Int. Ed.* **1998,** *37,* 344–346. doi:10.1002/(SICI)1521-3773(19980216)37:3<344::AID-ANIE344>3.0.CO;2-H
40. Bourissou, D.; Guerret, O.; Gabbaï, F. P.; Bertrand, G. *Chem. Rev.* **2000,** *100,* 39–91. doi:10.1021/cr940472u
41. Nonnenmacher, M.; Kunz, D.; Rominger, F.; Oeser, T. *Chem. Commun.* **2006,** 1378–1380. doi:10.1039/b517816a
42. Liske, A.; Verlinden, K.; Buhl, H.; Schaper, K.; Ganter, C. *Organometallics* **2013,** *32,* 5269–5272. doi:10.1021/om400858y
43. Vummaleti, S. V. C.; Nelson, D. J.; Poater, A.; Gómez-Suárez, A.; Cordes, D. B.; Slawin, A. M. Z.; Nolan, S. P.; Cavallo, L. *Chem. Sci.* **2015,** *6,* 1895–1904. doi:10.1039/C4SC03264K
44. Verlinden, K.; Buhl, H.; Frank, W.; Ganter, C. *Eur. J. Inorg. Chem.* **2015,** 2416–2425. doi:10.1002/ejic.201500174
45. Back, O.; Henry-Ellinger, M.; Martin, C. D.; Martin, D.; Bertrand, G. *Angew. Chem., Int. Ed.* **2013,** *52,* 2939–2943. doi:10.1002/anie.201209109
46. Rodrigues, R. R.; Dorsey, C. L.; Arceneaux, C. A.; Hudnall, T. W. *Chem. Commun.* **2014,** *50,* 162–164. doi:10.1039/C3CC45134H
47. Weiss, R.; Reichel, S. *Eur. J. Inorg. Chem.* **2000,** 1935–1939. doi:10.1002/1099-0682(200009)2000:9<1935::AID-EJIC1935>3.0.CO;2-U
48. Reichel, S. Ph.D. Thesis, Universität Erlangen-Nürnberg, 1998.
49. Ramirez, F.; Desai, N. B.; Hansen, B.; McKelvie, N. *J. Am. Chem. Soc.* **1961,** *83,* 3539–3540. doi:10.1021/ja01477a052
50. Dyker, C. A.; Lavallo, V.; Donnadieu, B.; Bertrand, G. *Angew. Chem., Int. Ed.* **2008,** *47,* 3206–3209. doi:10.1002/anie.200705620
51. Fürstner, A.; Alcarazo, M.; Goddard, R.; Lehmann, C. W. *Angew. Chem., Int. Ed.* **2008,** *47,* 3210–3214. doi:10.1002/anie.200705798
52. Schmidbaur, H. *Angew. Chem., Int. Ed. Engl.* **1983,** *22,* 907–927. doi:10.1002/anie.198309071
53. Tonner, R.; Frenking, G. *Angew. Chem., Int. Ed.* **2007,** *46,* 8695–8698. doi:10.1002/anie.200701632
54. Guha, A. K.; Phukan, A. K. *Chem. – Eur. J.* **2012,** *18,* 4419–4425. doi:10.1002/chem.201103250
55. Nonnenmacher, M.; Kunz, D.; Rominger, F.; Oeser, T. *J. Organomet. Chem.* **2005,** *690,* 5647–5653. doi:10.1016/j.jorganchem.2005.07.033
56. Nonnenmacher, M.; Rominger, F.; Kunz, D. *Organometallics* **2008,** *27,* 1561–1568. doi:10.1021/om701196c
57. Brill, M.; Marrwitz (née Eisenhauer), D.; Rominger, F.; Hofmann, P. *J. Organomet. Chem.* **2015,** *775,* 137–151. doi:10.1016/j.jorganchem.2014.04.008
58. Canepa, G.; Brandt, C. D.; Werner, H. *Organometallics* **2004,** *23,* 1140–1152. doi:10.1021/om034348p
59. Chaplin, A. B.; Weller, A. S. *Organometallics* **2010,** *29,* 2332–2342. doi:10.1021/om100105p

60. Fu, C.-F.; Chang, Y.-H.; Liu, Y.-H.; Peng, S.-M.; Elsevier, C. J.; Chen, J.-T.; Liu, S.-T. *Dalton Trans.* **2009,** 6991–6998. doi:10.1039/b906016b
61. Buhl, H.; Ganter, C. *J. Organomet. Chem.* **2016,** *809,* 74–78. doi:10.1016/j.jorganchem.2016.02.034
62. Neveling, A.; Julius, G. R.; Cronje, S.; Esterhuysen, C.; Raubenheimer, H. G. *Dalton Trans.* **2005,** 181–192. doi:10.1039/b414040k
63. Bittermann, A.; Herdtweck, E.; Härter, P.; Herrmann, W. A. *Organometallics* **2009,** *28,* 6963–6968. doi:10.1021/om900785p
64. Bittermann, A.; Härter, P.; Herdtweck, E.; Hoffmann, S. D.; Herrmann, W. A. *J. Organomet. Chem.* **2008,** *693,* 2079–2090. doi:10.1016/j.jorganchem.2008.01.039
65. Sanderson, M. D.; Kamplain, J. W.; Bielawski, C. W. *J. Am. Chem. Soc.* **2006,** *128,* 16514–16515. doi:10.1021/ja067475w
66. Katakis, D.; Gordon, G. *Mechanisms of Inorganic Reactions;* John Wiley & Sons: New York, NY, U.S.A., 1987.
67. Basolo, F.; Pearson, R. G. Mechanismen in der anorganischen Chemie. Thieme: Stuttgart, Germany, 1973.
68. Crozet, D.; Gual, A.; McKay, D.; Dinoi, C.; Godard, C.; Urrutigoïty, M.; Daran, J.-C.; Maron, L.; Claver, C.; Kalck, P. *Chem. – Eur. J.* **2012,** *18,* 7128–7140. doi:10.1002/chem.201103474
69. Alcarazo, M.; Roseblade, S. J.; Cowley, A. R.; Fernández, R.; Brown, J. M.; Lassaletta, J. M. *J. Am. Chem. Soc.* **2006,** *127,* 3290–3291. doi:10.1021/ja0423769
70. Enders, D.; Breuer, K.; Raabe, G.; Runsink, J.; Teles, J. H.; Melder, J.-P.; Ebel, K.; Brode, S. *Angew. Chem., Int. Ed. Engl.* **1995,** *34,* 1021–1023. doi:10.1002/anie.199510211
71. Martin, D.; Baceiredo, A.; Gornitzka, H.; Schoeller, W. W.; Bertrand, G. *Angew. Chem., Int. Ed.* **2005,** *44,* 1700–1703. doi:10.1002/anie.200462239
72. Arduengo, A. J., III; Dias, H. V. R.; Harlow, R. L.; Kline, M. *J. Am. Chem. Soc.* **1992,** *114,* 5530–5534. doi:10.1021/ja00040a007
73. Herrmann, W. A.; Elison, M.; Fischer, J.; Köcher, C.; Artus, G. R. J. *Chem. – Eur. J.* **1996,** *2,* 772–780. doi:10.1002/chem.19960020708
74. Arduengo, A. J., III; Goerlich, J. R.; Marshall, W. J. *J. Am. Chem. Soc.* **1995,** *117,* 11027–11028. doi:10.1021/ja00149a034
75. Denk, K.; Sirsch, P.; Herrmann, W. A. *J. Organomet. Chem.* **2002,** *649,* 219–224. doi:10.1016/S0022-328X(02)01133-6
76. Alder, R. W.; Allen, P. R.; Murray, M.; Orpen, A. G. *Angew. Chem., Int. Ed. Engl.* **1996,** *35,* 1121–1123. doi:10.1002/anie.199611211
77. Selenourea **4a** was already prepared by Weiss and co-workers, see [39,47], however, no ^{77}Se NMR chemical shift was reported.
78. Reed, A. E.; Weinstock, R. B.; Weinhold, F. *J. Chem. Phys.* **1985,** *83,* 735–746. doi:10.1063/1.449486
79. Luy, J.-N.; Hauser, S. A.; Chaplin, A. B.; Tonner, R. *Organometallics* **2015,** *34,* 5099–5112. doi:10.1021/acs.organomet.5b00692
80. Duddeck, H. *Prog. Nucl. Magn. Reson. Spectrosc.* **1995,** *27,* 1–323. doi:10.1016/0079-6565(94)00005-F
81. Becke, A. D. *Phys. Rev. A* **1988,** *38,* 3098–3100. doi:10.1103/PhysRevA.38.3098
82. Perdew, J. P. *Phys. Rev. B* **1986,** *33,* 8822–8824. doi:10.1103/PhysRevB.33.8822
83. Schäfer, A.; Horn, H.; Ahlrichs, R. *J. Chem. Phys.* **1992,** *97,* 2571–2577. doi:10.1063/1.463096
84. Weigend, F.; Ahlrichs, R. *Phys. Chem. Chem. Phys.* **2005,** *7,* 3297–3305. doi:10.1039/b508541a
85. Weigend, F. *Phys. Chem. Chem. Phys.* **2006,** *8,* 1057–1065. doi:10.1039/b515623h
86. Becke, A. D. *J. Chem. Phys.* **1993,** *98,* 5648–5652. doi:10.1063/1.464913
87. Lee, C.; Young, W.; Parr, R. G. *Phys. Rev. B* **1988,** *37,* 785–789. doi:10.1103/PhysRevB.37.785
88. Schäfer, A.; Huber, C.; Ahlrichs, R. *J. Chem. Phys.* **1994,** *100,* 5829–5835. doi:10.1063/1.467146
89. *TURBOMOLE,* V6.3.1; University of Karlsruhe and Forschungszentrum Karlsruhe GmbH, 1989–2007, TURBOMOLE GmbH, since 2007: Karlsruhe, Germany, 2011, http://www.turbomole.com.
90. Treutler, O.; Ahlrichs, R. *J. Chem. Phys.* **1995,** *102,* 346–354. doi:10.1063/1.469408
91. von Arnim, M.; Ahlrichs, R. *J. Comput. Chem.* **1998,** *19,* 1746–1757. doi:10.1002/(SICI)1096-987X(19981130)19:15<1746::AID-JCC7>3.0.CO;2-N
92. van Wüllen, C. *J. Comput. Chem.* **2011,** *32,* 1195–1201. doi:10.1002/jcc.21692
93. Deglmann, P.; Furche, F.; Ahlrichs, R. *Chem. Phys. Lett.* **2002,** *362,* 511–518. doi:10.1016/S0009-2614(02)01084-9
94. Deglmann, P.; Furche, F. *J. Chem. Phys.* **2002,** *117,* 9535–9538. doi:10.1063/1.1523393
95. Ahlrichs, R.; Bär, M.; Häser, M.; Horn, H.; Kölmel, C. *Chem. Phys. Lett.* **1989,** *162,* 165–169. doi:10.1016/0009-2614(89)85118-8
96. Armbruster, M. K.; Weigend, F.; van Wüllen, C.; Klopper, W. *Phys. Chem. Chem. Phys.* **2008,** *10,* 1748–1756. doi:10.1039/b717719d
97. Peng, D.; Middendorf, N.; Weigend, F.; Reiher, M. *J. Chem. Phys.* **2013,** *138,* 184105. doi:10.1063/1.4803693
98. Eichkorn, K.; Treutler, O.; Öhm, H.; Häser, M.; Ahlrichs, R. *Chem. Phys. Lett.* **1995,** *240,* 283–290. doi:10.1016/0009-2614(95)00621-A
99. Eichkorn, K.; Treutler, O.; Öhm, H.; Häser, M.; Ahlrichs, R. *Chem. Phys. Lett.* **1995,** *242,* 652–660. doi:10.1016/0009-2614(95)00838-U
100. Eichkorn, K.; Weigend, F.; Treutler, O.; Ahlrichs, R. *Theor. Chem. Acc.* **1997,** *97,* 119–124. doi:10.1007/s002140050244
101. Deglmann, P.; May, K.; Furche, F.; Ahlrichs, R. *Chem. Phys. Lett.* **2004,** *384,* 103–107. doi:10.1016/j.cplett.2003.11.080
102. Weigend, F. *Phys. Chem. Chem. Phys.* **2002,** *4,* 4285–4291. doi:10.1039/b204199p
103. Sierka, M.; Hogekamp, A.; Ahlrichs, R. *J. Chem. Phys.* **2003,** *118,* 9136–9148. doi:10.1063/1.1567253
104. Andrae, D.; Häußermann, U.; Dolg, M.; Stoll, H.; Preuß, H. *Theor. Chim. Acta* **1990,** *77,* 123–141. doi:10.1007/BF01114537
105. Grimme, S.; Antony, J.; Ehrlich, S.; Krieg, H. *J. Chem. Phys.* **2010,** *132,* 154104. doi:10.1063/1.3382344
106. *POV-RayTM for Windows,* v3.6.2; Persistence of Vision Pty. Ltd.: Williamstown, Victoria, Australia, http://www.povray.org/.

License and Terms

This is an Open Access article under the terms of the Creative Commons Attribution License (http://creativecommons.org/licenses/by/4.0), which permits unrestricted use, distribution, and reproduction in any medium, provided the original work is properly cited.

The license is subject to the *Beilstein Journal of Organic Chemistry* terms and conditions: (http://www.beilstein-journals.org/bjoc)

The definitive version of this article is the electronic one which can be found at: doi:10.3762/bjoc.12.178

BEILSTEIN JOURNAL OF ORGANIC CHEMISTRY

Thiophene-forming one-pot synthesis of three thienyl-bridged oligophenothiazines and their electronic properties

Dominik Urselmann, Konstantin Deilhof, Bernhard Mayer and Thomas J. J. Müller*

Full Research Paper

Open Access

Address:
Institut für Organische Chemie und Makromolekulare Chemie, Heinrich-Heine-Universität Düsseldorf, Universitätsstr. 1, D-40225 Düsseldorf, Germany

Email:
Thomas J. J. Müller* - ThomasJJ.Mueller@uni-duesseldorf.de

* Corresponding author

Keywords:
C–C coupling; copper; cyclic voltammetry; DFT; microwave-assisted synthesis; multicomponent reactions; palladium; phenothiazines; thiophenes

Beilstein J. Org. Chem. **2016,** *12,* 2055–2064.
doi:10.3762/bjoc.12.194

Received: 13 May 2016
Accepted: 11 August 2016
Published: 20 September 2016

This article is part of the Thematic Series "Organometallic chemistry".

Guest Editor: B. F. Straub

© 2016 Urselmann et al.; licensee Beilstein-Institut.
License and terms: see end of document.

Abstract

The pseudo five-component Sonogashira–Glaser cyclization synthesis of symmetrically 2,5-diaryl-substituted thiophenes is excellently suited to access thienyl-bridged oligophenothiazines in a one-pot fashion. Three thienyl-bridged systems were intensively studied by UV–vis and fluorescence spectroscopy as well as by cyclic voltammetry. The oxidation proceeds with lower oxidation potentials and consistently reversible oxidations can be identified. The Stokes shifts are large and substantial fluorescence quantum yields can be measured. Computational chemistry indicates lowest energy conformers with sigmoidal and helical structure, similar to oligophenothiazines. TD-DFT and even semiempirical ZINDO calculations reproduce the trends of longest wavelengths absorption bands and allow the assignment of these transitions to possess largely charge-transfer character from the adjacent phenothiazinyl moieties to the central thienyl unit.

Introduction

Oligothiophenes [1-8] have adopted a dominating role among functional π-electron systems [9]. In particular, they have received attention as hole-transport materials in organic light emitting diodes [10-15], organic field-effect transistors [16-22], and organic photovoltaics [23-26]. Likewise their smaller congeners, 2,5-di(hetero)aryl substituted thiophenes [4,5], are equally relevant as charge-carrying materials [2,3,27,28] and organic semiconductors [29,30] in electronic [31] and optoelectronic devices [32-34]. As reversibly oxidizable units 2,5-di(hetero)aryl-substituted thiophenes are additionally interesting as redox switchable molecular wires [35,36] in unimolecular electronics [37-40].

In comparison to thiophene, phenothiazine, a tricyclic dibenzo-1,4-thiazine, possesses a significantly lower oxidation potential, similar to aniline. However, phenothiazine derivatives form stable deeply colored radical cations with perfect Nernstian reversibility [41-44]. Over the past one and a half decades the

synthetic and physical organic chemistry of oligophenothiazines have been intensively studied in linear [45] and cyclic [46] topologies, as diphenothiazinyl dumbbells brigded by heterocycles [47-49], and as acceptor [50,51], ferrocenyl [52], and alkynyl [53-55] substituted (oligo)phenothiazines. Their pronounced reversible oxidation potentials, their electro- and photochromicity [56], and their luminescence [57,58] have rendered (oligo)phenothiazines interesting candidates as donors in donor–acceptor conjugates with photo-induced electron-transfer characteristics [59-63], as hole-transport materials [64], for applications in mesoporous organo silica hybrid materials [65], and as chromophores in dye-sensitized solar cells [66-68]. Furthermore, (oligo)phenothiazines in their native reduced forms display a pronounced ability to form self-assembled monolayers on gold [69-71] as well as on zinc and iron oxide surfaces [72].

Conceptually, thienyl-bridged oligophenothiazines can be considered as a novel type of structurally well-defined electron-rich oligophenothiazine–thiophene hybrids (Figure 1). Thereby, the strong intramolecular electronic coupling of (oligo)phenothiazines [45,64] and the low torsional displacement from a coplanar arrangement of both redox moieties of the dumbbells might represent conjugatively linked nanometer-scaled novel multistep redox active oligomers.

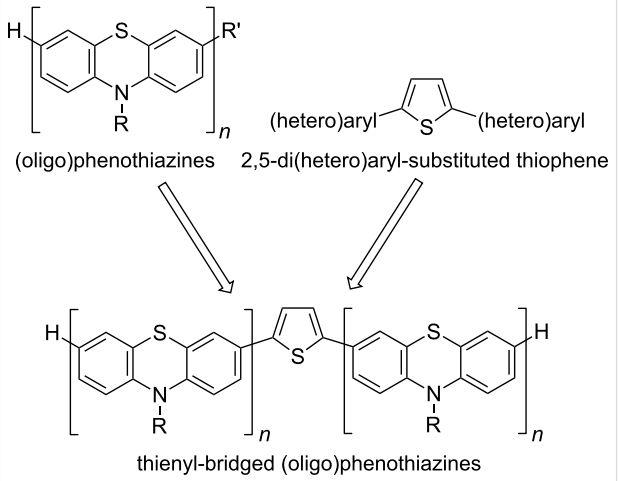


Figure 1: Thienyl-bridged oligophenothiazines as topological hybrids of (oligo)phenothiazines and 2,5-di(hetero)aryl substituted thiophene.

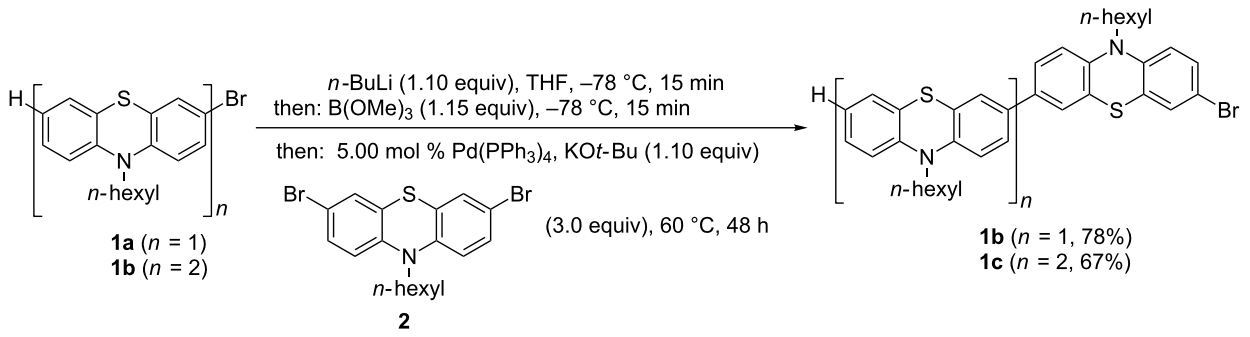
As part of our concept to develop novel multicomponent strategies for the synthesis of functional π-electron systems [73], we reasoned that our recently reported one-pot consecutive Sonogashira–Glaser sequence [74] and the resulting application to pseudo five-component syntheses of 2,5-di(hetero)arylthiophenes [75,76] as well as intensively blue luminescent 2,5-di(hetero)arylfurans [77] could open a highly convergent thiophene forming approach to the proposed title compounds. Here, we report the pseudo five-component synthesis of three thienyl-bridged oligophenothiazines by a one-pot Sonogashira–Glaser cyclization sequence and the electronic characterization by electronic spectroscopy, cyclic voltammetry, and quantum chemical computations.

Results and Discussion

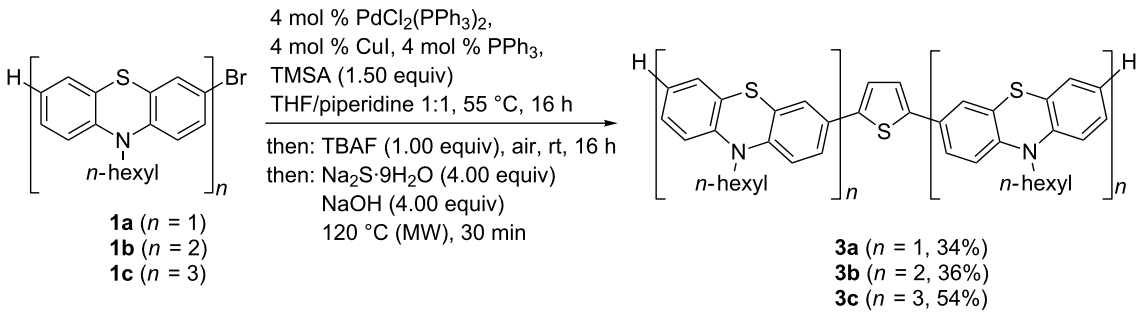
Synthesis of thienyl-bridged oligophenothiazines

Although the thienyl bridge can be introduced by Suzuki coupling as previously reported [48], we decided to transpose a methodology initiated by a Sonogashira–Glaser sequence [74] also for probing delicate oxidative dimerization conditions with easily oxidizable phenothiazinyl moieties. According to our recent study on the formation of butadiynyl-bridged diphenothiazines [54] we were optimistic to probe this unusual approach. First, three different bromo-substituted (oligo)phenothiazine substrates **1** had to be prepared. 3-Bromo-10-hexyl-10*H*-phenothiazine (**1a**) was synthesized according to the literature by hexylation of 3-bromo-10*H*-phenothiazine [45]. The 7-bromo-substituted phenothiazines **1b** and **1c** were prepared in good yields according to our one-pot bromine-lithium-exchange-borylation-Suzuki (BLEBS) sequence [78], employing an excess of 3,7-dibromo-10-hexyl-10*H*-phenothiazine (**3**) [45] as a coupling component in the Suzuki step (Scheme 1).

With three bromo-substituted (oligo)phenothiazines **1** in hand the consecutive pseudo five-component Sonogashira–Glaser cyclization synthesis [75] was successfully performed furnishing three symmetrical thienyl-bridged oligophenothiazine dumbbells **3** as yellow greenish resins in yields of 34–54% (Scheme 2). The molecular composition of the thienyl-bridged oligophenothiazines **3** is unambiguously supported by mass spectrometry (MALDI–TOF). The proton and carbon NMR spectra unambiguously support the formation of the oligomers **3**, and expectedly, in agreement with the molecular symmetry, the appearance of one (**3a**), two (**3b**), and three (**3c**) distinct resonances for the nitrogen-bound methylene carbon nuclei in the ^{13}C NMR spectra additionally supported the assigned structures. Combustion analyses of compounds **3b** and **3c** indicate that water and THF (compound **3b**) and water (compound **3c**) are present as solvent inclusion in the resins that cannot be removed even upon extensive drying under vacuo. However, HPLC traces with UV detection support that the materials consist of single specimen with over 99% purity. Taking into account that five new bonds are being formed in this consecutive pseudo five-component process the yield per bond forming step counts for 81–88%, albeit a Pd/Cu mediated air oxidation step is involved.



Scheme 1: One-pot bromine-lithium-exchange-borylation-Suzuki (BLEBS) synthesis of 7-bromo-substituted phenothiazines **1b** and **1c** with 3,7-dibromo-10-hexyl-10*H*-phenothiazine (**2**).



Scheme 2: Pseudo five-component Sonogashira-Glaser-cyclization synthesis of thienyl-bridged oligophenothiazine dumbbells **3**.

Electronic spectra and oxidation potentials

The electronic properties of the three thienyl-bridged oligophenothiazines **3** were experimentally investigated by absorption and emission spectroscopy and by cyclic voltammetry (Table 1).

Cyclic voltammetry discloses the oxidation potential as an electronic ground state property. Therefore, the ease of oxidation of the title compounds **3** in comparison to the model 10-hexyl-10*H*-phenothiazine with $E_0^{0/+1}$ = 730 mV was measured. All three thienyl-bridged oligophenothiazines **3** display cathodically shifted first oxidations in comparison to the model, however, with significantly more complex cyclovoltammetric signatures (Figure 2). The simplest representative, 2,5-bis(phenothiazinyl)thiophene **3a**, possesses two reversible oxidation waves at $E_{1/2}$ = 650 and 760 mV with Nernstian behavior (Figure 2, top),

Table 1: UV–vis and emission data and oxidation potentials of thienyl-bridged oligophenothiazines **3** (recorded in CH_2Cl_2, T = 298 K; bold values: absorption and emission maxima used for determining the Stokes shift).

compound	absorption $\lambda_{max,abs}$ (ε) [nm]	emission $\lambda_{max,em}$ [nm] (Φ_f) [%][a]	Stokes shift[b] $\Delta\tilde{\nu}$ [cm^{-1}]	$E_{1/2}$ [mV]
3a	246 (39600), 261 (39100), 318 (27000), **395** (33100)	**506** (18)	5600	650, 760
3b	266 (52100), 284 (45900), 319 (32500), **404** (27700)	**502** (16)	4800	620–1010,[c] 1320–1520[c,d]
3c	267 (103000), 283 (116200), 327 (61000), **379** (51900)	**521** (15)	7200	550–950[e]
10-hexyl-10*H*-phenothiazine	258, **312**	**444** (–)	9600	730

[a]Recorded in CH_2Cl_2 at c(**3**) = 10^{-7} M with coumarin 151 in ethanol/water 1:1 (w/w) as a standard (Φ_f = 0.88). [b]$\Delta\tilde{\nu} = 1/\lambda_{max,abs} - 1/\lambda_{max,em}$ [cm^{-1}]; the UV–vis and emission data in bold face were applied for calculating the corresponding Stokes shifts. [c]Oxidation and reduction half-waves are not resolved but superimpose. [d]Shoulder. [e]Position of the oxidation half-wave without distinct reduction half-wave.

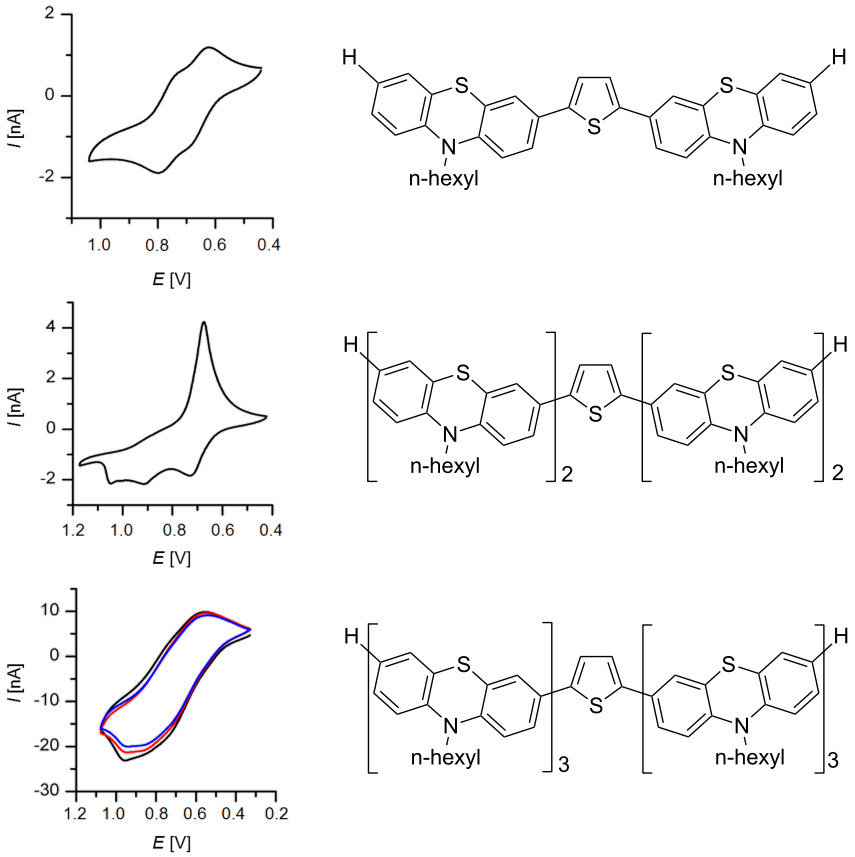


Figure 2: Cyclic voltammograms of compounds **3** (recorded in CH_2Cl_2, T = 293 K, electrolyte n-$Bu_4N^+PF_6^-$, Pt working electrode, Pt counter electrode, Ag/AgCl reference electrode, v = 50 mV/s (**3a** and **3b**), v = 100 mV/s (**3c**, multisweep experiment, 1. cycle (black), 2. cycle (red), 3. cycle (blue)).

indicating that the thiophene bridge enables electronic communication between both electrophore moieties. The first oxidation potential of 2,5-bis(diphenothiazinyl)thiophene **3b** is cathodically shifted and appears at a peak potential of $E_{1/2}$ = 620 mV, however, without displaying Nernstian behavior (Figure 2, center). Two further oxidation waves can be detected; yet, the corresponding reduction half-waves are absent. Only an increased reduction half wave indicates the presence of multiply oxidized specimens that are reduced at the same potential as a consequence of electrode deposition. For the 2,5-bis(triphenothiazinyl)thiophene **3c** no distinct reversible oxidation waves can be identified but rather a continuous oxidation window ranging from 500 to 1000 mV (Figure 2, bottom). Yet, the multisweep experiment indicates that within this window oxidation and reduction occurs in a reversible fashion.

However, the cyclic voltammograms of this system containing six phenothiazines conjugatively linked via a symmetrically substituted thiophene bridge do not obey a strictly Nernstian behavior. Thereby, a first oxidation potential of $E_{1/2}$ = 550 mV was estimated. Interestingly, by carefully selecting the applied reversal voltage thienyl-bridged oligophenothiazines **3** can be reversible charged and discharged, a property that is highly desired for molecular electronics applications.

The absorption spectra undoubtedly follow the Lambert–Beer law in a broad concentration range (as studied for compounds **3b** and **3c**, see Supporting Information File 1, Figures S3 and S4). In addition this behavior underlines that no aggregation of the molecules has to be taken into account at the concentration level of absorption and emission spectroscopy. In the UV–vis spectra, most characteristically, four absorption bands are found, three at shorter wavelengths arising from the phenothiazinyl moieties and the longest wavelength maximum can be assigned to the central 2,5-di(hetero)aryl-substituted thiophene part (Figure 3). This assignment is based on the molar decadic extinction coefficients that increase with the number of phenothiazinyl units (Table 1). However, the increasing number of phenothiazinyl moieties enhances the donor character of the substituents on the thiophene core. In turn the thienyl moiety behaves as an acceptor due to its higher oxidation potential. Interestingly, the redshift of the longest wavelength absorption

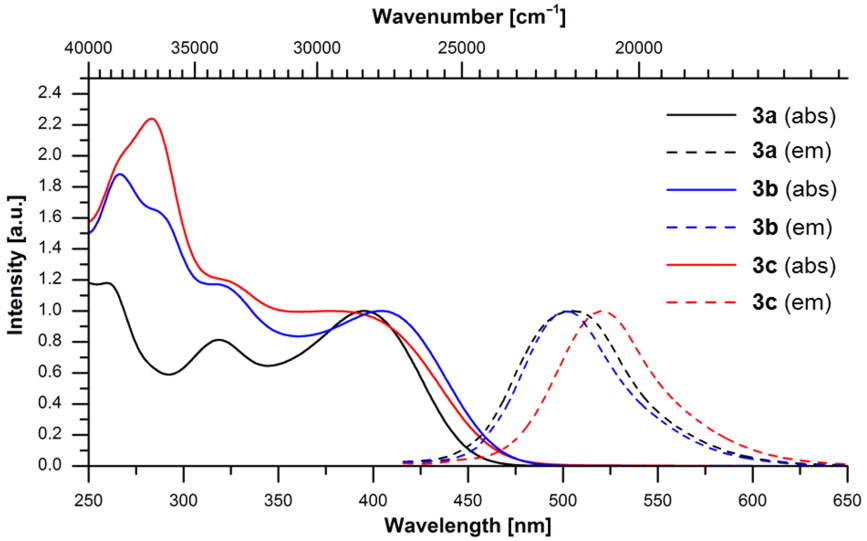


Figure 3: UV–vis (solid lines) and fluorescence spectra (dashed lines) of the thienyl-bridged oligophenothiazines **3** (recorded in CH_2Cl_2, T = 298 K).

band is relatively moderate, presumably as a consequence of only a modest delocalization of the complete π-electron systems in the electronic ground state.

In the emission spectra broad shortest wavelength bands appear in a region from 502 to 521 nm with large Stokes shifts $\Delta\tilde{\nu}$ between 4800 and 7200 nm (Figure 2), which are typical for oligophenothiazines [45]. However, the lack of a systematic trend with the numbers of phenothiazinyl units indicates that the excited state property is strongly affected by local conformational biases arising from the planarization of electronic ground state butterfly conformation of phenothiazines in the excited state [57,79]. Also the fluorescence quantum yields Φ_f with 15 to 18% essentially remain constant within this series, although, the increasing number of sulfur-containing heterocycles suggests an increase in fluorescence deactivating spin–orbit coupling. In comparison to the consanguineous oligophenothiazines [45] the compounds **3** display considerable lower fluorescence quantum yields.

Computations and electronic structure

The electronic properties of the three thienyl-bridged oligophenothiazines **3** were further investigated by computational studies on the DFT level of theory. First the ground state geometries of structures **3a**, **3b**, and **3c** (the *n*-hexyl substituents were truncated to ethyl groups for reducing the computational time) were optimized by DFT calculations with the B3LYP functional and the 6-311G(d,p) basis set as implemented in the program package Gaussian 09 [80]. In addition the minima structures were confirmed by the absence of imaginary vibrations in the analytical frequency analyses. The inspection of the computed molecular structures **3** indicates that these molecules adopt sigmoidal and helical minimum conformers (Figure 4) as already shown for consanguineous series of higher oligophenothiazines [45].

With these geometry-optimized structures in hand the electronic absorptions were calculated with the semiempirical ZINDO-CI, and TD-DFT (B3LYP and CAM-B3LYP, an implemented hybrid exchange-correlation functional [81], using the polarizable continuum model (PCM) [82] applying dichloromethane as solvent) methods and the results were compared with the experimentally obtained UV–vis absorption spectra (see Supporting Information File 1, Table S2) and the calculated energies of the FMOs (frontier molecular orbitals) (see Supporting Information File 1, Table S3).

Although a perfect numerical match of experimentally and computationally determined absorption bands cannot be expected for conformationally flexible complex molecules with extended π-conjugation, the trend of the longest wavelength absorption bands from the UV–vis spectra is correctly reproduced. Furthermore, for all three methods and for all three structures this longest wavelength absorption can be assigned to S_1 states that predominantly consist of HOMO to LUMO transitions with dominant oscillator strengths. For the thienyl-bridged 2,5-bis(terphenothiazinyl)thiophene **3c**, containing the symmetrical conjugative ligation of two terphenothiazinyl moieties to the thienyl bridge, in the TD-DFT methods significant contributions of HOMO-2 to LUMO transitions contribute to the corresponding S_1 states. The inspection of the Kohn–Sham FMOs, contributing to the S_1 states and representing the longest wavelength absorption bands, indicates that the nature of these transitions possesses predominantly a charge-transfer character from

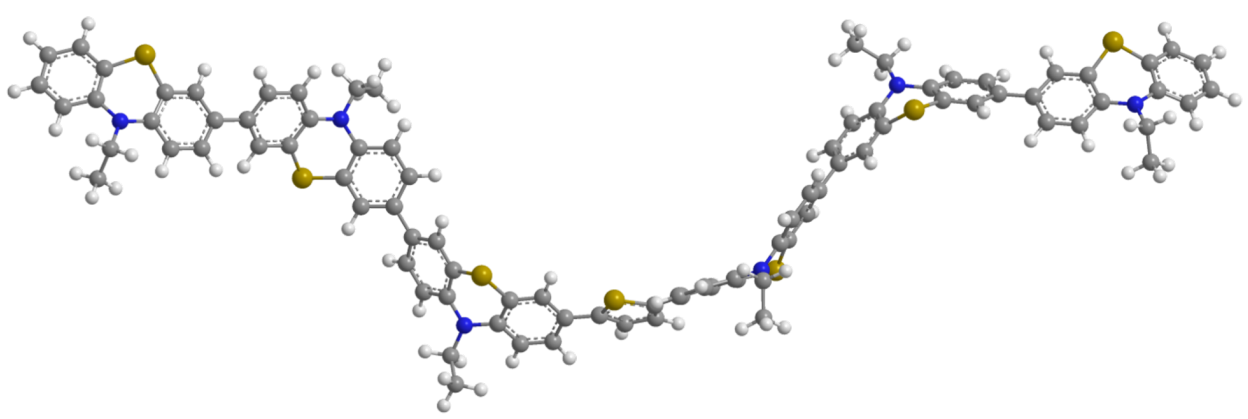


Figure 4: DFT-calculated minimum conformer of the 2,5-bis(terphenothiazinyl)thiophene **3c** (calculated with the B3LYP functional and the 6-311G(d,p) basis set).

the adjacent phenothiazinyl moieties to the central thiophene part. The intense coefficient density in the center of the structures in both HOMO (HOMO-2) and LUMO additionally supports and rationalizes the dominant magnitude of the oscillator strengths *f*, corresponding with significant decadic molar extinction coefficients of the associated bands (Figure 5). In principle these phenothiazine conjugates can be considered as donor–acceptor–donor systems, a topology that can be favorably developed further in molecular electronics.

Conclusion

In summary, we could show that the pseudo five-component Sonogashira–Glaser cyclization synthesis of symmetrically 2,5-diaryl-substituted thiophenes can be efficiently transposed to

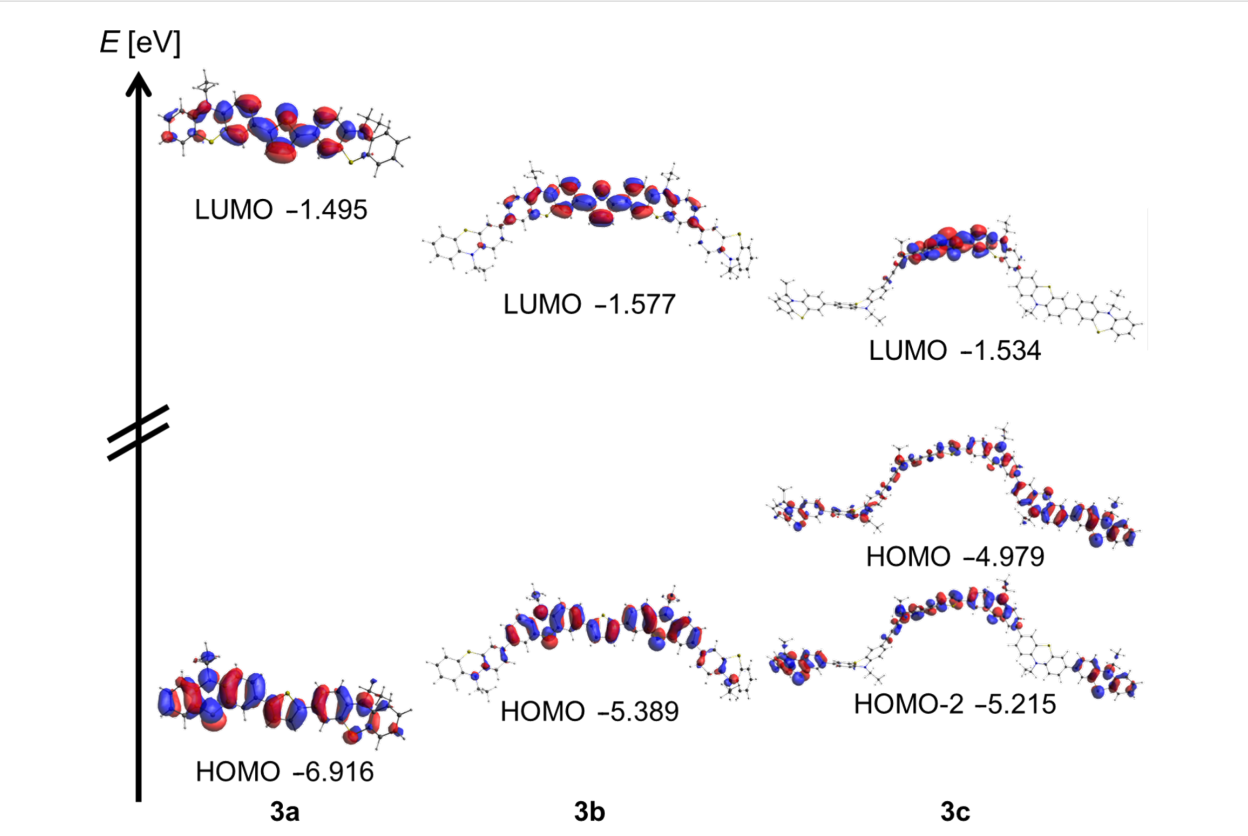


Figure 5: Relevant Kohn–Sham FMOs contributing to the S_1 states that are assigned to the longest wavelengths absorption bands of thienyl-bridged oligophenothiazines **3** (calculated with the B3LYP functional in vacuo and the 6-311G(d,p) basis set).

access thienyl-bridged oligophenothiazines in a one-pot fashion starting from 3-bromo(oligo)phenothiazines. Most remarkably, the oxidative conditions of the central Glaser step employing air as oxidant does not interfere with the oxidation sensitive (oligo)phenothiazinyl moieties. The electronic properties of the obtained three thienyl-bridged systems were intensively studied by UV–vis and fluorescence spectroscopy as well as by cyclic voltammetry. With increasing numbers of phenothiazinyl electrophore units the oxidation proceeds with lower oxidation potentials and for the 2,5-bis(terphenothiazinyl)thiophene even a consistently reversible oxidation area can be found. As already shown for oligophenothiazines and typical for many 3-(hetero)arylphenothiazines the Stokes shifts are large and substantial fluorescence quantum yields can be measured. Computational chemistry supports lowest-energy conformers with sigmoidal and helical structure, similar to oligophenothiazines. Furthermore, TD-DFT and even semiempirical ZINDO calculations on geometry-optimized simplified structures of the title compounds nicely reproduce the trends of longest wavelength absorption bands and allow the assignment of these transitions to be largely charge-transfer from the adjacent phenothiazinyl moieties to the central thienyl unit. This represents in principle a donor–acceptor–donor topology, suitable for further development toward molecular electronics. Studies employing the presented synthetic methodology and the concept of bridging oligophenothiazines with conjugating bridges of variable electronic nature are currently underway.

Experimental

3a (general procedure GP): 3-Bromo-10-hexyl-10*H*-phenothiazine (**1a**) (725 mg, 2.00 mmol) and dry THF (10.0 mL) were placed in a microwave vessel with septum (80 mL) and the mixture was deaerated by a constant stream of nitrogen through a syringe for 10 min. Then $PdCl_2(PPh_3)_2$ (56.0 mg, 0.08 mmol), CuI (15.0 mg, 0.08 mmol), PPh_3 (21 mg, 0.08 mmol), (trimethylsilyl)acetylene (0.56 mL, 2.00 mmol), and piperidine (5.00 mL, 50.4 mmol) were added. The closed vessel under nitrogen was heated at 55 °C (oil bath) for 16 h. Next, TBAF·$3H_2O$ (631 mg, 2.00 mmol) was added and the vessel open to ambient atmosphere was then stirred at room temp for 16 h. Then, sodium sulfide nonahydrate (960 mg, 4.00 mmol) and potassium hydroxide (224 mg, 4.00 mmol) were added and the reaction mixture in the closed vessel was heated at 120 °C in the microwave cavity for 30 min. After cooling to room temperature the solvents were removed in vacuo and the residue was filtered with THF through a short plug of Celite® and silica gel. The solvents were removed in vacuo and the residue was purified by chromatography on silica gel (hexane/dichlormethane 10:1) giving 218 mg (34%) of compound **3a** as a yellow greenish resin. R_f 0.53 (hexane/acetone 10:1); ^{1}H NMR (300 MHz, acetone-d_6) δ 0.84 (t, ^3J = 7.1 Hz, 6 H), 1.21–1.33 (m, 8H), 1.39–1.51 (m, 4H), 1.78 (quint, ^3J = 7.5 Hz, 4H), 3.92 (t, ^3J = 7.0 Hz, 4H), 6.90–6.97 (m, 2H), 6.97–7.03 (m, 4H), 7.14 (dd, ^3J = 7.7 Hz, ^4J = 1.5 Hz, 2H), 7.16–7.23 (m, 2H), 7.29 (s, 2H), 7.41 (d, ^4J = 2.1 Hz, 2H), 7.44 (dd, ^3J = 8.4 Hz, ^4J = 2.2 Hz, 2H); ^{13}C NMR (75 MHz, acetone-d_6) δ 14.3 ($2CH_3$), 23.3 ($2CH_2$), 27.1 ($2CH_2$), 27.5 ($2CH_2$), 32.2 ($2CH_2$), 47.9 ($2CH_2$), 116.7 (2CH), 116.8 (2CH), 123.4 (2CH), 124.5 (2CH), 124.5 (2CH), 124.8 ($2C_{quat}$), 125.4 (2CH), 126.1 ($2C_{quat}$), 128.1 (2CH), 128.4 (2CH), 129.6 ($2C_{quat}$), 142.5 ($2C_{quat}$), 145.5 ($2C_{quat}$), 145.8 ($2C_{quat}$); MS (MALDI) *m/z*: 646.3 ($[M]^+$); UV–vis (CH_2Cl_2), λ_{max} [nm] (ε): 246 (39600), 261 (39100), 318 (27000), 395 (33100); IR (KBr) $\tilde{\nu}$ [cm^{-1}]: 3057 (w), 2951 (w), 2926 (w), 2851 (w), 1917 (w), 1597 (w), 1576 (w), 1539 (w), 1489 (w), 1458 (s), 1398 (w), 1362 (w), 1331 (m), 1285 (w), 1248 (m), 1238 (m), 1225 (w), 1192 (w), 1161 (w), 1134 (w), 1103 (w), 1038 (w), 1022 (w), 968 (w), 926 (w), 908 (w), 874 (w), 793 (s), 745 (s), 704 (w), 681 (w), 669 (w), 646 (w), 625 (w); anal. calcd for $C_{40}H_{42}N_2S_3$ (647.0): C, 74.26; H, 6.54; N, 4.33; found: C, 74.17; H, 6.79; N, 4.05.

3b: According to the GP by reaction of 7-bromo-10,10'-dihexyl-10*H*,10'*H*-3,3'-biphenothiazine (**1b**, 1.29 g, 2.00 mmol) after chromatography on silica gel (hexane/THF 20:1) gave 435 mg (36%) of compound **3b** as a yellow greenish resin. ^{1}H NMR (600 MHz, $CDCl_3$) δ 0.65–0.82 (m, 12H), 1.10–1.23 (m, 16H), 1.26–1.36 (m, 8H), 1.62–1.76 (m, 8H), 3.62–3.79 (m, 8H), 6.64–6.84 (m, 10H), 6.93–7.09 (m, 6H), 7.09–7.26 (m, 12H); ^{13}C NMR (151 MHz, $CDCl_3$) δ 14.1 (CH_3), 22.7 (CH_2), 26.7 (CH_2), 26.7 (CH_2), 26.8 (CH_2), 26.9 (CH_2), 31.5 (CH_2), 47.5 (CH_2), 47.6 (CH_2), 115.3 (CH), 115.4 (CH), 115.5 (CH), 115.5 (CH), 122.4 (CH), 123.1 (CH), 124.2 (CH), 124.4 (C_{quat}), 124.4 (C_{quat}), 124.6 (CH), 124.8 (C_{quat}), 125.1 (CH), 125.1 (CH), 125.2 (CH), 125.3 (CH), 127.3 (CH), 127.5 (CH), 128.9 (C_{quat}), 134.2 (C_{quat}), 134.4 (C_{quat}), 141.9 (C_{quat}), 143.7 (C_{quat}), 144.2 (C_{quat}), 144.3 (C_{quat}),145.1 (C_{quat}); MS (MALDI) *m/z*: 1208.5 ($[M]^+$); UV–vis (CH_2Cl_2), λ_{max} [nm] (ε): 266 (52100), 284 (45900), 319 (32500), 404 (27700); IR (KBr) $\tilde{\nu}$ [cm^{-1}]: 2951 (w), 2922 (w), 2853 (w), 1456 (s), 1416 (w), 1375 (w), 1364 (w), 1331 (m), 1292 (w), 1238 (m), 1192 (w), 1138 (w), 1105 (w), 1063 (w), 1040 (w), 872 (m), 797 (s), 745 (s), 727 (w), 706 (w), 611 (w); anal. calcd for $C_{76}H_{80}N_4S_5{\cdot}H_2O{\cdot}2C_4H_8O$ (1209.8 + 18.0 + 144.2): C, 73.53; H, 7.20; N, 4.08; found: C, 73.39; H, 7.36; N, 4.29; HPLC (*n*-hexane) t_R [min] (%) = 4.49 (99).

3c: According to the GP by reaction of 7-bromo-10,10',10''-trihexyl-10*H*,10'*H*,10''*H*-[3,3',7',3'']terphenothiazin (**1c**, 1.85 g, 2.00 mmol) after chromatography on silica gel (hexane/THF 7:1 to 3:1) gave 955 mg (54%) of compound **3c** as a yellow greenish resin. ^{1}H NMR (600 MHz, $CDCl_3$) δ 0.75–0.88 (m, 18H), 1.08–1.33 (m, 24H), 1.31–1.40 (m, 12H), 1.66–1.81 (m, 12H), 3.60–3.89 (m, 12H), 6.68–6.88 (m, 14H), 7.00–7.11

(m, 6H), 7.13–7.37 (m, 20H); ^{13}C NMR (151 MHz, $CDCl_3$) δ 14.05 (CH_3), 14.06 (CH_3), 22.64 (CH_2), 22.66 (CH_2), 26.69 (CH_2), 26.72 (CH_2), 26.8 (CH_2), 26.88 (CH_2), 26.90 (CH_2), 31.5 (CH_2), 47.5 (CH_2), 47.6 (CH_2), 47.63 (CH_2), 115.31 (CH), 115.37 (CH), 115.42 (CH), 115.46 (CH), 115.48 (CH), 122.3 (CH), 123.1 (CH), 124.2 (CH), 124.42 (C_{quat}), 124.44 (C_{quat}), 124.57 (CH), 124.68 (C_{quat}), 124.72 (C_{quat}), 124.8 (CH), 125.12 (CH), 125.14 (CH), 125.18 (CH), 125.19 (CH), 125.25 (CH), 125.29 (CH), 127.25 (CH), 127.5 (CH), 128.9 (C_{quat}), 134.18 (C_{quat}), 134.23 (C_{quat}), 134.30 (C_{quat}), 134.37 (C_{quat}), 141.9 (C_{quat}), 143.7 (C_{quat}), 143.9 (C_{quat}), 144.0 (C_{quat}), 144.20 (C_{quat}), 144.22 (C_{quat}), 145.1 (C_{quat}); MS (MALDI) *m/z*: 1770.7 ($[M]^+$); UV–vis (CH_2Cl_2), λ_{max} [nm] (ε): 267 (103000), 283 (116200), 327 (61000), 379 (51900); IR (KBr) $\tilde{\nu}$ [cm^{-1}]: 3024 (w), 2951 (w), 2922 (w), 2851 (w), 1603 (w), 1574 (w), 1454 (s), 1416 (w), 1377 (w), 1331 (w), 1294 (w), 1238 (m), 1190 (w), 1140 (w), 1105 (w), 1063 (w), 1038 (w), 968 (w), 928 (w), 910 (w), 872 (w), 802 (s), 745 (m), 729 (w), 691 (w); anal. calcd for $C_{112}H_{118}N_6S_7 \cdot H_2O$ (1772.63 + 18.0): C, 75.13; H, 6.76; N, 4.69; found: C, 74.89; H, 6.50; N, 4.53; HPLC (*n*-hexane/THF 99.5:0.5) t_R [min] (%) = 2.92 (99).

Supporting Information

The Supporting Information contains all experimental procedures, spectroscopic and analytical data of compounds **3**, and copies of NMR spectra of compounds **3**, copies of the HPLC-traces of compounds **3b** and **3c**, Lambert-Beer plots of compounds **3b** and **3c**, computed xyz-coordinates of the thienyl-bridged oligophenothiazines **3a**, **3b**, and **3c**, computed UV–vis spectra of ZINDO-CI and TD-DFT (B3LYP, CAM-B3LYP) calculated structures of **3a**, **3b**, and **3c**, computed FMOs (frontier molecular orbitals) of the calculated structures **3a**, **3b**, and **3c**.

Supporting Information File 1

Experimental and analytical data.
[http://www.beilstein-journals.org/bjoc/content/supplementary/1860-5397-12-194-S1.pdf]

Acknowledgements

The authors cordially thank the Fonds der Chemischen Industrie and the Deutsche Forschungsgemeinschaft (Mu 1088/9-1) for financial support.

References

1. Otero, R.; Gallego, J. M.; Vázquez de Parga, A. L.; Martín, N.; Miranda, R. *Adv. Mater.* **2011,** *23,* 5148–5176. doi:10.1002/adma.201102022
2. Zhao, X.; Zhan, X. *Chem. Soc. Rev.* **2011,** *40,* 3728–3743. doi:10.1039/C0CS00194E
3. Shirota, Y.; Kageyama, H. *Chem. Rev.* **2007,** *107,* 953–1010. doi:10.1021/cr050143+
4. Barbarella, G.; Melucci, M.; Sotgiu, G. *Adv. Mater.* **2005,** *17,* 1581–1593. doi:10.1002/adma.200402020
5. Mishra, A.; Ma, C.-Q.; Bäuerle, P. *Chem. Rev.* **2009,** *109,* 1141–1276. doi:10.1021/cr8004229
6. *Handbook of Oligo- and Polythiophenes;* Fichou, D., Ed.; Wiley-VCH GmbH & Co. KGaA: Weinheim, Germany, 1999. doi:10.1002/9783527611713
7. Müllen, K.; Klärner, G. In *Electronic Materials: The Oligomer Approach;* Müllen, K.; Wegner, G., Eds.; Wiley-VCH Verlag GmbH & Co. KGaA: Weinheim, Germany, 1998.
8. Hotta, S. Chapter 8. In *Handbook of Organic conducting Molecules and Polymers;* Nalwa, H. S., Ed.; Wiley: Chichester, United Kingdom, 1997; Vol. 2.
9. Müller, T. J. J.; Bunz, U. H. F., Eds. *Functional Organic Materials. Syntheses, Strategies, and Applications;* Wiley-VCH Verlag GmbH & Co. KGaA: Weinheim, Germany, 2007. doi:10.1002/9783527610266
10. Yook, K. S.; Lee, J. Y. *Adv. Mater.* **2012,** *24,* 3169–3190. doi:10.1002/adma.201200627
11. Zhong, C.; Duan, C.; Huang, F.; Wu, H.; Cao, Y. *Chem. Mater.* **2011,** *23,* 326–340. doi:10.1021/cm101937p
12. Geiger, F.; Stoldt, M.; Schweizer, H.; Bäuerle, P.; Umbach, E. *Adv. Mater.* **1993,** *5,* 922–925. doi:10.1002/adma.19930051210
13. Fichou, D. *J. Mater. Chem.* **2000,** *10,* 571–588. doi:10.1039/A908312J
14. Mitschke, U.; Bäuerle, P. *J. Mater. Chem.* **2000,** *10,* 1471–1507. doi:10.1039/A908713C
15. Perepichka, I. F.; Perepichka, D. F.; Meng, H.; Wudl, F. *Adv. Mater.* **2005,** *17,* 2281–2305. doi:10.1002/adma.200500461
16. Wang, C.; Dong, H.; Hu, W.; Liu, Y.; Zhu, D. *Chem. Rev.* **2012,** *112,* 2208–2267. doi:10.1021/cr100380z
17. Horowitz, G.; Fichou, D.; Peng, X.; Xu, Z.; Garnier, F. *Solid State Commun.* **1989,** *72,* 381–384. doi:10.1016/0038-1098(89)90121-X
18. Garnier, F.; Horowitz, G.; Peng, X.; Fichou, D. *Adv. Mater.* **1990,** *2,* 592–594. doi:10.1002/adma.19900021207
19. Garnier, F.; Hajlaoui, R.; Yassar, A.; Srivastava, P. *Science* **1994,** *265,* 1684–1686. doi:10.1126/science.265.5179.1684
20. Sirringhaus, H.; Kawase, T.; Fried, R. H.; Shimoda, T.; Inbasekaran, M.; Wu, W.; Woo, E. P. *Science* **2000,** *290,* 2123–2126. doi:10.1126/science.290.5499.2123
21. Ong, B. S.; Wu, Y.; Liu, P.; Gardner, S. *J. Am. Chem. Soc.* **2004,** *126,* 3378–3379. doi:10.1021/ja039772w
22. Waldauf, C.; Schilinsky, P.; Perisutti, M.; Hauch, J.; Brabec, C. J. *Adv. Mater.* **2003,** *15,* 2084–2088. doi:10.1002/adma.200305623
23. Son, H. J.; He, F.; Carsten, B.; Yu, L. *J. Mater. Chem.* **2011,** *21,* 18934–18945. doi:10.1039/C1JM12388B
24. Facchetti, A. *Chem. Mater.* **2011,** *23,* 733–758. doi:10.1021/cm102419z
25. Schulze, K.; Uhrich, C.; Schüppel, R.; Leo, K.; Pfeiffer, M.; Brier, E.; Reinold, E.; Bäuerle, P. *Adv. Mater.* **2006,** *18,* 2872–2875. doi:10.1002/adma.200600658
26. Noma, N.; Tsuzuki, T.; Shirota, Y. *Adv. Mater.* **1995,** *7,* 647–648. doi:10.1002/adma.19950070709
27. Hughes, G.; Bryce, M. R. *J. Mater. Chem.* **2005,** *15,* 94–107. doi:10.1039/B413249C
28. Kulkarni, A. P.; Tonzola, C. J.; Babel, A.; Jenekhe, S. A. *Chem. Mater.* **2004,** *16,* 4556–4573. doi:10.1021/cm049473l

29. Wu, W.; Liu, Y.; Zhu, D. *Chem. Soc. Rev.* **2010,** *39,* 1489–1502. doi:10.1039/B813123F
30. Yamada, H.; Okujima, T.; Ono, N. *Chem. Commun.* **2008,** 2957–2974. doi:10.1039/B719964C
31. Yamao, T.; Shimizu, Y.; Terasaki, K.; Hotta, S. *Adv. Mater.* **2008,** *20,* 4109–4112. doi:10.1002/adma.200800942
32. Masui, K.; Mori, A.; Okano, K.; Takamura, K.; Kinoshita, M.; Ikeda, T. *Org. Lett.* **2004,** *6,* 2011–2014. doi:10.1021/ol049386z
33. Campbell, N. L.; Duffy, W. L.; Thomas, G. I.; Wild, J. H.; Kelly, S. M.; Bartle, K.; O'Neill, M.; Minter, V.; Tufn, R. P. *J. Mater. Chem.* **2002,** *12,* 2706–2721. doi:10.1039/B202073B
34. Kitamura, T.; Lee, C. H.; Taniguchi, Y.; Fujiwara, Y.; Sano, Y.; Matsumoto, M. *Mol. Cryst. Liq. Cryst.* **1997,** *293,* 239–245. doi:10.1080/10587259708042774
35. James, D. K.; Tour, J. M. Molecular Wires. *Molecular Wires and Electronics;* Topics in Current Chemistry, Vol. 257; Springer: Berlin, Germany, 2005; pp 33–62. doi:10.1007/b136066
36. Robertson, N.; McGowan, C. A. *Chem. Soc. Rev.* **2003,** *32,* 96–103. doi:10.1039/B206919A
37. Metzger, R. M. *J. Mater. Chem.* **2008,** *18,* 4364–4396. doi:10.1039/B802804B
38. Forrest, S. R. *Nature* **2004,** *428,* 911–918. doi:10.1038/nature02498
39. Carroll, R. L.; Gorman, C. B. *Angew. Chem., Int. Ed.* **2002,** *41,* 4379–4400. doi:10.1002/1521-3773(20021202)41:23<4378::AID-ANIE4378>3.0.CO;2-A
40. Tour, J. M. *Acc. Chem. Res.* **2000,** *33,* 791–804. doi:10.1021/ar0000612
41. Okada, K.; Imakura, T.; Oda, M.; Murai, H.; Baumgarten, M. *J. Am. Chem. Soc.* **1996,** *118,* 3047–3048. doi:10.1021/ja9539352
42. Duesing, R.; Tapolski, G.; Meyer, T. J. *J. Am. Chem. Soc.* **1990,** *112,* 5378–5379. doi:10.1021/ja00169a071
43. Jones, W. E., Jr.; Chen, P.; Meyer, T. J. *J. Am. Chem. Soc.* **1992,** *114,* 387–388. doi:10.1021/ja00027a073
44. Daub, J.; Engl, R.; Kurzawa, J.; Miller, S. E.; Schneider, S.; Stockmann, A.; Wasielewski, M. R. *J. Phys. Chem. A* **2001,** *105,* 5655–5665. doi:10.1021/jp0037293
45. Sailer, M.; Franz, A. W.; Müller, T. J. J. *Chem. – Eur. J.* **2008,** *14,* 2602–2614. doi:10.1002/chem.200701341
46. Memminger, K.; Oeser, T.; Müller, T. J. J. *Org. Lett.* **2008,** *10,* 2797–2800. doi:10.1021/ol800920d
47. Franz, A. W.; Popa, L. N.; Rominger, F.; Müller, T. J. J. *Org. Biomol. Chem.* **2009,** *7,* 469–475. doi:10.1039/B814850C
48. Hauck, M.; Turdean, R.; Memminger, K.; Schönhaber, J.; Rominger, F.; Müller, T. J. J. *J. Org. Chem.* **2010,** *75,* 8591–8603. doi:10.1021/jo101997t
49. Jahnke, A. C.; Spulber, M.; Neuburger, M.; Palivan, C. G.; Wenger, O. S. *Chem. Commun.* **2014,** *50,* 10883–10886. doi:10.1039/C4CC03806A
50. Franz, A. W.; Popa, L. N.; Müller, T. J. J. *Tetrahedron Lett.* **2008,** *49,* 3300–3303. doi:10.1016/j.tetlet.2008.03.071
51. Sailer, M.; Nonnenmacher, M.; Oeser, T.; Müller, T. J. J. *Eur. J. Org. Chem.* **2006,** 423–435. doi:10.1002/ejoc.200500539
52. Sailer, M.; Rominger, F.; Müller, T. J. J. *J. Organomet. Chem.* **2006,** *691,* 299–308. doi:10.1016/j.jorganchem.2005.08.012
53. Krämer, C. S.; Müller, T. J. J. *Eur. J. Org. Chem.* **2003,** 3534–3548. doi:10.1002/ejoc.200300250
54. Krämer, C. S.; Zeitler, K.; Müller, T. J. J. *Org. Lett.* **2000,** *2,* 3723–3726. doi:10.1021/ol0066328
55. Müller, T. J. J. *Tetrahedron Lett.* **1999,** *40,* 6563–6566. doi:10.1016/S0040-4039(99)01402-1
56. Zhou, G.; Pschirer, N.; Schöneboom, J. C.; Eickemeyer, F.; Baumgarten, M.; Müllen, K. *Chem. Mater.* **2008,** *20,* 1808–1815. doi:10.1021/cm703459p
57. Hauck, M.; Stolte, M.; Schönhaber, J.; Kuball, H.-G.; Müller, T. J. J. *Chem. – Eur. J.* **2011,** *17,* 9984–9998. doi:10.1002/chem.201100592
58. Hauck, M.; Schönhaber, J.; Zucchero, A. J.; Hardcastle, K. I.; Müller, T. J. J.; Bunz, U. H. F. *J. Org. Chem.* **2007,** *72,* 6714–6725. doi:10.1021/jo070922l
59. Bucci, N.; Müller, T. J. J. *Tetrahedron Lett.* **2006,** *47,* 8329–8332. doi:10.1016/j.tetlet.2006.09.075
60. Bucci, N.; Müller, T. J. J. *Tetrahedron Lett.* **2006,** *47,* 8323–8327. doi:10.1016/j.tetlet.2006.09.076
61. Bay, S.; Villnow, T.; Ryseck, G.; Rai-Constapel, V.; Gilch, P.; Müller, T. J. J. *ChemPlusChem* **2013,** *78,* 137–141. doi:10.1002/cplu.201200279
62. Bay, S.; Makhloufi, G.; Janiak, C.; Müller, T. J. J. *Beilstein J. Org. Chem.* **2014,** *10,* 1006–1016. doi:10.3762/bjoc.10.100
63. Bay, S.; Müller, T. J. J. *Z. Naturforsch., B: J. Chem. Sci.* **2014,** *69,* 541–553. doi:10.5560/ZNB.2014-4060
64. Müller, T. J. J.; Franz, A. W.; Barkschat (née Krämer), C. S.; Sailer, M.; Meerholz, K.; Müller, D.; Colsmann, A.; Lemmer, U. *Macromol. Symp.* **2010,** *287,* 1–7. doi:10.1002/masy.201050101
65. Zhou, Z.; Franz, A. W.; Hartmann, M.; Seifert, A.; Müller, T. J. J.; Thiel, W. R. *Chem. Mater.* **2008,** *20,* 4986–4992. doi:10.1021/cm800804t
66. Meyer, T.; Ogermann, D.; Pankrath, A.; Kleinermanns, K.; Müller, T. J. J. *J. Org. Chem.* **2012,** *77,* 3704–3715. doi:10.1021/jo202608w
67. Tian, H.; Yang, X.; Chen, R.; Pan, Y.; Li, L.; Hagfeldt, A.; Sun, L. *Chem. Commun.* **2007,** 3741–3743. doi:10.1039/B707485A
68. Park, S. S.; Won, Y. S.; Choi, Y. C.; Kim, J. H. *Energy Fuels* **2009,** *23,* 3732–3736. doi:10.1021/ef900207y
69. Lambert, C.; Kriegisch, V. *Langmuir* **2006,** *22,* 8807–8812. doi:10.1021/la061404t
70. Barkschat, C. S.; Stoycheva, S.; Himmelhaus, M.; Müller, T. J. J. *Chem. Mater.* **2010,** *22,* 52–63. doi:10.1021/cm901514t
71. Franz, A. W.; Stoycheva, S.; Himmelhaus, M.; Müller, T. J. J. *Beilstein J. Org. Chem.* **2010,** *6,* No. 72. doi:10.3762/bjoc.6.72
72. Rechmann, J.; Sarfraz, A.; Götzinger, A. C.; Dirksen, E.; Müller, T. J. J.; Erbe, A. *Langmuir* **2015,** *31,* 7306–7316. doi:10.1021/acs.langmuir.5b01370
73. Levi, L.; Müller, T. J. J. *Chem. Soc. Rev.* **2016,** *45,* 2825–2846. doi:10.1039/C5CS00805K
74. Merkul, E.; Urselmann, D.; Müller, T. J. J. *Eur. J. Org. Chem.* **2011,** 238–242. doi:10.1002/ejoc.201001472
75. Urselmann, D.; Antovic, D.; Müller, T. J. J. *Beilstein J. Org. Chem.* **2011,** *7,* 1499–1503. doi:10.3762/bjoc.7.174
76. Klukas, F.; Perkampus, J.; Urselmann, D.; Müller, T. J. J. *Synthesis* **2014,** 3415–3422. doi:10.1055/s-0034-1379074
77. Klukas, F.; Grunwald, A.; Menschel, F.; Müller, T. J. J. *Beilstein J. Org. Chem.* **2014,** *10,* 672–679. doi:10.3762/bjoc.10.60
78. Franz, A. W.; Müller, T. J. J. *Synthesis* **2008,** 1121–1125. doi:10.1055/s-2008-1032118
79. Yang, L.; Feng, J.-K.; Ren, A.-M. *J. Org. Chem.* **2005,** *70,* 5987–5996. doi:10.1021/jo050665p
80. *Gaussian 09,* Revision A.02; Gaussian, Inc.: Wallingford, CT, U.S.A., 2009.

81. Yanai, T.; Tew, D. P.; Handy, N. C. *Chem. Phys. Lett.* **2004,** *393,* 51–57. doi:10.1016/j.cplett.2004.06.011
82. Scalmani, G.; Frisch, M. J. *J. Chem. Phys.* **2010,** *132,* 114110. doi:10.1063/1.3359469

License and Terms

This is an Open Access article under the terms of the Creative Commons Attribution License (http://creativecommons.org/licenses/by/4.0), which permits unrestricted use, distribution, and reproduction in any medium, provided the original work is properly cited.

The license is subject to the *Beilstein Journal of Organic Chemistry* terms and conditions: (http://www.beilstein-journals.org/bjoc)

The definitive version of this article is the electronic one which can be found at: doi:10.3762/bjoc.12.194